

**AIR POLLUTION AND HEATH:
IDENTIFICATION OF CHEMICAL AND
PHYSICAL EXPOSURE METRICS FOR
EPIDEMIOLOGICAL RESEARCH**

By

Araceli Sánchez Jiménez

**Submitted in partial Fulfilment of the Requirements for the Degree of
Doctor of Philosophy**

(February 2010)

University of Strathclyde

Department of Civil Engineering

Glasgow, UK

DECLARATION OF AUTHOR'S RIGHTS

This thesis is the result of the author's original research. It has been composed by the author and has not been previously submitted for examination which has led to the award of a degree.

The copyright of this thesis belongs to the author under the terms of the United Kingdom Copyright Acts as qualified by the University of Strathclyde Regulation 3.51. Due acknowledgement must always be made of the use of any material contained in, or derived from, this thesis.

Signed:

A handwritten signature in blue ink, appearing to read 'D. A. G. H.', is written over a faint, light blue circular watermark or stamp.

Date: 26 February 2010

ACKNOWLEDGMENTS

First, I would like to thank my supervisor Dr. Iain Beverland for all his instructions and his constant support and patience in every aspect throughout the whole project.

I am also very grateful to Dr. Mat Heal and Dr. Leon Hibbs for their valuable comments.

I would like to express my thanks to all those who passed by 3.16 during the duration of the project: Alia, Nick, Panos, Marco, David, Graníee, Edriana, Alvis, Sornnarín, Antoine, Caroline and the technicians who assisted me on several occasions, Gerry, Francis and Gavin.

Special gratitude also goes to Glasgow City Council for providing me with access to their air pollution monitoring stations, National Physical Laboratories, AEA technologies and DEFRA who kindly assisted me when I needed it.

Finally, I would like to express my thanks to Chris Haikney for his continuous encouragement and help during my study.

Thank you all!!

ABSTRACT

The chemical components of particles and particle number concentration (PNC) are thought to be more relevant to describe the health effects of traffic-related air pollutants than the conventionally measured particle mass. However, they are not routinely measured and their temporal and spatial variation is not well characterized. Temporal correlations between pollutants are not well understood, making it difficult to identify what components in the pollution mix are responsible for observed health effects.

Hourly and daily PNC, PM₁₀ and PM_{2.5} mass and light absorbance of filters, elemental carbon (EC), organic carbon (OC), NO_x (NO₂ + NO), CO, SO₂, and hydrocarbons (1,3-butadiene, benzene, toluene, ethylbenzene and xylenes) concentrations were measured at paired sites (kerbside/street canyon vs. background) in London and Glasgow to examine their temporal and spatial variations. Simple metrics of air pollution such as light absorbance of filters and nitrogen oxides concentrations (including measurements with passive diffusion tubes, PDTs) were examined as possible indicators of temporal and spatial variations in PNC, water-soluble metals (Ti, V, Cr, Mn, Fe, Ni, Cu, As, Cd, Pb and Zn) bound to PM₁₀ (in Glasgow) and PM_{2.5} (in London) and polycyclic aromatic hydrocarbons (PAHs) in Glasgow.

The spatial gradients between paired sites were larger for PNC and NO₂ than for PM₁₀. Correlations of PNC and PM₁₀ between paired sites were moderate ($r \approx 0.5-0.6$) in London and Glasgow and NO₂ and NO_x correlations were moderate in London ($r \approx 0.5$) and moderate to high in Glasgow ($r \approx 0.6-0.8$). The r -values did not change with the averaging period used (hourly or daily). Correlations of daily measurements of water-soluble metals between paired sites were high ($r > 0.8$) for V and As and moderate to high ($r = 0.5-0.7$) for Fe, Ni, Zn, Cu, Cd and Pb in London but not in Glasgow ($r < 0.4$). Daily measurements of absorbance of PM_{2.5} in London and absorbance of PM₁₀ in Glasgow were not correlated between paired sites. PAHs concentrations were below the limit of detection.

Nitrogen oxides best represented the temporal variation of traffic-related air pollutants. However, a different pattern of correlations was observed between background and kerbside/street canyon sites. Hourly and daily NO₂ and NO_x were moderately to highly correlated with PNC ($r = 0.5-0.8$), PM₁₀ ($r = 0.4-0.8$) at the background and kerbside sites; 1,3-butadiene and benzene ($r = 0.6-0.9$) at the kerbside sites and with daily Fe, Cu, As, Pb and Zn at the background sites ($r = 0.5-0.7$) but not at the kerbside sites. The absorbance of the filter mass was correlated with Mn, Fe, Cu, As, Cd, Pb and Zn at the background sites but not at the kerbside sites. The spatial variations (daily kerbside- background increments) of NO₂ and NO_x explained 70 % of the variance in the daily increments in PNC at both paired sites, in London and Glasgow and 70 % of the increments in Cu and Ni at Glasgow but not at London. Weekly NO₂ and NO_x concentrations derived from PDTs explained up to 70 % of the variance in PNC, 1,3-butadiene, benzene, toluene, ethylbenzene and xylenes.

The variability in the between-pollutant correlations between background and street canyon sites highlights the influence of street building geometry on pollutants dispersion and suggests that results from one monitoring site may not be generalised to other locations. NO₂ and NO_x concentrations represent well the spatial differences in PNC but their use as surrogates for metals cannot be extrapolated to all locations. The high temporal correlation between NO₂, PNC and hydrocarbons implies that epidemiological studies based on time series analyses may not distinguish between their separate health effects. PDTs are a useful tool to build NO₂ maps across large areas, which can be used to represent variations in PNC and hydrocarbons. These maps could be used in epidemiological studies examining the relationship between air pollution and health.

ABBREVIATIONS AND DEFINITIONS

ACS	American Cancer Society
AQEG	Air Quality Expert Group
AUN	Automatic Urban Network
APHEA	Air Pollution and Health
BADC	British Atmospheric Data Centre
BCPC	Butanol Condensation Particle Counter
BC	Black Carbon
BMRC	British Medical Research Council
BS	Black Smoke
BSI	British Standard Institute
BST	British Standard Time
BTEX	Benzene, Toluene, Ethylbenzene and Xylene
CAFE	Clean Air for Europe
CEN	European Standardization Committee
CI	Confidence Interval
COX-2	Cyclooxygenase-2: enzyme responsible for inflammation and pain
COPD	Chronic Obstructive Pulmonary Disease
DEFRA	Department of Environment and Rural Affairs
DNA	Deoxyribonucleic acid
EGF	Epidermal Growth Factor
FDMS	Filter Dynamics Measurement System
FEV	Forced Expiratory Volume
FVC	Forced Vital Capacity
GC-MS	Gas Chromatography Mass spectrometry
GM-CSF	Granulocyte Monocyte Colony Stimulating Factor
GMT	Greenwich Mean Time
GSH	Glutathione

HEAPSS	Health Effects of Air Pollution on Susceptible Subpopulations
HEI	Health Effects Institute
IARC	International Agency for Research on Cancer
ICAM-1	Inter-Cellular Adhesion Molecule 1
IL	Interleukin
ICP-MS	Ionization Coupled Plasma Mass Spectrometry
IQR	Inter Quartile Range
ISO	International Standard Organization
NAQA	National Air Quality Archive
NLCS	Netherlands Cohort Study on Diet and Cancer
NERC	Natural Environmental Research Council
NETCEN	National Environmental Technology Centre
NF- κ B	Nuclear Factor kappa B
NIST	National Institute of Standard and Technology
NMMPS	National Morbidity, Mortality and Air Pollution Study
LOD	Limit of Detection
NPL	National Physical Laboratories
LSR	Linear Square Regression
LUR	Land Use Regression
PNC	Particle Number Concentration
NAEI	National Atmospheric Emission Inventory
NO _x	Sum of NO ₂ and NO (expressed as NO ₂)
PAHs	Polycyclic Aromatic Hydrocarbons
PAN	Peroxy Acetyl Nitrate
PCBs	Polychlorinated biphenyls
PDTs	Passive Diffusion Tubes
PEACE	Pollution Effects on Asthmatic Children in EU
PEFR	Peak Expiratory Flow Rate
PM _x	Particulate Matter with an aerodynamic diameter of less

	than $x \mu\text{m}$ collected with 50 % efficiency
PNC	Particle Number Concentration
PTFE	Polytetrafluoroethylene
PTV	Programmable Temperature Vaporising
RAIAP	Respiratory Allergy and Inflammation due to Ambient Particles
RANTES	Regulated on Activation Normal T Cell Expressed and Secreted. A cytokine that is a member of the interleukin-8 family of cytokines
RH	Relative Humidity
RMA	Reduced Major Axes
ROS	Reactive Oxygen Species
RSD	Relative Standard Deviation
SPALDIA	Swiss Study on Air Pollution and Lung Disease in Adults
SD	Standard Deviation
SE	Standard Error
TEA	Triethylamine
TEOM	Tapered Element Oscillating Microbalance
TNF- α	Tumour Necrosis Factor- α
TSP	Total Suspended Particles
ULTRA	Dutch for Exposure and risk assessment for fine and ultrafine particles in ambient air
VCM	Volatile Correction Model
VOCs	Volatile Organic Compounds
WCPC	Water Condensation Particle Counter

TABLE OF CONTENTS

DECLARATION OF AUTHOR’S RIGHTS	i
ACKNOWLEDGEMENTS.....	ii
ABSTRACT	iii
ABBREVIATIONS AND DEFINITIONS.....	iv
CONTENTS	vii-xiii
LIST OF FIGURES	xiv-xvi
LIST OF TABLES.....	xvii-xx
CHAPTER 1 INTRODUCTION AND GENERAL BACKGROUND	1
1.1 Introduction.....	2
1.2 Chemical & Physical Characteristics of Traffic-related Air Pollutants.....	3
1.2.1 Particulate matter	3
1.2.1.1 Physical characteristics of particulate matter.....	4
1.2.1.2 Chemical composition of particulate matter	9
1.2.2 Nitrogen oxides	13
1.2.3 Ozone	15
1.2.4 Carbon monoxide.....	16
1.2.5 Sulphur dioxide.....	16
1.2.6 Hydrocarbons.....	17
1.2.7 Diesel exhaust	17
1.3 Hazards from traffic-related air pollutants.....	19
1.3.1 Particulate matter	20
1.3.2 Polycyclic Aromatic Hydrocarbons	27
1.3.3 Metals.....	28
1.3.4 Interactive effects between the components of PM ₁₀	30

1.3.5 Nitrogen dioxide.....	31
1.3.6 Ozone	32
1.3.7 Carbon monoxide.....	33
1.3.8 Sulphur dioxide.....	33
1.3.9 Hydrocarbons.....	34
1.3.10 Interactive effects of PM and gaseous pollutants.....	35
1.3.11 Summary	35
CHAPTER 2 LITERATURE REVIEW OF EPIDEMIOLOGICAL STUDIES AND HEALTH EFFECTS OF AIR POLLUTION.....	37
2.1 Introduction.....	38
2.2 Epidemiological Studies on Short-term Exposure	38
2.2.1 Epidemiological short-term studies on the effects of PM ₁₀	39
2.2.2 Epidemiological short-term studies on gaseous pollutants	42
2.2.3 Epidemiological short-term studies on the health effects of transition metals	43
2.3 Epidemiological Studies on Long-term Exposure	44
2.4 Errors & Gaps in Air Pollution Exposure Assessment Studies	45
2.5 Correlations Between Traffic-Related Air Pollutants.....	50
2.5.1 Introduction.....	50
2.5.2 Studies on the correlations between particle number and co-pollutants.....	51
2.5.3 Studies on the correlation between transition metals and co-pollutants	55
2.5.4 Studies on the correlations between PAHs and co-pollutants.....	57
2.6 Summary Literature Review	60

CHAPTER 3 AIMS AND OBJECTIVES OF THE RESEARCH.....	62
3.1 Aims of the Research	63
CHAPTER 4 METHODOLOGY.....	65
4.1 Introduction.....	66
4.2 Overview of experimental design for the main study	66
4.3 Details of the Monitoring Sites involved in the main study	70
4.4 Equipment Operation for Particle Sampling.....	77
4.4.1 Water & Butanol based condensation particle counters	77
4.4.2 Partisol sampler and TEOM analyser	80
4.4.3 Respirable dust sampler	82
4.5 Gravimetric Analysis for PM ₁₀ & Respirable Dust Filters.....	83
4.6 Reflectance Analyses of PM ₁₀ & Respirable Dust Filters	88
4.7 Sequential Extraction of Particulate-bound PAHs & Transition Metals from PM ₁₀ Filters	92
4.7.1 Cleaning and storage	92
4.7.2 Extraction procedure	93
4.7.3 Assessment of losses of metals during the PAHs extraction	95
4.7.4 Efficiency of the PAH extraction.....	97
4.8 PAH Analyses	97
4.8.1 Gas Chromatography Mass Spectrometry	97
4.9 Metal Analysis	99
4.9.1 ICP-MS	99
4.9.2 Quality Assurance	104
4.9.3 Metal concentration in field blanks and limits of detection.....	105

4.10 Overview of the experimental design for assesment of the performance of NO ₂ and NO _x PDTs.....	107
4.10.1 Details of the monitoing sites for assessment of NO ₂ PDTs performance over time	107
4.10.2 NO ₂ passive diffusion samplers	110
4.10.3 NO _x passive diffusion samplers	111
4.10.4 Chemical quantification of NO ₂ and NO _x	112
4.10.4.1 Extraction of nitrite from exposed NO ₂ and NO _x PDTs	112
4.10.4.2 UV-molecular absorption theory	115
4.10.4.3 Operation of the spectrophotometer.....	116
4.10.4.4 Calculation of the ambient NO ₂ and NO _x concentrations.....	117
4.10.4.5 Quality assurance	120
4.11 Statistical Analyses of Data	120
CHAPTER 5 ASSESSMENT OF PRECISION AND COMPARABILITY OF MONITORING METHODS.....	124
5.1 Results	125
5.1.1 Equipment validation for gas sampling.....	125
5.1.1.1 Replicate precision of NO ₂ and NO _x PDTs	125
5.1.1.2 Effect of NO ₂ PDT exposure duration	129
5.1.1.3 Evaluation of the accuracy of the PDTs.....	135
5.1.1.3.1 Comparison of NO ₂ PDTs concentrations derived from 1-week exposure period with NO ₂ from a chemiluminescent analyser ..	135
5.1.1.3.2 Comparison of NO _x PDTs derived from 1-week exposure period with NO _x from a chemiluminescence analyser.	139
5.1.1.3.3 Comparison of NO ₂ PDTs derived from 4-weeks and 4*1-week with NO ₂ from a chemiluminiscence analyser	142

5.1.2	Equipment validation for particle sampling.....	144
5.1.2.1	Replicate precision of mass and absorbance of respirable dust filters....	144
5.1.2.2	Inter-comparison of Partisol and TEOM analyser	147
5.1.2.3	Comparison of water-based (Model 3785) & butanol-based (Model 3022A) condensation particles counters	154
5.1.3	Efficiency of the sequential extraction.....	166
5.1.3.1	PAHs concentrations.....	166
5.1.3.2	Losses of metals during the PAH extraction.....	167
5.2	Discussion	171
5.2.1	Performance of PDTs	171
5.2.1.1	Precision of PDTs	171
5.2.1.2	Biases of PDTs.....	171
5.2.2	Performance of the respirable dust samplers	177
5.2.3	Comparison of Partisol sampler and TEOM analyser	178
5.2.4	Performance of the water-based condensation particle counter.....	181
5.2.5	Efficiency of the sequential extraction.....	183
CHAPTER 6 SPATIAL & TEMPORAL VARIATIONS IN PARTICLE CHARACTERISTICS (MASS, NUMBER, ABSORBANCE, METAL COMPOSITION) AND GASEOUS POLLUTANTS IN GLASGOW AND LONDON		185
6.1	Results.....	186
6.1.1	Pollutant concentrations and diurnal variations	186
6.1.2	Temporal variability of pollutant concentrations at Glasgow.....	193
6.1.3	Correlations between a single pollutant measured at different sites.....	198
6.1.4	Correlation between different pollutants measured at the same site.....	203
6.1.4.1	Correlations between particle characteristics and gaseous pollutants....	216
6.1.4.2	Correlations between surrogates of BC, PM and PNC	219

6.1.4.3	Correlations between gaseous air pollutants.....	221
6.1.4.4	Correlations between water-soluble metals and traffic-related air pollutants.....	222
6.1.5	Correlations between the increments in pollutant concentrations.....	223
6.1.6	Variation of traffic-related air pollutants with wind speed and direction.....	228
6.2	Discussion.....	232
6.2.1	Spatial Variability of Air Pollutants.....	232
6.2.2	Diurnal pattern of traffic-related air pollutants in Glasgow.....	237
6.2.3	Correlations of the same pollutant measured at different sites.....	239
6.2.4	Correlation between different pollutants measured at the same site.....	242
6.2.4.1	Correlations between particle characteristics and gaseous pollutants....	243
6.2.4.2	Correlations between particle characteristics: number, mass and darkness.....	249
6.2.4.3	Correlations between water-soluble metals and traffic-related air pollutants.....	253
6.2.5	Correlations between the increments in pollutant concentrations.....	255
6.2.6	Summary correlations between traffic-related air pollutants.....	255
CHAPTER 7 USE OF NO₂ AND NO_x PDTs AS SURROGATES FOR AIR POLLUTION METRICS		258
7.1	Results.....	259
7.1.1	Use of PDTs to estimate the spatial variability of NO ₂ in Glasgow.....	259
7.1.2	Use of PDTs to assess the spatial variability of NO ₂ with increasing distance from a major road.....	260
7.1.3	Use of NO ₂ PDTs as surrogates for PNC.....	263
7.1.4	Use of NO ₂ & NO _x PDTs as surrogates for hydrocarbons.....	265
7.1.5	Use of NO ₂ & NO _x as surrogates for BS.....	268

7.2	Discussion	270
7.2.1	Use of PDTs to examine the spatial variability of NO ₂	270
7.2.2	Use of PDTs as surrogate for traffic-related air pollutants	273
CHAPTER 8 CONCLUSIONS, FURTHER WORK & LIMITATIONS OF THE PROJECT		276
8.1	Limitations of the Study & Further Work.....	277
8.2	Conclusions.....	279
8.3	Implications for epidemiological studies	282
8.4	Implications for air quality monitoring.....	283
REFERENCES.....		284

LIST OF FIGURES

Figure 1.1 Probability of aerosol penetration as a function of aerodynamic diameter, internationally agreed by CEN/ISO/ACGHI.....	6
Figure 1.2 Particle size distributions as a function of the number, surface area, and mass.	7
Figure 1.3 Composition of PM ₁₀ in the urban atmosphere. Mean values observed in London and Birmingham, 2000-2002. (Modified from Harrison, 2003b).....	10
Figure 1.4 Schematic representation of diesel exhaust particles (Matti Maricq, 2007).....	18
Figure 1.5 Signalling effects of particles known to lead to adverse health effects. Mn: Cu ²⁺ , Cr ³⁺ , Cr ⁴⁺ , Fe ³⁺ , V ³⁺ , V ⁵⁺ . Dashed line: animal data only..	22
Figure 4.1 Map of monitoring sites for the main study (Glasgow).....	71
Figure 4.2 Photographs to the North (top left), South (top right), East (bottom left) and West (bottom right) of the monitoring station at Hope St.	72
Figure 4.3 Photographs to the North (top left), South (top right), East (bottom left) and West (bottom right) of the monitoring station at St. Enoch Sq.....	73
Figure 4.4 Photograph of Glasgow City Council and the surrounding to the South (top right), East (bottom left) and West (bottom right) of the monitoring station at North Kensington. (Photos from www.airquality.co.uk).....	74
Figure 4.5 Map of the monitoring sites in London.	75
Figure 4.6 Photograph of Glasgow City Council and the surrounding to the South (top right), East (bottom left) and West (bottom right) of the monitoring station at Marylebone Rd.	76
Figure 4.7 Photograph of Glasgow City Council and the surrounding to the South (top right), East (bottom left) and West (bottom right) of the monitoring station at North Kensington.....	77.
Figure 5.1 Scatter plots and Reduced Major Axes (RMA) regression of duplicate 1-week NO ₂ exposure PDTs (a); 4-weeks NO ₂ exposure PDTs (b) and 1-week NO _x PDTs exposure.....	128
Figure 5.2 Comparison between NO ₂ PDT concentrations measured during 4-weeks exposure period and the averaged concentration of 4 consecutive 1 week exposure periods.	130
Figure 5.3 Comparison between NO ₂ concentrations measured during 4-weeks exposure period and the averaged concentration of 4 consecutive 1-week exposure periods at St. Enoch Sq. in 2005.	131

Figure 5.4 Scatter plot and Pearson correlation coefficient (r) of NO ₂ concentrations measured during 4 continuous weeks and the averaged concentration of 4 consecutive 1 week exposure periods.....	133
Figure 5.5 Scatter plot and Pearson correlation coefficient (r) of the ratio of NO ₂ concentration derived from 4-weeks exposure period over NO ₂ concentration derived from 4 consecutive weeks against the averaged NO ₂ concentration as measured by the analyser.....	134
Figure 5.6 Scatter plots and RMA relationship of NO ₂ measured by PDTs and NO ₂ measured with an analyser.....	136
Figure 5.7 Scatter plots and Pearson correlation coefficients (r) of PDTs: Analyser NO ₂ ratio against NO: NO ₂ & O ₃	138
Figure 5.8 Scatters and RMA relationship of NO _x measured by PDTs and NO _x measured by a chemiluminescence analyser at St. Enoch Sq., Hope St. and Montrose St.....	141
Figure 5.9 Boxplots of the concentration (left) and absorption coefficient (right) of PM ₄ sampled simultaneously with 6 respirable dust samplers at Rottenrow (background site) over 4 weeks, using pumps with previously used diaphragms.....	145
Figure 5.10 Boxplot of the concentration (left) and absorption coefficient (right) of PM ₄ sampled simultaneously with 6 samplers, at Rottenrow (background site) over 4 weeks, using pumps with new diaphragms.....	145
Figure 5.11 Replicate precision of PM ₄ concentration (left) and absorption coefficient (right) during the monitoring campaign at Hope St., St. Enoch Sq., and Montrose St. (n=15). Exposure period: 7 Jun-27 Jul 2006.....	147
Figure 5.12 Scatter plots, Reduced Major Axes (RMA) relationship and regression coefficient (R ²) of PM ₁₀ measurements taken with a Partisol and a 24-hrs averaged TEOM data with the default correction (3, 1.03); UK correction (3, 1.03, 1.3) and uncorrected at Hope St. (left) and St. Enoch Sq. (right).....	149
Figure 5.13 Scatter plot, Reduced Major Axes (RMA) relationship and regression coefficient (R ²) of PM ₁₀ measurements taken with a Partisol and a 24-hours averaged TEOM with the default correction (1.03,3); UK correction (1.03,3,1.3) and uncorrected data at Marylebone Rd. (left) and North Kensington. (right).....	152
Figure 6.1 Time series of particle number concentration (PNC), PM ₁₀ and NO ₂ at St. Enoch Sq. (urban centre), Hope St. (kerbside) and Montrose St. (urban background/street canyon) (8 Jun-31 Aug 2006). Data based on hourly averages.....	194
Figure 6.2 Time series plot of particle number concentration (PNC), PM ₁₀ and NO ₂ at Hope St., St. Enoch Sq. and Montrose St. on working days, Saturdays and Sundays (left) and time series plot of the ratios of weekday: weekend concentrations.....	196
Figure 6.3 Scatter plot and Spearman correlation coefficient of daily averaged particle number concentration (PNC) against black smoke (BS) at St. Enoch Sq. (Data period: Jan-May 07).....	221

Figure 6.4 Daily wind rose at Bishopton (Glasgow) (8 Jun- 31 Aug 2006).	228
Figure 6.5 Daily wind rose at Heathrow Airport (London) (selection of 26 days in 2006). 229	
Figure 6.6 Schematic representation of the street canyon at Hope St., Montrose St., and Marylebone Rd.	230
Figure 6.7 Schematic representation of wind flow and spatial variation of pollutant concentrations created when wind blows parallel to a regular street canyon (Scaperdas and Colvile, 1999).	254
Figure 7.1 Scatter plots, logarithmic, exponential, and power law curves of 5 week averaged NO ₂ concentrations and the averaged of the concentrations over the five weeks measured by PDTs against distance from Cathedral St.	261
Figure.7.2 Scatter plots, exponential and logarithmic curves of NO ₂ concentrations against distance from Cathedral St. (8,000-15,000 vehicles day ⁻¹).	263
Figure.7.3 Scatter plots, RMA relationship, and regression coefficient (R ²) of weekly averaged particle number concentration (PNC) vs. NO ₂ at St. Enoch Sq. (top), Hope St. (center) and Montrose St. (bottom).	265
Figure 7.4 Time series plot of weekly averaged VOCs, NO ₂ and NO _x measured with PDTs for all exposure period at Hope St.	266
Figure 7.5 Scatter plots, RMA relationship and regression coefficient (R ²) of weekly averaged black smoke (BS) vs. NO ₂ . and NO _x derived from PDTs and analyser.	268

LIST OF TABLES

Table 2.1 Summary review of studies on the correlations of particle number concentrations and other traffic-related air pollutants.	54
Table 2.2 Summary review of the studies of correlations between metals and other traffic-related air pollutants.	56
Table 2.3 Summary review of the studies of correlations between particle bound-PAHs (unless otherwise indicated) and other traffic-related air pollutants.....	59
Table 4.1 Pollutants measured as part of this project and those provided by the National Air Quality Archive (NAQA), monitoring equipment and monitoring sites.	69
Table 4.2 Location and classification codes of the monitoring sites in Glasgow (sites arranged from West to East).	71
Table 4.3 Location and classification codes of the monitoring sites (sites arranged from West to East).	75
Table 4.4 Operating parameters of TSI particle counters Model 3785 (water-based) & 3022A (butanol-based).	80
Table 4.5 Mass variability of a standard weight of 200 mg.	84
Table 4.6 Precision of Zefluor® blank filters weighed with the MC5 Sartorius® microbalance.	84
Table 4.7 Estimates of confidence interval (CI) and limits of detection (LOD) in weighing Zefluor® filters. $LOD=3*(SD \text{ day-to-day weight change} \times \sqrt{\frac{n+1}{n}})$	85
Table 4.8 Variability of blank reflectance of Zefluor® filters.	90
Table 4.9 Summary of isotopes chosen for each element and their possible polyatomic interferences.	102
Table 4.10 Limit of Detection (LOD) of quartz and PTFE field blank filters.	106
Table 4.11 Location and classification codes of the monitoring sites for the analysis of the performance of NO ₂ PDTs in Glasgow (sites arranged from West to East).	108
Table 4.12 Averaging time procedure for the analysis of air pollution data in Glasgow at the 3 AUN sites (Hope St, St. Enoch & Montrose St.).	122
Table 5.1 Monitoring sites and sampling periods for NO ₂ and NO _x PDTs.	126
Table 5.2 Summary statistics of the Relative Standard Deviation (RSD) of replicate measurements of NO ₂ and NO _x PDTs.	126

Table 5.3 Summary statistics of ratio of NO ₂ derived from 4 continuous weeks (4-weeks) over the NO ₂ concentration averaged from 4 separated weeks (4*1-week).....	132
Table 5.4 Summary statistics of the differences in NO ₂ measurements derived from 1-week exposure period and the averaged NO ₂ concentration measured by a chemiluminescence analyser.....	135
Table 5.5 Least Square Regression with (top values) and without intercept set to zero (bottom values) of NO ₂ PDTs vs. NO ₂ analyser.....	137
Table 5.6 Summary statistics of the differences in NO _x measurements derived from 1-week exposure periods and the NO _x concentration measured by a chemiluminescence analyser.....	140
Table 5.7 Least Square Regression with (top values) and without (bottom values) intercept forced to zero of NO _x PDTs vs. NO _x analyser.....	142
Table 5.8 Summary statistics of the differences in NO ₂ concentration derived from 4-weeks & 4*1-week PDTs exposure periods and the NO ₂ concentration measured by a chemiluminescence analyser.....	143
Table 5.9 Descriptive statistics of PM ₁₀ Partisol measurements and 24-hours averaged TEOM data with the default correction (3, 1.03), and UK correction (3, 1.03, 1.3) at Hope St. and St. Enoch Sq.....	150
Table 5.10 Descriptive statistics, of PM ₁₀ Partisol measurements and 24-hours averaged TEOM data with the default correction (3, 1.03), and UK correction (3, 1.03, 1.3) at Marylebone Rd. and North Kensington.....	153
Table 5.11 Summary of dates, sampling sites and technical faults of the water-based condensation particle counters (WCPC1 top and WCPC2 bottom).....	155
Table 5.12 Metal concentration (µg metal per g of PM ₁₀) found in the single metal extraction and the sequential extraction (PAHs and metals).....	168
Table 6.1 Descriptive statistics of traffic-related air pollutants at Glasgow (Hope St: kerbside/street canyon, St. Enoch Sq. urban centre; Montrose St: background/street canyon) (8 Jun to 31 Aug 2006) and London (Marylebone Rd: kerbside/street canyon; North Kensington: urban background).....	187
Table 6.2 Mean daily ratios of kerbside: background site concentrations in London and Glasgow.....	189
Table 6.3 Summary of annual median concentrations in 2006 at Glasgow sites (Hope St. St. Enoch Sq. and Montrose St.) and London sites (Marylebone Rd. and North Kensington).....	192

Table 6.4 Spearman correlation coefficient and sample size of pollutant concentrations between monitoring sites for hourly and daily averaged data at Glasgow (Hope St., St. Enoch Sq. & Montrose St. and London (Marylebone Rd.& North Kensington)	199
Table 6.5 Spearman correlation coefficients of water-soluble metal concentration in PM ₁₀ measured at Hope St. against St. Enoch Sq. in Glasgow and in PM _{2.5} at Marylebone Rd. against North Kensington in London.....	202
Table 6.6 Spearman correlation coefficient and scatter plot of hourly averaged traffic-related air pollutants at Hope St.	204
Table 6.7 Spearman correlation coefficient and scatter plot of daily averaged traffic-related air pollutants at Hope St..	205
Table 6.8 Spearman correlation coefficient and scatter plot of hourly averaged traffic-related air pollutants at St. Enoch Sq.....	207
Table 6.9 Spearman correlation coefficient and scatter plot of daily averaged traffic-related air pollutants at St. Enoch Sq.....	208
Table 6.10 Spearman correlation coefficient and scatter plot of hourly averaged traffic-related air pollutants at Montrose St (8 Jun-31 Aug 2006), (horizontal variables: x axes and vertical variables: y axes).	209
Table 6.11 Spearman correlation coefficient and scatter plot of daily averaged traffic-related air pollutants at Montrose St.....	209
Table 6.12 Spearman correlation coefficient hourly averaged traffic-related air pollutants at Marylebone Rd.	210
Table 6.13 Spearman correlation coefficient and scatter plots of daily traffic-related air pollutants at Marylebone Rd.....	211
Table 6.14 Spearman correlation coefficient hourly averaged traffic-related air pollutants at North Kensington.	213
Table 6.15 Spearman correlation coefficient and scatter plots of daily traffic-related air pollutants at North Kensington (horizontal variables: x axes and vertical variables: y axes.	214
Table 6.16 Scatter plot, RMA relationship, and regression coefficient (R ²) of the increments in PNC vs. increments in co-pollutants. The increments refer to the daily concentrations at Hope St. with the daily concentrations at St. Enoch Sq. subtracted.....	224
Table 6.17 Scatter plot, RMA relationship, and regression coefficient (R ²) of the increments in PNC vs. increments in co-pollutants. The increments refer to the daily	

concentrations at Marylebone Rd. with the daily concentrations at North Kensington subtracted	224
Table 6.18 Scatter plot, RMA relationship, and regression coefficient (R^2) of the increments in Cu and Ni vs. increments in PNC and nitrogen oxides. The increments refer to the daily concentrations at Hope St. with the daily concentrations at St. Enoch Sq. subtracted.....	226
Table 6.19 Scatter plot, RMA relationship, and regression coefficient (R^2) of the increments in Mn, Fe and Cu vs. increments in OC. The increments refer to the daily concentrations at Marylebone Rd. with the daily concentrations at North Kensington subtracted.	227
Table 7.1 Descriptive statistics of NO_2 ($\mu\text{g m}^{-3}$) measured by PDTs at different sites in Glasgow (sites arranged from west to east).....	259
Table 7.2 Scatter plots and Spearman correlation coefficient between NO_2 PDTs measured at different sites in Glasgow.	260
Table 7.3 Estimated parameters, regression coefficients (R^2) and p-value of the exponential, logarithmic and power relationship between NO_2 concentrations measured using PDTs at different distances from Cathedral St (x). (8,000-15,000 vehicles day ⁻¹).	262
Table 7.4 Estimated parameters of the logarithmic relationship of the relative NO_2 concentration (<i>C_{rel}</i> , reference distance of 3 m away from road in present study and 10 m in Gilbert et al. and Pleijel et al. studies) contributed by a major road and the distance to the road.	272

CHAPTER 1

INTRODUCTION AND GENERAL

BACKGROUND

1.1 INTRODUCTION

In recent years, there have been increased concerns about the health effects of air pollution (Brunekreef and Holgate, 2002; Dockery and Stone, 2007; Pope et al., 2009). Epidemiological studies worldwide have shown significant associations between particulate matter (PM), gaseous pollutants (nitrogen dioxide, NO₂, carbon monoxide, CO, sulphur dioxide, SO₂ and ozone, O₃) and increased morbidity and mortality (Schwartz et al., 1991, 2004; Dockery et al., 1993; Saldiva et al., 1995; Pope et al., 1995, 2002, 2004; Ostro et al., 1996; Lee et al., 2000; Samet et al., 2000; Omori et al., 2003; Aunan et al., 2004; Filleul et al., 2005).

Concentration of particles in 2005 in the UK were estimated to result in an average loss of life expectancy of 7-8 months (DEFRA, 2007). Beyond compromising the health of the population, air pollution also affects the economy. The health impact of particulate air pollution in the UK for 2005 was estimated at between £8.5 and £20.2 billion (DEFRA, 2007). Therefore, air pollution policies have been introduced in most urbanised countries. However, to implement effective air quality standards it is of fundamental importance to know which specific components of the air pollutant mixture are responsible for the observed health effects (Roberts and Martins, 2006).

Road transport is the main cause of air pollution in industrialised countries (DETR, 1997, Briggs et al., 1997; Wrobel et al., 2000). However, for logistical reasons not all pollutants can be monitored. Since the 1980s, measurements of PM₁₀ (defined as the mass of particles with an aerodynamic diameter < 10 µm deposited with 50 % efficiency) and NO₂ have been used as surrogates for human exposure to air pollution. However, these studies have been hampered by difficulties in characterizing spatial-temporal variations of NO₂ and PM₁₀ and by the degree of correlation between PM₁₀ and NO₂ with other traffic-related air pollutants. There are concerns about how representative of the adverse health effects these pollutants are. Therefore, the characterization of the chemical components of PM and their relationships with other gaseous pollutants is fundamental to understanding the toxic effects of air pollution. It has further importance in the attempt to implement air quality standards which reflect desired public health outcomes.

1.2 CHEMICAL & PHYSICAL CHARACTERISTICS OF TRAFFIC-RELATED AIR POLLUTANTS

This section describes the main traffic-related air pollutants namely PM, organic carbon (OC), elemental carbon (EC), metals, polycyclic aromatic hydrocarbons (PAHs), nitrogen oxides (NO₂, NO and NO_x) CO, SO₂ and hydrocarbons (1,3-butadiene, benzene, toluene, ethylbenzene, m/p-xylene and o-xylene). O₃ is also included although it is not directly emitted by vehicles. O₃ is formed in reactions involving nitrogen oxides and must be considered alongside them. A special section is dedicated to diesel exhaust due to the toxic effects and characteristics of this particular pollutant mixture.

1.2.1 Particulate matter

Airborne PM is a complex mixture of organic and inorganic substances that exist in liquid or solid states and range in diameter from less than 10 nm to 100 µm (QUARG, 1996). The most important distinction drawn is between primary and secondary atmospheric particles.

Primary particles are emitted directly to the atmosphere from anthropogenic and natural sources including the incomplete combustion of fossil fuel, or volcanic eruptions.

Secondary particles are formed by chemical and physical reactions in the atmosphere.

Primary and secondary particles are both subject to transformations in size, number, chemical composition, and shape until they are removed from the atmosphere.

In the UK, the main sources of particles are vehicle emissions, secondary aerosols from long range transport (e.g. ammonium sulphates and ammonium nitrates) and wind-blown material (Harrison et al., 1997).

There are several methods commonly used to measure airborne particles:

Gravimetric methods measure the mass of particles within a specific size range. The mass of particles can be described in terms of Total Suspended Particles (TSP, which refers to the mass of particles below 40-50 μm) and PM_x (defined as particle matter which passes a sampler entry of $x \mu\text{m}$ with 50 % efficiency).

Optical methods measure the reflectance of particles deposited onto a filter. This can be transformed into mass value, known as black smoke (BS), or into an absorption coefficient. Both methods provide indirect measurement of elemental or black carbon (BC), the material in PM with the highest absorption properties (Horvath, 1993). In the late 1990s, measurements of particle number concentration (PNC, particles per volume unit) started to be collected. This also used optical means.

EU and the UK legislation regulates PM_{10} concentrations. The current threshold annual limit value is $40 \mu\text{g m}^{-3}$. Annual $\text{PM}_{2.5}$ concentrations are recommended not to exceed $25 \mu\text{g m}^{-3}$. However, there is no threshold value for elemental carbon or elemental carbon surrogates and PNC (EC, 1996).

1.2.1.1 Physical characteristics of particulate matter

The behaviour of particles in the atmosphere and within the human respiratory system is determined largely, but not wholly, by their physical properties. These properties are related to particle size, shape and surface area (QUARG, 1996).

Particle size (calculated as the aerodynamic diameter of spherical particles) mostly depends on the process that generated the particle. Size influences the transport and removal of particles from the atmosphere, their chemical and physical properties, and the region of deposition in the respiratory tract. Particles are divided into coarse, fine and ultrafine fractions, based on their formation processes. *Coarse particles* ($> 2.5 \mu\text{m}$) refer to those particles produced by mechanical processes such as erosion and abrasion (e.g. from vehicle wear, road surface, building materials). Coarse biological material and sea spray (Seinfeld and Pandis, 1998). *Fine particles* ($< 2.5 \mu\text{m}$) originate mostly from combustion sources, including power generation

and wood burning (Seinfeld and Pandis, 1998). *Ultrafine particles*, UFPs ($< 0.1 \mu\text{m}$) also originate in combustion processes, (e.g. vehicle exhaust) and in gas-to-particle conversion processes (nucleation and condensation) of atmospheric gases (AIRNET, 2004).

Studies on human inhalability have shown that owing to the size selective nature of particle removal mechanisms in the nasal passages and lung airways, the size distribution of particles is vital to understand their health effects (Donalson and Borm, 2007). Therefore, in health studies definitions of aerosol size fractions are expressed as curves that relate the probability of aerosol penetration as a function of the aerodynamic size.

The European Standardization Committee (CEN, 1992), the International Organization for Standardization (ISO, 1995) and the American Conference for Governmental Industrial Hygienist, (ACGHI, 1995) convention defined three health related particle sizes corresponding to three regions in the respiratory tract: *inhalable particles* are defined as the fraction of particles with a probability of penetration of 50 % for particles below $100 \mu\text{m}$ in aerodynamic diameter, covering the whole range of particles potentially inhaled through the nose or mouth by humans; *thoracic particles* cover the fraction of particles with a probability of penetration of 50 % for particles below $11.64 \mu\text{m}$ in aerodynamic diameter; and *respirable particles* cover the fraction of particles with a probability of penetration of 50 % for particles below $4.25 \mu\text{m}$ in aerodynamic diameter. Respirable particles can penetrate deep into the unciliated airways of the lung (alveolar region). Figure 1.1 shows the three health related particle sizes.

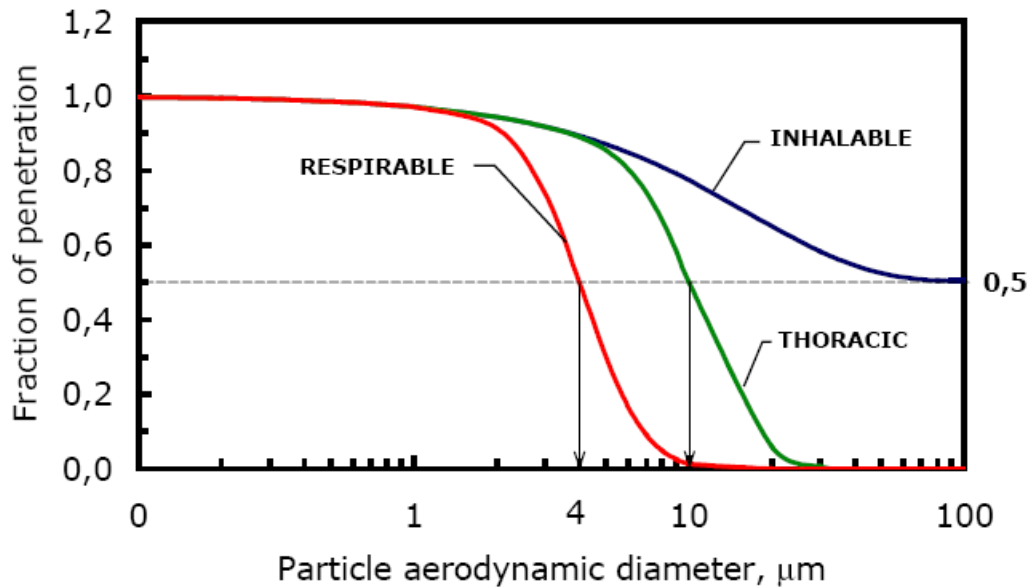


Figure 1.1 Probability of aerosol penetration as a function of aerodynamic diameter, internationally agreed by CEN/ISO/ACGIH.

Particle shape also influences particle toxicity. Particles from combustion sources tend to be spherical, while land material presents a granular shape. Long fibre particles, e.g. asbestos, are more difficult to clear from the lung than spherical particles (Champion and Mitragotri, 2006), which makes them of greater health concern.

Particle surface area is another important characteristic, especially of non-spherical particles. There are two definitions of particle surface: the *Brunauer, Emmett and Teller (BET) surface area* is related to the number of adsorption sites available on the particles (Gregg et al., 1995), and the *active surface* is a measure of the integral collision cross section of the particles (Baltensperger et al, 2001). That is, the actual surface that can adsorb or react with other compounds. Therefore, the larger the active surface the greater the potential toxic effects.

Particle charge is the result of the distribution of polar molecules at the surface of the particle. It depends on the original emission process, the ions present in the air, the length of the particle's suspension time, and the atmospheric humidity. Airborne particle charge gradually decreases from the time of emission, reaching a neutral state about 30 minutes after emission (Donaldson and Borm, 2007). Deposition of

inhaled particles may be significantly increased by the electrical charges on particles (Vincent, 1985).

More information about particle characteristics can be obtained from measurements of particle number, mass, or surface area as a function of the particle size, known as particle modes. The location of the modes, as a function of the size, are different when based on particle number, mass, or surface (Figure 1.2).

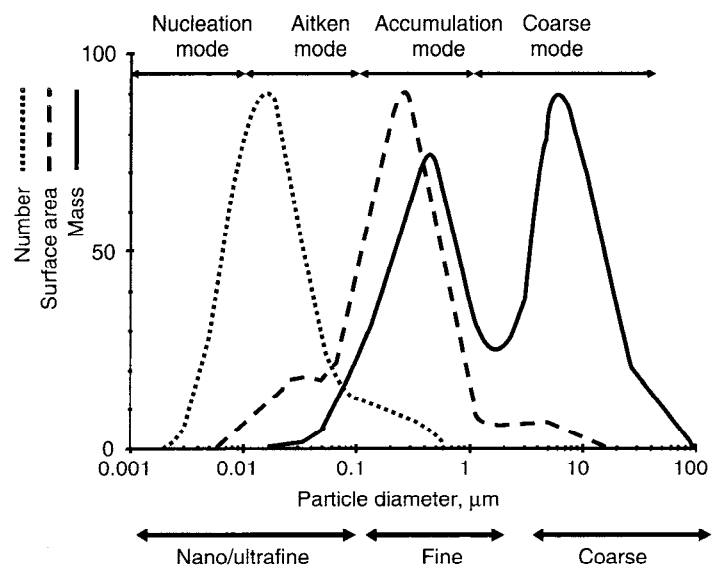


Figure 1.2 Particle size distributions as a function of the number, surface area, and mass (Donaldson & Borm, 2007).

The number distribution of urban particles is quite variable and depends on the proximity to source (Lingard, 2006) and type of source (Junker et al., 1999). The highest number of particles is located in the nucleation mode.

Most of the surface area is in particles between 0.1 and 0.5 μm . Thus, gas-to-particle processes occur mostly within this range.

The mass distribution of urban particles is characterized by two modes with a maximum in the accumulation range (0.1-1.0 μm), and another smaller peak in the nucleation mode (Whitby and Sverdrup, 1980). Particles larger than 1 μm are said to belong to the coarse mode and those smaller than 1 μm are said to belong to the fine

mode. The fine mode includes the accumulation and nuclei mode. The modes as a function of particle mass are described as follows:

Nucleation mode particles (0.005–100 nm) are produced by gas-to-particle conversion, as well as by combustion processes in which hot, supersaturated vapours are formed and undergo condensation. They also serve as nuclei for condensation of low-vapour-pressure gas-phase substances. Because of their small size, they account for only a few percentage of the mass. Their numbers rapidly diminish as they coagulate with each other to form larger particles (Shi et al., 2001). This mode is sub-divided into the nuclei mode (particles < 20 nm) and Aitken mode (particles between 20-100 nm) because of the different physico-chemical characteristics of particles in both size ranges.

Accumulation mode particles (0.1-1 μm) are formed by coagulation of particles in the nucleation mode and from condensation of vapours onto the surface of existing particles. Their rate of growth depends on the number of particles present and their velocity and surface area. Accumulation mode particles have longer atmospheric residence time than nucleation mode particles because removal by diffusion and sedimentation processes is very slow (Junker et al., 1999). In addition, coagulation of accumulation particles is a very slow process (Seinfeld and Pandis, 1998). Therefore, they can remain in the atmosphere for long periods and can travel long distances. They account for little of the particle numbers (0.1-10 %) though make up a great proportion of the aerosol mass (up to 90 %) (AQEG, 2005).

The coarse mode (> 1 μm) consists of particles generated by mechanical attrition processes and those formed by coagulation of accumulation particles or condensation of gases onto particles. When coarse particles exceed 2 μm in diameter they are efficiently removed from the atmosphere by sedimentation and impaction (Hinds, 1982). The boundaries for coarse particles are not very precise. When based on the mass mode coarse particles are referred to as those larger than 1 μm , whereas when the size distribution is not considered, coarse particles refers to those larger than 2.5 μm .

In summary, these distributions show that ultrafine particles ($< 0.1 \mu\text{m}$) are very abundant in terms of numbers, whereas the mass is concentrated in particles larger than $0.1 \mu\text{m}$. However, current legislation does not take into account the particle modes. As mentioned above, the parameters under regulation are PM_{10} and $\text{PM}_{2.5}$.

A major contributor to ultrafine particles in urban cities is vehicle exhaust, mostly from diesel engines (Kittelson, 1998). Non-exhaust emissions from vehicles contribute mostly to the coarse fraction ($> 10 \mu\text{m}$) (AQEG, 2005). However, a fraction is also emitted in the ultrafine size because of the large frictional heat on tyres and brakes (Luhana, 2004). Non-exhaust emissions are more difficult to estimate than those from the exhaust, since they depend on individual vehicle characteristics and operation. In the UK, it is estimated that 8 % of particles of $< 0.1 \mu\text{m}$ come from tyre and brake material (AQEG, 2005).

1.2.1.2 Chemical composition of particulate matter

The composition of airborne particles is very diverse and depends upon time and space (APEG, 1999). Major chemical components of particles include sulphates, nitrates, ammonium, sodium chloride (NaCl), elemental and organic carbon, mineral particles, and coarse, iron-rich particles generated by vehicles (APEG, 1999). Chemically bound water is also present.

Figure 1.3 shows typical composition of PM_{10} found in the UK atmosphere at background and roadside sites.

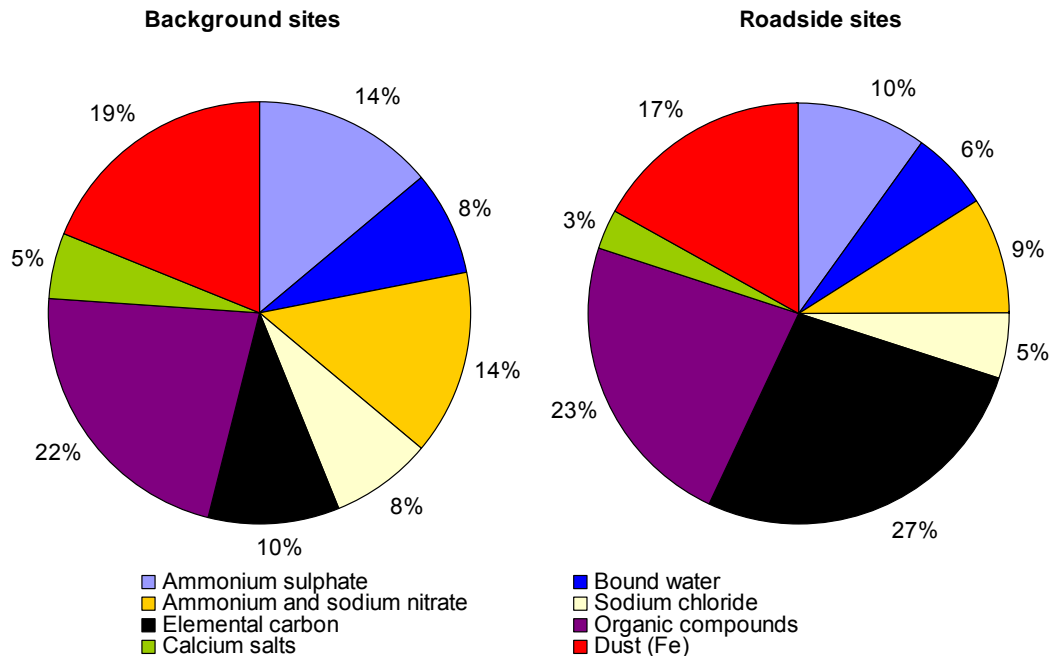


Figure 1.3 Composition of PM₁₀ in the urban atmosphere. Mean values observed in London and Birmingham, 2000-2002. (Modified from Harrison, 2003a).

The concentrations of EC and OC are much higher at sites close to traffic emissions than at background sites.

Sulphates ((NH₄)₂ SO₄), nitrates (NH₄NO₃) and sea salt (NaCl) absorb water vapour from the atmosphere, above a relative humidity (RH) point known as the deliquescence value, which usually exceeds 70 % (Seinfeld and Pandis, 1998). Some of this water can be retained when particles are sampled and weighed for mass concentration (Price, 2003). The precise amount of water quantified in a PM sample depends on its composition and the RH it experiences prior to weighing in the laboratory. It is important to note that although these compounds begin to lose water gradually upon a reduction in RH, they lose it all when exposed to a RH far below the deliquescence value (Seinfeld and Pandis, 1998).

Particle composition also varies with particle size, because of the differences in the particle formation processes. For example, EC and PAHs tend to be abundant in the fine fraction (< 2.5 μm) since they are formed in high temperature combustion processes (Harrison et al., 2003a), whereas silicon, from the resuspension of soils and surface dusts, is normally found in coarse particles (>2.5 μm) (AQEG, 2005).

Metals from combustion sources (Ni, Cd, Cr, Pb, Mn) are also found mainly in the fine fraction, whereas metals from soil resuspension (e.g. Fe and Mn) and abrasion of vehicle tyres and brakes (Zn, Cu, Fe) are more abundant in the coarse fraction, (Voutsas and Samara, 2002; Harrison et al., 2003b).

Metals bound to particles derived from vehicle exhaust emissions have been shown to have a higher solubility in water than those from industrially derived particles (Voutsas and Samara, 2002; Fernández Espinosa et al., 2002; Kyotani et al., 2002); with a higher proportion of water-soluble metals in PM_{2.5} than in PM₁₀ (Kyotani and Iwatsuki, 2002; Heal et al., 2005).

Metals from fly ash are usually in an insoluble oxide form (Fe₂O₃, Fe₃O₄, and CuO). However Fe (II), in the presence of acidic water droplets, can react with nitrates, sulphates, oxalate and humic-like substances in the atmosphere to form soluble compounds (Schroeder et al., 1987). Waste incinerators also contribute to metal concentrations with large amounts of soluble Zn, Cd and Pb (Germani and Zoller, 1994).

PAHs are emitted from the incomplete combustion of fossil fuel, power generation and wood burning processes (Bjorseth, 1985). PAHs from vehicle exhaust come from the fuel PAHs that survive combustion, and are also formed in chemical reactions of non-PAH fuel components. Lubricating oil in the engine may also contribute to the exhaust components (WHO, 2005). The USEPA (ATSDR, 2005) has listed 16 PAHs as priority pollutants based on toxicity, potential for human exposure, frequency of occurrence at hazardous waste sites, and the extent of information available: fluorene, phenanthrene, anthracene, fluoranthene, naphthalene, acenaphthene, acenaphthylene, chrysene, benzo[g,h,i]perylene, benzo[k]fluoranthene, benzo[a]pyrene, benzo[a]anthracene, dibenzo[a,h]anthracene, benzo[b]fluoranthene and pyrene.

PAHs with two or three aromatic rings are mainly released in the gas phase, while PAHs containing three or more aromatic rings (e.g. benzo[a]pyrene) are generally in the particulate phase, adsorbed onto the respirable fraction (PM₄) of airborne

particles (Li et al., 2003a). The half-life of low molecular weight PAHs is in the order of a few days, though it can be longer for high molecular weight PAHs adsorbed onto PM (Mumtaz., 1996). During their existence in the atmosphere, all but the most inert PAHs are likely to participate in complex homogeneous and heterogeneous chemical and photochemical reactions. These processes can transform PAHs into other species, which may have very different physical, chemical, and toxic characteristics. For example, pyrene, a non-toxic, and non-carcinogenic PAH, can react with NO_x and nitric acid in the air to yield various nitro-pyrenes. These are highly potent mutagens (Heflich et al., 1985).

Diesel vehicles emit mostly low molecular weight PAHs including fluorene, phenanthrene and naphthalene whereas gasoline engine vehicles emit higher molecular weight PAHs including benzo[a]pyrene and dibenzo[a,h]anthracene (Junker et al., 2000). Size distribution analysis of PAHs has shown that they are mostly absorbed on particles of around 100 nm in diameter (Miguel et al., 1998). The estimated contribution of road transport to the total PAH emissions in the UK was 64 % in 2005 (NAEI, 2007).

Carbonaceous material is a by-product of the combustion of liquid and gaseous fuel. It consists of aggregated spherules of highly structured graphite (EC) and amorphous carbon structures (OC) (Seinfeld and Pandis, 1998). Both forms are known simply as soot. Soot, as well as carbon, also contains 1-3 % hydrogen and 5-10 % oxygen, the latter due to partial surface oxidation (Seinfeld and Pandis, 1998).

EC consists of layers of carbon arranged in the hexagonal structure of graphite. EC has high adsorptive properties, which make it a carrier for harmful substances, including high molecular weight non-volatile compounds (Seinfeld and Pandis, 1998). EC is also called BC, and it is the component mostly responsible for the light absorbing characteristics of PM (Horvath, 1983). Measurements inside tunnels have found that over 85 % of the EC emitted by vehicles is in particles below 0.2 μm (Venkataraman and Friedlander, 1994).

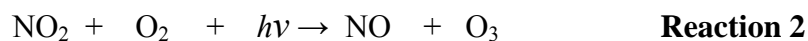
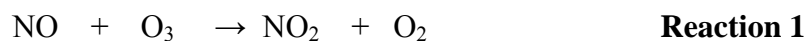
OC consists of hundreds, possibly thousands, of separate compounds that contain more than 20 carbon atoms and includes some compounds with potentially carcinogenic effects, such as PAHs, polychlorinated biphenyls (PCBs), benzene, toluene, ethylbenzene and m/p- and o-xylenes, the (the last four are referred to collectively as BTEX) (Seinfeld and Pandis, 1998).

1.2.2 Nitrogen oxides

Nitrogen oxides are a gaseous mixture of nitrogen dioxide (NO₂) and nitrogen monoxide (NO) collectively referred as NO_x. Other nitrogen oxides (generally present at lower concentrations) include NO₃, N₂O₃ and N₂O₄.

NO is formed from the oxidation of atmospheric nitrogen (N₂) during high temperature combustion processes. Further oxidation of NO by O₃ leads to the formation of NO₂ (secondary NO₂) (Reaction 1). However, NO₂ is also formed directly by diesel vehicles (mainly when moving slowly) (AQEG, 2004). This is known as primary NO₂. Since 1998, primary emissions of NO₂ have increased in the UK because of an increase in diesel vehicles, implementation of particle traps in buses and increasing background O₃ (AQEG, 2007). Carslaw and Beevers (2005) found that a significant amount of the variation observed between NO₂ concentrations at monitoring sites in London was the result of varying amounts of primary NO₂ being emitted by road vehicles, and not differences in secondary NO₂ emissions.

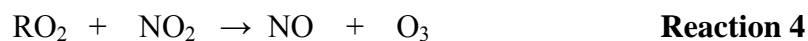
A photochemical equilibrium between NO and NO₂ results from the following reactions:



Hence, formation of NO₂ depends on the amount of O₃ and visible light. The minimum lifetime of individual NO₂ molecules under summertime conditions in the

UK is in the order of 100 seconds, with a mean daylight lifetime of 3 minutes. In winter, this is typically longer by a factor of two or three (AQEG, 2004).

NO₂ can also be formed by reaction of NO with O₂. However, the reaction time constant depends on the square of NO concentration, resulting in a very slow process only important during some episodes of winter smog, where NO concentrations tend to be very high. Therefore, NO and O₃ are usually considered as the limiting factors for NO₂ formation. Close to the emission source, NO is in large excess and the availability of O₃ limits the quantity of NO₂ that can be produced by this reaction (Kirby et al., 2000). At locations far from traffic emissions, those with low NO concentrations, O₃ is present in excess. At intermediate locations where neither NO nor O₃ is in large excess, Reaction 1 progressively depletes both NO and O₃ and the reaction time constant can become very long. For example an air mass containing 15 ppb of both pollutants (approximately 30 µg m⁻³ of NO and O₃) typically requires 30 minutes for 90 % conversion of NO (or O₃) to NO₂ by Reaction 1 (AQEG, 2004). However, the presence of Volatile Organic Compounds (VOCs) influences the photochemical equilibrium, with net production of O₃ through the following reactions:



Where, HO₂ are peroxy radicals and RO₂ are organic compounds containing oxygen. For reactions 3 and 4 to contribute significantly to NO and NO₂ formation, high concentrations of HO₂ are needed to initiate the process.

Other reactions of RO₂ with NO₂ lead to the production of unstable organic peroxy nitrates. The simplest example of this class of compound is peroxy acetyl nitrate (PAN), a contributor to photochemical smog. These compounds act as long-range carriers of NO_x and contribute to measurements of NO₂ made by chemiluminescent analysers (AQEG, 2004).

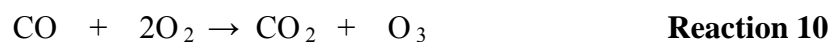
NO₂ emissions from road traffic was responsible for 34 % of the total emissions in the UK in 2005 (NAEI, 2007).

1.2.3 Ozone

Ground level ozone is not emitted directly into the atmosphere but is a secondary pollutant formed by complex photochemical reactions. These reactions involve VOCs (e.g. hydrocarbons and peroxy radical) and carbon monoxide. The reaction of VOCs and nitrogen oxides also produces O₃, as seen in Reaction 4. The reactions involved in the formation of O₃ from CO are shown below as described by Marston (1999):



The net effect is:



The reactions involving VOCs are more complex, but as for CO, the oxidation of NO to NO₂ is the step, which leads to O₃ formation. O₃ is removed by reaction with NO (Reaction 1). Therefore in areas with little traffic influence, where NO_x and CO are not abundant, O₃ concentration may be higher than in urban polluted locations.

Since O₃ formation requires the presence of sunlight, measurements of O₃ concentration display strong seasonal and diurnal patterns, with higher

concentrations in summer. O₃ can be transported over distances of hundreds or even thousands of kilometres and is regarded as a regional air pollution problem (WHO, 2003).

1.2.4 Carbon monoxide

Carbon monoxide (CO) is a by-product of the incomplete combustion of hydrocarbons. In combustion chambers with high temperature and O₂ supply, the combustion product of hydrocarbons is CO₂. However, in vehicle engines, the combustion of the fuel-air mixture is incomplete, leading to CO. Exhaust concentrations of carbon monoxide increase with lower (richer) air-to-fuel ratios and decrease with higher ratios. Improvements in engine design and changes in engine operating conditions as well as implementation of catalytic converters to trap CO (and also NO and hydrocarbons) have contributed to reduce CO emissions (NAEI, 2007).

CO is very stable in air with a lifetime of 30 to 90 days prior to its eventual oxidation to carbon dioxide (CO₂) (Seinfeld and Pandis 1998). Road transport is the main source of CO, accounting for 47 % of total emissions in the UK in 2005 (NAEI, 2007). The combustion of coal, wood and organic matter, for example in incinerators, also contributes to CO levels.

1.2.5 Sulphur dioxide

Sulphur dioxide (SO₂) is an acidic gas, soluble in water. SO₂ is oxidised by hydroxide radical to sulphuric acid, contributing to the formation and growth of new particles (Jeong et al., 2006).

SO₂ in vehicle exhausts comes from the incomplete combustion of sulphur in the fuel. Therefore, the amount of SO₂ released depends on the type of fuel used. The reduction of sulphur in fuel has significantly reduced the SO₂ emissions caused by road transport (NAEI, 2007).

1.2.6 Hydrocarbons

Hydrocarbons are compounds consisting of a structure of carbon and hydrogen without a functional group, ranging from simple methane (CH₄) to combinations of 19 or more carbon atoms. The most important hydrocarbons in relation to human health are 1,3-butadiene and BTEX (Fernández-Martínez et al., 2001). Road transport was the main source of 1,3-butadiene and benzene in the UK in 2005 (NAEI, 2007). There are two types of emissions: combustion derived and fuel derived (unburned fuel). Ethylbenzene, m/p-xylene and o-xylene have been identified as fuel derived hydrocarbons, whereas benzene and toluene have been found to be produced from both categories (Field et al., 1992).

Hydrocarbons play a significant role in particle formation (Reisell et al., 2003) and, in the presence of NO_x, they react with OH radicals to form O₃ thus modifying the oxidizing capacity of the atmosphere (Atkinson, 2000; Monod, 2001).

Benzene is the most stable of the BTEX group, with a lifetime of 9.4 days, while xylenes are the most unstable with estimated atmospheric lifetimes of 11.8, 19.4 and 20.3 hours for m-xylene, p-xylene and o-xylene, respectively (assuming an OH radical concentration of 10⁶ radical cm⁻³) (Monod, 2001). The lifetime of ethylbenzene is 1.6 days (assuming an OH radical concentration of 10⁶ radical cm⁻³) (Monod, 2001).

BTEX are also emitted from other fossil fuel-burning including power plants, chemical plants and petroleum refineries as well as vegetation (Fernández-Martínez et al., 2001).

1.2.7 Diesel exhaust

Diesel exhaust is a complex mixture of gaseous and particulate components, each of which comprises thousands of different substances. The gaseous fraction consists primarily of carbon dioxide, carbon monoxide, nitric oxide, nitrogen dioxide and to a lesser extent, sulphur oxides, aldehydes, ammonia and hydrocarbons, including benzene, 1,3-butadiene, PAHs and nitro-PAHs (IPCS, 1996).

The particulate fraction consists of conglomerates of carbonaceous material with organic and inorganic compounds adsorbed to its surface (IPCS, 1996). Particles start forming in the engine cylinder, at temperatures of 1000 to 2800 K. Vapours, including PAHs, condense onto carbonaceous material and form the first spherules. Particle growth occurs through coagulation and further condensation of vapours. Particles are released as conglomerates of 14-40 nm in diameter. When they leave the engine cylinder, the temperature drops to 800 K and particles grow by further adsorption of high molecular weight organic compounds and metallic ash to form agglomerates of 60-100 nm (AQEG, 2005). These are known as primary emitted accumulation particles.

Besides these primary emitted accumulation particles, nucleation particles are formed by condensation of the exhaust vapours during post-emission cooling and dilution (Charron and Harrison, 2003). Figure 1.4 shows a schematic representation of diesel particles. The properties of the diesel fuel (density, distillation temperature, sulphur and PAH content) have a considerable influence on emitted particle mass and their organic and elemental carbon content (WHO, 2005; Sandip et al., 2004).

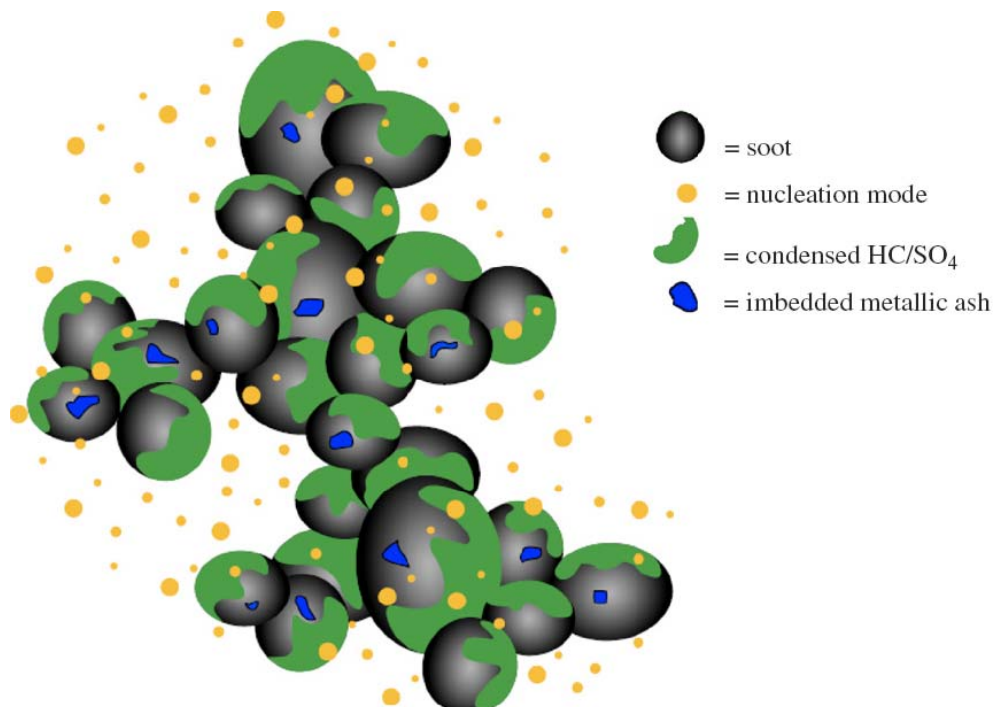


Figure 1.4 Schematic representation of diesel exhaust particles (Matti Maricq, 2007).

Typically, diesel particles have a total mass composition of 25-60 % EC (Seigneur et al., 2003) and 20-50 % OC (Shi et al., 2000). Sulphate and nitrate may account for up to 12 % and 4 % mass, respectively (Shi et al., 2000). PAHs and metals account for less than 2 % of the mass (ICPS, 1996). The following metals have been detected in diesel exhaust: Ba, Ca, Cr, Cu, Fe, Pb, Mn, Ni, P, Na, Si and Zn (ICPS, 1996).

Light diesel engines found in automobiles and light trucks emit less CO than gasoline engines (APEG, 1999), though they emit higher concentrations of PM (AQEG, 2005) and nitrogen oxides (Ono-Ogasawara and Smith, 2004). PM emissions have been reduced due to the use of filter traps. However, there is evidence to suggest that these filters produce primary NO₂ since they use NO to oxidise particles (Carslaw and Beevers, 2005).

Diesel engine exhaust is classified as a “probably carcinogenic pollutant to humans” by the International Agency for Research on Cancer (IARC, 1989), the Health Effects Institute (HEI, 1995), the World Health Organisation (WHO, 1996) and the US Environmental Protection Agency (USEPA, 2002).

1.3 HAZARDS FROM TRAFFIC-RELATED AIR POLLUTANTS

This section provides an overview of current understanding of the potential effects of PM, NO₂, CO, SO₂ and O₃ on human health. The focus of this review is on the biological mechanisms that trigger the observed health effects. Emphasis has been put on studies that have examined which pollutant or pollutant metrics are more responsible for the observed health effects.

Most of the current understanding is based on experiments using animals and cell-cultures. Human exposure studies are fewer in number and the exposure periods are limited. In addition, most of the reviewed studies used pollutant concentrations much higher than those found in ambient air, and therefore unrepresentative of typical exposure scenarios. Despite these limitations, information from toxicological studies is fundamental to aid the understanding of the separate and combined effects of air pollutants and the exposure-response relationship.

1.3.1 Particulate matter

Toxicological studies in humans and animals have shown that PM can attack the functioning of the lungs, the blood vessels, and the heart (Seaton et al., 1995, Van Eeden et al., 2005). The heterogeneous and chemically complex nature of PM makes it difficult to identify which individual components and/or physical parameters are responsible for causing the adverse effects or whether it is a combination of these (Brunekreef and Holgate, 2002).

The aerodynamic diameter of particles is one of the key characteristics influencing their deposition in the respiratory tract (Zielinski et al., 1998; McClellan et al., 2000). Once inhaled, particles greater than 10 μm are expelled through the nose and pharynx. Smaller particles deposited in the larynx and trachea (2.5-10 μm) and bronchioles (< 2.5 μm) are expelled by the action of ciliated cells with mucus or by coughing (Zielinski et al., 1998). In contrast, particles deposited in the alveoli (< 0.1 μm) are not subject to the action of ciliated cells. The alveoli do not consist of ciliated cells but of Type I epithelial cells, designed for gaseous exchange, and Type II epithelial cells, which reduce alveolar surface tension and also participate in defence functions (Donaldson and Borm, 2007). Therefore, particles that reach the alveolar region are cleared by specialised defence cells called macrophages, which remove exogenous substances towards ciliated airways or into the lymphatic system (McClellan, 2000). However, water- and lipid-soluble particle compounds can be dissolved into lining fluids and gain access to the blood system, where they can be transported to any organ (AIRNET, 2004).

Clearance of particles deposited in the larynx and alveoli by mucociliary transport and macrophages is estimated to be complete within 24 hours (Donaldson and Borm, 2007). However, ultrafine particles (< 100 nm) can be retained for longer periods (Wiebert et al., 2006) since macrophages are less efficient at removing particles of this size (Seaton et al., 1995). Furthermore, ultrafine particles can reduce the ability of macrophages to remove other particles, which increases the risk of inflammation (Donaldson et al., 2002). This removal mechanism may be impaired in children, the elderly, and individuals with respiratory illnesses (AIRNET, 2004).

When macrophages take in a pathogenic substance they activate the expression of pro-inflammatory mediators (cytokines), including Tumour Necrosis Factor- α (TNF- α) and interleukin-6 (IL-6) to recruit more defence cells (neutrophils and more macrophages) to the lungs (Donaldson et al., 2002 ; Jiménez et al., 2002; Brown et al., 2004). Brown et al. (2004) demonstrated that the activation of pro-inflammatory transcription factors in macrophages, including the transcription nuclear factor kappa (NF- κ) occurs via a Ca^{2+} influx across the plasma membrane.

Particles and macrophages interact with epithelial cells. Particles can damage Type I epithelial cells, which are replaced by Type II that later on differentiate to Type I. An increase in the cell proliferation rate increases the possibility that mutations remain uncorrected, thus becoming permanent (Donaldson and Borm, 2007). The interaction of macrophages with Type II epithelial cells results in an upregulation of the Inter-Cellular Adhesion Molecule 1 (ICAM-1), which recruits leukocytes (Brown et al., 2007). Additionally, Type II epithelial cells also activate the expression of pro-inflammatory mediators, including IL-8 and TNF- α which are regulated by the transcription nuclear factor kappa B NF- κ B (Schins et al., 2000). However, only a few studies have been able to demonstrate this *in vitro*, because the surface of particles adsorbs these pro-inflammatory mediators resulting in an underestimation of the amount produced (Seagrave et al., 2004; Veranth et al., 2007).

PM also triggers inflammation through the production of reactive oxygen species (ROS). PM participate in redox chemistry, in which the particles accept electrons from reducing agents and pass them on to O_2 molecules to generate ROS (Li et al., 2003a; Pourazar et al., 2005; Risom et al., 2005). ROS are generated in organisms in response to exogenous exposures, including cigarette smoke and O_3 . However, if ROS are produced in large concentrations a state of oxidative stress occurs as an exacerbation of the organism's response to these exogenous substances. ROS are released by defence cells (macrophages, leukocytes) during phagocytosis and also directly by some particle components, including the transition metal ions Cu^{2+} , Cr^{3+} , Cr^{4+} , Fe^{3+} , V^{3+} , V^{5+} (Donaldson and Borm, 2007). ROS are prone to react and inhibit functioning of proteins and lipids (AIRNET 2004). ROS also react with DNA, and

therefore ROS are potential inducers of cancer (Upadhyay et al., 2003; Risom et al., 2005). Additionally, oxidative stress initiates an intracellular signalling cascade involving the activation of phosphatase and kinase enzymes as well as NF- κ B (Jiménez et al., 2000; Pourazar et al., 2005) which, as mentioned above, increases the expression of pro-inflammatory mediators.

Figure 1.5 shows a diagram of the signalling pathways triggered by PM.

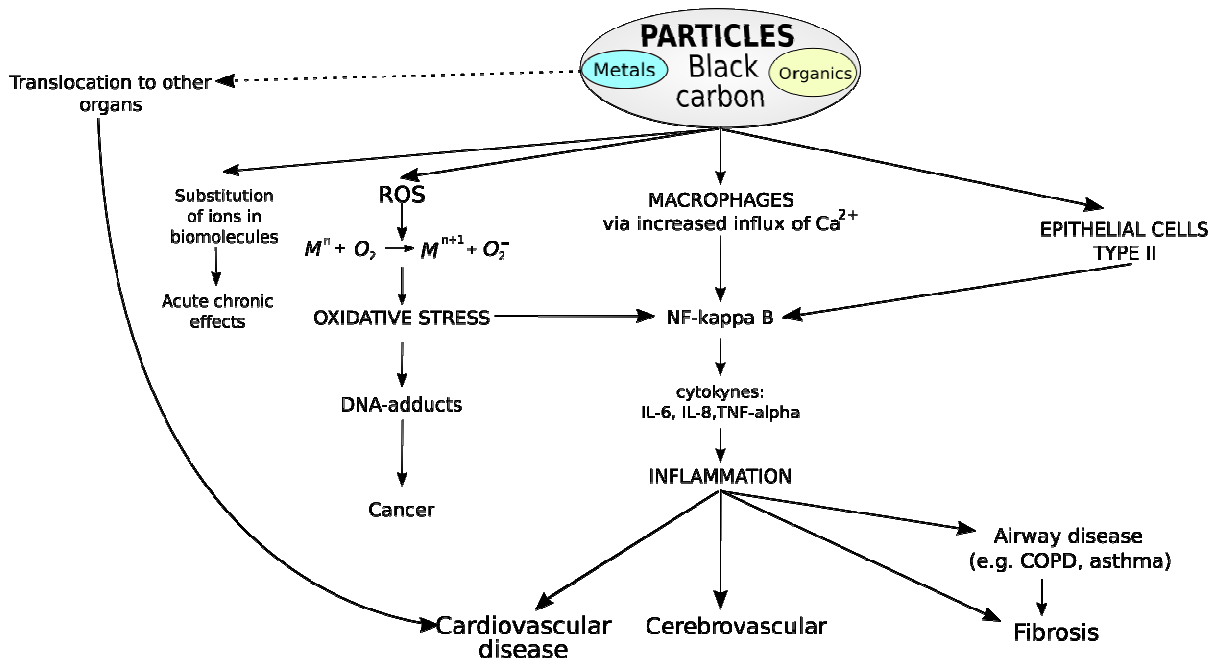


Figure 1.5 Signalling effects of particles known to lead to adverse health effects. Mn: Cu^{2+} , Cr^{3+} , Cr^{4+} , Fe^{3+} , V^{3+} , V^{5+} . Dashed line: animal data only. (From Donaldson & Borm, 2007).

A prolonged inflammatory state can result in heart attack, stroke, age related disorders (Buschini et al., 2001; Valko et al., 2006), lung inflammation (which exacerbates Chronic Obstructive Pulmonary Disease, COPD), and cystic fibrosis (Seaton et al., 1995; Brown et al., 1996; Heunks et al., 2000). Oxidative stress has also been linked with asthma exacerbation (Li et al. 2003b) and cerebrovascular effects (Thomson et al, 2007).

Some antioxidants, such as glutathione (GSH), and N-acetylcysteine have the ability to block the release of pro-inflammatory mediators (Rahman and Macnee, 2000; Dick et al., 2003). Behndig et al. (2006) in an experiment with human subjects exposed to diesel exhaust ($100 \mu g m^{-3}$ PM_{10} , 10.4 ppm CO, 1.3 ppm NO, 0.4 ppm

NO₂ and 1.3 ppm hydrocarbons) concluded that diesel exhaust causes bronchial inflammation, but suggest that the movement of glutathione (GSH) and urate onto the lung surface protects against inflammation in the alveolar region.

A key question is whether inflammation is mediated by the physical properties of the particles (small size and high surface area), the carbonaceous material, adsorbed compounds on the particle surface (e.g. transition metal, and organic compounds) or a combination of these.

Experimental studies have shown that UFPs have greater toxic effects: their larger surface area, which acts as a catalytic surface for ROS formation; their high concentration of toxic chemical compounds and their ability to translocate to other organs have been suggested as the factors behind their greater toxicity when compared with larger size fractions.

Brown et al. (2001) found that ultrafine polystyrene particles (65 nm) produced greater inflammation in rat lungs than fine polystyrene particles (232 and 535 nm), suggesting the parameter driving toxicity was the large surface area. In a follow-up study, Donaldson et al. (2002) observed that inflammation was independent of the release of transition metals from ultrafine BC.

In vitro studies using human cells have shown similar results. Monteiller et al. (2007) showed larger pro-inflammatory effects for TiO₂ and BC UFPs than for the same mass dose of fine particles in human alveolar cells, suggesting the importance of particle surface area on inflammation.

In contrast, other studies have attributed the greater inflammogenic effects of UFPs to their higher content of toxic compounds rather than to their higher surface area. Shi et al. (2003) found higher hydroxyl radical production in water suspensions of ambient PM₁, when compared to PM_{2.5} and PM₁₀. PM₁ was the size fraction with the highest metal content (Fe and Cu). Furthermore, Shi et al. (2003) and Baulig et al. (2004) found that the higher hydroxyl radical production was correlated with the Fe and Cu content. However, when human bronchial epithelial cells were exposed to

PM_{2.5} samples with different metal and PAH content, they exhibited similar levels of cytotoxicity, intracellular ROS production, and proinflammatory cytokine release (granulocyte macrophage colony-stimulating factor, GM-CSF, and TNF- α) (Baulig et al., 2004). Baulig et al. suggested that the absence of an apparent particle composition effect might have been the result of the lack of sensitivity of the biomarkers used, components' bioavailability and/or the possible particle-metal interactions. Xia et al. (2004) also found that aliphatic, aromatic and polar organic compounds, fractionated from diesel exhaust, and ambient UFPs induced mitochondrial perturbation (including an increase in the superoxide radical O_2^-) in mouse cells, but polystyrene nanoparticles (< 100 nm) did not, suggesting that the toxic effect of particles was due to adsorbed chemical components. Gerlofs-Niland et al. (2007) exposed rats to PM_{2.5-10} and PM_{0.1-2.5} from different sites across EU, via tracheal instillation. Samples from high-traffic sites showed higher toxicity than those less influenced by traffic. The authors argued as possible reasons the higher concentration of Ba, Zn and K in the samples from the high-traffic sites.

Kunzli et al. (2006) examined the correlation between the oxidative properties of PM_{2.5} collected at several locations in EU and their characteristics (PM_{2.5} mass, absorbance and mass concentration of chemical components: S, Si, Al, Fe, Zn, Pb and Cu). None of the characteristics served as a surrogate for the annual mean redox activity of PM_{2.5}. The redox activity changed both temporally at each sampling site and regionally between cities.

Investigations in animal studies have suggested the occurrence of translocation of UFP from the lungs to other organs. Nemmar et al. (2001) observed passage of UFPs into the blood circulation of hamsters after 30 minutes of instillation, which leads to thrombus formation in peripheral veins and arteries. Oberdörster et al. (2002) reported translocation of UFPs to the liver 1 day after rats were exposed to ultrafine carbon and to the brain in a follow-up study (Oberdörster et al., 2004). Experiments in humans have shown a mass fraction of translocated particles no greater than 1 % of the dose delivered (Donaldson and Borm, 2007). These results add very valuable information. However, some issues are still under debate including the transport

mechanisms, the characteristics of the particles able to translocate (mainly size and charge) and the fraction of particles translocated in relation to the total delivered dose.

The carbonaceous core of particles (as opposed to the extractable components adsorbed onto a particle's surface) has also been associated with inflammation of the lung. Yanagisawa et al. (2003) found that the residual carbonaceous nuclei of diesel particles contributed to the aggravation of lung inflammation in mice. In a similar experiment, Pan et al. (2004) showed that washed PM (PM residue after extraction with organic and acid solvents) could still generate ROS in a buffer solution.

According to these findings, the main factors contributing to the toxicity of ultrafine particles are their larger surface area, their larger concentration of toxic chemical compounds, and their ability to pass the epithelial lining layer into the blood system. However, it seems that each factor exerts its toxicity through a different mechanism. Therefore, a single bioassay is not enough to assess the toxicity of particles (Steenenberg et al., 2006).

Despite these unresolved questions, these findings explain the higher toxicity of diesel particles compared with those from other sources. Diesel particles are in the ultrafine fraction, and have a high content of adsorbed toxic compounds (including organic compounds, PAHs and metals). Both of these factors are related to toxic effects on human health.

The EU project "Respiratory Allergy and Inflammation due to Ambient Particles" (RAIAP) clustered the chemical constituents of PM according to the biological response they provoked. Respiratory allergy in animal models was related to particles originating from traffic, industrial combustion, incinerators and coal and wood smoke. Pro-inflammatory responses were associated with crustal material and sea spray. Secondary inorganic aerosols and long-range transport aerosols were related to systemic allergy (Steenenberg et al., 2006).

Experiments in humans have confirmed the hypothesis that particles can generate a systemic inflammatory response both in the airways and in the circulatory system involving different cell types (Salvi et al., 1999, 2000; Guio et al. 2000; Stenfors et al., 2004; Tornqvist et al., 2007). Thus confirming the findings of the *in vitro* and animal studies mentioned earlier. However, in all reviewed human studies, such effects were noticed only at concentrations above $100 \mu\text{g m}^{-3}$. These concentrations may be found at “hot spots” (e.g. street canyons, tunnels) in urban cities, but are well above the EU Air Quality limit value ($40 \mu\text{g m}^{-3}$).

Ghio et al. (2000) exposed healthy individuals to ambient $\text{PM}_{0.1-2.5}$ ($23-311 \mu\text{g m}^{-3}$) for 2 hours. Eighteen hours after exposure, individuals showed mild inflammation (measured as an increase in neutrophils) in bronchial and alveolar cells, although no effects on lung function were observed. An increase in levels of the blood clotting protein fibrinogen, related to heart attacks, was also reported. Tornqvist et al. (2007) reported impairment in the vasodilatation system 18 hours after a group of healthy individuals were exposed to $300 \mu\text{g m}^{-3}$ of PM_{10} from diesel exhaust. Salvi et al. (1999, 2000) reported increases in neutrophil and platelet levels in peripheral blood after 1 hour of exposure to diesel exhaust ($300 \mu\text{g m}^{-3}$ PM_{10} , 2 ppm of NO_2 , 4.46 ppm of NO, 7.5 ppm of CO, 4.3 ppm of total hydrocarbons and $4.3 \cdot 10^6$ particles cm^{-3}) in healthy individuals.

Studies of human subjects have also reported asthma exacerbation after exposure to diesel exhaust. Stenfors et al. (2004) found an increase in IL-10 (a protein associated with airway inflammation and asthma) in a group of asthmatic individuals exposed to $108 \mu\text{g m}^{-3}$ PM_{10} for 6 hours. Healthy individuals exposed to the same conditions exhibited an increase of IL-8 and neutrophils, these are related to inflammation but not asthma. Nordenhäll et al. (2001) reported bronchial hyperresponsiveness (a marker of asthma) and increases in both airway resistance and IL-6, but not IL-8, one day after a group of asthmatic individuals were exposed for 1 hour to $300 \mu\text{g m}^{-3}$ PM_{10} from diesel exhaust.

Individual differences in the toxic effects of exposure to different particle sizes have been reported: Peters et al. (1997) examined the effect of PM on peak expiratory

flow rate (PEFR, a measure of airway obstruction), finding larger effects for PM₁ compared to PM₁₀.

1.3.2 Polycyclic Aromatic Hydrocarbons

PAHs' toxicity relates to their ability to dissolve in epithelium lining fluids. This results in their selective retention in the trachea and bronchial regions of the respiratory tract (AIRNET, 2004). Two approaches have been used to predict the toxicity of the PAH mixture. The first uses benzo[a]pyrene concentration, one of the most potently carcinogenic PAHs, as a measure of the dose of the PAH mixture. This approach assumes a constant PAH composition throughout a mixture. Concerns have been raised about this approach due to the variable composition (and therefore carcinogenicity) of PAHs ambient samples (AIRNET, 2004). The second approach uses the sum of different PAH concentrations weighted for their carcinogenic potency relative to that of benzo[a]pyrene, using the list developed by Nisbet and Lagoy (1992). Neither of the above approaches takes into account potential interactions between mixture components (AIRNET, 2004).

PAHs do not have intrinsic redox activity, although they can undergo transformations to become chemically active compounds that can then induce ROS generation (Penttinen et al., 2001; Shi et al., 2003; Baulig et al., 2003, Risom et al., 2005). PAHs can also bind covalently to DNA, forming these DNA adducts is what makes them potential inducers of cancer (Castaño-Vinyals et al., 2004; Kok et al., 2005; Rossner Jr. et al., 2007). They also stimulate alveolar macrophages and epithelial cells to release pro-inflammatory mediators (Kawasaki et al., 2001; Li et al., 2003a; Vogel et al., 2005). The mediators recruit defence cells which PAHs also have direct effects upon (Donalson and Borm, 2007). In this way, PAHs can induce respiratory and cardiovascular disease. Some studies have suggested PAHs can induce immunoglobulin-E and histamine production. These two species are implicated in the development of allergy and chronic asthma (Tsien et al., 1997; Schober et al., 2007).

Most of these studies have used organic solvents to extract the PAHs adsorbed onto PM, instead of fluids simulating the lining layer of the lung. Some authors have therefore argued that the amount of bioavailable PAHs would be too low to trigger the effects described earlier. For example, Buddingh et al. (1981) reported that only 0.005 % of the adsorbed benzo[a]pyrene content (as determined by Soxhlet extraction in toluene) was eluted in human plasma, swine serum, swine lung homogenate and swine lung washings. In contrast, Gerde et al. (2001) found that 1 hour after dogs inhaled benzo[a]pyrene adsorbed on the carbonaceous core of diesel soot, the adsorbed benzo[a]pyrene was mostly metabolized into conjugated phase II metabolites.

Occupational exposure to particles containing PAHs has shown an elevated concentration of PAH-DNA adducts in the exposed human subjects, which may reflect the level of cancer risk (Castaño-Vinyals et al., 2004).

1.3.3 Metals

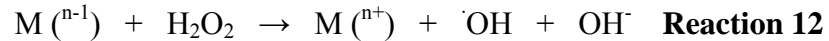
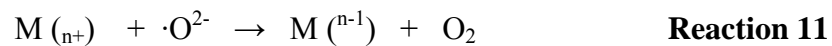
The potential toxicity of metals depends on their chemical form, oxidation state, affinity for metal protein chelators (e.g. transferrin, lactoferrin, ferritin and caeruloplasmin), tendency to bioaccumulate in the human body and the synergistic and antagonistic effects of metal combinations (Donaldson and Borm, 2007).

The solubility of the chemical form in which the metal is contained is fundamental in determining metal bioavailability and therefore toxicity. Metals in soluble chemical forms, such as sulphate, are released from particles in the form of ions, causing toxic effects, whereas metals in insoluble forms such as oxides tend to remain attached to the particle (Costa and Dreher, 1997). Exchangeable metals (those attached weakly to the particle surface) are also soluble in water (Fernández Espinosa, 2001).

The oxidation state of the metal plays an important role. Metals with more than one stable oxidation state can participate in electron transfer reactions and therefore possess the potential to generate oxidative stress (Lloyd et al., 1997). This includes the entire first row of transition metals in the periodic table, with the exception of Zn

(i.e. Sc, Ti, V, Cr, Mn, Fe, Co and Cu). Metals with only one stable oxidation state, including Cd, Ni, Pb and Zn, can also cause oxidative stress to cells and tissues, this through depletion of glutathione and protein-bound sulphhydryl groups (Stohs and Bagchi., 1995).

Cu, Co, Cr, Fe, Mn, Ni, Zn and V, especially in their soluble forms, have been shown to generate Reactive Oxygen Species (ROS) (Pritchard et al. 1996; Carter et al. 1997; Donaldson et al., 1997; Frampton et al., 1999; Shi et al., 2003; Valavanidis et al., 2005). The process of radical formation by soluble metals involves redox cycling of the metal ions via the Fenton reaction (Lloyd et al., 1997). This reaction was first studied for Fe, however other metals can follow the same cycle (Stohs et al. 1995). The metal facilitates the conversion of a superoxide anion ($O_2^{\cdot-}$) (Reaction 5) and hydrogen peroxide (H_2O_2) to hydroxyl radical ($\cdot OH$) (Reaction 6). This species has been suggested to initiate lipid peroxidation (Lundborg et al., 2007) and can also attack DNA (Lloyd et al., 1997)



$M^{(n+)}$: Cu^{2+} , Cr^{3+} , Cr^{4+} , Fe^{3+} , V^{3+} , V^{5+} (Stohs et al., 1995; Lloyd et al., 1997)

$M^{(n-1)}$: Cu^+ , Cr^{2+} , Cr^{3+} , Fe^{2+} , V^{2+} , V^{4+}

The oxidation state of the metal plays an important role in the Fenton reaction (Reactions 5 and 6). Lloyd et al. (1997) found that the greatest DNA damage occurred in the presence of Cr^{3+} , Cu^{2+} , Fe^{2+} , V^{5+} ions.

Jiménez et al. (2000) conducted an *in vitro* study on alveolar epithelial cells and showed that the inflammatory response of PM_{10} was the result of the activation of the Nuclear Factor kappa B (NF- κ B) through a mechanism that involved Fe. Chen et al. (2001) proposed the following order of metal capacity to generate NF- κ B:

$Cu^{2+} = Co > As^{3+} = As^{5+} > V^{5+} > Cr^{6+} = Ni^{2+}$

Adamson et al. (2000) reported that soluble Zn was the metal responsible for producing lung inflammation and fibrosis in mouse lung cells, after instillation of atmospheric dust. They found that the effects were minimal when mice were injected with solutions containing Cu, Fe, Al, Pb, Mg, or Ni, but not Zn.

Insoluble metals have also been related to the generation of ROS (Ghio et al., 1999; Knaapen et al., 2002; Shi et al., 2003).

Furthermore, metals can bind to specific proteins, and be transported to specific organs, where they can substitute polyvalent cations, including Ca, Zn and Mg. For example, Pb^{2+} can substitute Ca^{2+} and Zn^{2+} . These interactions affect different biological processes, including metal transport, energy metabolism, apoptosis (cell death), enzymatic processes, protein maturation, and genetic regulation, (Garza et al., 2006).

These studies suggest that soluble metals pose a higher potential hazard for human health than insoluble metals. Taking this into consideration, in this study only the water-soluble fraction of metals attached to PM was assessed. The choice of water as extractant is discussed in Section 4.7.

1.3.4 Interactive effects between the components of PM₁₀

From the previous review, it is clear that transition metals, PAHs and carbon particles all produce an inflammatory response in the lung. However, very few studies have reported on the interactions between these components.

Wilson et al. (2002) found that the addition of iron salts to ultrafine particles enhanced the influx of neutrophils in rat lungs.

Benzo[a]pyrene adsorbed onto BC was found to induce a time-dependant production of TNF- α . This effect was not observed in the presence of either benzo[a]pyrene or BC alone (Chin et al., 1998). However, this finding contrasts with the results reported by Kawasaki et al. (2001) where benzo[a]pyrene extracted from diesel particles was found to mimic the effects of ultrafine diesel particles.

Kok et al. (2005) found a positive correlation between DNA-adduct formation and the interaction of PAHs with transition metals in PM₁₀ and PM_{2.5}.

Studies on the effects of metal interactions have shown that Fe and V reduced the inflammatory effect of Ni compared with Ni on its own: this is due to their interference with Ni redox cycling (Kodavanti et al., 1997; Shi et al., 2003). However, Ni enhanced the effects of V when both metals were inhaled by rats (Campen et al., 2001). V was also found to interfere with the divalent metal transporter (DMT1) involved in the removal of Fe from the lung epithelium (Ghio et al., 2005).

Insoluble particles can cause accumulation of Fe in cells. The disruption of the normal transport of Fe in cells affects multiple biological mechanisms and induces oxidative stress. This trapping of Fe ions by carbonaceous particles occurs because Fe³⁺ has a high affinity for oxygen-containing groups (e.g C=O, COOH, C-OH), which are very abundant on the surface of carbonaceous material.

1.3.5 Nitrogen dioxide

NO₂ is a highly oxidizing gas with low solubility in water that reacts with components in the lining fluid of the respiratory tract (AIRNET, 2004).

In vitro studies on lung epithelial cells have shown that the mechanism through which nitrogen dioxide affects human health is the formation of ROS that can cause damage or stress to cells leading to release of proinflammatory mediators (Jorres et al., 1995; Devlin et al., 1999; Bayram et al. 2001 and Frampton et al., 2002).

NO₂ also increases susceptibility to infection by viruses and bacteria. It interacts with macrophages, suppressing their capacity to deactivate viruses (Frampton et al., 1989) and with lymphocytes (Damji and Richters, 1989). Chauhan et al. (2003) reported that exposure to NO₂ in the week before the start of a respiratory viral infection, and at levels within current air quality standards, was associated with an increase in the severity of a resulting asthma exacerbation.

1.3.6 Ozone

O₃ is a powerful oxidant (more powerful than NO₂), with low solubility in water, which enables it to reach the alveolar region of the respiratory tract. Epidemiological studies have linked exposure to O₃ with respiratory symptoms including chronic cough (Mathieu-Nolf et al., 2002; Castillejos et al., 1992) and reduction in lung function (Brauer and Brook, 1997).

In vitro studies have shown that exposure to O₃ causes inflammation in bronchial and alveolar epithelial cells by increasing the release of cytokines and other pro-inflammatory mediators including IL-8, TNF- α , granulocyte monocyte colony stimulating factor (GM-CSF), InterICAM-1, and Regulated on Activation Normal T Cell Expressed and Secreted (RANTES) (Rusznak et al., 1996; Schierhorn et al., 1999; Bayram et al., 2001; Stenfors et al., 2002). Cells of asthmatic individuals were found to release greater concentrations of pro-inflammatory mediators than cells from non-asthmatic individuals (Bayram et al., 2001, Stenfors, et al., 2002).

Studies of repeated exposure to O₃ concentrations of 240 $\mu\text{g m}^{-3}$ (6.6 hours/day, for four days) in individuals with asthma and rhinitis indicated that persistent damage to lung cells is cumulative even though functional adaptation takes place (Holz et al., 2002).

O₃ has also been found to induce DNA damage via the production of hydroxyl radicals in experiments in aqueous solution (Ito et al., 2005).

Experiments in animals have shown that O₃ can modulate the expression of genes involved in vasoregulatory pathways in the brain, and therefore induce cerebrovascular effects (Thomson et al., 2007). Thomson et al. reported that the same effect caused by O₃ was also caused independently by PM, concluding that these effects were additive.

In these studies the exposure concentrations were higher than the European and UK limit value (120 $\mu\text{g m}^{-3}$ for 8 hours average, WHO, 2005), though similar to those

found in some EU countries in summer time (e.g. France registered peak concentrations of $417 \mu\text{g m}^{-3}$ in the summer of 2003, Vautard et al., 2005).

1.3.7 Carbon monoxide

CO diffuses rapidly across the respiratory tract reaching the alveoli and blood vessels (AIRNET, 2004). The toxicity of CO is due to the displacement of oxygen from haemoglobin, which leads to the formation of carboxyhaemoglobin (COHb). Consequently, the transport of oxygen to the tissues and organs decreases (Prockop and Chichkova, 2007). Formation of COHb is relatively fast because of haemoglobin's much higher affinity for CO compared to oxygen (210 times) (Prockop and Chichkova, 2007). COHb release depends on its concentration. A 50 % reduction in blood concentration may take between 4 and 6 hours (Prockop and Chichkova, 2007).

Studies on human subjects have shown symptoms at CO concentrations much higher than normal ambient levels. A group of susceptible individuals with angina pectoris experienced chest pain, due to narrowing of the heart vessels, at COHb concentrations of 2.5-3.0 %, levels that can be reached at ambient CO concentrations of 40 mg m^{-3} (AIRNET, 2004). However, this concentration is much higher than that found even at traffic "hot spots" such as tunnels ($20\text{-}30 \text{ mg m}^{-3}$) (Han and Naeher, 2006). Healthy adults have been found not to experience symptoms at concentrations below 5 % COHb (ICPS, 1999). However, concentrations between 5.1-8.2 % have resulted in damage to the nervous system (reduced co-ordination and driving ability, and impaired wakefulness) (Raub and Benignus, 2002). Headaches, weakness, fatigue, and sleepiness have been observed at COHb concentrations below 20 % (Abelsohn et al., 2002).

1.3.8 Sulphur dioxide

SO₂ can be inhaled as a gas or adsorbed onto the surface of particles. Inhaled SO₂ is dissolved in the fluid of the airways forming bisulphite and sulphite ions, which interact with nerve receptors in the trachea and bronchi causing airway narrowing

(AIRNET, 2004). SO₂ adsorbed onto particles can be transported up to the lungs (Mehlman et al., 1983).

Experiments in epithelial cells have found that exposure to SO₂ increased the levels of asthma-related genes. For example, Ruijin et al. (2007) observed a dose-dependant increase in epidermal growth factor receptor (EGF), ICAM-1, and cyclooxygenase-2 (COX-2), all of them related to asthma, in bronchial epithelial cells exposed to SO₂ and its derivatives (bisulphite and sulphite ions). These genes induced the generation of inflammatory repair molecules, which in high concentrations cause injury to the airway epithelium. Ruijin et al. suggested that repeated cycles of lung injury followed by repair might cause cell proliferation and differentiation and that this could be the cause of the structural changes in lung function. Winterton et al. (2001) found an increase in TNF- α in asthmatic subjects who experienced a 12 % decrease in Forced Expiratory Volume in one second (FEV₁, a measurement of lung function) after exposure to SO₂.

These associations have been confirmed by experiments in humans. However, in most of the cases only asthmatic individuals were symptomatic. Bethel et al. (1983) observed airway narrowing in a group of asthmatics exposed to 500 ppb of SO₂ for 5 minutes. Exposure to lower concentrations, 200 ppb over 1 hour, resulted in a small increase in the respiratory rate of asthmatics, but not of healthy individuals (Tunnicliffe et al, 2003). Horstman and Folinsbee (1989) reported that, in general, non-asthmatic subjects are unresponsive to SO₂ concentrations below 500 ppb, a level much higher than the current Air Quality UK limit value (100 ppb for 15 minutes average).

1.3.9 Hydrocarbons

Benzene and 1,3-butadiene are of particular concern since they are known to be genotoxic carcinogens (IARC, 1982, 2008). Levels of toluene and xylenes are suspected to have synergic effects with benzene (Buczynska et al., 2009).

In addition, hydrocarbons are precursors of photochemical oxidants including O₃ through sunlight-driven chemical reactions in the presence of nitrogen oxides (Atkinson, 2000; Monod, 2001).

Acute health effects associated with exposure to benzene include dizziness, muscle weakness, confusion, and loss of coordination. These effects generally occur only at high concentrations and are not likely to be associated with vehicle exhaust (Chang et al., 2008).

Exposure to benzene has also been associated with leukemia, malignant lymphoma, multiple myeloma and lung cancer, as well as numerous disorders of the bone marrow depression in human subjects (Aksoy et al., 1985).

Toluene and xylenes in the vapour phase can be absorbed rapidly from the lungs, and liquid toluene is taken up readily from the gastrointestinal tract (Browning, 1965).

1.3.10 Interactive effects of PM and gaseous pollutants

Exposure to traffic-related air pollutants in the environment involves breathing in PM and gaseous pollutants together. Therefore, an understanding of their interactive effects is fundamental to an explanation of their toxic effects. However, very few studies have looked at the interaction of PM and gaseous pollutants.

Experiments in rats and cell-cultures have reported that exposure to O₃ resulted in an inflammation effect that was additive to that produced by PM alone (Adamson et al., 1999; Madden et al., 2000).

1.3.11 Summary

Particulate matter, NO₂, O₃, SO₂ and soluble metals produce airway inflammation. A possible mechanism is their ability to generate oxidative stress, which involves generation of cytokines by macrophages and epithelial cells via NF-κB and production of ROS. Inflammation and oxidative stress have been related to cardiopulmonary health effects.

Soluble particle components can also act directly upon lipids and proteins, inhibiting important processes. Consequently, a range of respiratory and cardiovascular symptoms have been reported, as well as lung cancer.

There is a large body of literature that suggests that ultrafine particles, transition metals (especially in soluble form) and PAHs play an important role in particle toxicity. However, it remains unclear which factor is more responsible for the observed health effects.

More research is needed on the toxicological effects of pollutant mixtures which simulate the real composition of air in the environment. This information would help epidemiological studies to better understand the health effects of the different pollutants.

CHAPTER 2

LITERATURE REVIEW OF EPIDEMIOLOGICAL STUDIES AND HEALTH EFFECTS OF AIR POLLUTION

2.1 INTRODUCTION

Epidemiological studies have shown consistent associations between traffic-related air pollutants and cardiopulmonary and respiratory illness in humans. Individuals with existing health conditions, the elderly and children are at higher risk of suffering from these effects (Zanobetti et al., 2000; Forastiere et al., 2005 and Goldberg et al., 2006). Evidence of socioeconomic differences in susceptibility has also been reported (Jerrett et al., 2001; O'Neill et al., 2003; Wheeler and Ben-Shlomo., 2005; Kingham et al., 2007).

Two main approaches have been used to assess the exposure populations, short and long term exposure studies. Short-term exposure studies examine the effects of day-to-day variations in pollutant metrics. Long-term exposure studies examine over longer periods (e.g. annual or decadal) the mean concentrations of a pollutant metric across different regions (Pope et al., 1995 and Janssen et al., 2003).

2.2 EPIDEMIOLOGICAL STUDIES ON SHORT-TERM EXPOSURE

Multiple studies of the health effects of short-term exposure to air pollution have found significant associations between PM₁₀ and both daily mortality and hospital admissions for respiratory and cardiovascular diseases, in Europe (Kunzli et al., 2000; Brauer et al., 2001; Katsouyanni et al., 2003), the US (Schwartz et al., 1991, 2004; Dokery et al., 1993; Pope et al., 1995, 2002, 2004; Samet et al., 2000; Dominici and Burnett, 2003) Asia (Omori et al., 2003; Aunan et al., 2004) and South America (Saldiva et al., 1995; Ostro et al., 1996, 2007). NO₂ has also been associated with increased mortality (Lanki et al., 2006; Samoli et al., 2006) and respiratory conditions such as asthma (Walters et al., 1995; Fusco et al., 2001) and COPD (Yang et al., 2005).

Three analytical methodologies have been used: time series analysis; case-crossover; and panel studies. In time series studies, day-to-day variation in air pollution levels is associated with health outcomes (mortality events and hospital admissions) in a single population. As these series analyses make comparisons across a large number

of years, it is necessary to control for factors which vary over time and correlate with pollutant concentrations and mortality counts, including seasonal patterns (Peng et al., 2005).

In case-crossover studies, for each studied subject the exposure concentration of a mortality case (case period) is compared to exposure concentration on a nearby day, where death did not occur (control period). This design does not require the use of complex models to control for seasonal patterns and other covariates (e.g. age, smoking) (Schwartz, 2004). However, the strategy used to choose the control period is important in terms of controlling for time-dependent confounding factors (e.g. weather and day of the week) (Janes et al., 2005).

In panel studies, a group of subjects is followed for several months and the effects of air pollution on their respiratory or cardiac symptoms are reported. The observation of these symptoms provides very valuable information about the health effects of air pollution, since there will be a larger number of people suffering from these symptoms than there are mortality cases or hospital admissions during a high pollution episode.

2.2.1 Epidemiological short-term studies on the effects of PM₁₀

Two large time series studies, in the US (National Morbidity, Mortality and Air Pollution Study, NMMAPS) and Europe (Air Pollution and Health, APHEA-2) conducted in the 1990s showed a link between daily mortality and exposure to PM₁₀. The American study showed an increase of 0.51 % in all mortality and 0.68 % in cardiorespiratory death occurring for each increase of 10 $\mu\text{g m}^{-3}$ in PM₁₀ concentrations (Samet et al., 2000). Because the study included 20 different cities, with differing pollution climates, it was able to address the influence of co-pollutants. The mortality effect was found to be not attributable to NO₂, CO, SO₂ or O₃. Only a slight increase in mortality was observed with increased O₃ levels in summer (Samet et al., 2000; Dominici and Burnett, 2003). Hospital admissions of individuals older than 65 increased by 1.5 % and 1.1 % for COPD and cardiovascular

disease, respectively, for each $10 \mu\text{g m}^{-3}$ increase in PM_{10} (Dominici and Burnett, 2003).

The European study reported a higher risk of all causes of mortality (0.6 %) and 0.76 % for cardiovascular mortality for each $10 \mu\text{g m}^{-3}$ increase in PM_{10} (Katsouyanni et al., 2001). The authors found that PM_{10} effects were stronger in areas with higher concentrations of NO_2 . Hospital admissions for COPD and cardiovascular diseases among people older than 65 were lower than those reported in the NMMAPS: for each increase of $10 \mu\text{g m}^{-3}$ PM_{10} the associated risks were 1.0 % and 0.5 % for COPD and cardiovascular disease respectively (Katsouyanni et al., 2001). An increase of $10 \mu\text{g m}^{-3}$ BS resulted in a risk of 1.1 % (Katsouyanni et al., 2001). The effects of NO_2 and BS suggested the importance of combustion processes (Katsouyanni et al., 2001; Analitis et al., 2006). However, separated risk estimates for NO_2 were not calculated.

Concerns about the statistical procedures used to control for time-varying measures in these studies resulted in a revision of the data, using different smoothing methods. The revised NMMAPS estimates were reduced to 0.21 % for all causes of mortality and 0.31 % for cardiovascular mortality (HEI, 2003). The European study results were more robust to the statistical procedures, and the different smoothing approaches used to validate the original results did not significantly alter the PM -mortality estimates (Atkinson et al., 2003).

These findings led the US Health Institute to invite research teams to re-analyse data from 17 other studies of PM_{10} and mortality. Data was re-analysed using different smoothing approaches. In general, large changes in the mortality estimates were found when data was analysed using more stringent convergence criteria. However, the associated mortality risk remained significant (HEI, 2003).

Other meta-analyses of time series studies have examined specific factors as potential confounders of PM_{10} and mortality. Levy et al. (2000) applied an empirical Bayesian model to time-series literature. The results showed a pooled estimate of a 0.7 % increase in mortality per $10 \mu\text{g m}^{-3}$ increase in PM_{10} concentrations. Greater

effects were found at sites with higher ratios of $PM_{2.5} / PM_{10}$, highlighting the role of fine particles on the health effects. Different climates, housing characteristics, demographics and concentrations of SO_2 and O_3 were found to have a measurable impact on the PM_{10} -mortality relationship.

In an attempt to improve air quality, the European Commission created a framework, the “Clean Air for Europe, CAFE” programme to provide an independent review of the health effects of air pollution. The CAFE programme carried out a meta-analysis of time-series studies and panel studies of PM_{10} and O_3 to calculate pooled risk estimates. The estimated summary risks for all causes of mortality were 1.006 % for either a $10 \mu g m^{-3}$ increase in PM_{10} or a $10 \mu g m^{-3}$ increase in BS and 1.003 % for an increase in $10 \mu g m^{-3}$ in O_3 (WHO, 2004). However, these results were strongly influenced by the data published in the APHEA project, since this study included 29 European cities, so the study was not as independent as it intended to be.

Some case-crossover studies have failed to show associations between PM and cardiovascular disease. For example, Levy et al. (2001) did not find associations between primary cardiac arrest and PM_{10} in a case-crossover study of 362 subjects without recognised heart disease. As a possible explanation for this, the authors suggested the low concentrations of PM_{10} during the studied period. In a similar cross-over design, Sullivan et al. (2003) examined the effects of $PM_{2.5}$ on cardiac arrest on 1206 subjects with and without prior cardiac disease. The results showed an effect only among smokers with prior heart disease. Neither of these studies examined the effects of NO_2 .

Cerebrovascular effects of PM_{10} were reported by Wellenius et al. (2005). The authors found PM_{10} , NO_2 and CO to be associated with hospital admissions for ischemic stroke in a crossover study of subjects aged ≥ 65 in 9 US cities.

The two study designs, time-series and cross-over, were applied to the same data in a study of PM_{10} and mortality in 14 US cities. Results were similar for both methods (Schwartz, 2004).

2.2.2 Epidemiological short-term studies on gaseous pollutants

Time-series studies on the effects of NO₂ are more scarce than those for PM₁₀. The largest study, mentioned earlier, APHEA-2 found a higher increase in mortality (0.80 %) for each 10 µg m⁻³ increase in PM₁₀ in areas with high NO₂, whereas in areas of low NO₂ concentrations the associated risk was 0.19 % (Katsouyanni et al., 2001). This finding can be interpreted in two ways: either NO₂ enhances the toxic effects of PM₁₀ or in areas with high NO₂ concentrations, there are other toxic compounds not present in areas with low NO₂. These compounds could be attached to PM₁₀ but are not represented by the particle mass or could be other, un-monitored pollutants emitted alongside NO₂.

A large panel study over 28 European regions, the Pollution Effects on Asthmatic Children in Europe (PEACE) project, did not show any effect of PM₁₀, NO₂ and SO₂ on respiratory symptoms (PEFR) and bronchodilator use during the winter of 1993/94 (Roemer, 1998, 2000a). Similar results were found by Peacock et al. (2003) in a study of 179 children in southern London during the winter of 1996/97. The authors regressed PEFR against concentrations of SO₂, PM₁₀, O₃ and NO₂. The results showed no clear effect of air pollutants on PEFR, although when PEFR was analysed as a binary variable (decrements more than 20 % below the median) instead of a continuous variable, NO₂ and PM₁₀ (but not SO₂ and O₃) showed negative effects. In contrast, a study in Southampton showed an association between exposure to NO₂ and reductions in PEFR. NO₂ was also associated with asthma exacerbation in the presence of viral infection (Chauhan et al., 2003). However, Chauhan et al. did not adjust for other pollutants. Another large panel study, covering 10 communities in California, reported positive associations between NO₂ and diagnosis of asthma (Gauderman et al., 2005). In Gauderman's study NO₂ was highly correlated with PM₁₀ and CO. Therefore, the reported NO₂-estimate should be considered an estimate of traffic-related air pollution in general and not only of NO₂ (Gauderman et al., 2005).

Results from panel studies are considered less reliable due to the relatively small groups studied and the existence of confounding long-term factors (Brunekreef and Holgate, 2002).

Effects of O₃ on mortality were also reported by Bell et al. (2005). The authors used different lag-times (O₃ concentrations on 0, 1 and 2 days previous to the health effect), age groups, cause-specific mortality, and concentration metrics from 39 time series studies. The associated risk found was 0.87 % for each 20 µg m⁻³ increase in O₃. Adjustment for PM₁₀ did not alter the results.

2.2.3 Epidemiological short-term studies on the health effects of transition metals

Few studies have focused on the association of transition metals attached to ambient PM and health outcomes. Sulphates of Fe, Ni and Zn in PM_{2.5} were associated with mortality in a time-series study of 8 cities in Canada from 1986 to 1996 (Burnett et al., 2000). The effect of the metals was greater than for the mass alone. In contrast, a large study in Edinburgh failed to show associations between metals and cardiovascular and respiratory mortality after adjustment for PM₁₀. However, in this case the concentrations of metals were not measured directly. Instead, a cluster-based meteorological approach was used to extrapolate the metal concentrations for the past eight years. The authors highlighted that the trajectory clustering methodology used to calculate the metal concentrations had limited precision when predicting the true metal concentrations (Beverland et al., 2002).

In a study in California, Cu, Ti and Zn were associated with cardiovascular disease among individuals older than 65. Zn showed larger effects than Cu and Ti and than PM_{2.5}. (Ostro et al., 2007).

Effects of transition metals on respiratory symptoms have shown conflicting results. In Italy, Lagorio et al. (2006) showed a decrease in lung function with increments of Zn and Fe in persons with COPD. The PEACE study only showed slight effects on Fe exposure on reduction of PEF_R (Roemer et al., 2000b). Hong et al. (2007) found

that Mn and Pb but not Al and Zn reduced the PEFR in schoolchildren beyond the reductions seen from exposure to ambient particles. In contrast, Roemer et al. (2007) did not find any association between Ni, Zn, V and Pb and reduction in PEFR. The different findings could be influenced by the interactive effects of metals discussed in Section 1.3.4.

2.3 EPIDEMIOLOGICAL STUDIES ON LONG-TERM EXPOSURE

Studies of long-term impacts of air pollution provide information about the extent to which long residence in a polluted city shortens life. The effects on mortality have been reported to be 5-10 times larger than those predicted by short-term studies (Künzli et al., 2001).

These studies are less common than short-term studies due to the longer period and higher costs involved. The first two large studies that linked PM with mortality by cardiopulmonary disease took place in the US in the 1980s: the Harvard Six Cities study (Dockery et al., 1993) and the American Cancer Society (ACS) study (Pope et al., 1995). The original conclusions of both studies were confirmed in follow up analyses (Krewski et al., 2000, 2004). In these extended studies, the increase in the risk of cardiopulmonary mortality for each $10 \mu\text{g m}^{-3}$ $\text{PM}_{2.5}$ increase was estimated to be 1.28 % and 0.93 % in the Harvard six cities study and ACS respectively; and 1.27 % and 1.14 % for lung cancer in the Harvard and ACS studies respectively (Laden et al., 2006; Pope et al., 2002, 2004). In a cohort study in the Netherlands, Hoek et al., (2000a) found an increase in cardiopulmonary mortality of 1.34 % for $10 \mu\text{g m}^{-3}$ increase in BS. In this study, the BS concentrations were calculated as a function of regional background and urban/local sources, instead of from a single central site, as in the American studies. The traffic indicator, living near a major road (< 100 m), showed a higher mortality risk (relative risk 1.95 %) than the BS concentration, suggesting that one single pollutant may not fully represent the mortality risk.

Other studies have addressed a range of traffic-related air pollutants. For example the SPALDIA study (Swiss Study on Air Pollution and Lung Disease in Adults) found

significant associations between NO_2 , SO_2 and PM_{10} and decreases in lung function (measured as reduction in Forced Vital Capacity, FVC, and FEV_1) (Ackermann-Liebrich et al., 1997) and increase in bronchitis symptoms, but not asthma (Zemp et al., 1999). The same pollutants were also associated with bronchitis but not asthma in children in 10 Swiss communities (Braun-Fahrlander et al., 1997). In both studies, the high temporal correlations between the pollutants prevented separation of their individual effects.

NO_2 and NO have been also associated with mortality from lung cancer and cardiopulmonary causes in cohort studies in France (Filleul et al., 2005) and Norway (Nafstad et al., 2003).

2.4 ERRORS & GAPS IN AIR POLLUTION EXPOSURE ASSESSMENT STUDIES

The previous sections discussed the different analytical approaches used in epidemiological studies and highlighted some potential biases. However, other important aspects can lead to errors in the associated risk estimates. The most important source of error is thought to be exposure misclassification (Brauer et al., 2002). How well do surrogate exposure metrics represent the pollutant exposure resulting in the observed health effects and how does the temporal and spatial distribution of the surrogate vary over the study area.

Most of the studies that have shown associations between air pollution and adverse health effects have used PM_{10} as a surrogate for air pollution exposure. However, PM contains a complex mixture of compounds with different toxicities. Furthermore, the composition of PM may have changed over the last ten years because of the introduction of new engine technologies, which release pollutants with different physical and chemical characteristics, and possibly different toxicity. Therefore, the mass of PM may not represent properly the observed health effects. Thus, in recent years, attention has focussed on examining whether specific components of PM_{10} result in a higher associated risk than PM alone.

A study of the effects of PM on risk of cardiovascular hospitalization in 14 US cities showed that the risk increased with the percentage of particles that came from traffic sources, and decreased with the percentage of particles from windblown dust (Janssen et al., 2003). This finding is of particular concern since in industrialized countries traffic-emissions account for up to 50 % of the total PM concentration (Briggs et al., 1997; Wrobel et al., 2000). In addition, particles emitted by traffic exhaust are very abundant in the ultrafine mode, which contributes greatly to the number of particles but not to the mass.

Therefore, the accuracy of PM as a surrogate for air pollution has been questioned. There are a growing number of studies using alternative surrogates considered more representative of exposure to traffic emissions, including BC and PNC. Several studies have reported higher health risk when BC was used as the exposure metric instead of PM (e.g. Peters et al., 2001; Schwartz et al., 2005). A growing number of studies are reporting associations between ultrafine particles and cardiovascular diseases. For example, in Europe, the ULTRA study followed for 6 months a group of adults aged 40-84 from Amsterdam, Erfurt and Helsinki with stable coronary disease. The results showed significant associations between ST-segment depression (an indicator of heart attack) and the number concentration of ultrafine particles, but not the mass of coarse particles $PM_{2.5-10}$. However, the effect of the number of ultrafine particles could not be separated from the other traffic pollutants measured, NO_2 and CO (Pekkanen et al., 2002). Another large study in 5 European cities, the HEAPSS project (Health Effects of Air Pollution on Susceptible Subpopulations) showed ultrafine particles and CO as the pollutants with the strongest associated risk of hospitalization for myocardial infarction (Paatero et al., 2005). Forastiere et al. (2003) also found a higher risk of coronary death associated with PNC than concentrations of $PM_{2.5}$.

Ultrafine particles have been also associated with respiratory symptoms (Peters et al., 1997). However, Osunsanya et al. (2001) highlighted that, whatever the effect of ultrafine particles, the effects of PM_{10} could not be dismissed.

Estimation of the effects of individual pollutants may lead to incorrect conclusions about health effects since the overall effect of air pollution will be a result of the contribution of each pollutant to the air mixture. The effects can also be confounded by other, unmeasured, pollutants highly correlated with the selected surrogate (Hoek et al., 2002a). To overcome this problem, some studies consider it is more realistic to assess the adverse health effects of a pollutant mix (Wong et al., 2002; Dominici and Burnett, 2003; Moolgavkar et al., 2003; Roberts and Martin, 2006). In these studies, each pollutant is assigned a weight and represents a contribution to the overall health effect.

The spatial variation of the air pollutant metric used is another important issue that must be taken into account to avoid bias in the exposure assessment. Most studies on long-term exposure have used the concentration of a metric measured at a single central site to represent population exposure for the entire studied area. However, this can lead to exposure misclassification due to the marked spatial variability in pollutant concentrations. Several studies have shown that ultrafine particles, BS, BC and NO₂ all exhibit large spatial variability, with concentrations higher near to highways and major roads (Shi et al., 1999; Fischer et al., 2000; Lanki et al., 2006; Zhu, 2002a, 2002b; Gilbert et al., 2003; Namdeo and Bell, 2005). However, the spatial variability of PM₁₀ is not as clear as for other pollutants. For example some studies have reported a marked spatial variability of PM₁₀ within cities (Cyrus et al., 1998; Shi et al., 1999; Brauer et al., 2000; Hoek et al., 2002b; Namdeo et al., 2005) whereas other studies have found an homogeneous distribution of PM₁₀ (Roorda-Knappe et al., 1998; Rööslly et al., 2001). The different results may be a consequence of the different contribution of long-range transported aerosols to PM₁₀ concentrations, as well as the effects of weather conditions on the dispersion.

It should be noted that the spatial gradients of pollutant metrics across a city are not of importance for studies based on time-series analysis so long as the pollutant is highly correlated across the studied area. However, spatial variations in the absolute values of air pollutants are important for long-term epidemiological studies.

Regarding the methodology used to assess spatial variation, it is important to highlight that a high temporal correlation of one pollutant metric between sites may not be accurate enough to describe the spatial variation of that pollutant, since a high correlation does not imply similar absolute concentrations at the sites. Pinto et al. (2004) examined the spatial variability of PM_{2.5} in 28 U.S cities, finding PM_{2.5} concentrations highly correlated between paired sites, but the absolute concentrations between paired sites were significantly different.

In recent years, research has focused on the improvement of exposure assessment methods. Multiple measurement sites, personal exposure and inclusion of meteorological variables are now used more frequently in exposure assessments. However, large monitoring networks are not always available. Instead, modelling techniques are often used to predict pollutant concentrations at each residence or in various microenvironments. The most common models used are Land Use Regression models (LUR) and dispersion models.

LUR models predict traffic-related air pollutants at the home address of each studied subject by using variables derived from geographical information systems (GIS), such as traffic and population density in a buffer, distance to major roads, land cover or altitude, and the annual pollutant concentrations measured at multiple sites. Briggs et al. (1997) pioneered the use of regression-based methods in the EU-funded project Small Area Variations in Air quality and Health (SAVIAH). Concentrations of NO₂ at subjects' addresses were estimated using traffic flow, land cover in a 300 m buffer, altitude and concentrations of NO₂ measured with passive samplers. The model was applied successfully in another location, after local calibration. The values of the regression coefficient (R^2) between model and observed annual NO₂ concentrations were between 58–76 % (Briggs et al., 2000). Similar results were reported in California using another LUR model: 79 % of NO₂ variability was explained, using traffic density in buffers of 40-300 m and 300-1000 m, road length, and distance from Pacific coast (Ross et al., 2006). Brauer et al. (2003) used a similar approach in a study of the Netherlands, Munich and Stockholm to estimate PM_{2.5}. Using traffic variables and distance to major road, the R^2 values between the modelled and

estimated concentrations were between 0.50 and 0.73. For prediction of filter absorbance the R^2 values were higher (0.66-0.81), highlighting the contribution of BC from traffic exhaust. Another study in the Netherlands, part of the Netherlands Cohort Study on Diet and Cancer (NLCS) study, used a more sophisticated approach. The model included a local contribution calculated from traffic variables, an urban contribution estimated from address density, number of inhabitants and land cover and a regional component estimated from daily concentrations at background sites. The regression model estimated 84 %, 44 %, 59 % and 56 % of the variance in NO_2 , NO, BS and SO_2 , respectively (Beelen et al., 2007).

LUR models have been successfully applied in long-term exposure studies. For example Morgenstern et al. (2007) in a cohort of 1 and 2 year old infants in Norway found significant associations between respiratory symptoms (sneezing, runny/stuffed nose and asthmatic/spastic/obstructive bronchitis) and $\text{PM}_{2.5}$ and absorbance of $\text{PM}_{2.5}$ estimated using a regression model based on land use, population density and length of road. However, LUR models are less reliable in assessing short-term exposure, since they do not account for temporal variability (e.g. meteorological factors). In those cases, it may be more appropriate to use dispersion models. Another limitation of LUR models is that extrapolation to other geographical areas is limited by the similarity of the traffic characteristics and land use compared with those areas where the model was developed (Jerrett et al., 2005).

Dispersion models consider spatial and temporal variability in air pollutants. They require meteorological, emission and topographical data. This data is combined in the model to simulate the transport and distribution of the pollutant in the urban area. The accuracy depends among other factors, on the type of dispersion considered. For example, a simple Gaussian plume model may not be realistic, since it assumes no chemical or removal processes of the pollutant, and therefore such models need to be validated with extensive networks (Jerrett et al., 2005). Another disadvantage is the large amount of input information required. However, these models may be very useful in estimating air pollutant concentrations in complex geographical locations such as street canyons.

In summary, LUR and dispersion models are very useful to assess personal exposure. However, they must be validated with real measurements. Therefore, to apply these models further information on the temporal and spatial variation of air pollutants in the studied area is needed.

On the other hand, if possible, PNC and chemical components of PM₁₀ should be measured together with the mass to better understand the toxic effects of PM. However, for financial and practical reasons it is difficult to measure multiple pollutant metrics at multiple locations. An alternative approach is to examine the correlations between pollutant measurements, with the aim of finding a surrogate for PNC and chemical components of PM₁₀, albeit with the difficulty of discriminating between their single and interactive effects.

2.5 CORRELATIONS BETWEEN TRAFFIC-RELATED AIR POLLUTANTS

2.5.1 Introduction

Previous studies have confirmed a high correlation between traffic-related air pollutants at individual sites. This section reviews studies on the correlations between PNC, transition metals and PAHs with other traffic-related air pollutants.

Different studies have used different statistical descriptors to measure the degree of correlation between co-pollutants. Studies where pollutant data was normally distributed have used parametric methods reporting Pearson correlation coefficients (r) and the square of the Pearson correlation coefficient, the regression coefficient (R^2). However, some studies where data was skewed have used non-parametric methods and have reported Spearman correlation coefficients. Pearson and Spearman correlation coefficients can be compared directly with each other (Miller, 2008). However, correlation coefficients and regression coefficients can not be compared as they measure different aspects of the association between pollutants. Therefore, the regression coefficients reported in the reviewed literature in sections 2.5.2 to 2.5.4 were transformed into Pearson correlation coefficients.

2.5.2 Studies on the correlations between particle number and co-pollutants

Most of the reviewed studies found a higher correlation between PNC vs. nitrogen oxides and CO than between PNC vs. PM₁₀ (Morawska et al., 1998; Cyrus et al., 2003a; Harrison and Jones, 2005; Johansson and Norman, 2007). This can be explained by the fact that PM₁₀ has a larger fraction of resuspended road dust and is strongly influenced by background particles (Harrison et al., 2000; Forastiere et al., 2005), while gaseous pollutants are released by the vehicle exhaust as ultrafine particles (Longley et al., 2005).

The degree of correlation reported between PNC and gaseous pollutants differs across the different reviewed studies. Comparisons are difficult because of the different characteristics of each study: time averaging period; distance of the monitor from the traffic source; particle size measured and meteorological conditions.

Paatero et al. (2005) developed a regularized linear model to predict PNC using data on NO, NO₂, CO, SO₂, O₃, PM₁₀, PM_{2.5} and meteorological variables (wind direction and speed, temperature and barometric pressure) from Augsburg, Barcelona, Helsinki, Rome, and Stockholm. The results showed NO₂ to be the most important explanatory variable, with an R² of 0.77, 0.80, 0.58, 0.84, 0.81 respectively for the five cities.

Longley et al. (2005) used a simple least squared linear model to predict PNC from NO_x and CO concentrations. The authors found R² of 0.85 and 0.78 (equivalent to r-values of 0.92 and 0.88 respectively) between fine particles (95-470 nm) vs. NO_x and CO respectively, for hourly averaged concentrations at an urban centre in Manchester. The separation between the gas and particle monitors was 600 m horizontally and 30 m vertically. Correlation coefficients for both ultrafine (13-35 nm) and nanoparticles (3-7.5 nm) vs. NO_x and CO were much lower. The authors examined the regression coefficients for each wind direction cluster, concluding that the correlation coefficients did not depend strongly on wind direction. However, Harrison and Jones (2005) in a similar study in London (at Marylebone Rd.) found an increase in R² from 0.63 to 0.96 (equivalent to r-values of 0.79 and 0.97

respectively), when the regression of PNC against NO_x was calculated only with PNC data corresponding to the wind direction with highest PNC. These contrasting results are likely to be due to the different topography surrounding the monitoring sites. Marylebone Rd. is located in a street canyon, where pollutants are driven by the wind flows in the street while the Manchester monitoring site in Longley's study was on top of a building, where air is more representative of background urban air.

Apart from wind direction, other factors reported to influence the correlations between particle number and co-pollutants include wind speed, particle size and the averaging period used in the regression analysis.

Noble et al. (2003) found higher correlation coefficients between ultrafine (20-100 nm) and accumulation particles (100-700 nm) and CO, NO, NO_2 and PM_{10} at wind speed below 3 m s^{-1} . However, Longley et al. (2005) found that the relationship between NO_x and ultrafine particles (13-35 nm) was weakened during periods of stagnation (wind speeds below 2 m s^{-1}), suggesting that stagnation increases NO_x concentrations, but does not affect ultrafine particles to the same extent due to their shorter atmospheric residence time.

Different particle sizes have resulted in different degrees of correlation with NO_x : total number of particles resulted in an r-value of 0.67 at an urban centre in Birmingham (Harrison and Jones, 2005), whereas particles in the size fraction of $0.095\text{-}0.47 \mu\text{m}$ vs. NO_x showed an $R^2 = 0.85$ ($r=0.92$) also in Birmingham (Longley et al., 2005). Noble et al. (2003) found similar Pearson correlation coefficients between PNC and NO_2 for particles in the size range ($0.1\text{-}0.7 \mu\text{m}$) ($r=0.65$) and ultrafine ($< 0.1 \mu\text{m}$) ($r=0.70$). Correlation coefficients for coarse particles ($1\text{-}10 \mu\text{m}$) vs. NO_2 were 0.31. Ketzler et al. (2003) examined the correlation between PNC and NO_x over a wide range of particle sizes (10-800 nm) at kerbside and background locations. Smaller particle sizes (10 to 200 nm) resulted in correlation coefficients of 0.7-0.85, decreasing to 0.5 for larger particles (800 nm). The decrease was more pronounced at the background site.

Different averaging periods have resulted in different degrees of correlation. Sardar et al. (2004) found higher Pearson correlation coefficients for daily average PNC vs. CO, NO and NO₂ in summer than for hourly average data, especially for receptor sites compared to source sites. Cyrus et al. (2003a) also found daily averaged PNC vs. NO_x and CO more highly correlated (Spearman correlation coefficients of 0.6) than hourly averaged data ($r=0.7$), at a background location. Daily averaged PNC vs. PM₁₀ also resulted in higher correlation coefficients than hourly averaging data, although the r -values were lower than those observed for PNC vs. NO_x.

The absorbance of PM deposited onto a filter has also been found to be correlated with particle numbers. Ruuskanen et al. (2001) found the absorbance of PM_{2.5} filters to be highly correlated with total PNC and accumulation mode particles ($r > 0.5$ and $r > 0.7$ respectively) in three urban background sites across Finland.

PM₁₀ and PM_{2.5} have shown lower correlation coefficients with PNC, than absorbance of PM and NO_x. Ruuskanen et al. (2001) reported correlation coefficients for PM_{2.5} and total PNC of 0.049, 0.32 and 0.58, however, correlations with the accumulation mode were much higher (0.66-0.9). Results published by the Air Quality Expert Group (AQEG, 2005) also showed very low correlations between total PNC vs. PM₁₀ and PM_{2.5}.

Table 2.1 summarises the findings and study characteristics of the reviewed studies on the correlations between PNC and other traffic-related air pollutants.

Table 2.1 Summary review of studies on the correlations of particle number concentrations and other traffic-related air pollutants.

Reference	Sampling period	Averaging time	Site characteristics	Particle Size	Statistical description of bivariate relationship	NO _x	NO ₂	NO	CO	O ₃	SO ₂	PM ₁₀	PM _{2.5}	Black carbon surrogate
Cyrus et al., 03a	Sep 95-Dec 98	1hr 24 hrs	1km from City Centre & 30m from road	TN, 0.01 - 2.5 µm	Spearman r		0.55 0.71	0.57 0.73	0.57 0.70		0.33 0.56	0.37 0.57		
AQEG, 05	Jan 01-Mar 02	1hr	Kerbside	TN	Pearson r	0.77						0.29	0.25	
Harrison et al., 03	Oct-Jan, 01	48 hrs	Roadside 43,000 veh/day	TN, > 7nm	Not specified	0.84								
Paatero et al., 05	99-02	24 hrs	Source & receptor sites	TN, > 7nm	Spearman r		0.33-0.67	0.45-0.72	0.29-0.65	-(0.17-0.8)	0.49-0.64			
Harrison & Jones, 05	00-03	24 hrs	5 Urban Centres	TN, > 7nm	Pearson r	0.42-0.67						0.37-0.56		
		24 hrs	2 Urban Background			0.30/0.40						0.14/0.22		
		1hr	Kerbside			0.79						0.54		
Sardar et al., 04	Jan-Dec, 02	1 hr	Source and receptor sites	TN, > 15 nm	Pearson r		0.17-0.5	0.06-0.65	0.13-0.66	-0.65 - 0.59		-0.16-0.27		
		24 hrs					0.07-0.68	0.30-0.66	0.00-0.63	-0.64 - 0.30	-0.32-0.10			
Ruuskanen et al., 01	Nov 96-Mar 97	24 hrs	3 Background sites	TN	Spearman r								0.050-0.58	0.56-0.67 ¹
				0.1 - 0.5 µm							0.66-0.90	0.73-0.87 ¹		
				0.01 - 0.1 µm							0.23-0.61	0.64-0.66 ¹		
Ketznel et al., 03	May-Nov, 01	30 min	Street Canyon	0.01 - 0.7 µm	Not specified	0.93			0.84					
		30 min	Street Canyon - Background	0.01 - 0.7 µm		0.90			0.82					
Penttinen et al., 01	Nov 96-Apr 97	24 hrs	50 m from busy road	TN	Spearman r		0.81	0.77	0.44					
				0.01 - 0.1 µm			0.81	0.76	0.43					
				0.1 - 1 µm			0.51	0.57	0.47					
Noble et al., 03	Nov-Dec, 99	1 hr	Pooled two trafficked places	0.02 - 0.1 µm	Pearson r		0.65	0.74	0.81	-0.45				
				0.1 - 0.7 µm			0.70	0.75	0.87	-0.31				
				1 - 10 µm			0.31	0.43	0.43	-0.07				
Moraska et al., 98	Jul 95-Apr 97	4 hrs	Background	0.016 - 0.626 µm	Pearson r	0.45			0.78	-0.14	0.38	0.25		0.38
				0.7 -30 µm		-0.04		0.16	0.08	0.12	0.36		0.37	
Longley et al., 05	Nov-Dec, 97	1 hr	Urban Centre	0.013 -0.035 µm 0.095 - 0.47 µm	Pearson r	0.46 0.92			0.39 0.88					

¹Absorbance PM_{2.5}, r, correlation coefficient; RD, roadside; TN, Total Number

2.5.3 Studies on the correlation between transition metals and co-pollutants

Transition metals bound to PM have been found to be associated with NO_x, and with the darkness of PM filters. Harrison et al. (2003) noted Spearman correlation coefficients between NO₂ and total metal content in PM₁₀ of 0.735 and 0.606, for Cu and Zn, respectively, in Birmingham. However, the least-squared regression coefficients were lower (< 0.5). Götschi et al. (2005) in a study across 21 European cities found PM_{2.5} concentrations and the absorbance of PM_{2.5} filters vs. Cu, Fe, Zn and Pb (total metal content in PM_{2.5}) to be highly correlated. Pearson correlation coefficients of the annual mean across cities were over 0.6 for all those metals. Less attention has been paid to the water-extractable fraction, despite this being the most bioavailable fraction in the human respiratory tract (Costa and Dreher, 1997). Hibbs (2002) found Spearman correlation coefficient of 0.5 and 0.7 between the water extractable fraction of Zn, Ni, Pb, V in PM₁₀ vs. BS and the water extractable fraction of Cu in PM₁₀ vs. BS, respectively in a central location in Edinburgh. Table 2.2 summarises these findings.

Table 2.2 Summary review of the studies of correlations between metals and other traffic-related air pollutants.

Reference	Surrogate for metals	Sampling period	Averaging time	Site characteristics	Characteristics of the metal extraction procedure	Statistical description of bivariate relationship	Cu	Fe	Ni	Zn	V	Cd	Pb
Harrison et al., 03	NO _x	Oct-Jan, 01	48 hrs	Roadside 43,000 veh/day	PM ₁₀ , Aqua Regia	Pearson r	0.68	-	-	-	-	-	0.58
					PM _{0.2} , Aqua regia		0.40	-	-	-	-	-	0.61
Harrison et al., 03	TN	Oct-Jan, 01	48 hrs	Roadsite 43,000 veh/day	PM ₁₀ , Aqua Regia	Pearson r	0.50	-	-	-	-	-	0.40
					PM _{0.2} , Aqua regia		0.35	-	-	-	-	-	0.46
Götschi et al., 05	PM _{2.5}	Jun 00-Dec 01	24 hrs	21 EU cities	PM _{2.5} , ED-XRF	Pearson r	0.63	0.85	-	0.46	0.18	-	0.88
	AbsPM _{2.5}						0.69	0.90	-	0.60	0.25	-	0.89
Hibbs., 02	PM _{2.5}	Sep 99-Sep 00	24 hrs	urban centre	PM _{2.5} , water-soluble	Spearman r	0.61	0.59	0.52	0.48	0.74	0.13	0.42
	PM ₁₀	Sep 99-Sep 00	24 hrs	urban centre	PM ₁₀ , water-soluble	Spearman r	0.54	0.51	0.55	0.47	0.61	0.21	0.41
	BS	Sep 99-Sep 01	25 hrs	urban centre	PM ₁₀ , water-soluble	Spearman r	0.72	0.23	0.46	0.49	0.48	0.19	0.45
	BS	Sep 99-Sep 02	26 hrs	urban centre	PM _{2.5} , water-soluble	Spearman r	0.71	0.42	0.39	0.55	0.48	0.19	0.49

AbsPM_{2.5}, Absorbance PM_{2.5}; ED-XRF: energy dispersive X-ray fluorescence spectrometry

2.5.4 Studies on the correlations between PAHs and co-pollutants

PAHs have also been found to be correlated with NO_x and CO. Lim et al. (1999) found highly significant correlation coefficients between the carcinogenic PAHs benz[a]anthracene benzo[b]fluoranthene, benzo[j+k]fluoranthene, benzo[a]pyrene, benzo[g,h,i]perylene, and indeno[1,2,3-cd]pyrene and NO_x and CO in a central site in Birmingham. Harrison et al. (2003), also found high correlations between particle-bound and vapour phase pyrene and fluoranthene and NO_x ($R^2=0.6$, $r=0.77$) in a central site in Birmingham.

In Greece, Mantis et al. (2005) found high correlation coefficients between PAHs vs. NO₂, NO and CO ($r=0.575$, 0.687 , 0.730 respectively) in a site influenced by traffic and in an urban-industrial site ($r=0.513$, 0.895 for PAHs vs. NO₂ and NO respectively). Correlation coefficients at a background site and a second site influenced by traffic were $r < 0.5$.

Several studies have shown a significant association between PAHs and absorbance of PM₁₀ or BS deposited on a filter. Fischer et al. (2000) as part of the SAVIAH study examined the correlations between concentrations of PAHs vs. mass and absorbance of PM₁₀ and PM_{2.5} at streets with high and low traffic densities in Amsterdam. The results showed Spearman correlation coefficients of 0.85 and 0.82 for $\Delta\sum\text{PAHs}$ vs. $\Delta\text{absorption of PM}_{10}$ & $\Delta\text{absorption of PM}_{2.5}$ filters respectively, where the increments (Δ) were the differences in concentration between high and low traffic streets. Kingham et al. (2000) as part of the same study examined the correlation between benzene, benzo[a]pyrene and sum of PAHs vs. PM₁₀, PM_{2.5} (mass and absorbance) in outdoor and indoor measurements in Huddersfield. In general, filter absorbance of PM_{2.5} showed higher correlations than mass of PM_{2.5} for most of the metals.

Papageorgopoulou et al. (1999) in a study of six towns in Greece also found significant correlations between PAHs and BS ($r=0.573$), the latter being comparable to measurements of filter absorbance.

Table 2.3 shows a summary of the reviewed studies on the associations of PAHs with other traffic-related air pollutants.

Table 2.3 Summary review of the studies of correlations between particle bound-PAHs (unless otherwise indicated) and other traffic-related air pollutants.

Reference	Surrogate for PAHs	Sampling period	Averaging time	Site characteristics	Particle size fraction	PAHs measured	Statistical description of bivariate relationship	Value of the statistical description of bivariate relationship
Harrison et al., 03	NO _x	Oct-Jan, 01	48 hrs	Roadsite	TSP+	Pyrene	Pearson r	> 0.70
				43,000 veh/day	vapour	Fluranthene		> 0.70
Mantis et al., 05	NO ₂	May 01-Jun 02	24 hrs	2 urban centre	PM ₁₀	∑ PAHs	Pearson r	0.27 & 0.57
				Industrial background				0.51
								0.27
Papageorgopoulou et al., 99	NO ₂	warm months in period Jan 96-Fe 97 cold months in period Jan 96-Fe 97	24 hrs	Grouped 6 urban sites	TSP	∑ PAHs	Spearman r	0.46
								-0.47
Mantis et al., 05	NO	May 01-Jun 02	24 hrs	Background Industrial	PM ₁₀	∑ PAHs	Pearson r	0.39
				2 urban sites				0.90
								0.33 & 0.69
Papageorgopoulou et al., 99	CO	warm months in period Jan 96-Fe 97	24 hrs	Grouped 6 urban sites	TSP	∑ PAHs	Spearman r	0.68
Lodovici et al., 03	CO	winter months 92-01	24 hrs	Traffic site		∑ PAHs	Pearson r	0.86
Lim et al., 99	CO	May-96	2 hrs	Heavily trafficked	PM ₁₀	B[b]F	Pearson r	0.93
						B[a]A		0.95
Mantis et al., 05	CO	May 01-Jun 02	24 hrs	urban site	PM ₁₀	∑ PAHs	Pearson r	0.73
Mantis et al., 05	SO ₂	May 01-Jun 02	24 hrs	Industrial	PM ₁₀	∑ PAHs	Pearson r	0.19
				2 urban sites				0.27 & 0.43
Papageorgopoulou et al., 99	O ₃	warm months in period Jan 96-Fe 97	24 hrs	Grouped 6 urban sites	TSP	∑ PAHs	Spearman r	-0.44
Papageorgopoulou et al., 99	BS	warm months in period Jan 96-Fe 97	24 hrs	Grouped 6 urban sites	TSP	∑ PAHs	Spearman r	0.53
Papageorgopoulou et al., 99	Pb	warm months in period Jan 96-Fe 97	24 hrs	Grouped 6 urban sites	TSP	∑ PAHs	Spearman r	0.73
Harrison et al., 03	PN	Oct-Jan, 01	48 hrs	43,000 veh/day veh/day	TSP+ vapour	3-Me-Phen 2-Me-Phen 1+9-Me-Phen 4,5-Me-Phen Pyrene Fluranthene	Pearson r	0.69 0.54 0.61 0.57 > 0.70 > 0.70
Fisher et al., 00	ΔPM ₁₀ ΔPM _{2.5} ΔAbsPM ₁₀ ΔAbsPM _{2.5}	Jan- Apr, 95	24 hrs	High - low traffic sites		∑ PAHs	Spearman r	0.58 0.57 0.85 0.82
Kingham et al., 00	AbsPM ₁₀ AbsPM _{2.5}	Feb-May, 95	24 hrs	Grouped traffic and background sites		∑ PAHs	Spearman r	0.34 0.34

ΔAbsPM_{2.5}, increments in absorbance PM_{2.5}; TSP, total suspended particles

Results from these studies suggest several factors influence the associations between these pollutants: meteorological conditions, location of the monitoring site relative to the pollutant source, and the measurement averaging period used. These factors interact with each other and hence a different averaging time and gaseous pollutant might better represent PNC, PAHs or metal concentrations at a specific sampling site, under specific meteorological conditions. Therefore, further information would help to generalise these observations.

2.6 SUMMARY LITERATURE REVIEW

A very large number of epidemiological studies have demonstrated consistent associations between traffic-related air pollutants and health outcomes. The associated estimates seem to be sensitive to the statistical model used to assign exposures to the subjects studied. However, exposure misclassifications due to the selection of monitoring sites and surrogate exposure metric have also possibly altered the magnitude of the apparent associations between exposure and health outcomes. To overcome this problem, several studies have developed sophisticated exposure models, which account for temporal and spatial variation of air pollutants and meteorological variables. However, application of these models requires validation with observations on the area of interest. In addition, because many of the exposure models provide estimates of annual averaged concentrations, their estimates of concentrations for shorter periods may be inaccurate for exposure assessment.

There remains considerable uncertainty in epidemiological and toxicological studies about which pollutant (or pollutant mix), causes the observed health effects. This uncertainty partly results from the high temporal correlation between pollutants. The resultant uncertainty about the effect of specific pollutants is hampering preventive strategies and policies.

In addition, despite the fact that toxicological studies have highlighted the importance of water-soluble metals on health, there are very few epidemiological

studies that have looked at the relationship between metal concentrations and health outcome.

Based on these concerns, examination of the spatio-temporal correlations of air pollutants is fundamental for better exposure assessment. An inexpensive, easy to operate and maintain metric such as NO₂ measured by passive diffusion tubes (PDTs) or filter absorbance would be helpful to estimate the spatial variability of other more toxic pollutants (e.g. particle numbers, transition metals and PAHs) since economic and logistical reasons make it impossible to monitor these pollutants simultaneously at a large number of sites.

CHAPTER 3

AIMS AND OBJECTIVES OF THE RESEARCH

3.1 AIMS OF THE RESEARCH

The overall aim of this research was to examine the spatial and temporal variations of different traffic-related air pollutants in urban environments to determine what implications these variations may have for epidemiological research. Five aims were posed:

- I. To examine the spatial contrast in pollutant concentrations between sites and the temporal correlation between pollutants at sites with different traffic intensities.
- II. To examine whether simple metrics of air pollution (e.g. light absorbance of filters and NO₂ & NO_x) predict temporal and spatial variations in other toxic traffic-related air pollutants (including water-soluble metals, PAHs and PNC).
- III. To examine to what extent the correlations between pollutant metrics change with the time averaging period (e.g. hourly and daily), between sites with different traffic intensity and street topography, as a result of dispersion from source.
- IV. To examine the performance of novel methodologies to measure particle darkness and particle number concentration.
- V. To examine whether PDTs are a useful technique to measure the spatial variability of NO₂ and NO_x and whether NO₂ and NO_x PDT measurements can be used to represent the spatial variability of other pollutants.

To answer the above aims the specific methodological objectives of the project were:

- (a) To collect data for PNC, PM₁₀, PM_{2.5}, absorbance of PM₁₀ and PM_{2.5}, BS, EC, OC, NO₂, NO, NO_x, CO, SO₂, O₃ and VOCs (1,3-butadiene and BTEX) at sites with different pollution concentrations in Glasgow and London.
- (b) To extract water-soluble metals and PAHs from filters of PM₁₀ and PM_{2.5}.

- (c) To measure PNC with a novel particle counter and the darkness of PM collected with a respirable sampler.
- (c) To measure NO₂ and NO_x using PDTs at sites with different pollution levels in Glasgow.

The answers to research questions I-IV will inform best practice in exposure assessment studies to account for spatial variability of pollutant concentration in urban environments and to evaluate which pollutants best represent exposure to traffic-related air pollution. Analysis of the correlations between pollutant metrics will also inform epidemiological studies based on time series analyses whether the effects of each air pollutant on health can be distinguished from each other.

Air pollution regulatory bodies will also benefit from the results, since the total number of sites where toxic and difficult to measure pollutants (e.g. PNC, metals) are monitored in a city are limited and usually restricted to one site due to practical constraints (including cost, space requirement of the equipment, security reasons, power supply). Consequently, information about the spatial variation of these pollutants is often non-existent in most cities, despite the fact that recent research has indicated that particles and their attached compounds are probably the most causative factors of the observed health effects of air pollution. Therefore, it would be very useful if a single and inexpensive method can be used to represent concentrations of these pollutants. NO₂ is a common pollutant used in health effects assessments. Measurements of NO₂ PDTs in the UK date back to 1960; therefore, for retrospective studies it is worth investigating whether NO₂ maps derived from PDTs measurements reflect variations in other pollutants.

CHAPTER 4

METHODOLOGY

4.1 INTRODUCTION

This chapter explains the monitoring strategy used to answer the research questions stated in Chapter 3. It also describes the monitoring sites where pollutants were sampled, the equipment used, and the chemical analyses performed. Sections 4.2 to 4.9 describes the methodology followed to answer research questions I to IV. This monitoring campaign is referred to in the text as the main study. Section 4.10 deals with the methodology followed to examine the performance of the NO₂ and NO_x PDTs (aim V).

4.2 OVERVIEW OF EXPERIMENTAL DESIGN FOR THE MAIN STUDY

The monitoring campaign took place in the City of Glasgow. It should be noted that the experimental work in London was limited to the extraction of water-soluble metals from the PM_{2.5} filters. The rest of the data was provided by the National Air Quality Archive (NAQA).

Glasgow is Scotland's largest city with a population of 580,690 in 2006 (GCC, 2008) situated on the River Clyde in the country's west central lowlands.

Glasgow is an ideal location for the study of traffic-related air pollutants since the major contributor of PM₁₀, NO₂, CO, benzene and 1,3-butadiene is road transport, accounting specifically for 51 % of PM₁₀, 75 %, of NO₂ 66 % of benzene and, 95 % of 1,3-butadiene (LAQM, 2003). The three main sites where monitoring took place were part of the air pollution Automatic Urban Network (AUN) run by the Department of Environment and Rural Affairs (DEFRA) (LAQM, 2003). The monitoring sites were located in the city centre at a kerbside/street canyon (Hope St.), urban centre (St. Enoch Sq.) and urban background/street canyon (Montrose St.). A motorway (M8) surrounds the City Centre. The prevailing winds are usually westerly, which blows the highway exhaust into the City Centre.

London is the largest metropolitan area in the UK and Europe, with a population of 7,556,900 in 2007 (Office of National Statistics, 2008). It is located in a valley and is frequently congested. Traffic is the main source of PM₁₀ and NO₂ (LAQN, 2008). An

inner ring road and an outer motorway (M25) encircle the centremost part of the city and it is intersected by a number of busy radial routes. The selected monitoring sites for the study were a kerbside/street canyon (Marylebone Rd.) and an urban background (North Kensington).

The research activities associated with the objectives indicated in Chapter 3 are described below:

1) Instrument inter-comparison study: the monitoring equipment used as part of this project was compared with that used by DEFRA in the city of Glasgow, whenever this was possible, to assess possible biases in the measurements. The different pollutants and monitoring methods inter-compared are described below:

PM₁₀: 24-hours gravimetric PM₁₀ measurements taken with a Partisol sampler 2025, were compared with measurements over the corresponding averaging period from a Tampered Element Oscillating Microbalance analyser (TEOM). Comparisons were made taking into account the mass correction factors applied to TEOM data (see Section 4.4.2 for details).

Respirable dust (PM₄): Six Higgins-Dewell cyclones attached to low volume pumps were run side by side from 18 November to 19 December 2005 to assess the measurement precision.

PNC: two Water-based Condensation Particle Counters (WCPCs) were co-located at St. Enoch Sq. beside a butanol condensation particle counter (BCPC) run by DEFRA and maintained by National Physical Laboratories (NPL). Comparisons between the three particle counters took place on different occasions throughout the entire project because of the continuous technical problems with the WCPCs (2-8 March 2006 and 17 February to 13 April 2007).

2) Collection of air pollution data: The aim of the monitoring campaign was to investigate whether local traffic density influences the correlations between traffic-related air pollutants. This was achieved by making use of the local authority's

existing automatic air pollution monitoring network to collect data for different pollutants from three sites with different traffic characteristics.

Measurements of particle characteristics (PNC, PM₁₀, PM_{2.5} and absorbance, transition metals and PAHs) and gaseous pollutants (NO_x, NO₂, CO, SO₂, O₃, and VOCs) were collected at 3 AUN sites in Glasgow (Hope St., St. Enoch Sq. and Montrose St.) from the 8 June to 3 August 2006 and two AUN sites in London at Marylebone Rd. and North Kensington in 2006 for those days on which data of most pollutants was available at the two sites. These days were 26 days in total on 13, 15, 16, 23, 24-26 June; 24-26, 31 October; 3, 8, 11, 12, 13, 17, 23, 27 November; 4, 6, 8, 10, 12, 14, 15 December 2006.

Unfortunately, data in the NAQA was not available for all pollutants at all the studied sites. In addition, it was not possible to measure PM₁₀ at the background site in Glasgow because of the absence of an accessible site to locate the Partisol sampler. Table 4.1 provides a list of the pollutants measured as part of this project and the data provided by the NAQA at each studied site.

Table 4.1 Pollutants measured as part of this project and those provided by the National Air Quality Archive (NAQA), monitoring equipment and monitoring sites.

Pollutant	Equipment	Monitoring sites				
		Glasgow			London	
		Hope St.	St. Enoch Sq.	Montrose St.	Marylebone Rd.	North Kensington
PM ₁₀	PARTISOL	√	√	-	NAQA	NAQA
	TEOM	NAQA	NAQA		NAQA	NAQA
PM _{2.5}	PARTISOL	-	-	-	NAQA	NAQA
Respirable Dust (PM ₄)	Cyclone	√	√	√	-	-
PNC	Water based-CPC	√	√	√	-	-
	Butanol based-CPC	-	NAQA	-	NAQA	NAQA
BS	BS monitor	-	NAQA	-	NAQA	-
EC	Ambient Carbon Particulate Monitor	-	-	-	NAQA	NAQA
	Ambient Carbon Particulate Monitor	-	-	-	NAQA	NAQA
Absorbance PM	measured on PM PARTISOL filters	√	√	-	√	√
Metals	extracted from PM filters	√	√	-	√	√
	extracted from PM filters	√	√	-	-	-
NO ₂ & NO _x	PDTs	√	√	√		
	Chemilumiscence Analyser	NAQA	NAQA	NAQA	NAQA	NAQA
O ₃	Ultra Violet Analyser	-	NAQA	-	NAQA	NAQA
SO ₂	Ultra Violet Analyser	-	NAQA	-	NAQA	NAQA
CO	Infra Red Analyser	NAQA	NAQA	NAQA	NAQA	NAQA
Hydrocarbons	Ultra Violet Analyser	NAQA	-	-	NAQA	-

√: measured as part of this project; NAQA: provided by the National Air Quality Archive; BS:Black Smoke; EC: elemental carbon; OC:organic carbon; CPC: condensation particle counter; PDTs: passive diffusion tubes; Hydrocarbons: includes 1,3-butadiene, benzene, toluene, ethylbenzene and xylenes

Data of the following pollutants was obtained from the NAQA: measurements of gaseous pollutants monitored with continuous analysers (NO₂, NO, NO_x, CO, SO₂, O₃, VOCs); PM₁₀ measured with a TEOM analyser, PM_{2.5} measured with a Partisol sampler, and PNC measured with a butanol-based condensation particle counter (BCPC). To complete these data sets the following pollutant metrics were measured: NO₂ and NO_x using PDTs; PM₁₀ using a Partisol sampler with subsequent extraction of metals and PAHs from the filters, and measurement of the reflectance of the mass deposited onto the filter. Transition metals were also extracted from the PM_{2.5} DEFRA filters and the reflectance was measured; mass and reflectance of respirable dust (PM₄) using Higgins-Dewell cyclones and low volume pumps, and PNC using a WCPC.

3) Measurement of NO₂ and NO_x using PDTs: NO₂ PDTs were deployed across Glasgow at sites with different pollution environments (background, industrial, suburban and urban centre sites) as per the DEFRA classification scheme (NAQAa, 2007). This monitoring campaign took place from 15 February to 10 May 2005. In addition, measurements at the three AUN sites in Glasgow were carried out from 8 June to 14 December 2006 and 22 May to 18 December 2007.

NO₂ PDTs were also used to examine the spatial variation of NO₂ with increasing distance from a major road. The experiment was repeated 5 times so as to obtain statistical power for the regression analysis. The first exposure period was in October 2005 and it was repeated on four other occasions from 20 November 2007 to 18 December 2007.

NO_x PDTs were deployed at the three AUN sites in Glasgow from 22 May to 18 December 2007.

4.3 DETAILS OF THE MONITORING SITES INVOLVED IN THE MAIN STUDY

A map with the location of the monitoring sites for the main study and details of the sites in Glasgow are shown in Figure 4.1 and Table 4.2, respectively.

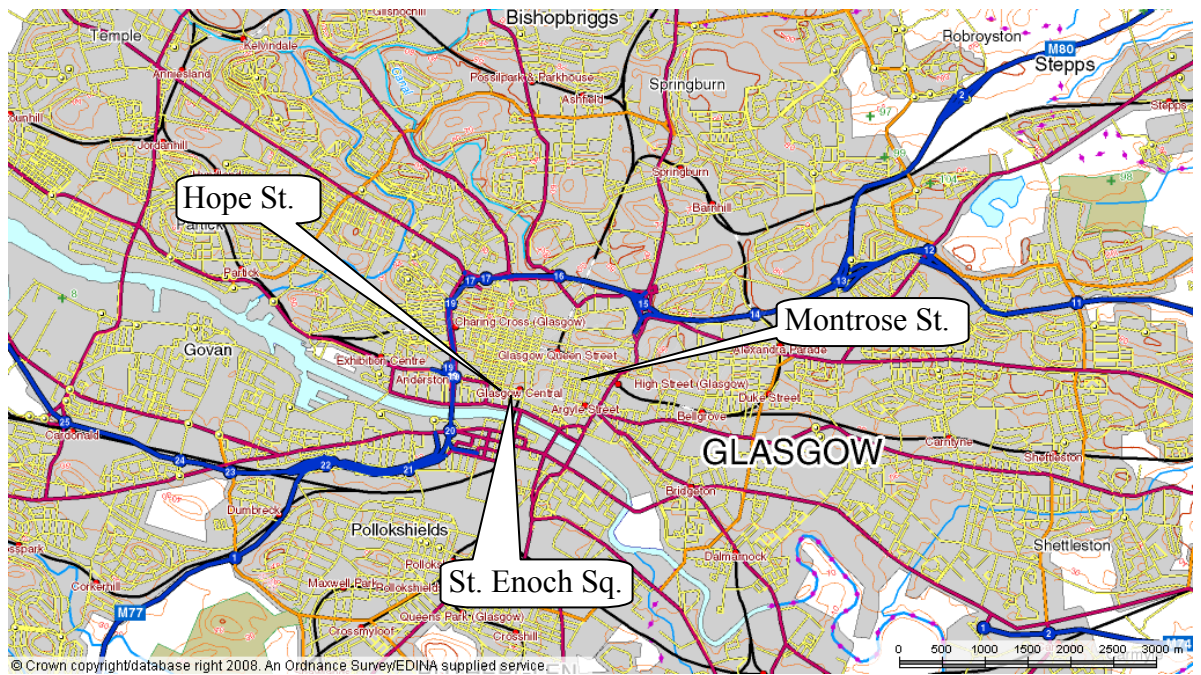


Figure 4.1 Map of monitoring sites for the main study (Glasgow).

Table 4.2 Location and classification codes of the monitoring sites in Glasgow (sites arranged from West to East).

Site Name	Grid Reference Easting	Grid Reference Northing	Location	Site type (DEFRA) ¹
Hope St.	2589	6651	End of Hope St.	Kerbside
St. Enoch Sq.	2589	6650	St. Enoch Sq.	Urban centre
Montrose St.	2595	6653	Glasgow City Chambers	Urban background

Hope St. (Kerbside, Glasgow)

The monitoring station was located at the southern end of Hope St. (Glasgow) at 1 m from the kerb of the East side of the street (which is oriented in a North-South direction). Figure 4.2 shows photographs of the surroundings in the four directions. The distance between buildings at either side of the street was approximately 20 m, and the building height was approximately 30 m on both sides of the street, forming what is known as a street canyon (two rows of buildings and a narrow street, where pollutants enter into a recirculation vortex, leading to a build up of concentrations). A junction 10 m south of the monitoring station was subject to frequent congestion during peak traffic flow periods (average traffic flows were estimated to be typically greater than 25,000 vehicles per day, NAQAb).

The monitoring equipment for the gaseous pollutants (NO_x , CO, SO_2 , BTEX, 1,3-butadiene), the TEOM analyser and WCPC were inside an air-conditioned self-contained monitoring station with the inlets positioned on the roof at a height of approximately 3 m. The Partisol sampler and the NO_2 PDTs were placed on the South side of the monitoring station. The Partisol inlet and NO_2 PDTs were approximately 2.5 m above ground level.



Figure 4.2 Photographs to the North (top left), South (top right), East (bottom left) and West (bottom right) of the monitoring station at Hope St. (Photos from www.airquality.co.uk).

St. Enoch Sq. (Urban Centre, Glasgow)

The monitoring equipment was within an air-conditioned self-contained station located in a pedestrian area surrounded by commercial premises. The site is classed as an urban centre. The nearest road was situated approximately 10 m from the site, with typical traffic flows estimated at approximately 20,000 vehicles per day (NAQAb). Figure 4.3 shows the geography surrounding the monitoring station. St. Enoch Sq. is approximately 300 m away from Hope St. Therefore, it is a good background site to examine the contribution of traffic to pollutant concentrations at Hope St.



Figure 4.3 Photographs to the North (top left), South (top right), East (bottom left) and West (bottom right) of the monitoring station at St. Enoch Sq. (Photos from www.airquality.co.uk).

The monitoring equipment for the gaseous pollutants (NO_x , CO , SO_2 , O_3), the TEOM analyser and BCPC were inside the monitoring station with the inlets positioned on the roof at a height of approximately 3 m. The Partisol sampler, NO_2 and NO_x PDTs were placed on the South side of the monitoring station. The Partisol inlet and PDTs were approximately 3 m above ground level.

Montrose St. (Urban Background/street canyon, Glasgow)

The monitoring equipment was located on the second floor of Glasgow City Chambers. The inlets for all monitored pollutants (PNC, PM_{10} , TEOM, NO_x , CO , SO_2 , and NO_2 & NO_x PDTs) were approximately 20 m above ground level, on Montrose St., around 2 m from the junction with Cochran St. The distance between buildings at either side of Montrose St. is approximately 10 m, and the building height was approximately 30 m on both sides of the street, forming a symmetrical street canyon (buildings at both sides with similar heights). The surroundings

comprise office buildings (Figure 4.4). Typical traffic flows are estimated between 8,000-15,000 vehicles per day (Henderson, 2005). The site is classed as an urban background (NAQAb). However, as it is located in an urban canyon, in this study it is referred to as urban background/street canyon.



Figure 4.4 Photograph of Glasgow City Council and the surrounding to the South (top right), East (bottom left) and West (bottom right) of the monitoring station at Montrose St. (Photos from www.airquality.co.uk).

Figure 4.5 shows a map with the location of the monitoring sites in London. Details of the sites are shown in Table 4.3.

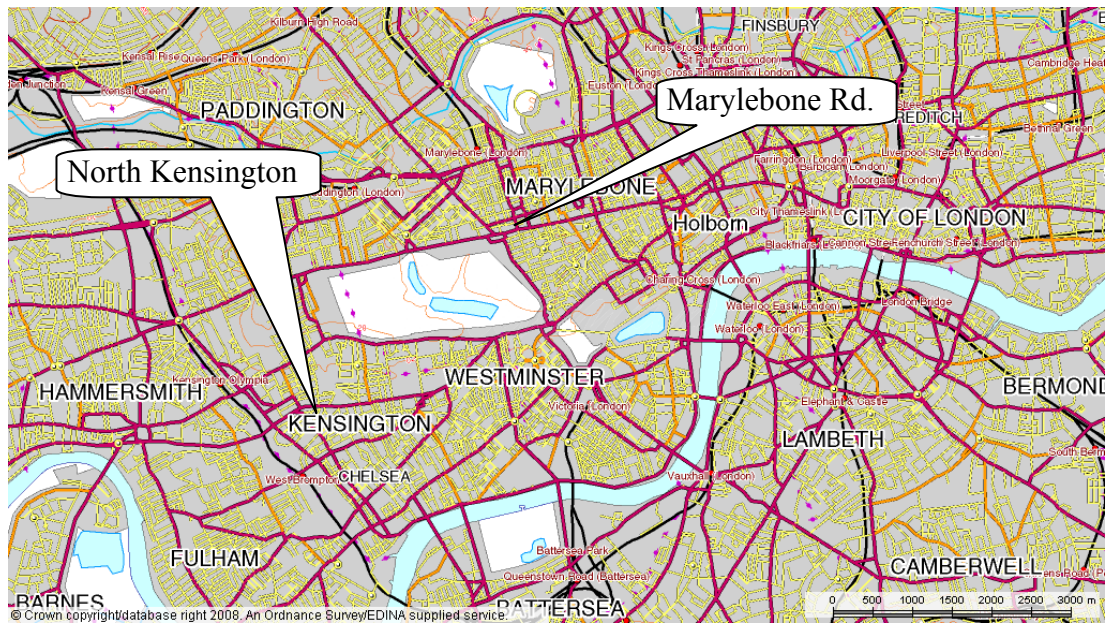


Figure 4.5 Map of monitoring sites in London.

Table 4.3 Location and classification codes of the monitoring sites (sites arranged from West to East).

Site Name	Grid Reference Easting	Grid Reference Northing	Address	Site type (DEFRA)
North Kensington	5240	1817	Sion Manning School, St. Charles' Square, London	Urban background
Marylebone Rd	5281	1820	Marylebone Rd. (opposite Madame Tussauds), London	Kerbside

A detailed description of the monitoring sites is provided below.

Marylebone Rd. (Kerbside, London)

The monitoring equipment was within an air-conditioned self-contained station located 1 m from the kerbside of Marylebone Rd., a 6 lane east/west trunk route, frequently congested road with around 80,000 vehicles per day (NAQA_c). There is a bus lane adjacent to the monitoring station, along which only buses and taxis circulate. Since buses and taxis use diesel, this site will have a larger influence of diesel exhausts compared to the other sites. The surrounding area forms a street canyon and comprises educational and commercial buildings plus housing. Figure 4.6 shows the surroundings of the monitoring station.



Figure 4.6 Photographs to the North (top left), South (top right), East (bottom left) and West (bottom right) of the monitoring station at Marylebone Rd. (Photos from www.airquality.co.uk).

North Kensington (Urban Background, London)

The monitoring equipment was within a self-contained station located in the grounds of Sion Manning School. The inlets were located 3 m above the ground. The site was located 7 km from west central London and is classified as urban background (NAQA_c). North Kensington is located at 4 km south from Marylebone Rd. making it a good background site for Marylebone Rd. (Carslaw et al., 2004; Jones and Harrison, 2005). Figure 4.7 shows the surroundings of the monitoring station.



Figure 4.7 Photograph of the North (top left), South (top right), East (bottom left) and West (bottom right) of the monitoring station at North Kensington. (Photos from www.airquality.co.uk).

4.4 EQUIPMENT OPERATION FOR PARTICLE SAMPLING

This section describes the monitoring equipment used during the main study. The BCPC and TEOM analyser used by DEFRA are briefly described, for comparison purposes with the WCPC and Partisol sampler respectively.

4.4.1 Water & Butanol based condensation particle counters

Condensation particle counters measure PNC in real time. Particles are grown to a size that can be detected optically. They rely on the difference between thermal diffusivity of air and mass diffusivity of a fluid in a laminar flow. The most widely used particle counters, and those used in this project, are manufactured by TSI (TSI Incorporated). The BCPC (Model 3022A) can detect particles of 7 nm diameter with 50 % efficiency (with the smallest detectable particle size =3 nm) (TSI, 2002). This model is used by DEFRA to monitor particle number counts across the UK (NAQAd). The monitoring site in Glasgow was located in St. Enoch Sq.

Henring et al. (2005) presented a new particle counter, marketed as TSI 3785, that uses water as the working fluid. In this model, particles down to 5 nm can be detected with 50 % efficiency (TSI, 2005). This water-based model was used in this project to monitor particles at Hope St. and Montrose St.

In the BCPC, the sample airflow is drawn into a heated chamber (35 °C) where it becomes saturated with butanol and flows into a cooled condenser tube (10 °C). When the sample aerosol starts to cool, butanol condenses onto the particles, increasing their size. At the end of the condenser, a nozzle accelerates particles through a laser beam. The light scattered at right angles from the particles strikes a photodetector. In the WCPC model, the temperatures have been reversed. First, the airflow passes through a conditioner chamber, where the walls are kept at 20 °C for normal operation. The airflow is brought to 100 % RH then, the air stream passes to the second part of the tube, the growth tube. Here the walls are wetted and heated to 60 °C to produce a high vapour pressure so that the partial pressure of water vapour is close to equilibrium vapour pressure. Diffusion of water vapour takes place toward the centreline of the tube. Since the mass diffusivity of water vapour is higher than the thermal diffusivity of air, a region of supersaturation with respect to water vapour is generated, producing condensational growth of particles (Hering et al., 2005).

In both models, particles are counted using different operation modes depending on the particle concentration. The BCPC uses three modes of particle counting: single particle real-time counting (for concentrations below 1,000 particles cm⁻³); single particle live-time (for concentrations between 1,000-10,000 particles cm⁻³); and photometric mode (for concentrations over 10,000 particles cm⁻³) (TSI, 2002). The WCPC only uses single particle live-time corrected (for concentrations below 20,000 particles cm⁻³) and photometric mode (for concentrations between 10,000-10⁷ particle cm⁻³) (TSI, 2005).

In the BCPC, in the single particle counting mode called *real time particle counting*; the concentration is calculated from the individual pulses from the photodetector. When a particle is in the optical viewing volume being detected, no other particles can be detected. Therefore, at concentrations over 1000 particle cm⁻³ the dead time

(the time a particle is waiting to be counted) increases and this needs to be subtracted from the effective sampling time. This time is called live-time (TSI, 2005). In the WCPC this dead time is multiplied by a constant value, regardless of particle concentration, calculated empirically for each instrument through dilution experiments with NaCl aerosol. This value accounts for the overlap of tails of adjacent pulses and extends the range of single particle counting to 20,000 particle cm^{-3} , while in the BCPC the single particle counting mode only works for concentrations below 10,000 particle cm^{-3} .

At concentrations over 10,000 particles cm^{-3} the BCPC uses the photometric mode. The WCPC between 10,000-20,000 particles cm^{-3} can use both modes and over 20,000 particles cm^{-3} uses only the photometric mode. In this mode, particle concentration is derived from the scattered light of the cloud of particles in the viewing volume and transformed empirically into concentration. The response time for the WCPC is 1.3 s (Hering et al., 2005) whereas for the BCPC it is between 7 and 10 s (Sem, 2002).

A summary of the characteristics of both models is given in Table 4.4.

Table 4.4 Operating parameters of TSI particle counters Model 3785 (water-based) & 3022A (butanol-based).

	TSI 3022A	TSI 3785
Minimum particle size detected (D_{50})	7 nm	5 nm
Maximum particle size detected	> 3 μm	> 3 μm (1 μm with cyclone)*
Particle concentration	0-10 ⁷ particle cm ⁻³	0-10 ⁷ particle cm ⁻³
Single particle counting	> 1,000 particles cm ⁻³ (real time) 1,000-10,000 particles cm ⁻³ (live time)	0 to ~ 20,000 cm ⁻³ (live time corrected)
Photometric mode	10 ⁴ - 10 ⁷ particles cm ⁻³ $\pm 10\%$ at < 5 x 10 ⁵ particles cm ⁻³ $\pm 20\%$ at > 5 x 10 ⁵ particles cm ⁻³	over ~ 2 x 10 ⁴ - 10 ⁷ particles cm ⁻³ $\pm 10\%$ at < 3 x 10 ⁴ particles cm ⁻³ Not specified
Aerosol Flow rate	High-mode: 1.5 \pm 0.15 L/min Low-mode: 0.3 \pm 0.15 L/min	1.0 \pm 0.1 L/min
Condensing fluid	Butanol	Distilled water

* TSI recommends the use of a cyclone to prevent particles larger than 1 μm from entering the system, since they can accumulate in the laser nozzle resulting in a decreased counting efficiency.

4.4.2 Partisol sampler and TEOM analyser

Gravimetric PM₁₀ measurements were taken with an R & R Partisol 2025 (Rupprecht & Patashnick Co. Inc., New York). The inlet used is designed to collect particles of 10 μm with an efficiency of 50 % at a flow of 16.7 L min⁻¹. Larger particles are removed by impaction.

The verification procedures required to maintain consistent operation of the Partisol sampler were performed using the operational guidance provided by USEPA (USEPA, 1998b) and the manufacturer (Rupprecht and Patashnick, 1999). The USEPA guidelines refer to measurement of PM_{2.5} with a Partisol sampler. However, the same procedure applies when using a PM₁₀ sampling head. The following checks were performed:

- Ambient air temperature: filters must be within ± 2 °C of the ambient temperature.
- Ambient pressure: filters must be within ± 10 mm Hg of the ambient pressure
- External Leak Check: pressure drop must not be more than 25 mm of Hg.
- Internal Leak Check: pressure drop must not be more than 140 mm of Hg.

- Volumetric flow was to be within $\pm 4\%$ of the specified flow (16.7 L min^{-1}).

Ambient temperature and pressure checks were performed at the beginning and end of the sampling campaign, since this was within the interval time of 4 weeks recommended by the USEPA (USEPA, 1998b). Temperature and pressure remained in the range specified above.

The external and internal leak checks were performed every 7 days to coincide with the filter exchange. The USEPA (USEPA, 1998b) recommends doing these checks every 5 days. However, this was considered unnecessary, since during a pilot monitoring period previous to the monitoring campaign in June 2006, leak checks were carried out satisfactorily every 7 days, and therefore it was decided that a 7-day interval was acceptable.

The flow was checked every 15 days, which is within the interval recommended by USEPA, USEPA (1998b). Flow measurements were made using an FTS (Streamline Flow Transfer Standard, Rupprecht & Patashnick Co. Inc., New York) certified against a National Institute of Standards and Technology (NIST)-traceable standard.

During the sampling campaign, the flow was halted on 4 occasions: once the Partisol at St. Enoch Sq. and 3 times the Partisol at Hope St. Filters sampled on these days were discarded. The halted flow was attributed to worn O-rings in the sampling head (Rupprecht and Patashnick, 2006). New O-rings were installed in both Partisol samplers.

Filters were exposed for 24-hours, with filter exchange taking place automatically at midnight. Filters were collected from the Partisol every 7 days. Therefore, they remained in the sampler for 6 days (plus the sampling day). The USEPA specification of 4 days is to avoid losses of semi volatile compounds (organic compounds, nitrate and sulphate), from the filters, which can occur at temperatures over 25°C . However, temperatures in Glasgow are rarely above 25°C , and therefore volatilization of compounds was not considered to be a major problem. The 95th

percentile of the hourly ambient temperature during the monitoring campaign was 22.2 °C. Temperatures exceeded 25 °C only for a period of 6 hours on the 18 July 2006 and 3 hours on the 19 July 2006.

Gravimetric data collected with the Partisol sampler was compared with data from the TEOM analyser averaged over the same time period. The TEOM analyser collects real time measurements of particulate mass. It consists of a filter cartridge on top of a hollow tapered crystal element. One end of the crystal is fixed and the other is free to vibrate at its natural frequency. The airflow passes through the filter and then through the crystal causing a decrease in the vibration. The change in the frequency of the vibration is proportional to the mass deposited on the filter. The inlet is heated to 50 °C to eliminate moisture (Rupprecht & Patashnick Co. Inc.).

TEOM data has a default correction factor of 3 $\mu\text{g m}^{-3}$ and slope correction of 1.03 (i.e. $3+1.03*\text{TEOM}$), denoted TEOM (1.03, 3). This correction factor was determined in the United States, using Arizona road dust to achieve US EPA certification (EQPM-1090-079) (Rupprecht and Patashnick, 1991). In the UK, a further slope correction factor of 1.3, denoted TEOM (1.03, 3, 1.3), is applied to all TEOM datasets to compensate for the losses of semi-volatile material (AQEG, 2005). The TEOM head is heated to 50°C to avoid water droplets entering the system, which has been reported to cause the loss of semi-volatile compounds (Green et al., 2001; DEFRA, 2003). The UK adjustment factor was calculated using measurements from co-location studies between the European Reference Method, which uses a gravimetric method, and the TEOM (APEG, 1999; DETR, 2000a and DETR, 2000b). Therefore, in this study PM_{10} gravimetric data was compared with uncorrected TEOM data, default corrected data and the UK corrected data (as it is shown in the NAQA).

4.4.3 Respirable dust sampler

The respirable dust sampler consists of a Higgins and Dewell type conductive plastic cyclone (SKC Inc., US) attached to an SKC universal sampling pump (Model 224-44XR). The cyclone holds a collection filter in a reusable cassette. A conductive tube

from Tygon® was used to connect the pump and the cyclone. The conductive material prevents particles from sticking to the walls, minimising particle losses.

The cyclone works as a particle-size selector. It is designed to meet the ISO/CEN/ACGHI respirable sampling curve (ISO 1995, CEN 1992, ACGHI 1999) with a 50 % cut-off point of $4.0 \mu\text{m}$ at 2.2 L min^{-1} (SKC Inc., US).

Filters were exposed for 7 days. Flow rates were adjusted on the first day of each sampling period and then measured on day 3 and 7 by using a flow meter (Aalborg Instruments & Controls Inc.) with a resolution of 0.05 L m^{-3} . An average flow rate was calculated from the three measurements. Each filter was exposed for 7 days to collect enough PM_4 for the subsequent analysis.

SKC pumps were operated according the manufacturer's guidance (SKC Inc., US). Inlets were placed 2.5 m above the ground and sheltered to protect them from rain. Filter holders and cyclones were washed in Decon 90, rinsed in $18 \text{ M}\Omega$ water and then air dried. The gravimetric procedure and filter handling was identical to that for the PM_{10} filters and is described in Section 4.7.

4.5 GRAVIMETRIC ANALYSIS FOR PM_{10} & RESPIRABLE DUST FILTERS

Gravimetric analysis was performed following USEPA guidance (USEPA, 1998a,b). The filters were weighed with a Sartorius® MC5 balance with a measurement resolution of $\pm 1 \mu\text{g}$. The mass output was automatically recorded. Filters were placed under an ionizing blower (Stat Attack IB-8, Bucks) before being weighed to neutralize any build up of electrostatic charges in the filter that could affect the mass measurement.

The filters were made of polytetrafluoroethylene (PTFE) Zeflour® (VWR International, Leicestershire, UK) with a pore size of $2 \mu\text{m}$ and 47 mm diameter for PM_{10} sampling and 25 mm diameter for PM_4 sampling.

To test the stability and sensitivity of the microbalance a standard class 1 weight of $200 \mu\text{g}$ accredited by NIST was weighed ten times per day for a five day period. To

ensure the accuracy of the balance during the subsequent weighing sessions, the standard (weight) was weighed at the beginning and end of each weighing session. The LOD ($\text{LOD}=3\times\text{SD}$) was calculated from these values (Table 4.5).

Table 4.5 Mass variability of a standard weight of 200 mg.

	5 days check n=50	All weighing sessions n=20
Mean (mg)	200.003	200.003
Median (mg)	200.003	200.002
SD (mg)	0.00086	0.00074
RSD	0.00043	0.00037
Maximum (mg)	200.005	200.004
Minimum (mg)	200.001	200.002
LOD (mg)	0.0026	0.0022

SD: standard deviation; RSD: relative standard deviation ($100\times\text{SD}/\text{mean}$); LOD: limit of detection

The mean difference between the mass weight and the mean of all mass measurements was therefore 3.0 μg and the LOD of the balance over the course of all weighing sessions was 2.2 μg . These are within the recommended USEPA values (3 μg difference and 5 μg LOD) (USEPA, 1998b).

The mass of the filters is less stable than the mass of standard weights because filters can have slight gains or losses of mass due to humidity changes or electrostatic effects. To assess filter precision, six laboratory blank filters (filters randomly selected from the same box as the exposed filters, though never taken out to the field) (25 mm for PM_4 sampling and 47 mm for PM_{10} sampling) were weighed three times per day, for 6 days to estimate the within-day and day-to-day variability. Results are shown in Table 4.6.

Table 4.6 Precision of Zefluor® blank filters weighed with the MC5 Sartorius® microbalance.

Values (μg)	PM_{10} (47 mm DIA)	PM_4 (25 mm DIA)
Mean SD of within-day weighings (n=6)	1.2	1.0
Mean SD of day-to-day weight changes (n=5)	1.3	0.6
Mean SD of between-day weighings (n=6)	2.9	1.7

DIA: diameter; SD: standard deviation

Based on the values from Table 4.6, 3.0 μg variability was allowed between two replicate measurements for both types of filters. This is within the USEPA

recommendations (4 μg variability between replicate measurements) (USEPA, 1998b).

The day to day mass change found in this study was slightly lower than that reported by Hibbs, (2002) (2.2 μg) using the same procedure and a balance of the same precision.

The LOD was defined as $3 \times \text{mean SD of day to day weight change} \times \sqrt{\frac{n+1}{n}}$ and the 95 % confidence interval (CI) for a single filter weighing were calculated as $1.96 \times \text{mean SD of within day weighing}$, as defined by Vaughan et al. (1989). The above formula for the LOD accounts for the combination of errors when subtracting the mean mass change of blank filters from the mass change in the sample filter. Results are shown in Table 4.7.

Table 4.7 Estimates of confidence interval (CI) and limits of detection (LOD) in weighing Zefluor® filters. $\text{LOD} = 3 \times (\text{SD day-to-day weight change} \times \sqrt{\frac{n+1}{n}})$.

Filter diameter (mm)	95% CI		LOD	
	μg	$\mu\text{g m}^{-3}$	μg	$\mu\text{g m}^{-3}$
PM ₁₀ (47 mm)	2.3	0.1	4.2	0.2
PM ₄ (25 mm)	1.2	0.1	2.0	0.1

Air volume: 24 $\text{m}^3 \text{ day}^{-1}$ for PM₁₀ filters and 22.2 $\text{m}^3 \text{ day}^{-1}$ for PM₄ filters

Measured PM₁₀ concentrations in this study ranged from 10 to 50 $\mu\text{g m}^{-3}$ and PM₄ from 8 to 25 $\mu\text{g m}^{-3}$. Therefore, for a 24-hours sample volume the LOD represents between 0.4-2.0 % of the PM₁₀ concentration and 0.4-1.25 % of the PM₄ concentration.

The LOD values compared well with those reported in the literature. Fisher et al. (2000) reported a LOD (calculated as $3 \times \text{SD of field blanks}$) of 7.2 $\mu\text{g m}^{-3}$ for 37 mm 2 μm pore filters. Hibbs (2002) reported a LOD of 0.3 $\mu\text{g m}^{-3}$.

The weighing room was not controlled for RH and temperature. The USEPA (USEPA, 1998b) and European guidelines (EN 14907) recommend conditioning the filters at 40 % and 50 % RH, respectively to avoid mass gain through water

absorption. However, Green et al. (2001) and Chow et al. (1995) found that mass gains do not occur until RH is over 60 % and 70 % respectively. In the present study, pre and post sampling filters were kept in a desiccator (inside the Petri dishes with the lids open) for 24-hours prior to weighing as recommended in ULTRA's project guidance (ULTRA, 1998a). The desiccant (silica gel) was changed regularly. The RH in the desiccator was between 26 % and 32 % and the room temperature ranged from 19 to 23 °C. To control for any humidity effect on the filters, six PM₁₀ and six PM₄ filters were used as control filters and weighed in each weighing session (1 control measured after every 3 filters). The mean change in mass of the control filters was subtracted from the observed mass of pre and post sampling filters. This adjustment does not take into account potential gains in mass on the deposited PM on the exposed filters. However, these were anticipated to be negligible for this procedure.

The procedure used to weigh the sample filters is described below:

1. The balance was left in standby mode continuously, and the ionizing blower was turned on 30 minutes prior to any measurement being taken.
2. Laboratory coats and gloves were stored in the weighing room and were used only for weighing to minimize contamination from the external environment.
3. The microbalance was cleaned with an antistatic cloth (supermarket brand) prior to use.
4. The draught shield was opened several times to equilibrate the air in the draught shield chamber with room air.
5. An internal calibration was made according to the microbalance's operating manual: the balance calibrates itself using a series of five internal calibration weights. This calibration was done automatically each time the temperature changed by 1 °C.

6. A standard class 1 weight (200 mg) was weighed. If the mass was larger or smaller than $200 \pm 3 \mu\text{g}$, the weight was weighed again. If the mass remained larger or smaller than $200 \pm 3 \mu\text{g}$ the balance was re-calibrated.
7. A Petri-dish was taken out of the dessicator and using working standard forceps previously washed with ethanol, the filter was taken and placed 5-10 cm from the ionizing blower for around 30 seconds. This time is sufficient to neutralize any build-up charge in air with RH over 20 %, such as that in the weighing room (USEPA, 1998b).
8. The filter was placed on the centre of the balance's weighing pan and the shield was closed. When a stable measure appeared, the value was recorded automatically in an Excel spreadsheet. The balance was left to zero itself and not by using the TARE button.
9. Each post-sampling filter was transferred to the Petri dish and returned to the dessicator and the pre-sampling filters were placed in the filter holder, inside the magazine and this within an insulated protective container for shipping to the field.
10. After 3 filters a control filter was weighed.

Steps 7-10 were repeated until all filters were weighed. Then all filters were re-weighed in order to have two replicates of each filter. If the second replicate differed, by more than $\pm 3 \mu\text{g}$ both measurements were discarded and the filter was weighed again twice. If the deviation remained above $\pm 3 \mu\text{g}$ then the filter was put back in the dessicator, conditioned for at least 24-hours and re-weighed again. This was necessary only with one filter batch.

The standard class 1 weight was weighed again at the end of every weighing session. The mass of the standard weights were always within $200 \pm 3 \mu\text{g}$.

The USEPA guidelines (USEPA, 1998b) indicate that Teflon® filters can exhibit a mass loss of up to $150 \mu\text{g}$ over a period of up to 6 weeks after removal from the original packaging due to outgassing from the filter media. The filters used in this project came from two different boxes. The box with the first filters used had been

opened more than 6 weeks prior to mass measurements and the second box was opened and left to condition for two weeks. Six new control filters were chosen at random from this new box and therefore any change in the filter weights should have been accounted for by the control filters.

After measuring reflectance the filters were kept in Petri dishes (wrapped in aluminium foil, and placed inside a dessicator, inside a freezer at -20°C) prior to chemical analysis.

4.6 REFLECTANCE ANALYSES OF PM_{10} & RESPIRABLE DUST FILTERS

The reflectance of PM_{10} and PM_4 filters was measured using a monochromatic reflectometer (EEL Model 43D, Diffusion Systems Limited, London, U.K) and transformed into an absorption coefficient using the ISO Equation 4.1 (ISO, 1993). The filter material does not affect absorption coefficients calculated by this method.

$$a = \frac{A}{2V} \ln\left(\frac{R_0}{R}\right) \quad \text{Equation 4.1}$$

Where:

a: absorption coefficient (m^{-1}).

A: area of the stain on the filter paper (m^2).

A: $\pi(d/2)^2$, where d is the inner diameter of the filter's poly support ring. For filters of 47 mm the value of A was $11.95 \times 10^{-4} \text{ m}^2$ and for filters of 25 mm $A = 3.46 \times 10^{-4} \text{ m}^2$.

V: volume sampled (m^3) (24.048 m^3 for PM_{10} filters and 22.046 m^3 for PM_4 filters).

R_0 : reflectance of a field blank filter.

R: reflectance of an exposed filter.

Two different methods for adjusting the reflectometer to 100 % reflectance were found in the literature. The British Standard Institute (BSI) specifies calibration of reflectance value to 100.0 % using a blank filter (BSI, 1969). This was the approach used in the UK black smoke network until its closure in 2005 and it is also the method used by NPL in the re-established BS network. The ULTRA project (ULTRA, 1998b) developed a method to select a representative control filter to calibrate the reflectometer. The reflectance of 5 blank filters was measured at 5 different points and the filter with the median reflectance value was selected as the control filter. Penttinen et al. (2000) used the white tile provided by the manufacturer to adjust the reflectometer to 100.0 %. Penttinen and the ULTRA project were interested in deriving an absorption coefficient using the ratio of reflectance values. Therefore, the method by which the spectrometer is calibrated should be irrelevant, as long as it has a linear response to light intensity. This stands in contrast to the BS method, where a concentration is derived from the reflectance value.

To study whether the method for adjusting the reflectance to 100.0 % affected the reflectance observed in exposed filters, 37 exposed filters were measured using both methods. The correlation coefficient was $r = 0.98$ and the mean RSD between both measurements was 1.8 %, which is within the acceptable deviation between measurements of a single filter recommended by the ULTRA project (ULTRA, 1998b). However, these values could differ if a different blank filter is used to calibrate the spectrometer, since the reflectance of blank filters can vary. To study this issue further the variability in blank reflectance of ten blank filters was examined. 10 PM_{10} and 10 PM_4 filters were chosen at random from the same box and their reflectance was measured (Table 4.8).

Table 4.8 Variability of blank reflectance of Zefluor® filters.

	PM ₁₀ filter blank	PM ₄ filter blank
Mean	100.65	99.60
Median	100.60	99.60
SD	0.99	0.86
RSD (%)	0.99	0.86
Minimum	99.90	99.30
Maximum	100.20	103.30

SD: standard deviation; RSD: relative standard deviation
(100*SD/mean)

The reflectance of blank filters varied slightly within filters from the same box and therefore it was considered that less error was introduced by using a fixed media, the white tile, to adjust the reflectance to 100.0 %. Therefore, results in this thesis are presented as adjusted with the white tile.

To confirm that the particles were uniformly distributed on the filter, the reflectance was measured at 5 different points of 10 PM₁₀ filters. The RSD among the 5 measurements ranged from 0.09 to 0.3 % and the correlation coefficient between reflectance measurements ranged from 0.97 to 0.99. Thus, for practical reasons, only two measurements were taken for each filter. It was considered unnecessary to perform this test on the filters used for sampling PM₄ since these filters have a much smaller diameter (25 mm) and the measuring head of the reflectometer covered most of the filter.

The reflectance was measured in a room with low lighting to eliminate the effects of sunlight and other light sources on the measurements. The detailed protocol is described below:

1. The reflectometer was switched on and allowed to warm up for at least 15 minutes.
2. The standard plate and reflectometer measuring head were cleaned with a lint-free cloth.
3. Before adjusting the measuring head, the reflectance reading was adjusted to zero using the zero control on the front panel of the reflectometer.

4. The measuring head was attached and positioned on the white standard tile. The reflectance was adjusted to 100.0 units using the coarse and fine controls. Then, the head was placed on the grey standard tile and adjusted to 33 ± 1.5 reflectance units. The head was then moved back to the white tile to ensure 100.0 % reflectance. This demonstrates the linearity of the reflectometer.
5. An exposed filter was removed from the Petri-dish, using plastic forceps previously washed with ethanol, and placed on the white tile.
6. The circular mask was placed centrally on the stain. It was checked carefully to ensure that none of the "clean/non exposed" part of the filter was visible through the hole, especially for the 25 mm filters, since the diameter was close to that of the underlying disk.
7. After every 5 filters measured the 100.00 % reflectance was rechecked by placing the head on the white tile. If the measurement remained at 100.00 units, the rest of the filters were measured. If the '100' setting had drifted, absorbance was re-adjusted to exactly '100.00' and the previous five filters re-measured to ensure that no error had been made.
8. The whole process was repeated to obtain two measurement replicates. If the duplicate measurement deviated by more than 3 % from the first measurement, both measurements were discarded and the filter was re-measured again twice. The mean of both measurements was calculated.

The only aspect of the above protocol that differs from the BS protocol is that the 100.0 % reflectance was adjusted using the white tile instead of a blank filter, and that two replicate measurements were taken for each filter, instead of one.

4.7 SEQUENTIAL EXTRACTION OF PARTICULATE-BOUND PAHS & TRANSITION METALS FROM PM₁₀ FILTERS

4.7.1 Cleaning and storage

The cleaning procedure for the glassware followed USEPA guidelines (USEPA, 1998c) for analysis of PAHs and Hibbs (2002) for analysis of metals. The combined procedure was as follows:

1. Glassware was soaked for 24 hours in a bath of 5 % v/v Decon 90 detergent in tap water.
2. Glassware was rinsed with a copious amount of hot tap water followed by rinsing with 18 MΩ water.
3. Finally, the glassware was rinsed with Aristar grade acetone (BDH, Poole, England) and AnalaR[®] grade hexane (BDH, Poole, England).
4. Glassware (except volumetric glassware) was heated in a muffle furnace at 400 °C for at least 8 hours to eliminate any trace of organic compounds.
5. Glassware was soaked for 24 hours in 10 % v/v Aristar grade HNO₃ in 18MΩ water.
6. Glassware was soaked for 24 hours in 18 MΩ water to rinse off the acid from the above stage.
7. Wrapped in aluminium foil and stored in a clean environment.

All soaking baths were covered and airtight.

Pipette tips were rinsed with standard grade acetone and hexane, left to air dry and then soaked according to steps 6-7.

The polypropylene containers used to store the metal extracts, were rinsed according to steps 1&2 and 5&6.

4.7.2 Extraction procedure

Particulate PAHs and transition metals were sequentially extracted following a modification of a procedure developed by Piñeiro et al. (2003). Piñeiro et al. digested TSP quartz filters in a microwave (power 400 W and irradiation time 20 min) with a hexane: acetone mix (1:1) to extract the PAHs. The residue was then digested with HNO₃ and HF to extract the full amount of total metal. The metal recoveries were not affected by the preceding extraction of PAHs Piñeiro et al. (2003).

In the present study, the same solvents as in Piñeiro's study were used to extract the PAHs, as they have been proven not to affect the release of metals from the filter. However, instead of using a microwave, filters were ultrasonicated in a water bath for 30 minutes. These conditions are less aggressive than those in a microwave and therefore should not cause the release of metals.

The ultrasonication time for the PAH extraction was based on that used by Fisher et al. (2000). Fisher et al. showed extraction efficiencies of 95-99 % using 30 minutes of ultrasonication in 2.5 mL of acetone. In the present study, with extraction by acetone and hexane, the influence of the ultrasonication time on the effectiveness of PAH extraction was examined by extracting 5 PM₁₀ filters three times. The detailed procedure is described in Section 4.7.3.

After the PAH extraction, filters were ultrasonicated in 18 MΩ water to extract the water-soluble metals following the procedure described by Hibbs (2002). Ultrapure water was selected as the bioavailable extractant based on results reported by Hibbs (2002). Hibbs observed that the use of phosphate-based solutions caused interferences in the Ionization Coupled Plasma Mass Spectrometry (ICP-MS) detection of some elements under study. Other extracts including potassium citrate and tris(ma) introduced unacceptable additional blank variability.

The details of the complete protocol of the sequential extraction are described below.

1. Filters were folded twice, using previously cleaned forceps, with the sampling side of the filter facing outwards and placed in a Pyrex test tube. This was done so that the entire filter was covered in the extracting solvent.
2. 2.500 ± 0.001 mL of acetone/hexane (1:1) (Aristar[®] grade acetone and AnalaR grade hexane, from BDH, Poole, England) were added to the Pyrex tube containing the filter.
3. 200 μ L of a standard solution of 125 ng mL^{-1} of 9 D-10 Acetanaphthene and D-12-Indenol (1,2,3-c,d)pyrene (qmx Laboratories, Augsburg, Germany) were added to each sample, to yield a final concentration in the middle of the calibration range. These standards were added to calculate the efficiency of the sequential extraction.
4. Tubes were covered with cling film, and sonicated for 30 minutes. The temperature was kept at 20 °C to avoid volatilization of acetone and PAHs.
5. 7 standard calibration solutions were prepared from a mix of 16 PAHs solution (qmx Laboratories, Augsburg, Germany). The concentrations ranged from 0.25 to 20 ng mL^{-1} . Deuterated standards were added to match the same range of concentrations.
6. The extracts and calibration solutions were stored in Teflon[®] sealed screw-cap amber borosilicate glass vials and kept inside a refrigerator below 4 °C until they were shipped to the Natural Environmental Research Council (NERC) Gas Chromatography Mass Spectrometry (GC-MS) facility in Bristol University for analysis.
7. The extracts were concentrated to 100 μ L in the NERC GC-MS facility with a gentle N₂ stream and analysed by GC-MS.
8. After the PAH extraction the filters were removed from the test tubes and placed in a fresh tube. They were allowed to air dry for approximately 30 minutes to evaporate the remaining acetone in the filter, since acetone can damage the mass spectrometer used for the analysis of the metal extracts.

9. 7.00 ± 0.05 mL of 18 M Ω water were added to each tube.
10. Tubes were covered with cling film and ultrasonicated for 60 minutes.
11. During the ultrasonication the temperature was not controlled and rose to approximately 36 °C (i.e. similar to the temperature conditions in the human lung).
12. 5.00 ± 0.05 mL of the extract were transferred to a polypropylene tube and acidified with 0.550 ± 0.001 mL of a solution of 20 % HNO₃ to avoid any metal being adsorbed to the walls of the storage container.
13. Containers were kept in a refrigerator under 4 °C until they were shipped to the NERC ICP-MS facility in Kingston University for analysis.
14. Shipping was carried out using an insulated container, where temperatures were kept at approximately 10 °C.

4.7.3 Assessment of losses of metals during the PAHs extraction

To test for losses of metal concentration during the PAH extraction the metal concentration in 3 filters analysed for PAHs and metal was compared with that of other 3 filters (which were expected to have the same amount of metals) which only underwent metal extraction. Since there was not replicate filters available, filters consisted of two halves of different filters: 6 filters (F) were cut in half (h), (F₁h₁, F₁h₂, F₂h₁, F₂h₂...) and two halves of different filters underwent extraction together so that the metal concentration in F₁h₁&F₂h₁ was equal to the metal concentration in F₁h₂&F₂h₂ (this assuming that the metals were distributed homogeneously in the filters).

The two halves of each filter (FMh₁ and FMh₂) did not have exactly the same mass. Therefore, to make the results comparable, metal concentration was expressed as $\mu\text{g metal g}^{-1}$ of PM₁₀. The mass of PM₁₀ in each filter half was calculated using Equation 4.2 (the equation refers to half 1, half 2 was calculated in a similar way).

$$PM_{10} F_n h_1 = \frac{FM_n h_1}{FM_n} \times PM_{10} F_n \quad \text{Equation 4.2}$$

Where,

$PM_{10} F_n h_1$: mass of PM_{10} in the half filter 1 (h_1) of filter n (F_n)

$FM_n h_1$: mass of half filter 1 of filter n (half filter + corresponding PM_{10})

FM_n : mass of the entire filter n (filter + PM_{10})

$PM_{10} F_n$: mass of PM_{10} in the entire filter n

n : 1, 2, 3.

The mass of PM_{10} in the two filter halves digested together (e.g $PM_{10} F_1 h_1$ & $PM_{10} F_2 h_1$) were added to give the total PM_{10} mass corresponding to each combined sample.

It would have been simpler to compare the metal concentration in two halves of the same filter. However, the expected metal concentration in half of a filter could have conceivably fallen below the LOD of the instrument, for metals of low concentrations (e.g. As, Cd, Ni, V and Pb). In fact, some PM_{10} filters collected in Glasgow showed mass of Ti, Ni and Cd below the LOD. A detailed description of metals below the LOD has been included in section 4.9.3.

Ideally, a certified reference material should have been used. However, at the time of conducting the experiments there were not such a material with certified values of water-soluble metals available at the National Institute of Standards and Technology (NIST). Furthermore, particles in reference material for PM are “free” i.e. they are not embedded in a filter, and therefore the analysis would not have been completely representative of the real conditions in this project. Therefore, the method described above was considered to be more appropriate.

4.7.4 Efficiency of the PAH extraction

To examine the influence of the ultrasonication time on the extraction efficiency of the PAHs, 5 PM₁₀ filters were extracted 3 times according to the procedure in section 4.7.2 (steps 1-6). After each extraction the extract was stored in a borosilicate screw-cap vial, the filter transferred to a fresh tube and the extraction repeated and so on until 3 extractions were performed.

4.8 PAH ANALYSES

This section describes briefly a gas chromatography mass spectrometer instrument. The instrument was operated by members of the NERC GC-MS facility at Bristol University.

4.8.1 Gas Chromatography Mass Spectrometry

The coupling of GC with a mass spectrometer detector provides high sensitivity and selectivity along with the ability to separate the components of complex samples.

In GC the sample is injected into a carrier gas (mobile phase) which flows through a column packed with a porous/adsorbent material (stationary phase). The molecules in the sample are partitioned between the two phases. The ratio of the concentration of molecules in the mobile phase over the concentration of molecules in the stationary phase is characteristic of each compound. This allows each compound to spend a different time in the stationary phase. This time is called retention time. Thus, each compound enters the ionization chamber of the detector at a different time, which allows its identification and quantification. There are two types of ionization techniques: electron or chemical ionization. In the second, molecular species tend to be relatively stable when compared with their analogous molecular ion. This improves the likelihood of detecting the molecular species and so compared with electron ionization, molecular peaks tend to be intense and fragmentation relatively sparse.

After ionization, the positive ions are accelerated and enter a magnetic field where they are deflected into circular paths, the radii of which are proportional to the square root of their mass to charge ratio (m/e). The m/e ratio of a single charged ion is given by Equation 4.3:

$$\frac{m}{e} = \frac{B^2 r^2}{2V} \quad \text{Equation 4.3}$$

Where B is the strength of the magnetic field, r is the radius of the path and V is the potential gradient used to accelerate the electrons (McMaster & MacMaster, 1998).

In this study, a ThermoQuest Trace Mass® GC-MS fitted with a high temperature capillary column (50m x 0.22 mm internal diameter × 0.25 µm film thickness) (HT-8) was used. The sample was discharged directly into the column (by means of a syringe) instead of the sample being injected into a heated tube where it is vaporised and swept away by the carrier gas. On-column injection has the advantage of not over-heating the sample meaning that thermally labile solutes are not decomposed and it provides better column efficiencies.

The GC was operated in constant flow mode at a flow rate of 1 mL min⁻¹. Samples were introduced via a programmable temperature vaporising (PTV) injector programmed to rise from 75 °C to 320 °C at 14.5 °C per second and hold at 320 °C for 61 minutes. Splitless time was 1 minute with a split flow of 10 1 mL min⁻¹. The temperature programme was 70 °C rising at 15 °C to 320°C and holding there for 45 minutes. The ionization mode was electron ionization set to 70 eV, source temperature 200 °C and a transfer line temperature of 320 °C.

The MS detector was a photomultiplier detector, which operated in full-scan analysis mode, scanning m/z 50-300 with a scan time of 0.6 seconds and a multiplier voltage of 350 V.

4.9 METAL ANALYSIS

This section briefly describes the characteristics of an ICP-MS instrument. The analysis was done under the guidance of members of staff of the NERC ICP-MS facility, Kingston University.

4.9.1 ICP-MS

For this project, a Thermo Elemental PlasmaQuad® was used. The sample was drawn into the nebuliser with a peristaltic pump. Then it is passed to a spray chamber and from there to the central channel of the ICP, the torch. The torch, which consists of 3 concentric quartz tubes, induces plasma formation by collision of accelerated electrons with a flow of argon (Ar) atoms. When the sample reaches the plasma it is evaporated, then atomised and finally ionized.

The plasma with the ionized sample is transferred to the quadrupole through the instrument interface: the plasma ion population is driven through a cone with 1 mm aperture, to an expansion chamber where it reaches supersonic speeds. A representative sample of the plasma ion population passes through another cone (microskimmer) of 0.7 mm. Then, it is led through a series of lenses with different voltages, which separate the positive ions from the UV photons. The positive ions reach the quadrupole.

The quadrupole acts as a mass filter allowing only ions of the specified mass to charge ratio (m/e) to pass through to the detector (a dynode). The quadrupole consists of four cylindrical molybdenum rods to which are applied different potentials. The four rods are arranged with one pair in the X plane and one in the Y plane. As ions enter the quadrupole, they begin to oscillate in both the X and the Y planes. By sweeping these potentials, only ions of a particular mass are able to resonate at the correct frequency and pass through the quadrupole at any time.

The dynode detector works on the principle of electron multiplication: an ion striking the first dynode releases electrons, which accelerate towards and into the dynode beneath, releasing more electrons. The resulting electron cloud is counted as single

pulse. The voltage of the pulse is then transformed to a frequency via a voltage to frequency converter (VFC) and related to the concentration of the element in the sample by use of a calibration curve.

Interferences in ICP-MS are classified as:

1. *Spectral interferences*: when the quadrupole cannot distinguish the mass of two ions, the signals appear overlapped. These interferences can arise from:
 - Isobaric overlap: caused because two ions have very similar masses. For example ^{58}Ni (57.9307) and ^{58}Fe (57.9332). These interferences can be avoided by selecting isotopes with different masses.
 - Polyatomic ions: are formed in the plasma and can overlap with some of the metals of interest. For example, $^{35}\text{Cl}^{16}\text{O}$ overlaps with ^{51}V . These interferences can be important if the concentration of the interfering ions in the sample are high.
 - Refractory oxide ions: these species occur either as a result of incomplete dissociation of the sample matrix or from recombination in the plasma. For example, formation of $^{47}\text{Ti}^{16}\text{O}$ and $^{49}\text{Ti}^{17}\text{O}$ in the plasma interferes with ^{63}Cu and ^{66}Zn respectively. However, because of the low concentration of Ti compared to Zn and Cu the interferences are insignificant.
 - Double charged ions: they can be formed in the plasma and since the detector works on a mass to charge ratio, this can cause interferences for ions whose mass is half of the mass of the isotopes in the sample. However, generally ICP instruments are set up so that they do not produce double charged ions
2. *Non spectral interferences*: these are due to matrix effects, in which the analyte sensitivity is influenced by the reagents or other sample constituents. For example, high concentrations of Na (over $200\ \mu\text{g mL}^{-1}$) or Fe, Mn or Ca ($500\ \mu\text{g mL}^{-1}$) can suppress or enhance the signals of other metals (Jarvis, 1992). However, the concentrations dealt with in this work were lower than those values.

Table 4.9 shows the isotopes chosen for each element and their potential polyatomic interferences.

Table 4.9 Summary of isotopes chosen for each element and their possible polyatomic interferences.

Element	Isotope (m/e)	Abundance of analysis isotope (%)	Dominant polyatomic interferences
Ti	47	7.8	$^{30}\text{Si}^{16}\text{O}^1\text{H}$
	49	5.5	$^{32}\text{S}^{16}\text{O}^1\text{H}$, $^{35}\text{Cl}^{14}\text{N}$, $^{37}\text{Cl}^{12}\text{C}$
V	51	99.7	$^{35}\text{Cl}^{16}\text{O}$
Cr	52	83.8	$^{35}\text{Cl}^{17}\text{O}$, $^{37}\text{C}^{15}\text{N}$, $^{40}\text{Ar}^{12}\text{C}$
Mn	55	100	$^{40}\text{Ar}^{14}\text{N}^1\text{H}$
Fe	57	2.14	$^{40}\text{Ar}^{16}\text{O}^1\text{H}$
Ni	60	26.2	$^{44}\text{Ca}^{16}\text{O}$, $^{43}\text{Ca}^{16}\text{O}^1\text{H}$
Cu	63	69.1	$^{40}\text{Ar}^{23}\text{Na}$
	65	48.9	$^{32}\text{S}^{33}\text{S}$
Zn	66	27.8	$^{35}\text{Cl}^{15}\text{N}^{16}\text{O}$, $^{32}\text{S}^{33}\text{S}$
	68	15.86	$^{40}\text{Ar}^{12}\text{C}^{16}\text{O}$
As	75	100	$^{40}\text{Ar}^{35}\text{Cl}$
Cd	111	12.86	
Pb	208	52.38	

Interferences of combinations of Ar, O, H and N are present across all samples and blanks, since they are formed in the Ar plasma and therefore will be removed by blank correction. However, polyatomic species containing ions which were only present in the sample extracts (e.g. Na or Cl from dissolved sea salt, or S from dissolved sulphate) could pose a problem.

For example, $^{35}\text{Cl}^{14}\text{N}$ and $^{37}\text{Cl}^{12}\text{C}$ species interfere with the isotope ^{49}Ti resulting in higher concentrations for ^{49}Ti than those of the isotope ^{47}Ti . The coefficient of determination between both was relatively low (0.41) (Figure 4.8). Therefore, only concentrations of the ^{47}Ti isotope were presented in the results section. Interferences from SiOH on ^{47}Ti are not thought to be a problem since Si in PM is mostly in the form of water-insoluble silicates. Therefore, Si concentration in the sample extracts was likely to be negligible.

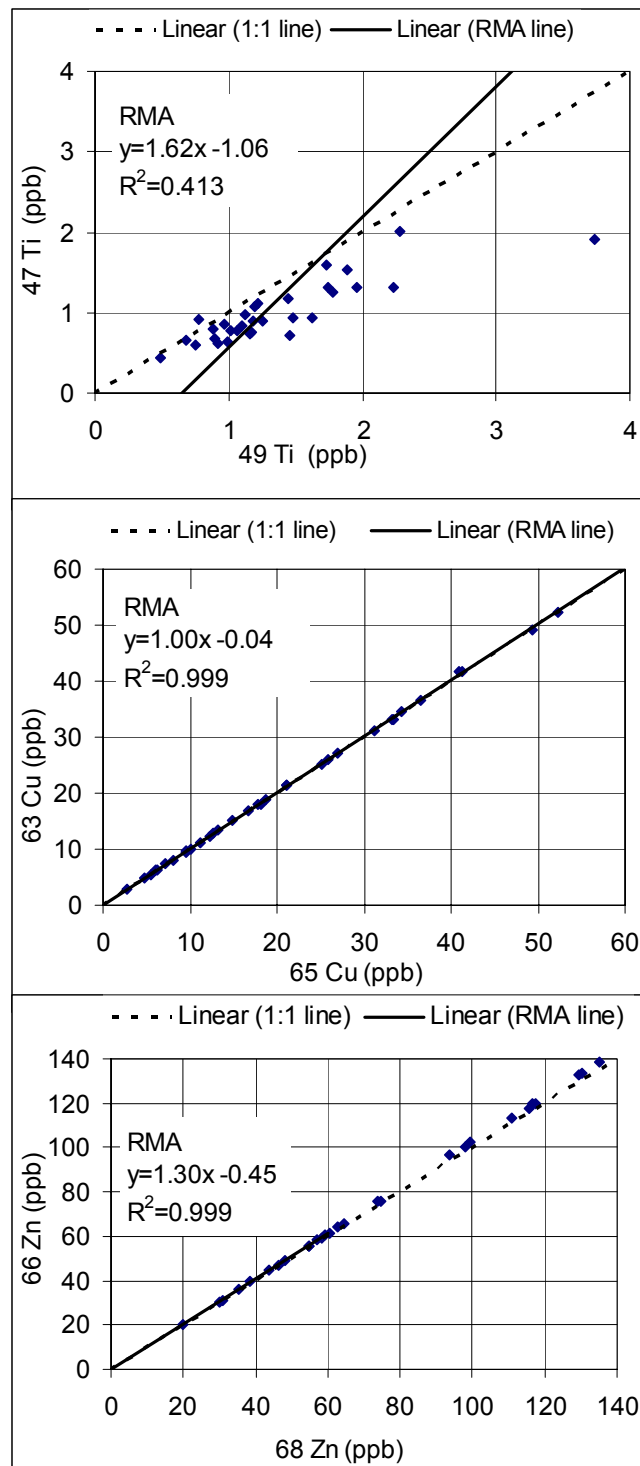


Figure 4.8 Relationship between Ti (top), Cu (middle) and Zn (bottom) isotopes.

The polyatomic species $^{40}\text{Ar}^{23}\text{Na}$ could have affected ^{63}Cu . However, concentrations of the two Cu isotopes (63 and 65) were very similar to each other. The slope and intercept of the Reduced Major Axes (RMA) regression equation between both

isotopes were not significantly different from 1 and zero, respectively (at $p=0.05$ significance level) and the regression coefficient was 0.999 (Figure 4.4). The differences ($^{63}\text{Cu} - ^{65}\text{Cu}$) ranged from -0.2 to -0.6 ppb, which is well below the ambient Cu concentrations found in the filters (mean of 20 ppb).

Similarly, $^{35}\text{Cl}^{15}\text{N}^{16}\text{O}$ could have affected measurements of ^{66}Zn . However, concentrations of the isotopes ^{66}Zn and ^{68}Zn were very similar (Figure 4.4) with differences ranging from 0.3 to 6.5 ppb, which are very low compared to the Zn concentrations (around 90 ppb). The slope and intercept of the regression equation for both isotopes were not significantly different from 1 and zero respectively and the regression coefficient was 0.999.

Mathematical equations for the correction of the mentioned interferences were not used since the use of these equations links one metal with the metal used to make the adjustment, which may affect the correlations of metals with other pollutants. Since one of aim this project was the determination of the relationships between metals and other pollutants, rather than determination of the absolute metal concentrations, interferences were not corrected.

4.9.2 Quality Assurance

Calibration was achieved using multi-element standards (Spex, US: ISO90001 certified) made up in 2 % Aristar[®] nitric acid (BDH, Poole, Dorset) in nanopure water.

A total of 53 samples were analyzed, in two separate runs. Each run took 7 hours and therefore a degree of drift within the run (decrease or increase in the detector signal for a given ion concentration) could potentially have occurred. To correct for this possible instrumental drift a standard solution of 10 ppb was analysed every 5 samples. In total, this solution was analysed 13 times in each run. The concentrations for all metals were stable throughout the run. The mean RSD for all of the metal concentrations was 0.5 % for run 1 and 0.7 % for run 2, which indicates that the detector response was very stable throughout the entire analysis.

4.9.3 Metal concentration in field blanks and limits of detection

The following approach was followed to calculate the metal concentrations in the blank filters, the LODs and metal concentrations in exposed filters. The approach aimed to maximise the number of data points available for the analysis of the temporal and spatial correlations between metals and co-pollutants.

- In the field blanks, concentrations of metals above or below the sum of two times the SD plus the mean were considered outliers and excluded from the dataset (Heal et al. 2007).
- The median concentration of metals in the 6 field blanks was subtracted from the concentration of metals found in the exposed filters.
- LODs were calculated as the mean concentration of the laboratory blanks plus 3 times its SD (with the outliers excluded).

Metal concentrations in the exposed filters below the LODs were left in the data set if they were above zero. If they were negative or zero they were removed from the dataset, as recommended by Brown et al. (2008). Brown et al. recommend this approach rather than assigning an arbitrary fraction of the LOD (e.g. LOD/2), since the latter can bias the statistics. However, it has to be borne in mind that values below the LOD have more uncertainty than values over the LOD.

Metal concentration in the quartz field blanks (quartz filters were used at the London sites) and PTFE field blanks (PTFE filters used at the Glasgow sites) are shown in Table 4.10.

Table 4.10 Limit of Detection (LOD) of quartz and PTFE field blank filters.

Metal	Quartz filters (London sites) n=6				PTFE filters (Glasgow sites) n=2			
	Median (ng ml ⁻¹)	SD	LOD (ng ml ⁻¹)	LOD (ng m ⁻³)	Mean (ng ml ⁻¹)	SD	LOD (ng ml ⁻¹)	LOD (ng m ⁻³)
Ti	0.767	0.344	1.03	0.307	0.473	0.117	0.350	0.113
V	0.034	0.019	0.056	0.017	0.165	0.014	0.042	0.013
Cr	7.14	1.70	5.11	1.52	0.692	0.116	0.349	0.113
Mn	0.744	0.119	0.358	0.106	0.344	0.132	0.395	0.128
Fe	12.9	3.39	10.2	3.02	5.27	2.75	8.26	2.67
Ni	0.944	0.138	0.415	0.123	0.955	0.335	1.00	0.325
Cu	2.01	0.707	2.12	0.630	1.04	0.556	1.67	0.538
Zn	1.92	1.97	5.92	1.76	89.6	8.58	25.7	8.32
As	0.020	0.007	0.020	0.006	0.002	0.004	0.011	0.004
Cd	0.011	0.005	0.016	0.005	0.086	0.013	0.039	0.013
Pb	0.112	0.059	0.178	0.053	0.762	0.239	0.718	0.232

Quartz blank filters showed higher metal concentration than PTFE blank filters except for Cd and Pb. LODs were lower for Ti, V, Cr, Cu, Fe and As in PTFE filters. However, Mn, Ni, Zn, Cu and Pb showed lower LODs in quartz filters. The lower LOD in quartz filters was a result of the higher sample size used in calculating the SD of quartz filters (SD of 6 filters), while the SD for PTFE filters was calculated with the values from two filters. Therefore, a slight difference in the two PTFE blank filters resulted in a high SD.

If the number of samples with metal concentration below the LOD exceeded 25 % of the total number of samples, results for that metal were removed from the data set (the sample sizes were n=26 and n=17 at London sites, and Glasgow sites respectively). Therefore, if the metal concentration was below the LOD in more than 7 samples and more than 4 samples in London and Glasgow respectively, data for that metal was excluded from the analysis.

The filters used at the Glasgow sites (including the field blanks) were contaminated with Zn. The contamination was not homogenous across the samples, as when the concentrations found in the blanks were subtracted from those found in the filters, some samples showed negative concentrations. Therefore, results could not be corrected. The reason for this contamination remained unknown.

Following is a description of the metals that showed concentrations below the LOD and those that were excluded from the dataset.

Cr: all sample filters at London sites (all data removed from the data set).

Ti: 23 sample filters at Marylebone Rd. and 16 at North Kensington (all data removed from the dataset); 9 sample filters at St. Enoch Sq. (data removed from the dataset); 3 sample filters at Hope St. (values left in dataset).

Mn: 1 sample filters at North Kensington (value left in data set).

Ni: 4 sample filters at Marylebone Rd., 1 sample at Hope St. and 1 sample at St. Enoch Sq. (all these values were left in the data set).

Fe: 5 sample filters at North Kensington (all values left in data set).

Cd: 1 sample filters at Hope St. (value left in the data set).

4.10 OVERVIEW OF THE EXPERIMENTAL DESIGN FOR ASSESSMENT OF THE PERFORMANCE OF NO₂ AND NO_x PDTs

The performance of the NO₂ and NO_x PDTs was evaluated by comparing their measurements with those averaged from a chemiluminescence analyser at the three AUN sites described earlier (kerbside:Hope St., urban centre:St. Enoch Sq. and background/street canyon: Montrose St.) from 8 June to 10 August 2006.

In addition, the influence of exposure time on the performance of the NO₂ tubes was studied by comparing measurements from PDTs exposed for 4 weeks with the average of the measurements from 4 PDTs exposed over 4 consecutive periods of 1 week. This experiment took place from 15 February to 10 May 2005 at the BS network of monitoring sites in Glasgow (Baillieston, Cardonald, Carmyle, Dalmarnock, Springburn, St. Enoch Sq.). These sites are described in section 4.10.1.

4.10.1 Details of the monitoring sites for assessment of NO₂ PDTs performance over time

The monitoring sites (Cardonald, Springburn, Dalmarnock, Carmyle and Baillieston) were part of the BS and sulphur dioxide DEFRA monitoring network (the network

stopped operating in 2005), managed by the National Environmental Technology Centre (NETCEN). Therefore, NETCEN classification and DEFRA equivalent site type have been included in Table 4.11. A map with the location of the sites is shown in Figure 4.9.

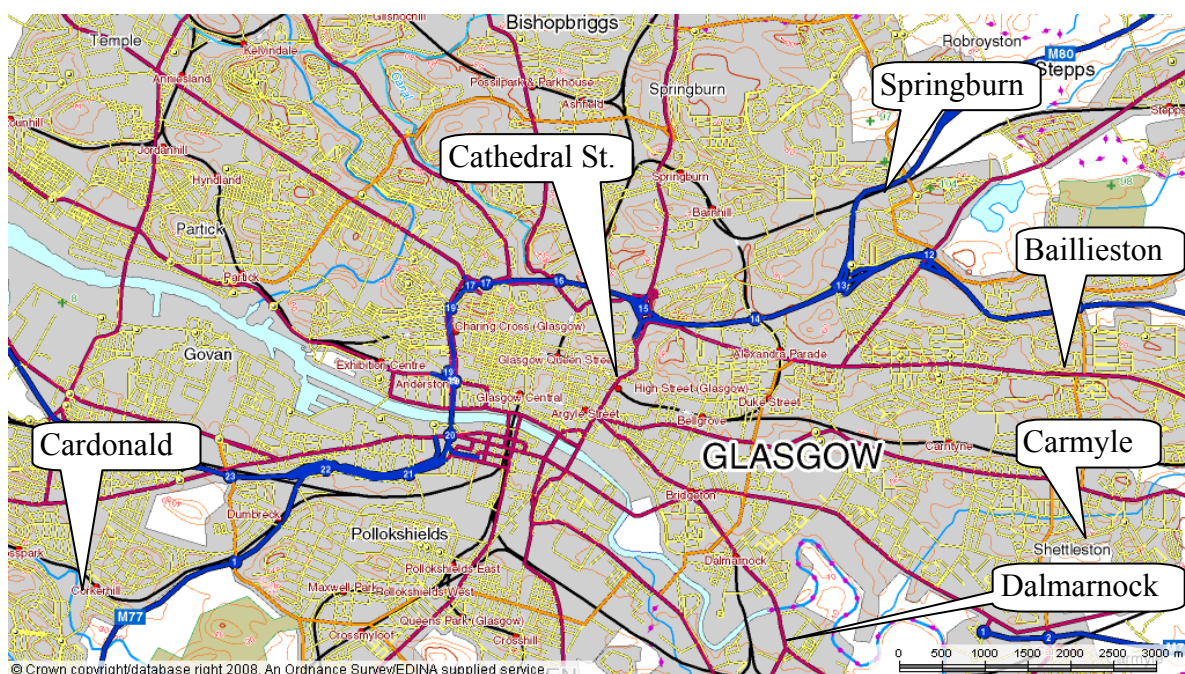


Figure 4.9 Map of monitoring sites for the study of the performance of NO₂ PDTs in Glasgow.

Table 4.11 Location and classification codes of the monitoring sites for the analysis of the performance of NO₂ PDTs in Glasgow (sites arranged from West to East).

Site Name	Grid Reference Easting	Grid Reference Northing	Address	Site environment (NETCEN) ¹	Site type (DEFRA) ¹
Cardonald	2533	6641	74 Berryknowes Rd.	B3/E	Suburban
Cathedral St.	2595	6656	Allan Glen Place	-	-
Springburn	2611	6678	Wellfied Nursery School, 308 Edgefauld Rd.	B2	Suburban
Dalmarnock	2612	6627	Dalmarnock Sewage works, Cotton St.	C2	Urban industrial
Carmyle	2653	6622	St. Joachins Primary School, Montrose Av.	C2	Urban industrial
Baillieston	2679	6642	St. Bridget Primary School, Swinton St.	A3	Urban background

interspersed with, other areas with low potential air pollution output (parks, fields, coast).

B1: Residential area with medium-density housing, typically an inner suburb or housing estate, surrounded by other built-up areas.

B2: Predominantly B1, but interspersed with some industrial undertakings.

C2: Industrial area interspersed with domestic premises of high density or in multiple occupation.

E: Smoke control area or smokeless zone (the letter to be added to the primary classification).

¹NAQAa

Cardonald (Suburban, Glasgow)

The NO₂ diffusion tubes were located in the grounds of a medical centre. They were attached to a lamppost approximately 4 m above the ground. The surrounding

environment is classified as B3/E equivalent to suburban (NAQAa). Two roads (A739 & A761) run approximately 50 m from the monitoring site.

Cathedral St. (Glasgow)

Cathedral St. is a 4 lane road, carrying approximately 8,000 to 15,000 vehicles day⁻¹ (Henderson, 2005), with frequent buses and congestion during the morning and afternoon rush hours. This site was selected to examine the decay of NO₂ with distance from a busy road. The diffusion tubes were located along Allan Glen Place, a perpendicular pathway to the North of Cathedral St. PDTs were located at distances of 3, 5, 25, 45, 65, 85, and 105 m from Cathedral St.

Springburn (Suburban, Glasgow)

The NO₂ diffusion tubes were located in the back yard of Wellfield nursery school. They were attached to a post approximately 3 m above the ground. The site environment is classified as B2, equivalent to suburban (NAQAa). The nearest road (A803) was approximately 50 m away from the monitoring site and a railway line runs 40 m from the monitoring site.

Dalmarnock (Urban Industrial, Glasgow)

The NO₂ diffusion tubes were attached to a lamp post approximately 3 m above the ground. The site environment is classified as C2 equivalent to urban industrial (NAQAa). There were sewage works and a railway lane approximately 500 m away from the monitoring site.

Carmyle (Urban Industrial, Glasgow)

The NO₂ diffusion tubes were located in the playground of St. Joaquins Primary School. They were attached to a post approximately 3 m above the ground. The site environment is classified as C2 equivalent to urban industrial (Table 4.11). A motorway (M8) runs approximately 100 m north from the monitoring site.

Baillieston (Urban background, Glasgow)

The NO₂ PDTs were located in the back yard of St. Bridget's Primary school. They were attached to a post approximately 3 m above the ground. The site environment is classified as A3, equivalent to urban background (NAQAa). There was a railway line 3.5 km north and a landfill site approximately 3 km from the monitoring site.

4.10.2 NO₂ passive diffusion samplers

The tubes used in this project were standard Palmes-type acrylic diffusion tubes from Gradko International. The tubes were made of acrylic plastic, 7 cm long, with grey-coloured rubber caps holding 2 stainless steel grids (mesh size 4x4 mm²) impregnated in an adsorbent. During exposure, the end without the grids is open to the atmosphere.

The tubes operate on the principle of molecular diffusion: NO₂ molecules diffuse from an area of high concentration (open end) to an area of low concentration (closed end) where they are trapped as nitrite ions (NO₂⁻) in the adsorbent to be quantified by ultra-visible (UV) spectrophotometry (Palmes, 1976).

The tubes were re-used during the project. In the absence of international or European guidelines, the cleaning procedure and assembly was done following Heal et al. (2005a). In 2008, DEFRA published practical guidance on the use of NO₂ diffusion tubes (AEA, 2008). The DEFRA specifications for cleaning and re-use of tubes did not differ significantly from those used in this project. A detailed comparison of DEFRA procedure and that followed in this study for cleaning and preparation of NO₂ PDTs is provided in section 4.4.3.

The tubes, caps, and grids were cleaned thoroughly with Decon 90 and rinsed in 18 MΩ water. Grids were ultrasonicated in an ultrasonic bath (FS 100b, Decon Lab Ltd) for 30 minutes, rinsed with 18 MΩ water, left overnight at 105 ± 2 °C to evaporate the water and then cooled off in a dessicator, inside a beaker covered with cling film until they were used. Cleaned tubes were double wrapped and stored in plastic bags. The tubes were prepared as described below:

1. Grids were dipped into a solution of 50 % triethylamine (TEA) and 50 % acetone, swirled well and left for approximately 5 minutes.
2. Grids were transferred onto tissue paper using stainless steel tweezers and patted gently with another piece of tissue paper to remove excess solution.
3. Two grids were fitted in the grey caps. Then the tube was inserted in the cap and the other end was capped with the white cap.
4. Tubes were double wrapped and stored in plastic bags in a refrigerator (below 4 °C) until they were exposed, within 4 weeks. After exposure they were stored (again double wrapped) inside a refrigerator until they were analyzed, within 4 weeks.

4.10.3 NO_x passive diffusion samplers

The NO_x passive diffusion system consists of two tubes. One tube is a conventional NO₂ PDT prepared as described in section 4.4.1. The other tube has two reagents: oxidizing granules (containing K₂Cr₂O₄) to oxidize NO to NO₂ and TEA to trap the oxidized NO₂. The tubes, caps, grids and oxidizing granules were supplied by Gradko International. The TEA/acetone solution was prepared as described in section 5.2.1. The tubes were assembled in the laboratory following instructions from Stuchbury (2006):

1. 500 ± 1 mg of the oxidizing granules (weighed in a Sartorius, MC1 balance) were placed in a black cap and held in place with a metallic grid two hours before exposure, to minimize degradation of the oxidant.
2. A red open cap containing two grids impregnated in TEA/acetone was fitted into the black cap. The rim of the red cap had a thickness of 1 mm to prevent contact between the two grids (that holding the TEA/acetone and the grid holding the oxidizing granules) (Figure 4.10).
3. A tube was inserted into the red cap and capped with a white cap.

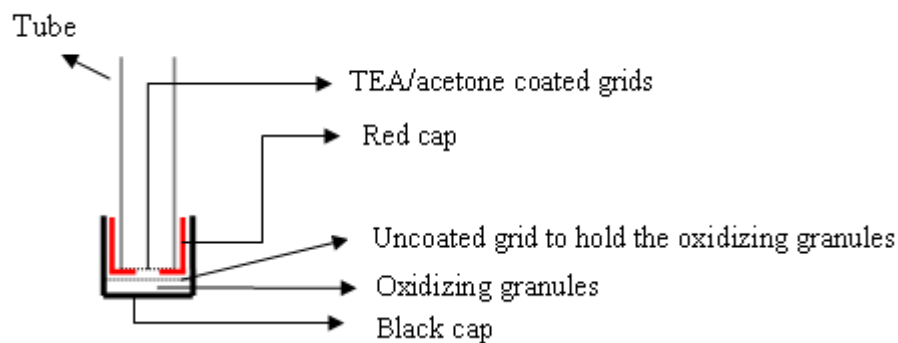


Figure 4.10 Schematic representation of a NO_x tube.

Two NO₂ tubes and two NO_x tubes were exposed for each sampling period (7 days) to provide duplicate measurements. The distance between NO₂ and NO_x tubes was approximately 10 cm.

After exposure, the red and black caps (with the oxidizing granules) were removed and a closed grey cap was used to hold the TEA/acetone coated grids. Tubes were double wrapped in plastic bags and stored in a refrigerator (below 4 °C) until analysis, within 4 weeks.

4.10.4 Chemical quantification of NO₂ and NO_x

4.10.4.1 Extraction of nitrite from exposed NO₂ and NO_x PDTs

NO₂ PDTs were analysed following the procedure developed by Heal (2005). NO_x tubes were analyzed as NO₂ tubes, since the NO had been oxidized to NO₂ and trapped in the absorbent as nitrite. The nitrite was released with water and trapped with sulfanamide. Then, a solution of N-1-Naphthyl ethylene diamine dihydrochloride (NEDA) was added. NEDA reacts with the sulfanamide to form an azo dye complex, the intensity of which is determined by spectrophotometry. Exposed tubes and field blank tubes were analysed in the same way. The details of the procedure are as follows:

1. 1500 ± 1 µL of deionised water was added to each tube so the nitrite is dissolved.
2. Tubes were re-capped, swirled gently, and left for half an hour.

3. After half an hour, caps were removed from the sample tubes.
4. $1500 \pm 1 \mu\text{L}$ of sulphanilamide solution was added to each tube, including the calibration tubes. The sulphanilamide solution was prepared by dissolving 2 g of AnalaR® sulphanilamide (BDH, Poole, England) and $5.00 \pm 0.05 \text{ mL}$ of 88 % AnalaR® orthophosphoric acid (H_3PO_4) (BDH, Poole, England) in 100 mL of 18 MΩ water. The orthophosphoric acid is added to keep the pH low, a requirement for the subsequent extraction of nitrite. The solution was kept in a dark glass bottle in a refrigerator (below 4°C) and used in subsequent analyses. A fresh solution was prepared every 3 months.
5. $150 \pm 1 \mu\text{L}$ of NEDA solution was added to each tube, including the calibration tubes. The time between the addition of the sulfanamide and NEDA was kept to a minimum to maximize the development of the diazo coloured product. The NEDA solution was prepared by dissolving $0.700 \pm 0.001 \text{ g}$ of AnalaR® NEDA (BDH, Poole, England) in 500 mL of 18 MΩ water. This solution was stored in a dark glass bottle inside a refrigerator and re-used in subsequent analyses. A fresh solution was prepared every 3 months.
6. Tubes were capped, inverted and shaken briefly. They were shaken regularly for a further half an hour for the colour to develop.
7. After half an hour, the solution was poured into a cuvette and the light absorption of the azo compound measured by spectrophotometry.

Analysis of the concentration of nitrite by spectrophotometry required the preparation of calibration standards, i.e. a series of solutions of known nitrite concentrations, which covers the expected nitrite concentration in the tubes. These calibration standards were prepared as follows:

Approximately 2.0 g of AnalaR® NaNO_2 (BDH, Poole, England) was dried in an oven at $105 \pm 2^\circ\text{C}$ overnight followed by cooling in a dessicator. NaNO_2 is a hygroscopic compound and therefore it is necessary to evaporate the water before it can be weighed accurately.

Then, $1.5000 \pm 0.0001 \text{ g}$ of NaNO_2 was dissolved in 1 L of 18 MΩ water. $0.09 \pm 0.01 \text{ g}$ of AnalaR® NaOH (BDH, Poole, England) was added to prevent

liberation of unstable nitrous oxide by any CO₂ present. 1000 ± 1 µL of HPLC grade chloroform (Aldrich, Milwaukee, Wisconsin) was added to prevent bacterial growth. This stock solution of 1000 mg NO₂⁻ L⁻¹ was kept in the fridge and used in subsequent analyses within 3 months.

For each batch of tubes analysed a solution of 1 mg L⁻¹ nitrite was prepared from the stock solution by dilution in 18 MΩ water.

In order to calibrate the spectrophotometer, 8 calibration standard solutions were prepared by dilution from the nitrite subsidiary solution (of concentration 1 mg L⁻¹) in 18 MΩ water. The calibration standards were prepared in tubes without grids.

Recently, DEFRA published guidance for the use and preparation of NO₂ PDTs (DEFRA, 2008). The recommended procedures are similar to those used for this project (Dr. Heal also contributed to the DEFRA guidance document). The minor differences between the DEFRA guidelines and those followed in this project are described below.

Calculation of the coefficient of diffusion of NO₂ in air: DEFRA recommends calculating the coefficient of diffusion based on the UK's average temperature over the last 10 years (11 °C). In this project, the temperature used was the average temperature over the exposure period as measured at the British Atmospheric Data Centre (BADC) meteorological station at Bishopton. The measured T at the station could have been slightly different from that at the monitoring sites, introducing a minor source of error to the calculation. However, this error was probably smaller than that introduced if a fixed T of 11 °C had been used.

Automated shaking: DEFRA guidelines recommend the use of automated agitation of the tubes after adding the sulphanamide and NEDA to facilitate the reaction. In this work, the tubes were agitated manually. Vigorous manual agitation is not likely to be much different from automated agitation (Heal, 2005). DEFRA's reasons for the use of automated agitation are to generate harmonisation between different laboratories and avoid inconveniences such as strain injury (DEFRA, 2008).

4.10.4.2 UV-molecular absorption theory

UV spectrometers consist of a light source (an incandescent bulb for the visible wavelengths, or a deuterium arc lamp in the ultraviolet), a sample holder and a diffraction grating or monochromator which filters the light so that only light of a single wavelength reaches the detector (Donbrow, 1966).

The most common detectors are photodiodes or charge coupled devices (CCD). Photodiodes are used in spectrometers with monochromators, and diffraction gratings are used with CCDs. The light source can be a single or double beam. Single beam instruments provide accurate measurements, assuming that the radiation source is stable. However, by using a double beam any variation in the radiation source, sensitivity of the detector, or in the amplification electronics is eliminated as a source or error since the signal from the radiation source is divided in two: a reference beam and a sample beam.

Monochromatic light is passed through the solution containing the compound of interest. The power of the incident beam P° and the power of the emerging beam, P , are measured. If the path of the beam is divided into many infinitesimally thin segments, the power of the light will be diminished by the same fraction as it passes through each segment. This can be assumed because the amount of absorbent material encountered by the beam in each segment will be the same. Expressing this mathematically, the fractional decrease in power, $-dP/P^{\circ}$, depends on the amount of the absorbent material in the segment, dL and a proportionality constant, k (Equation 4.4). Thus, it predicts a linear relationship between absorbance and concentration (Donbrow, 1966).

$$-\frac{dP}{P^{\circ}} = KdL \quad \text{Beer-Lambert Law} \quad \text{Equation 4.4}$$

To find the total amount of absorption over the whole path (L), $-dP/P^{\circ}$ is integrated between 0 and L . After taking logarithms the final equation is given as Equation 4.5:

$$A = \varepsilon LC \quad \text{Equation 4.5}$$

$$A \text{ (absorbance)} = \text{Log } P/P \quad \text{Equation 4.6}$$

ϵ (absorptivity): is a function of the compound that is absorbing the radiation and the wavelength of the radiation

L: is the length of the path

C: is the concentration of absorbent atoms

If the sample concentration is too high to permit accurate analysis in the linear response range, there are two alternatives to bring the absorbance into the optimum working range: sample dilution, or use of an alternative wavelength having a lower absorptivity. In this project, the first alternative was chosen.

4.10.4.3 Operation of the spectrophotometer

In this study, a UV single beam SP6-250 Pye Unicam® spectrophotometer was used. It was operated as follows:

1. The spectrophotometer was switched on and left to warm up for 30 minutes.
2. The wavelength was set to a value at which the absorbance of the compound was greatest (540 nm). This was checked by measuring the absorbance of 5 solutions at different wavelengths from 520-560 nm.
3. A cuvette containing the reagents added to the exposed tube (18 M Ω water, sulfanamide and NEDA) was used to adjust the absorbance to zero. This eliminated the effect of any nitrite present in the reagents. This zero calibration solution was re-checked after every 3 exposed tubes to control the effect of any drift in the electronic response of the spectrophotometer. If the absorbance of the calibration solution was different from zero, the spectrometer was adjusted to zero again and the three last tubes were measured again.

4. In samples where the absorbance was out of the linear range a dilution was made by pipetting 1 mL of the solution (sulfanamide and NEDA) and 1 mL of a mixed solution of sulfanamide and NEDA into a fresh tube. This happened only with the NO_x PDTs collected at Hope St.

To check for drifts in the linearity of the response of the spectrophotometer the calibration standards were run at the beginning and end of each batch. The Relative Standard Deviation (RSD) between the slopes of the calibration curves was always lower than 3 %.

The response of the spectrometer was very stable throughout the complete study period. In total 29 calibrations were performed. The RSD of the slope of the calibration curves was 9.0 %.

4.10.4.4 Calculation of the ambient NO₂ and NO_x concentrations

The collected mass of nitrite in the tubes was converted into concentration using Fick's law, which states that the flux is proportional to the concentration gradient (Equation 4.7):

$$J = D_{12} : \frac{(C_1 - C_0)}{z} \quad \text{Fick's Law} \quad \text{Equation 4.7}$$

Where:

J: the flux of gas 1 (NO₂ or NO) through gas 2 (air) across unit area in the z direction.

C₀: concentration of the gas (NO₂ or NO) at the absorbent end of the tube, which is maintained at zero (since it is assumed that the absorbent captures and converts all gas NO₂ to nitrite and that in the case of NO diffusion, NO is oxidised to NO₂ and then converted to nitrite).

C₁: average concentration of the gas at the open end of the tube over the exposure period.

z : the length of the diffusion path.

D_{12} : the molecular diffusion constant of gas 1 in gas 2, which is temperature (T) dependant and is calculated using Equation 4.8:

$$D_{12} : D_{273} (T/273)^{1.81} \quad \text{Equation 4.8}$$

D_{12} for NO_2 and NO was calculated for each exposure period using the averaged T as measured at Bishopton weather station. Data was provided by BADC (BADC, 2008).

Therefore the quantity in ng (Q) of gas 1 transferred to a tube of length (L) over a specific period of time (t) is given by Equation 4.9:

$$Q = D_{12} \frac{(C_1 - C_0)at}{L} \quad \text{Equation 4.9}$$

Where:

a : cross-sectional area of tube (0.916 cm^2)

L : length of tube (7.1 cm)

t : length of exposure period (604800 s for 1 week period of exposure)

Since $C_0=0$, the concentration of ambient gas in the air is:

$$C_1 = \frac{QL}{D_{12}at} \quad \text{Equation 4.10}$$

Q was obtained as the average of the two replicates of mass of nitrite in the tube estimated from the linear regression equation of the calibration graph of standard nitrite solutions.

Calculation of NO₂ concentrations

NO₂ concentrations were calculated by entering the mass of nitrite collected in the NO₂ tube into Equation 4.10

Calculation of NO concentration

NO concentration was calculated as follows:

First, the mass of NO was calculated by subtracting the mass of nitrite collected in the NO₂ tube (Q_{NO_2}) from the mass of nitrite collected in the NO_x tube (Q_{NO_x}) (both tubes were exposed in parallel) and converted into equivalent mass of NO (Equation 4.11):

$$Q_{NO} = (Q_{NO_x} - Q_{NO_2}) \times \frac{MW_{NO_2}}{MW_{NO}} \quad \text{Equation 4.11}$$

Where MW_{NO_2} and MW_{NO} are the molecular weight for NO₂ and NO, respectively.

Secondly, NO concentrations were calculated as described in Equation 4.7, using the corresponding coefficient of diffusion for NO and the averaged T for the measuring period.

Calculation of NO_x concentration

NO_x concentrations were calculated by adding the NO₂ concentration and the NO concentration (expressed as NO₂):

$$C_{NO_x} = C_{NO_2} + C_{NO} \text{ (as NO}_2\text{)} \quad \text{Equation 4.12}$$

Where C_{NO} (as NO₂) is:

$$C_{NO} \text{ (as NO}_2\text{)} = C_{NO} \times \frac{MW_{NO}}{MW_{NO_2}} \quad \text{Equation 4.13}$$

All PDT concentrations (NO_2 , NO and NO_x) were corrected for temperature and pressure using Equation 4.11 for comparison with data from the chemiluminescence analyser. Chemiluminescence measurements are reported at a temperature of 293 K (20 Celsius) and pressure of 101.3 kPa for comparison with EU Limit Values or Air Quality Standard Objectives (DEFRA, 2008):

$$C_{293} = C_T \frac{T}{293} \quad \text{Equation 4.14}$$

4.10.4.5 Quality assurance

Leakage around the end caps and any possible contamination during the preparation and analysis of the tubes was tested by exposure of field blanks (a tube treated as the exposed tubes but never exposed). The mean NO_2 concentration from 189 field blanks was $1.2 \mu\text{g m}^{-3}$, much lower than the lowest measured NO_2 concentration ($7.13 \mu\text{g m}^{-3}$).

The limit of detection (LOD) of the method was calculated as three times the mean plus three times the Standard Deviation (SD) of the 189 field blanks (Miller and Miller, 1993). Field blanks were used instead of laboratory blanks (tubes with no grids) because they provide more information about possible contamination since they are treated identically to exposed tubes. The LOD was $6.4 \mu\text{g m}^{-3}$.

The precision of the measurement method was assessed by taking duplicate measurements at each site. The RSD between the two measurements was calculated. Replicates with a value of RSD greater than 10 % were excluded (10 out of 285). An RSD of 10 % is considered acceptable for this type of analysis (Kirby et al., 2000).

4.11 STATISTICAL ANALYSES OF DATA

Monitoring equipment recorded data at different time resolutions and therefore hourly, daily and weekly means were calculated to examine the inter-pollutant correlations at different averaging periods. Daily means were calculated from hourly data, from midnight to midnight and weekly means were calculated from hourly data

from 1 pm to noon to coincide with the exchange of NO₂-PDTs and PM₄ filters. Weekly means of BS were calculated from daily observed data (coinciding with the same period for which NO₂ tubes and PM₄ filters were exposed) as follows: weighing of the days at either end of the week reduced by a factor of 2 in the computation of the 7-day mean.

Data from the continuous analysers at AUN sites was provided by the NAQA as hourly mean Greenwich Mean Time (GMT) ending time (from 15 minutes instrument resolution time). In contrast, data for the butanol based-CPC was provided as hourly means beginning time (from 15 minutes instrument resolution time). Therefore, data for the butanol-based CPC was changed to the conventional format of beginning time. All data presented in the thesis has been presented as GMT beginning time. Data for the WCPC was recorded with a resolution time of 1 minute. 15 minute averages were calculated for comparison with the BCPC. Hourly averages were calculated from the 15 minute averages. Table 4.12 shows the resolution times and mean calculations for the different pollutants.

Table 4.12 Averaging time procedure for the analysis of air pollution data in Glasgow at the 3 AUN sites (Hope St, St. Enoch & Montrose St.).

Pollutant Parameter	Equipment	Resolution time	Means		
			Hourly	Daily	Weekly
PM ₁₀	PARTISOL	24 hrs	NA	Direct obs.	NA
	TEOM	15 mins	hh:15 to hh:00	01 to 00 h	NA
Respirable Dust (PM ₄)	SKC pump	7 days	NA	NA	Direct obs.
PNC	Water based-CPC	1 min	hh:15 to hh:00 (from 15 min averages)	01 to 00 h	13pm to noon
	Butanol based-CPC	15 mins	hh:15 to hh:00	01 to 00 h	13pm to noon
BS	BS monitor	24 hrs	NA	Direct obs.	[(Thurs/2)+Fri+Sat+Sun+Mon+Tues+Wed+(Thurs/2)]/7
Metals	Extracted from PM ₁₀ & PM _{2.5} filters	24 hrs	NA	Direct obs.	NA
PAHs	Extracted from PM ₁₀ filters	24 hrs	NA	Direct obs.	NA
NO ₂ & NO _x	PDTs	7 days	NA	NA	Direct obs.
	Chemiluminescence Analyser	15 mins	hh:15 to hh:00	01 to 00 h	13pm to noon
O ₃	Ultra Violet Analyse	15 mins	hh:15 to hh:00	01 to 00 h	13pm to noon
CO	Infra Red Analyser	15 mins	hh:15 to hh:00	01 to 00 h	-
Hydrocarbons	Gas Chromatograph	15 mins	hh:15 to hh:00	01 to 00 h	13pm to noon

BS: black smoke; NA: Not applicable; PNC: particle number concentration; Direct obs: direct observation
- weekly averaged were not calculated

Means were calculated only when there were no more than 25 % of missing data, i.e. no more than 15 minutes missing for hourly means; no more than 6 alternate missing hours, or no more than 4 consecutive missing hours for daily means, and no more than 2 days for weekly means. Daily means were allowed only 4 consecutive missed hours, since it was observed that more than 4 missed hours at night or during rush hour could substantially change the daily mean. However, if up to 6 hours were missed at different times of the day the daily mean value was not changed to a great extent.

The precision of the monitoring equipment (two replicates measurements) and the agreement between two different instruments was evaluated in two ways, as the $RSD=(100 \times (SD/Mean))$ and as the bivariate relationship between the two measurements. The coefficient of determination (R^2) was also calculated to determine the strength of the relation between the two measurements.

Student t-test were used to compare the means of two samples (two replicate measurements or two measurements from two different instruments).

The bivariate relationship between different monitoring equipment as well as between the increments in pollutant metrics was calculated using the RMA method, which accounts for variance along both variables and is recommended in air pollution studies (Ayers, 2001).

In RMA, the ratio of the SD of data variable sets (SD_y , SD_x) is used to determine the slope (b) of the equation:

$$b = \frac{SD_y}{SD_x} \quad \text{Equation 4.15}$$

As the RMA line passes through (\bar{x}, \bar{y}) the intercept (a) is calculated in the same way as Least Square Regression (LSR):

$$a = \bar{y} - b\bar{x} \quad \text{Equation 4.16}$$

In general, the concentrations of pollutant metrics were not normally distributed and therefore non-parametric methods (Spearman correlation coefficient) were used to calculate the correlation coefficient between pollutant metrics.

CHAPTER 5

ASSESSMENT OF PRECISION AND COMPARABILITY OF MONITORING METHODS

5.1 RESULTS

The equipment used in this project was validated by comparing it with monitoring equipment used by DEFRA. This chapter presents the results of the samplers' performance and the results from these instrument intercomparisons: NO₂ and NO_x PDTs vs. chemiluminescence analyser; TEOM vs. Partisol sampler and WCPC vs BCPC. The assessment of the efficiency of the sequential extraction for PAHs and metals is also included.

5.1.1 Equipment validation for gas sampling

5.1.1.1 Replicate precision of NO₂ and NO_x PDTs

The precision of the PDTs was evaluated in two ways: as the RSD of the replicate measurements (Table 5.2) and as the RMA relationship between both replicate measurements (Figure 5.1).

The different exposure periods and monitoring sites for NO₂ PDTs exposed during 1-week and 4-weeks and NO_x PDTs exposed during 1-week are shown in Table 5.1.

Table 5.1 Monitoring sites and sampling periods for NO₂ and NO_x PDTs.

NO ₂ 1-week exposure	Baillieston	15 Feb - 10 May 2005
	Cardonald	
	Carmyle	
	Dalmarnock	
	Springburn	
	St. Enoch Sq.	15 Mar - 19 Dec 2005 8 Jun - 14 Dec 2006 22 May - 18 Dec 2007
Hope St.		8 Jun - 14 Dec 2006 22 May - 18 Dec 2007
	Montrose St	15 Feb - 10 May 2005 8 Jun - 14 Dec 2006 22 May - 18 Dec 2007
NO ₂ 4-weeks exposure	Baillieston	15 Feb - 10 May 2005
	Cardonald	
	Carmyle	
	Dalmarnock	
	Springburn	
	Montrose St	
St. Enoch Sq.	15 Mar - 19 Dec 2005	
NO _x 1-week exposure	St. Enoch Sq.	22 May - 14 Aug 2007
	Montrose St	
	Hope St.	

Table 5.2 Summary statistics of the Relative Standard Deviation (RSD) of replicate measurements of NO₂ and NO_x PDTs.

	NO ₂ PDTs		NO _x PDTs
	1-week	4-weeks	1-week
n	237	23	35
Mean RSD (%)	7.37	5.10	3.46
SD	7.50	4.55	3.77
Range	0 - 33.6	0 - 17.8	0 - 16.4

The mean RSD was higher for NO₂ PDTs 1-week measurements (7.4 %), than for 4-weeks (5.1 %) and NO_x PDTs 1-week (3.5 %).

The maximum RSD values reached were 33.6 % for NO₂ 1-week exposure; 18 % for NO₂ 4-weeks exposure and 16 % for NO_x 1-week exposure.

Figure 5.1 shows the scatter plot, RMA relationship and regression coefficient (R^2) between replicate measurements.

In the scatter plot for NO_x replicates (Figure 5.1 bottom), the units used were ng of trapped nitrite in the tube, instead of $\mu\text{g m}^{-3}$ of NO_x because there were no duplicate

measurements in $\mu\text{g m}^{-3}$ for NO_x (see section 4.4.6 for details of calculation of NO_x concentrations).

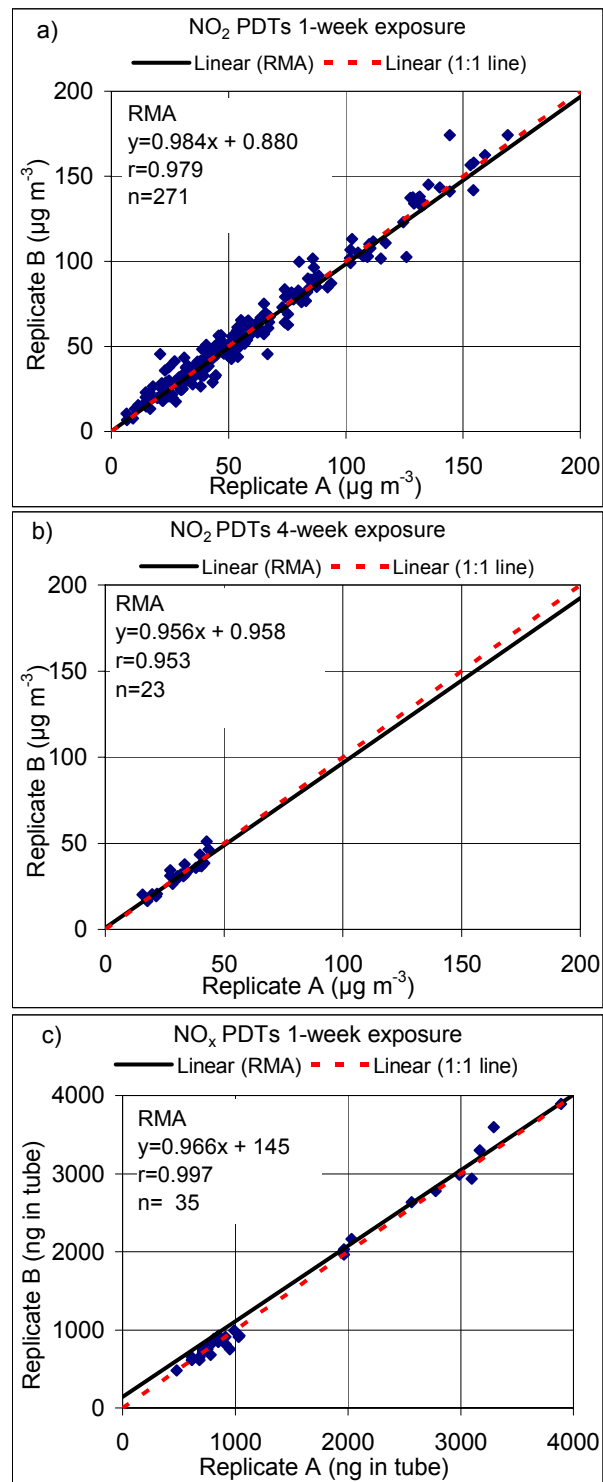


Figure 5.1 Scatter plots and Reduced Major Axes (RMA) regression of duplicate 1-week NO₂ exposure PDTs (a); 4-weeks NO₂ exposure PDTs (b) and 1-week NO_x PDTs exposure (c).

The correlation coefficient was statistically significant at $p>0.001$, 2-tailed, in the three cases. The slope and intercept of the RMA relationships for NO₂ replicate

determinations (1 & 4-weeks exposure periods) were not statistically significantly different from 1 and 0, respectively ($p < 0.05$). The intercept of the RMA relationship for the NO_x replicates (145 ng) was equivalent to a concentration of $6 \mu\text{g m}^{-3}$ expressed as NO_2 (at $T=13.3 \text{ }^\circ\text{C}$, which was the averaged T during the exposure period), which was well below the minimum NO_x concentration collected in the tubes ($17.1 \mu\text{g m}^{-3}$, expressed as NO_2).

Table 5.2 and Figure 5.1 include all NO_2 PDTs replicates available, with the aim of showing worst case scenarios for measurement precision. However, for the subsequent analyses (of spatial variability and temporal correlations) only those measurements with a replicate precision below 10 % were included in the analyses. From the total number of replicates (including 1-week and 4-week NO_2 PDTs and NO_x PDTs) only 8 % of the measurements were discarded.

5.1.1.2 Effect of NO_2 PDT exposure duration

The effect of the exposure duration on the precision of the NO_2 measurements was assessed by comparing the concentration derived from 4 continuous monitoring weeks (denoted 4-weeks) with that averaged for 4 separate weeks (denoted 4*1-weeks). The 4-weeks exposure period was selected since local authorities often measure NO_2 using PDTs for 4 continuous weeks.

Figure 5.2 shows the results of the measurements at Montrose, Cardonald, Dalrnarnock, Carmyle, Baillieston and St. Enoch Sq. At the latter site, measurements were continued for a longer period. These extra measurements are shown in Figure 5.3.

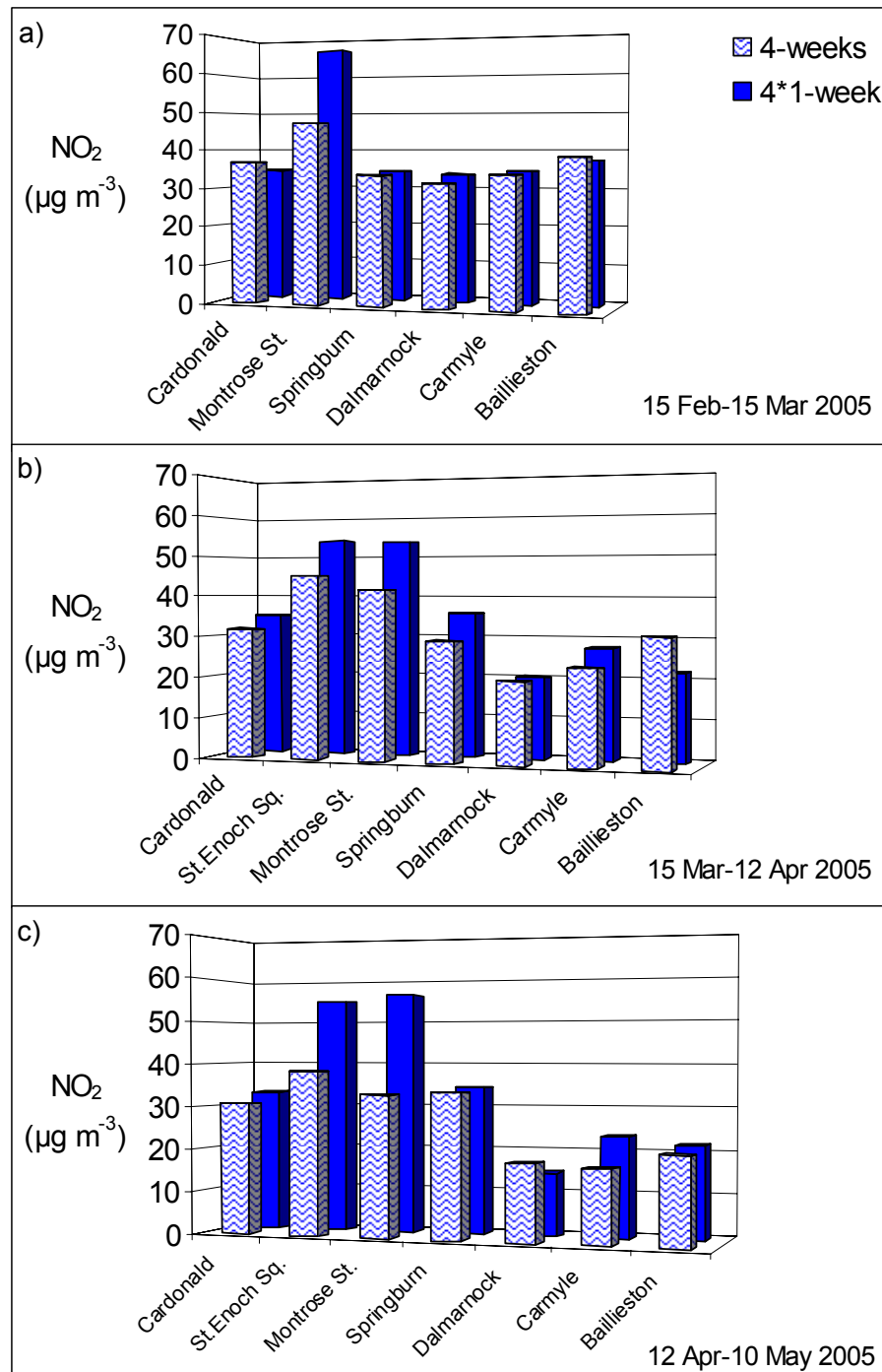


Figure 5.2 Comparison between NO₂ PDT concentrations measured during 4-weeks exposure period (denoted 4-weeks) and the averaged concentration of 4 consecutive 1 week exposure periods (denoted 4*1-week). Data for St. Enoch Sq. from 15 Feb-15 Mar 2005 was not available. Site classification: Montrose St. (background/street canyon); St. Enoch Sq. (urban centre); Cardonald & Springburn (suburban); Baillieston (urban background); Dalmarnock & Carmyle (urban industrial). Sites are arranged approximately from W to E.

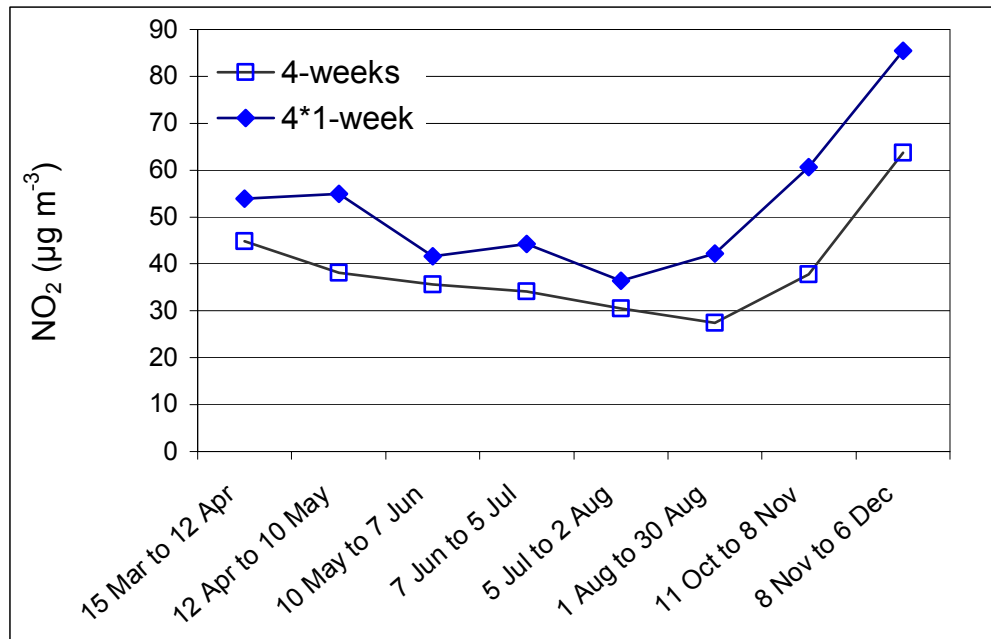


Figure 5.3 Comparison between NO₂ concentrations measured during 4-weeks exposure period (denoted 4-weeks) and the averaged concentration of 4 consecutive 1-week exposure periods (denoted 4*1-week) at St. Enoch Sq. in 2005.

Figure 5.2 and 5.3 show that the concentrations derived from 4 continuous weeks of exposure were lower than the corresponding average of 4 consecutive weeks at all sites for all periods, with the infrequent and relatively marginal exceptions of Cardonald from 15 February to 15 March; Baillieston from 14 March to 12 April and Dalmarnock 12 April to 10 May.

Table 5.3 shows the summary statistics of the comparison between the NO₂ concentrations derived for 4*1-week and 4 consecutive weeks.

Table 5.3 Summary statistics of ratio of NO₂ derived from 4 continuous weeks (4-weeks) over the NO₂ concentration averaged from 4 separated weeks (4*1-week).

Site classification	Site Name	n	Ratio : 4-weeks : 4*1-week		Paired t-test
			Mean	SD	p-value
Background/street canyon	Montrose St.	3	0.69	0.10	0.031
Urban centre	St.Enoch Sq.	8	0.75	0.09	0.001
Suburban	Cardonald	3	0.97	0.09	0.615
	Springburn	2	0.90	0.11	0.420
	Baillieston	3	1.13	0.26	0.433
Background	Carmyle	3	0.83	0.14	0.154
	Dalmarnock	3	1.05	0.36	0.819
All sites	All sites	25	0.87	0.19	0.001

SD:standard deviation. Significant p-values in bold.

The differences in concentrations were statistically significant only at Montrose St. and St. Enoch Sq. ($p < 0.05$, 2-tailed), the sites with the highest NO₂ concentrations. NO₂ concentrations at these two sites correspond to 1,500-2,000 ng mass of nitrite in the PDT, whereas at the other sites the mass of nitrite in the PDT was generally below 1,500 ng.

The two sets of data (4*1-week and 4-weeks) were significantly correlated ($r=0.888$, $p < 0.01$ (2-tailed) (Figure 5.4) suggesting that the differences were indicative of a systematic effect depending on the magnitude of average NO₂ concentration.

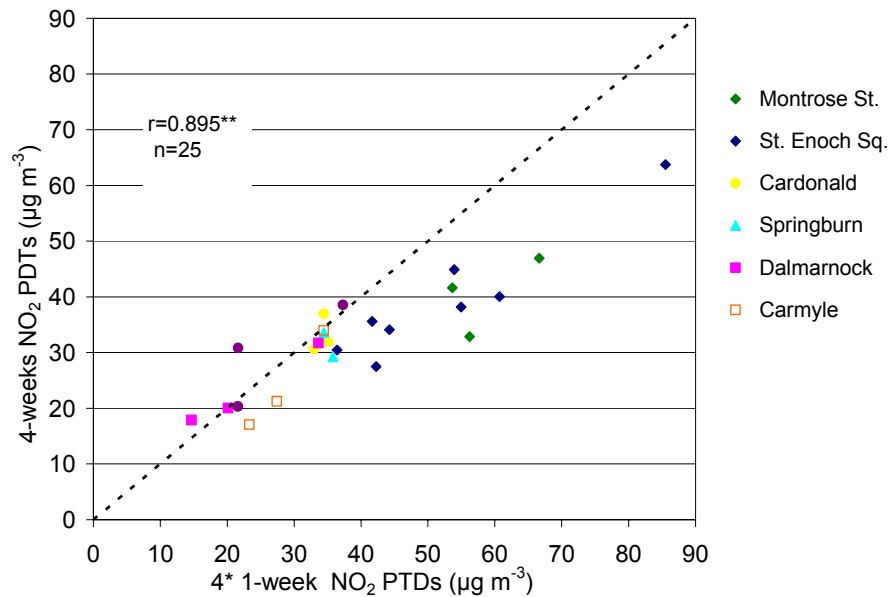


Figure 5.4 Scatter plot and Pearson correlation coefficient (r) of NO₂ concentrations measured during 4 continuous weeks (denoted 4-weeks) and the averaged concentration of 4 consecutive 1 week exposure periods (denoted 4*1-week). Exposure periods: 15 Feb to 10 May 2005 for all sites, except for St. Enoch Sq. (15 Mar to 6 Dec 2005). ** Correlation significant at 0.01 (2-tailed).

Data at St. Enoch Sq. and Montrose St. showed greater underestimation for the 4-weeks period. Since NO₂ concentrations at these two sites were higher than at the other sites it is possible that high NO₂ concentrations were saturating the TEA absorbent over the 4-weeks period resulting in an underestimation of the NO₂ concentration. If this was the case then an increase in underestimation should be observed with increasing ambient NO₂ concentrations.

To test this hypothesis the ratio of 4-weeks: 4*1-week NO₂ concentration was plotted against the averaged mean 4-weeks chemiluminescence analyser NO₂ concentrations at St. Enoch Sq. and Montrose St. (Figure 5.5).

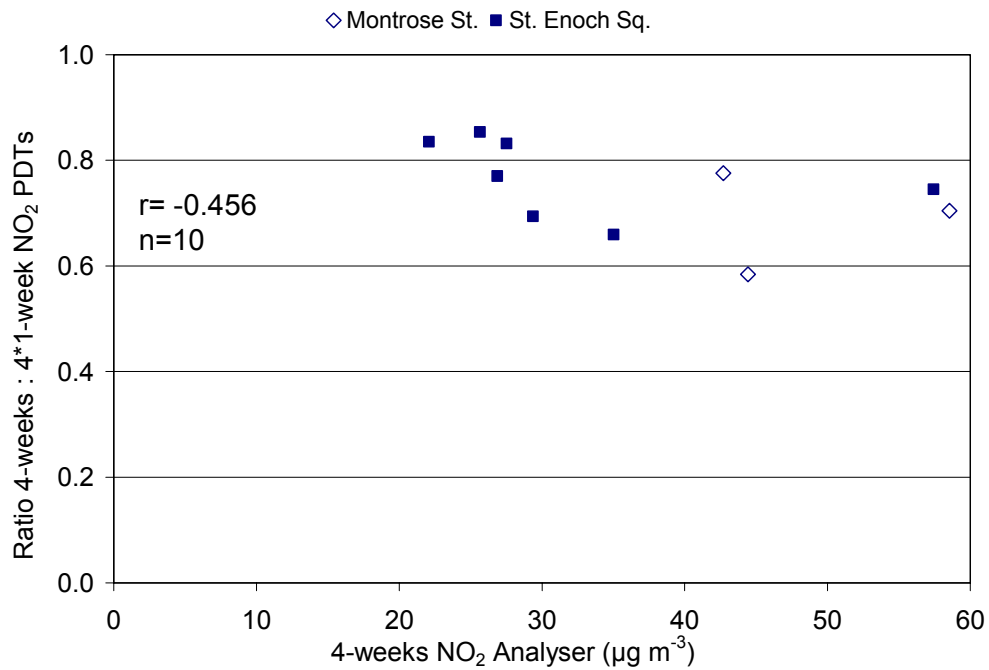


Figure 5.5 Scatter plot and Pearson correlation coefficient (r) of the ratio of NO₂ concentration derived from 4-weeks exposure period over NO₂ concentration derived from 4 consecutive weeks (4*1-week) against the averaged NO₂ concentration as measured by the analyser. Exposure periods: Montrose St. (15 Feb-May); St. Enoch Sq. (15 Mar-Dec 2005). r -value was not statistically significant.

The correlation coefficient was not statistically significant, though at St. Enoch Sq. the scatter plot showed a tendency for greater underestimation as the analyser NO₂ concentrations increased.

Further analyses of the comparison between NO₂ measured by the analyser and the PDTs for the two different exposure periods (4-weeks and 4*1-week) are shown in Section 5.1.1.3.3, alongside a comparison of NO₂ derived from 1-week exposure and the corresponding NO₂ from the analyser.

5.1.1.3 Evaluation of the accuracy of the PDTs

5.1.1.3.1 Comparison of NO₂ PDTs concentrations derived from 1-week exposure period with NO₂ from a chemiluminescent analyser

Table 5.4 shows a summary of statistics comparing NO₂ derived from 1-week PDT exposure and the averaged NO₂ concentrations measured with a chemiluminescence analyser. The PDTs : analyser ratios indicated overestimation by the PDTs. A paired t-test was performed to examine whether the differences in concentration were statistically significant. The correlation coefficient indicates whether these differences in concentrations were systematic or random.

Table 5.4 Summary statistics of the differences in NO₂ measurements derived from 1-week exposure period and the averaged NO₂ concentration measured by a chemiluminescence analyser.

1 week exposure NO ₂		St. Enoch Sq.	Hope St.	Montrose St.
PDTs : analyser	n	83	50	51
	Mean	1.56	1.61	1.06
	SD	0.38	0.23	0.15
	Range	0.90 - 2.37	1.10 - 2.19	0.67 - 1.47
PDTs vs. analyser	p-value	0.000	0.000	0.004
	Paired t-test			
	r	0.767**	0.850**	0.815**

SD: standard deviation. Significant p-values in bold. ** Correlation is significant at 0.01 level (2-tailed). Exposure periods: St. Enoch Sq. (15 Mar-19 Dec 2005; 8 Jun-14 Dec 2006 & 22 May-18 Dec 2007); Hope St. (8 Jun-14 Dec 2006 & 22 May to 18 Dec 2007) and Montrose St. (15 Feb-10 May 2005; 8 Jun-14 Dec 2006 & 22 May -14 Aug 2007).

The differences in concentration measured by the PDTs and analyser were statistically significant ($p < 0.001$, 2-tailed) at St. Enoch Sq. and Hope St., whereas at Montrose St. the differences were significant at $p = 0.004$ level (2-tailed).

The high correlation coefficients between NO₂ concentrations measured by the PDTs and the analyser were indicative of a systematic effect depending on the NO₂ concentration.

Figure 5.6 shows the regression coefficients, scatter plots and the RMA relationships between the 1-week NO₂ concentrations derived from the PDTs and the corresponding averaged data from the analyser at the three sites.

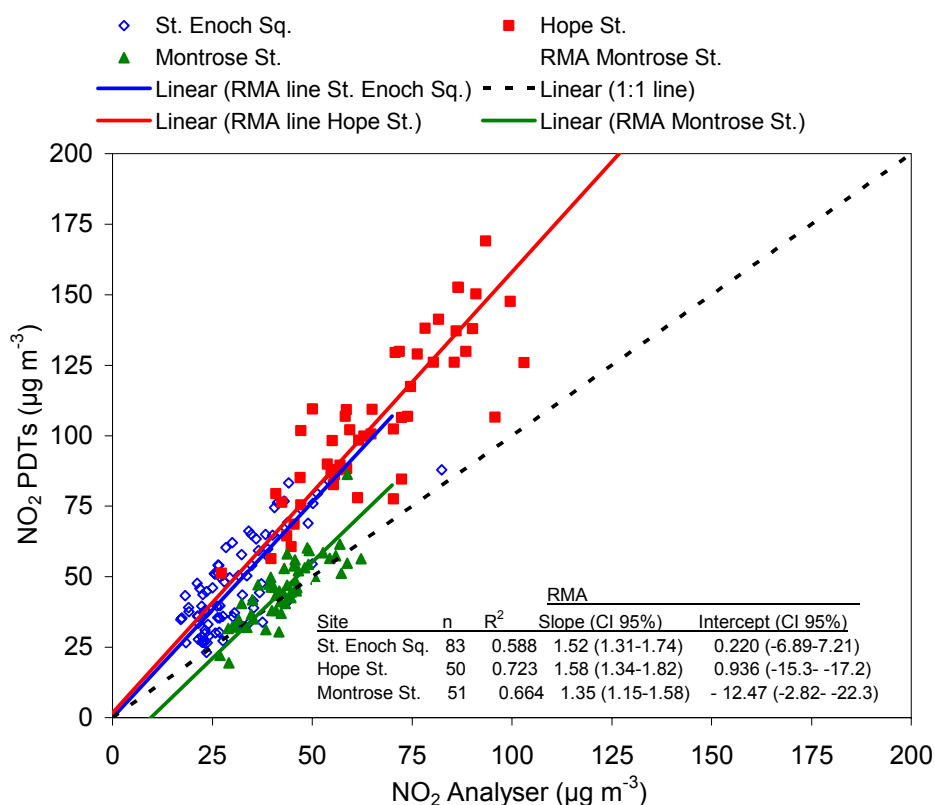


Figure 5.6 Scatter plots and RMA relationship of NO₂ measured by PDTs and NO₂ measured with an analyser. Exposure periods: St. Enoch Sq. (15 Mar-19 Dec 2005; 8 Jun-14 Dec 2006 & 22 May-18 Dec 2007); Hope St. (8 Jun-14 Dec 2006 & 22 May-18 Dec 2007) and Montrose St. (15 Feb-10 May 2005; 8 Jun-14 Dec 2006; 22 May-18 Dec 2007).

The regression coefficient was moderately high at the three sites. The slope of the RMA equation was significantly different from 1 at the three sites (at $p=0.05$ significance level) while the intercept was only significantly different from 0 at Montrose St. (at $p=0.05$ level, 2-tailed). It could be argued that the uncertainty from the NO₂ PDTs concentrations is higher than that from the measurements taken with the analyser and therefore LSR would be a more appropriate regression method. In addition, all NO₂ measurements were above $25 \mu\text{g m}^{-3}$ and therefore concentrations below this value are not well represented in the RMA regression showed in Figure 5.6. Previous studies (Atkins et al., 1986; Gerboles and Amantini, 1993) have shown that the relationship between PDTs and analyser do not produce a significant intercept at low concentrations ($20 \mu\text{g m}^{-3}$). Therefore, the application of forced to zero regression could have provided a better estimation of the relationship between PDTs and analyser.

This observation was proven by comparing the LSR equation not forced and forced to zero intercept (Table 5.5).

Table 5.5 Least Square Regression with (top values) and without intercept set to zero (bottom values) of NO₂ PDTs vs. NO₂ analyser. Exposure periods: St. Enoch (15 Mar-19 Dec 2005; 8 Jun- 14 Dec 2006 & 22 May-18 Dec 2007); Hope St. (8 Jun-14 Dec 2006 & 22 May-18 Dec 2007) and Montrose St.

Site	n	R ²	Slope	CI 95%	Intercept	CI 95%
St. Enoch Sq.	83	0.588	1.17	(0.952-1.38)	11.3	(4.15-18.3)
	83	0.953	1.49	(1.42-1.57)	-	
Hope St.	50	0.723	1.34	(1.10-1.58)	16.7	(0.103-33.3)
	50	0.980	1.58	(1.51-1.64)	-	
Montrose St.	51	0.664	1.11	(0.880-1.33)	-1.75	(-11.6-8.15)
	51	0.981	1.07	(1.02-1.11)	-	

Exposure periods: St. Enoch Sq. (15 Mar-19 Dec 2005; 8 Jun- 14 Dec 2006 & 22 May-18 Dec 2007); Hope St. (8 Jun-14 Dec 2006 & 22 May-18 Dec 2007) and Montrose St. (15 Feb-10 May 2005; 8 Jun- 14 Dec 2006; 22 May-18 Dec 2007).

LSR forced to zero intercept resulted in a slope not statistically significantly different from 1 (at p=0.05, 2-tailed) and a regression coefficient very close to 1 at Montrose St. The slopes for St. Enoch Sq. and Hope St. were similar to those obtained by RMA regression. The slopes of LSR not set to zero intercept were obviously larger than those obtained with RMA since the $\text{slope}_{\text{RMA}} = \text{slope}_{\text{LSR}} / \text{correlation coefficient}$.

To examine the influence of ambient NO, NO₂ and O₃ concentrations on the overestimation by the passive samplers, the overestimation expressed as the ratio of NO₂ concentration PDTs to analyser was plotted against the concentration ratio analyser NO: NO₂ and analyser O₃: NO₂ (Figure 5.7). The NO: NO₂ and O₃: NO₂ concentration ratios were used as independent variables instead of the absolute concentration of NO and O₃ because the ratios provide more information than the absolute values of NO and O₃ about the relative concentrations of NO₂, NO and O₃ due to the continuous reactions between the 3 gases.

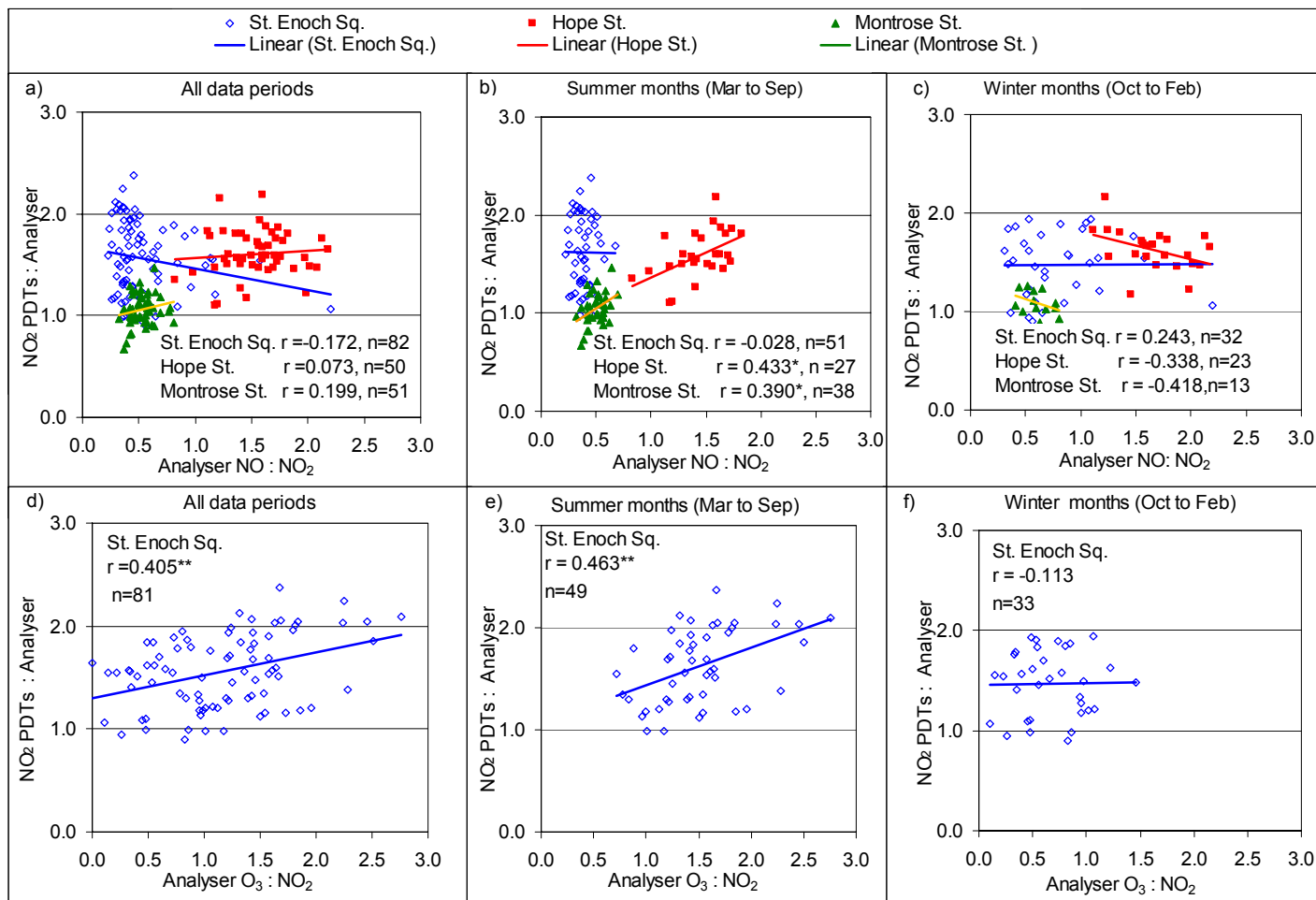


Figure 5.7 Scatter plots and Pearson correlation coefficients (r) of PDTs:Analyser NO₂ ratio against NO:NO₂ & O₃:NO₂ measured by a chemiluminescence analyser for all data periods (a & d); summer (b & e) and winter (c & f) at St. Enoch Sq., Hope St. and Montrose St. (O₃ data were only available to St. Enoch Sq.). **Correlation significant at the 0.01 level (2-tailed); *Correlation significant at the 0.05 level (2-tailed).

Data for the entire period did not show a positive dependency of NO₂ overestimation by the passive samplers with the ratio of NO: NO₂ at any of the sites. However, when only summer data (March to September) was considered, a weak dependence on NO: NO₂ was found at Hope St. and Montrose St. but not at St. Enoch Sq. This caused an increase in overestimation with an increase in the ratio NO: NO₂. In winter (October to February), the opposite trend was observed, though the r-values were not statistically significant.

At St. Enoch Sq. (the only site where there were data of O₃) the excess of NO₂ created in the tube was dependent on the O₃ concentration over the summer but not over the winter.

5.1.1.3.2 Comparison of NO_x PDTs derived from 1-week exposure period with NO_x from a chemiluminescence analyser.

Table 5.6 shows summary statistics of the ratio of 1-week NO_x PDTs over the NO_x concentration derived from the chemiluminescence analyser for the same exposure period.

Table 5.6 Summary statistics of the differences in NO_x measurements derived from 1-week exposure periods and the NO_x concentration measured by a chemiluminescence analyser.

		NO _x	NO ₂	NO	
St. Enoch Sq.	n	12	12	12	
	PDTs/ Analyser	Mean	1.67	1.94	1.13
		SD	0.18	0.18	0.44
		Range	1.41 - 2.03	1.56-2.24	0.57-1.95
		p-value	0.000	0.000	0.260
PDTs vs. Analyser	r	0.793**	0.878**	0.626*	
Hope St.	n	12	12	12	
	PDTs/ Analyser	Mean	1.06	1.58	0.82
		SD	0.18	0.13	0.26
		Range	0.77 - 1.35	1.42-1.81	0.31 - 1.14
		p-value,	0.960	0.000	0.022
PDTs vs. Analyser	r	0.900**	0.973**	0.496*	
Montrose St.	n	12	12	12	
	PDTs/ Analyser	Mean	0.91	1.02	0.77
		SD	0.07	0.09	0.15
		Range	0.78-0.99	0.943-1.19	0.54 -0.98
		p-value,	0.002	0.737	0.000
PDTs vs. Analyser	r	0.826**	0.895**	0.259	

Significant p-values in bold. Exposure period: 22 May-14 Aug 2007.

NO_x derived from the passive samplers overestimated the concentration measured by the analyser at St. Enoch Sq. The differences between PDTs and analyser were statistically significant ($p < 0.001$, 2-tailed). However, at Montrose St., the PDTs underestimated the NO_x concentration measured by the chemiluminescence analyser (the differences between PDTs and analyser were statistically significant at $p = 0.002$ level, 2-tailed). At Hope St. both monitoring devices measured similar concentrations and the difference between PDTs and analyser were not significantly different ($p > 0.05$, 2-tailed).

NO₂ PDTs concentrations were overestimated at the three sites, whereas NO PDTs concentrations were underestimated at Hope St. and Montrose St. but compared well with those averaged from the analyser at St. Enoch Sq.

As was the case for NO₂, the biases of measuring NO_x by passive samplers were systematic, as indicated by the high correlation coefficient between PDTs and analyser.

Figure 5.8 shows the scatter plots, RMA regression equation and regression coefficient between NO_x derived from PDTs and analyser at the three sites.

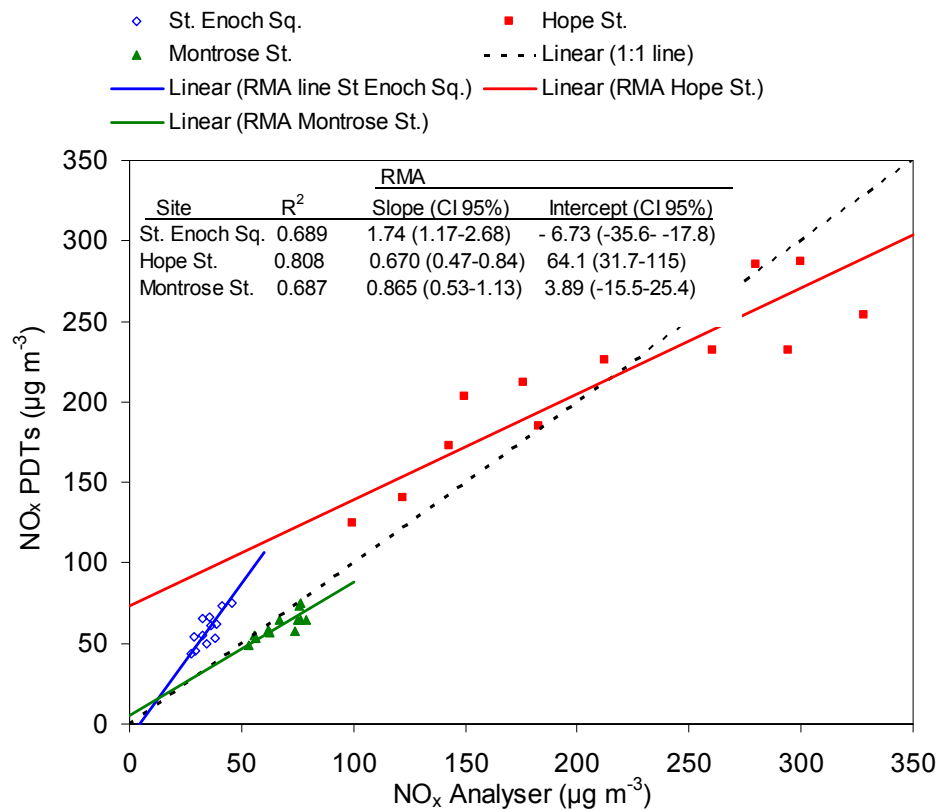


Figure 5.8 Scatters and RMA relationship of NO_x measured by PDTs and NO_x measured by a chemiluminescence analyser at St. Enoch Sq., Hope St. and Montrose St. Exposure period: 22 May-14 Aug 2007 (n=12 at the three sites).

The regression coefficients were moderately high at the three sites. The slope and intercepts were significantly different from 1 and zero, respectively at Hope St. and St. Enoch Sq. (at $p=0.05$ level, 2-tailed) but not at Montrose St.

As discussed in Section 5.1.1.3.1, for the regression of NO_2 PDTs vs. NO_2 analyser, the regression equation was calculated using the Linear Square Regression (LSR) method with and without the intercept set to zero (Table 5.7).

Table 5.7 Least Square Regression with (top values) and without (bottom values) intercept forced to zero of NO_x PDTs vs. NO_x analyser.

Site	n	R ²	Slope	(CI 95 %)	Intercept	(CI 95 %)
St. Enoch Sq.	12	0.689	1.45	(0.764-2.13)	3.68	(-20.7-28.0)
	12	0.992	1.55	(1.45-1.64)	-	
Hope St.	12	0.808	0.592	(0.40-0.80)	88.4	(41.9-132)
	12	0.973	0.958	(0.851-1.06)	-	
Montrose St.	12	0.687	0.712	(0.37-1.05)	14.2	(-9.04-37.8)
	12	0.994	0.918	(0.87-0.96)		

Exposure period: 22 May- 14 Aug 2007.

The LSR forced to zero intercept resulted in a slope not significantly different from 1 (at $p=0.05$, 2-tailed) at Montrose St. and Hope St. However, at Hope St. the regression line did not match the pattern of the data points, since in this case, the intercept was very high and approximation to zero was not adequate. Results for St. Enoch Sq. were similar for LSR with and without set to zero intercept and similar to those obtained by RMA regression.

5.1.1.3.3 Comparison of NO₂ PDTs derived from 4-weeks and 4*1-week with NO₂ from a chemiluminescence analyser

Table 5.8 shows summary statistics for the comparison between NO₂ concentrations measured by PDTs and those measured by the analyser for the two exposure periods (4-weeks and 4*1-week).

Table 5.8 Summary statistics of the differences in NO₂ concentration derived from 4-weeks & 4*1-week PDTs exposure periods and the NO₂ concentration measured by a chemiluminescence analyser.

		4*1-week & analyser		4-weeks & analyser
Montrose St.	PDTs:analyser	n	3	3
		Mean	1.17	0.80
		SD	0.08	0.12
		Range	1.07 - 1.21	0.71 - 0.94
	Paired t-test	p-value	0.111	0.043
	Correlation Coefficient	r	NA	NA
St. Enoch Sq.	PDTs:analyser	n	7	7
		Mean	1.65	1.26
		SD	0.15	0.16
		Range	(1.41 - 1.88)	(1.05 - 1.53)
	Paired t-test	p-value	0.000	0.003
	Correlation Coefficient	r	0.964**	0.949**

NA: Not applicable; SD: standard deviation. Significant p-values in bold. ** Correlation significant at the 0.01 level (2-tailed). Exposure periods: St. Enoch Sq. (15 Mar-19 Dec 2005; 8 Jun-14 Dec 2006 & 22 May-18 Dec 2007); Montrose St. (15 Feb-10 May 2005; 8 Jun-14 Dec 2006 & 22 May-14 Aug 2007).

With the exception of 4-weeks PDTs at Montrose St., PDTs overestimated the NO₂ concentrations measured by the chemiluminescence analyser. The overestimation was higher for 4*1-week exposure periods than for exposure of 4 continuous weeks. This was expected since the 4-weeks exposure period was found to underestimate the concentration measured by 4 consecutive weeks (see Table 5.3). Paired t-test showed that the differences between 4*1-week and those derived from the analyser were statistically significant at Montrose St. ($p < 0.05$, 2-tailed) and St. Enoch Sq. ($p < 0.001$, 2-tailed), whereas the differences between 4-weeks and those derived from the analyser were significant only at St. Enoch Sq. ($p < 0.05$, 2-tailed).

However, despite the differences in the absolute NO₂ concentrations, measurements of NO₂ derived from 4*1-week and 4-weeks exposures at St. Enoch Sq., were statistically significantly correlated with the NO₂ concentrations measured by the analyser ($r=0.964$ for 4*1-week vs. analyser and $r=0.949$ for 4-weeks PDTs vs. analyser) (only at St. Enoch Sq. were there sufficient data to calculate correlations). This result suggests that the differences in the concentrations measured by both devices were systematically dependant on ambient NO₂ concentrations. At Montrose St. there were only 3 data points available; these indicated a substantially lower overestimation of 4*1-week vs. analyser and an underestimation of 4-weeks vs. analyser.

5.1.2 Equipment validation for particle sampling

5.1.2.1 Replicate precision of mass and absorbance of respirable dust filters

The precision of the respirable dust samplers (Higgins and Dwell cyclone and SKC personal pump) was assessed by running 6 samplers side by side over a period of 4 weeks in the University premises with the inlets located outdoors towards a quiet street in a background area (Rottenrow).

Figure 5.9 and Figure 5.10 show a boxplot with the concentration and absorption coefficient values of the six samplers for each week, during two inter-comparison exercises: a first one with previously used diaphragms in the pumps (Figure 5.9) and a second one with new diaphragms (Figure 5.10).

Figure 5.9 shows a high variability in the PM₄ mass and absorption coefficient measured with the different samplers. The mean RSD for the 4 weeks was 16.1 % for the mass and 52.9 % for the absorption coefficient. This high level of imprecision was attributed to the changes in the flow rate. In most of the pumps, the flow was unstable, varying between 2.2 to 1.6 L min⁻¹. To improve the flow stability new diaphragms were installed in all the pumps resulting in a decrease in flow variability and consequently, higher precision of the mass concentration (RSD=9.7 %) and absorption coefficient (RSD=5.8 %) (Figure 5.10).

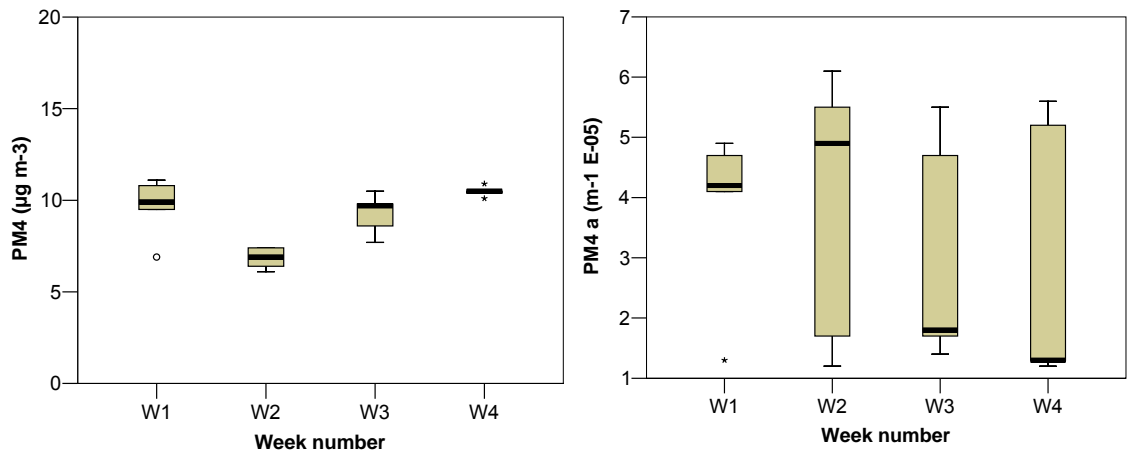


Figure 5.9 Boxplots of the concentration (left) and absorption coefficient (right) of PM₄ sampled simultaneously with 6 respirable dust samplers at Rottenrow (background site) over 4 weeks, using pumps with previously used diaphragms. Exposure period: 21 Nov-19 Dec 2005. Box limits are the 25th and 75th percentiles. The solid line in the box is the median and the whiskers are the 10th and 90th percentiles.

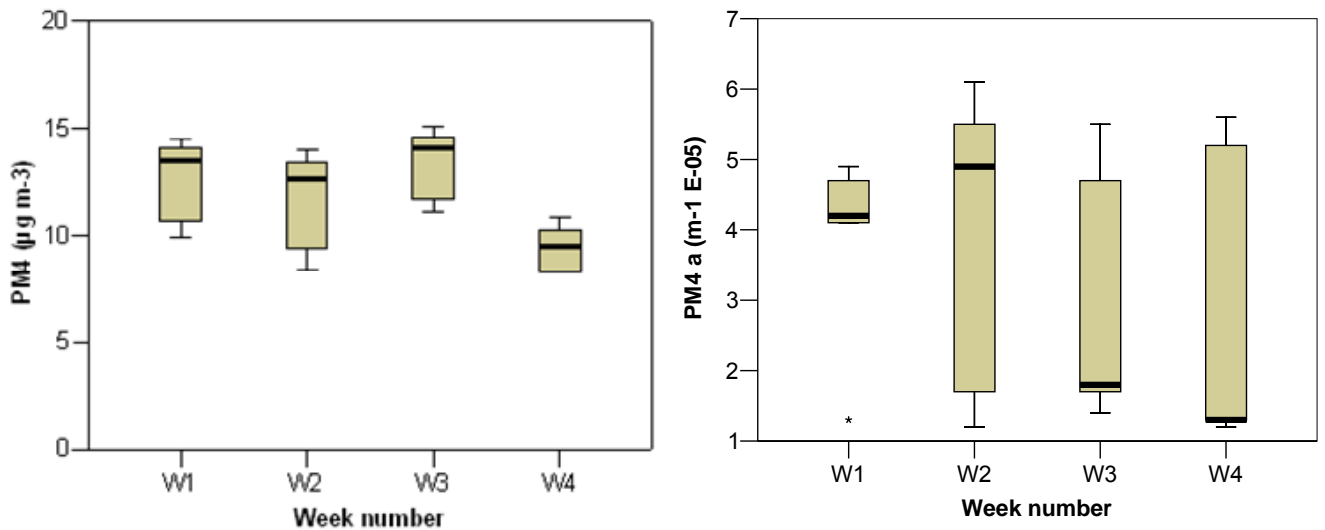


Figure 5.10 Boxplot of the concentration (left) and absorption coefficient (right) of PM₄ sampled simultaneously with 6 samplers, at Rottenrow (background site) over 4 weeks, using pumps with new diaphragms. Exposure period: 16 Feb-20 Mar 2006. Box limits are the 25th and 75th percentiles. The solid line in the box is the median and the whiskers are the 10th and 90th percentiles.

Since the precision of the samplers using pumps with the new diaphragms was acceptable, two respirable dust samplers were set up at each monitoring site (St. Enoch Sq., Hope St. and Montrose St.) simultaneously with NO₂ PDTs, particle counters and

Partisol sampler (except at Montrose St.). Figure 5.11 shows the scatter plot and correlation coefficient of the PM₄ concentration and absorption coefficient of the two replicates collected at the three sites.

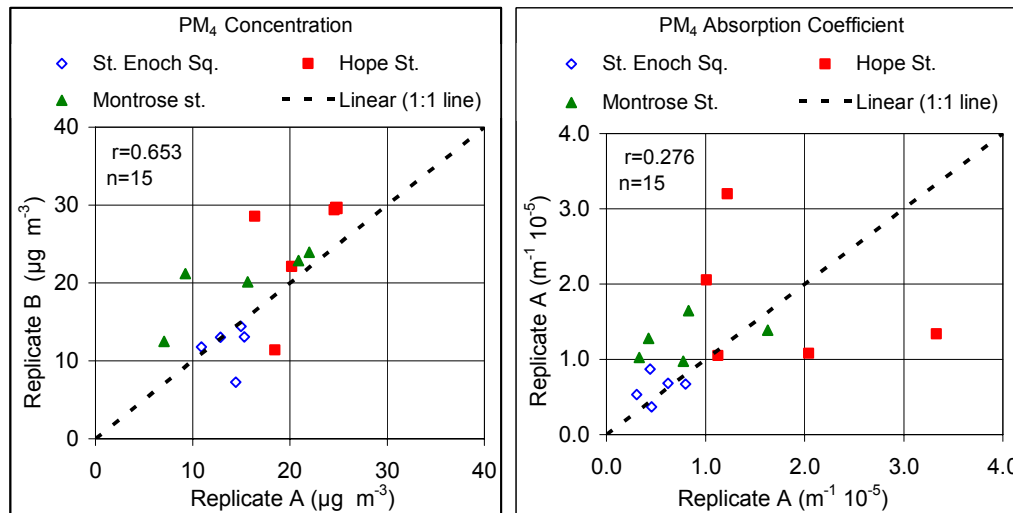


Figure 5.11 Replicate precision of PM₄ concentration (left) and absorption coefficient (right) during the monitoring campaign at Hope St., St. Enoch Sq., and Montrose St. (n=15). Exposure period: 7 Jun-27 Jul 2006.

During the monitoring campaign one sampler failed at each site because the sampler's diaphragm wore out, having to be replaced with another sampler. Replicate measurements at Hope St. for both PM₄ mass and absorption coefficient showed a higher dispersion at Hope St. compared to St. Enoch Sq. and Montrose St. The correlation coefficient between samplers was relatively low, especially the r-value between of the absorption coefficient replicates (r=0.276). The RSD (%) was 19.7 % and 37 % for the mass and absorption coefficient, respectively. Therefore, the quality of the data was not considered acceptable and the results were not included in the analysis of pollutant correlations.

5.1.2.2 Inter-comparison of Partisol and TEOM analyser

This section shows the results of the inter-comparison study between the gravimetric method for PM₁₀ measurements using Partisol 2025 and the real-time analyser Tampered Element Oscillating Microbalance (TEOM) at two sites with different pollution levels: Hope St. (kerbside/street canyon) and St. Enoch Sq. (urban centre).

Figure 5.12 shows the scatter plots, correlation coefficient, and RMA linear relationship between the PM_{10} measurements collected with the Partisol sampler and the corresponding 24-hours averaged TEOM data. TEOM data is presented with the default correction factor of $3 + 1.03 \cdot TEOM$ (denoted TEOM (3, 1.03)); the correction factor applied in the UK (default correction plus a further correction of 1.3 in the slope, denoted TEOM (3, 1.03, 1.3)) and without any correction factor (full details of these correction factors are given in section 4.3.2). TEOM data were obtained from the NAQA where it is reported with the UK (3, 1.03, 1.3) correction factor.

Data were collected from 8 June to 21 July 2006. Instrument faults meant that simultaneous data for the two monitoring sites were available for only 8 days. Therefore, to increase the statistical power, scatter plots and the RMA relationship are not presented only with simultaneous data but with all data available at each site ($n=15$ and $n=18$ at St. Enoch Sq. and Hope St., respectively).

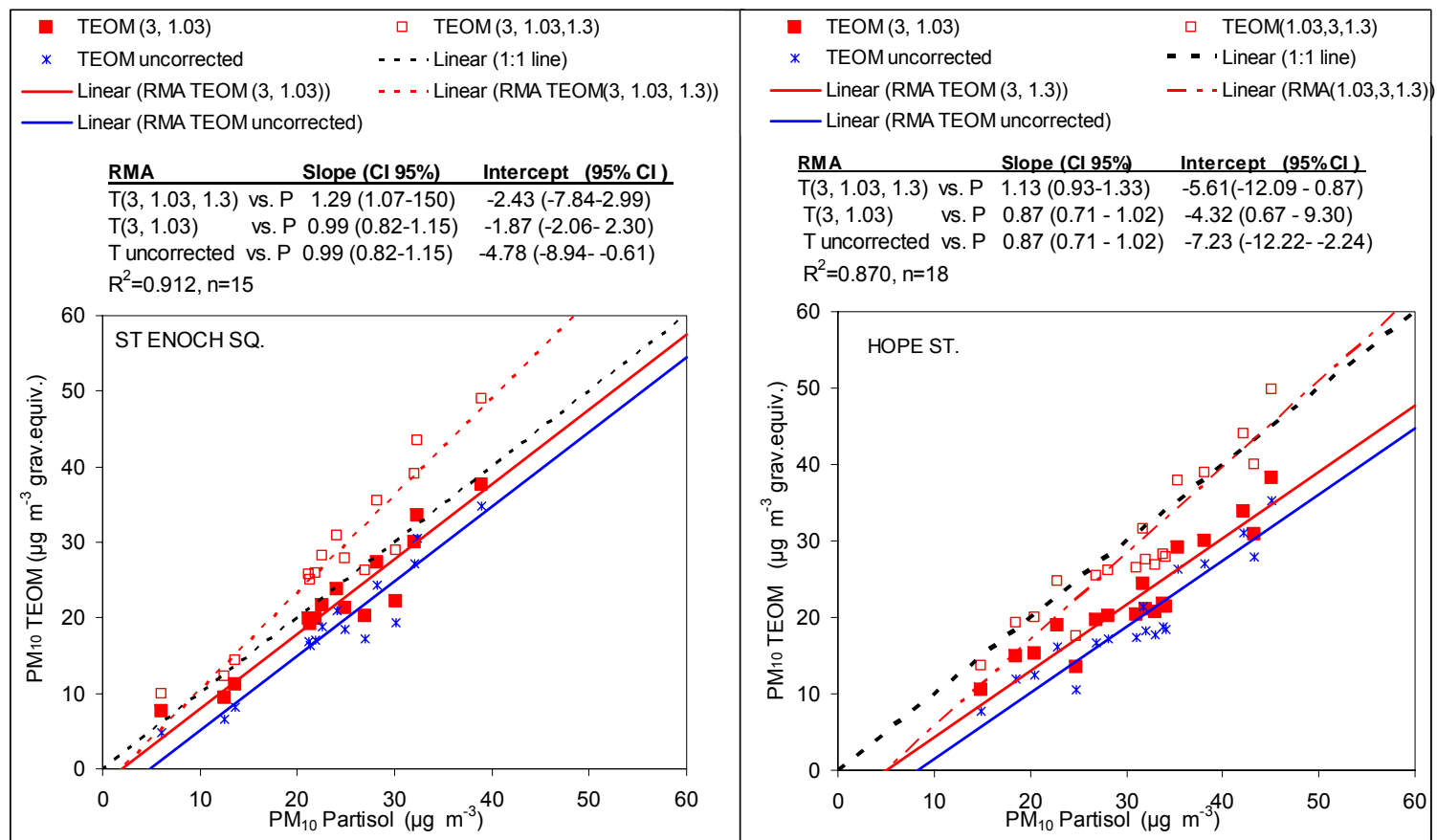


Figure 5.12 Scatter plots, Reduced Major Axes (RMA) relationship and regression coefficient (R^2) of PM_{10} measurements taken with a Partisol and a 24-hrs averaged TEOM data with the default correction (3, 1.03); UK correction (3, 1.03, 1.3) and uncorrected at Hope St. (left) and St. Enoch Sq. (right). Exposure period: 8 Jun- 21 Jul 2006.

PM₁₀ measurements collected with both monitors were statistically significantly correlated (0.01 level, 2-tailed) at both sites. At Hope St., the relationship that was closest to the 1:1 line was that with the (1.03, 3, 1.3) corrected TEOM data, which is the factor used in the UK. In contrast, at St. Enoch Sq. application of the default correction factor (1.03, 3) resulted in a closer relationship to the 1:1 line, than the (1.03, 3, 1.3) correction factor. This result suggests that the further correction of 1.3 on the slope applied by the UK authorities is unnecessary at St. Enoch Sq. and would result in overestimation of the PM₁₀ concentrations as measured by the Partisol.

Table 5.9 shows the mean and median of the PM₁₀ measurements collected with the Partisol and those averaged from the TEOM analyser using the default correction factor (3, 1.3) and the UK correction factor (1.03, 3, 1.3). The mean of the RSD for each day is also shown, as are the p-values of the paired t-test between Partisol and TEOM measurements.

Table 5.9 Descriptive statistics of PM₁₀ Partisol measurements and 24-hours averaged TEOM data with the default correction (3, 1.03), and UK correction (3, 1.03, 1.3) at Hope St. and St. Enoch Sq. RSD (%) and paired t-test between Partisol data and TEOM data with the different correction factors. Exposure period: 8 Jun- 21 Jul 2006.

		n	Mean ($\mu\text{g m}^{-3}$)	Median ($\mu\text{g m}^{-3}$)	Mean daily RSD (%) (Partisol, TEOM)	p-value paired t-test (Partisol, TEOM)
Hope St.	Partisol	18	30.9	31.9	NA	NA
	TEOM(3, 1.03, 1.3)	18	29.2	27.2	7.48	0.057
	TEOM(3, 1.03)	18	22.5	20.9	23.0	0.000
St. Enoch Sq.	Partisol	15	23.8	24.1	NA	NA
	TEOM(3, 1.03, 1.3)	15	28.2	27.8	12.6	0.000
	TEOM(3, 1.03)	15	21.7	21.4	9.18	0.000

NA: Not applicable. Significant p-values in bold.

At Hope St., application of the 1.3 factor reduced the significance of the difference between Partisol and TEOM in the paired t-test compared to the default correction (3, 1.03). At St. Enoch Sq., both correction factors resulted in significant differences from the PM₁₀ concentration measured by the Partisol. Correction factor (3, 1.03, 1.3) overestimated the Partisol measurements, whereas correction factor (3, 1.03) resulted in an underestimation.

The mean of the RSD (%) between Partisol and TEOM measurements corrected with factor (3, 1.03, 1.3) was only 7.48 %. At St. Enoch Sq., the RSD was larger since the correction factor (3, 1.03, 1.3) resulted in statistically different concentrations between Partisol and TEOM.

The paired TEOM and Partisol PM₁₀ dataset from Hope St. and St. Enoch was limited and cannot be considered to represent the annual trend. However, it gives an insight into the possible unsuitability of relying upon the UK 1.3 factor to correct TEOM measurements.

To investigate whether similar relationships between TEOM and Partisol at Hope St. and St. Enoch Sq. were observed at other locations, simultaneously PM₁₀ measurements at North Kensington and Marylebone during 2006 were examined. Figure 5.13 shows the scatter plot, correlation coefficient, and RMA linear relationship between the PM₁₀ Partisol measurements and the 24-hours averaged TEOM. As for St. Enoch Sq. and Hope St. TEOM data is also shown with the UK correction factor (3, 1.03, 1.3), with the default correction factor (3, 1.03) and as uncorrected data.

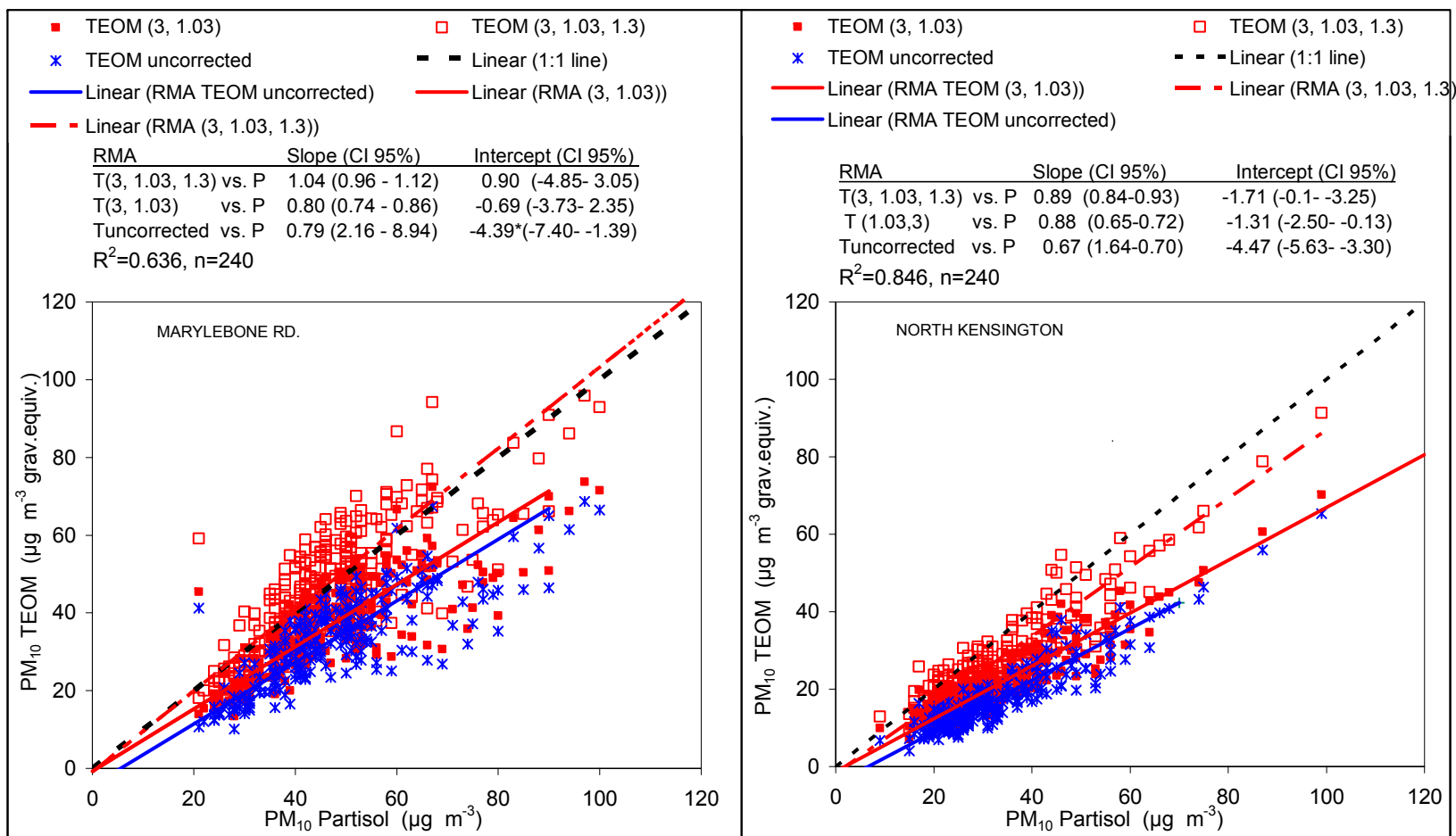


Figure 5.13 Scatter plot, Reduced Major Axes (RMA) relationship and regression coefficient (R^2) of PM_{10} measurements taken with a Partisol and a 24-hours averaged TEOM with the default correction (1.03,3); UK correction (1.03,3,1.3) and uncorrected data at Marylebone Rd. (left) and North Kensington. (right). Exposure period: 18 Jan- 31 Dec 2006.

PM₁₀ data collected by the TEOM and Partisol was statistically significantly correlated ($p < 0.001$, 2-tailed) at Marylebone Rd. and North Kensington.

At both sites the relationship that was closest to the 1:1 line was that with the TEOM corrected for (3, 1.03, 1.3), which is the correction used in the UK. However, at Marylebone Rd. such correction resulted in slightly higher PM₁₀ readings for the TEOM than for the Partisol, whereas at North Kensington the PM₁₀ Partisol readings were higher than those of the TEOM.

Table 5.10 shows the mean and median of the PM₁₀ measurements collected with the Partisol and those averaged from the TEOM analyser with the default correction factor (3, 1.3) and the UK correction factor (1.03, 3 1.3). The mean of the RSD of PM₁₀ concentration measured with both monitors for each day is also shown, in addition to the p-values of the paired t-test between Partisol and TEOM measurements.

Table 5.10 Descriptive statistics, of PM₁₀ Partisol measurements and 24-hours averaged TEOM data with the default correction (3, 1.03), and UK correction (3, 1.03, 1.3) at Marylebone Rd. and North Kensington. RSD (%) and paired t-test between Partisol data and TEOM data with the different correction factors. n=240. Exposure period: 1 Jan-31 Dec 2006.

		Mean ($\mu\text{g m}^{-3}$)	Median ($\mu\text{g m}^{-3}$)	Mean daily RSD (%) (Partisol, TEOM)	p-value Paired t-test (Partisol, TEOM)
Marylebone Rd.	Partisol	47.2	45.0	NA	NA
	TEOM(3, 1.03, 1.3)	48.3	48.3	10.9	0.059
	TEOM(3, 1.03)	37.1	37.1	18.0	0.000
North Kensington	Partisol	32.4	28.5	NA	NA
	TEOM(3, 1.03, 1.3)	27.0	23.5	14.8	0.000
	TEOM(3, 1.03)	20.8	18.0	31.1	0.000

NA: Not applicable. Significant p-values in bold.

At Marylebone Rd. the further correction factor of 1.3 (3, 1.03, 1.3) applied in the UK seemed appropriate as differences with PM₁₀ Partisol measurements were not statistically significantly different ($p > 0.001$). However, at North Kensington the UK correction factor (3, 1.03, 1.3) resulted in statistically significant lower concentrations compared to PM₁₀ Partisol measurements.

The mean of the daily RSD between TEOM corrected with (3, 1.03, 1.3) and Partisol at Marylebone Rd. (for which PM₁₀ differences were not statistically significant) was 10.9%. At North Kensington the mean of the RSD between the TEOM and partisol was

higher than at Marylebone Rd. since the differences between TEOM (3, 1.03, 1.3) and Partisol were statistically significant.

5.1.2.3 Comparison of water-based (Model 3785) & butanol-based (Model 3022A) condensation particles counters

This section describes the results of the inter-comparison studies of PNC measured with a WCPC and BCPC. The relationships of PNC measured by both particle counter models vs. nitrogen oxides concentrations are also shown.

Table 5.11 shows a summary of the dates, deployment sites, and technical faults encountered with the WCPCs.

Table 5.11 Summary of dates, sampling sites and technical faults of the water-based condensation particle counters (WCPC1 top and WCPC2 bottom).

WCPC1 serial No. 70515012				
Start date	End date	Deployment site	Purpose / Repair description	Reason ending
02-Mar-06	08-Mar-06	St.Enoch Sq.	Comparison with BCPC	Study completed
10-Mar-06	May 06	St.Enoch Sq.	Familiarization with software	Drop in flow-rate
23-May 06	01-Jun-06	TSI Company	Restoration of flow-rate Installation of new wick	
08-Jun-06	11-Aug-06	Montrose St.	Correlation with co-pollutants	Drop in flow-rate
18 Aug-06	03-Jan-07	TSI Company	Cleaning of lazer nozzle Installation of new wick Installation of 1 µm cyclon Extended photometric calibration	
25-Jan-07	29-Jan-07	Strathclyde University	Comparison with WCPC 2	Taken to field site
31-Jan-07	13-Apr-07	St.Enoch Sq.	Comparison with BCPC	Zero reading due to damaged wick
14-Jun-07	15-Jun-07	Strathclyde University	Checked by TSI engineer: Installation of new wick New maintainance guidelines	
15-Jun-07	22-Jun-07	Strathclyde University	Comparison with WCPC 2	
01-Jul-07	25-Aug-07	St. Enoch Sq.	Comparison with BCPC	
01-Sep-07	18-Oct-07	Hope St.	Correlation with co-pollutants	Low readings. Wick turned around
18-Oct-07	16-Dec-07	Hope St.	Correlation with co-pollutants	Zero reading due to damaged wick
01-Feb-08			New wick installed	
01-Feb-08	07-Apr-08	Hope St.	Comparison with WCPC 2 & NO _x	Drop in flow-rate
WCPC2 Serial No. 70515013				
Start date	End date	Deployment site	Purpose / Repair description	Reason ending
02-Mar-06	08-Mar-06	St.Enoch Sq.	Comparison with BCPC	Study completed
10-Mar-06	May 06	St.Enoch Sq.	Familiarization with software	Drop in flow-rate
23-May 06	01-Jun-06	TSI Company	Restoration of flow-rate Installation of new wick	
08-Jun-06	13-Jul-06	Hope St.	Correlation with co-pollutants	Drop in flow-rate
25 Jul-06	03-Jan-07	TSI Company	Cleaning of lazer nozzle Installation of new wick Installation of 1 µm cyclon Extended photometric calibration	
25-Jan-07	29-Jan-07	Strathclyde University	Comparison with WCPC 1	Taken to field site
31-Jan-07	13-Apr-07	St.Enoch Sq.	Comparison with BCPC	Zero reading due to damaged wick
14-Jun-07	15-Jun-07	Strathclyde University	Checked by TSI engineer: Installation of new wick New maintainance guidelines	
15-Jun-07	22-Jun-07	Strathclyde University	Comparison with WCPC 1	
01-Jul-07	31-Aug-07	St. Enoch Sq.	Comparison with BCPC	
01-Sep-07	02-Oct-07	St. Enoch Sq.	Correlation with co-pollutants	Low readings. Wick turned around
02-Oct-07	16-Dec-07	St. Enoch Sq.	Correlation with co-pollutants	Zero reading due to damaged wick
01-Feb-08			New wick installed	
01-Feb-08	14-Jul-08	St. Enoch Sq.	Comparison with WCPC 1 & NO _x	Zero reading due to damaged wick

The two WCPCs were set up at the monitoring station at St. Enoch Sq. on 2 March 2006 to compare their measurements with those from a BCPC run by DEFRA and maintained by NPL. They were continuously running until May 2006, when the flow rate of both WCPCs dropped by more than 20 % from the initial level of 1 L min⁻¹.

The instrument manufacturer and supplier (TSI Ltd.) suggested that the drop in flow could be due to water in the pump system and that drying the machine should enable the flow to be raised to 1 L min^{-1} . The particle counters were dried according to the manufacturer's instructions (left to run overnight without water), which resulted in the flow rate being restored to 1 L min^{-1} . However, after two days the flow dropped again, by more than 20 %. The instruments were returned to the company, where the flow was again restored to 1 L min^{-1} and new wicks were installed. On 8 June 2006 the WCPC 1 was installed at Montrose St. and WCPC 2 at Hope St. as part of the monitoring campaign aiming to simultaneously measure PM_{10} , PNC and nitrogen oxides.

On 13 July and on 11 August 2006, respectively the WCPC 2 and WCPC 1 experienced the same technical problem (reduction of the specified flow rate of 1 L min^{-1}) and they were sent to the company for repair. In January 2007, the instruments were returned to the University. The manufacturers indicated that the reason for the fault was "a build up of dirty aerosols in the optical nozzle" (Cussens, 2006). The laser nozzle was cleaned and to overcome this problem a cyclone was installed to prevent particles larger than $1 \mu\text{m}$ from entering the system.

Figure 5.14 shows the scatter plots of the inter-comparison studies of PNC measured with the WCPCs vs. PNC measured with the BCPC in Mar 2006 (2-8 March, before the instruments were repaired) and in 2007 (14-28 February; 2-21 March and 1-13 April). Data for 2007 was sub-divided by calendar months to examine the effect of the wick's apparent lifetime on the relationship between PNC measured by the WCPC vs. PNC measured by the BCPC.

Data from 5-9 April 2007 has been presented in a separate scatter plot (Figure 5.15) because during these days concentrations reached up to $300,000 \text{ particles cm}^{-3}$, and therefore the axes's scale for these days did not match those for the rest of the measurements. These exceptionally high concentrations were possibly caused by the use of diesel power generators and open gas cookers as part of a street market on the square where the monitoring station was located.

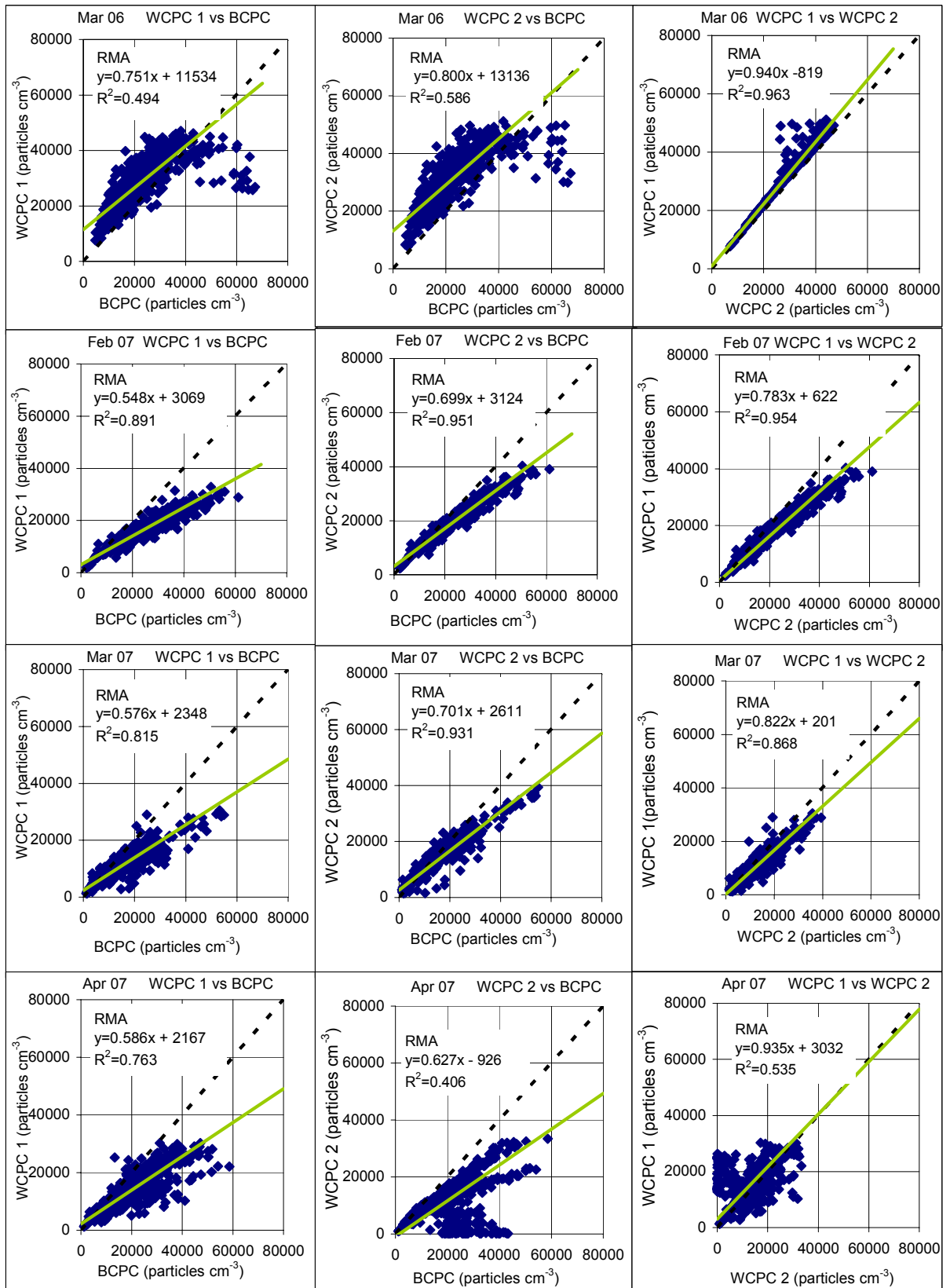


Figure 5.14 Scatter plots, RMA relationship and regression coefficient (R^2) of the two water-based condensation particle counters (WPCPC1 & 2) and butanol-based condensation particle counter (BCPC) from 2- 8 Mar 2006, $n=624$ (before the WPCPCs were repaired) and from 17-22 Feb 2007, $n=497$; 2- 21 Mar 2007 and 1-13 (except 5-8 Apr 2007) after they underwent a major repair. Data are 15-min averages.

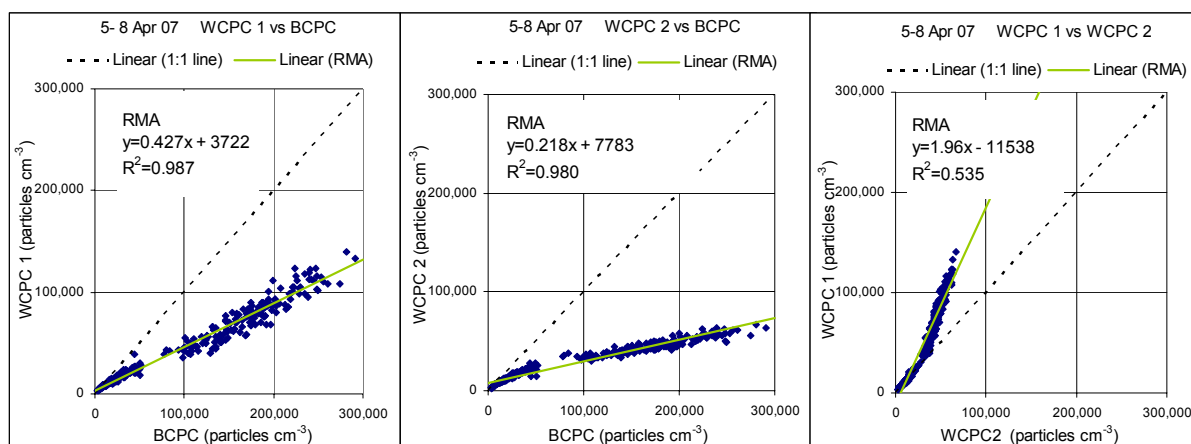


Figure 5.15 Scatter plots, RMA relationship and regression coefficient (R^2) of the two water-based condensation particle counters (WCPC 1 & 2) and butanol-based condensation particle counter (BCPC) from 5 - 9 Apr 07, during a high pollution episode. Data are 15-min averages.

The scatter plots of WCPCs vs. BCPC showed a more clear linear relationship in the inter-comparison studies in 2007, after the instruments were repaired, than that observed in March 2006.

The precision of the WCPC and BCPC during March 2006 was not very high. The RSDs for WCPC1 & BCPC and WCPC2 & BCPC, were relatively high: 25 % and 28 %, respectively and the $R^2=0.494$ and $R^2=0.586$ for WCPC1 & BCPC and WCPC2 & BCPC, respectively. The precision of the two WCPCs was very high ($R^2= 0.963$ and mean RSD=7 %). However, there was an episode of high PNC, where WCPC1 underestimated the PNC as measured by WCPC2 (Figure 5.14, top-right graph).

The scatter plots of data collected in March 2006 clearly showed two different patterns with a steep change at 40,000 particles cm^{-3} (as measured by the BCPC). Below 40,000 particles cm^{-3} there was a linear relationship between the two models ($R^2=0.729$ & 0.727 for WCPC1 & 2 vs. BCPC, respectively), notwithstanding that the WCPCs overestimated the readings taken by the BCPC (the mean ratios of WCPC: BCPC were 1.43 and 1.56 for WCPC1 and WCPC2, respectively). However, above 40,000 particles cm^{-3} there was no clear functional relationship between the two models. Measurements over 40,000 particles cm^{-3} by the BCPC, corresponded to WCPC measurements between 30,000 and 50,000 particles cm^{-3} . The ratios of WCPC: BCPC for paired data with PNC > 40,000 particles cm^{-3} (as measured by the BCPC) dropped to 0.75 and 0.85 for WCPC1: BCPC and WCPC2: BCPC, respectively.

The scatter plots of data in February and March 2007 (Figure 5.14) and during the high pollution episode from 5 to 9 April (Figure 5.15) showed a clear linear relationship between both models for the full range of concentrations. The regression coefficients were higher than those observed in March 2006, before the instruments were repaired (Figure 5.14).

Measurements taken by the WCPCs underestimated slightly those taken by the BCPC for the whole of the concentration range measured, unlike in the previous inter-comparison study in March 2006, where underestimation by the WCPCs occurred only over concentrations above 40,000 particles cm^{-3} . The underestimation in 2007 may have arisen partly from the introduction of a 1 μm size selective inlet, as part of new guidelines issued by TSI. The average ratios WCPC: BCPC from February to March 2007 were 0.82 and 0.98 for WCPC1: BCPC and WCPC2: BCPC respectively. The underestimation by the WCPC increased with increasing PNC as measured by the BCPC (clearly shown in Figures 5.14 and 5.15). During the high pollution episode (Figure 5.15) the WCPCs did not register concentrations above 150,000 particle cm^{-3} , while the BCPC registered up to 300,000 particle cm^{-3} . This resulted in a much lower slope between WCPC vs. BCPC than that observed for February and March 2007 where concentrations were below 40,000 particles cm^{-3} (Figure 5.14).

In addition, the linear relationship between the two particle counter models was sometimes obscured due to the aging of the condensation wick. It was observed that the end of the wick proximate to the laser (where the growth of particles takes place) became discoloured after approximately 4-6 weeks of continuous running and it was not wet. If the wick does not wet properly particles are not grown and therefore they are not efficiently counted. As a consequence, the underestimation by the WCPCs increased as the wick aged, as shown by comparing the scatter plots of data collected in February 2007 with those from April 2007 (Figure 5.14). The scatter plots in February are closer to the 1:1 line than those in April. In addition, the discrepancies between measurements by both particle counter models also increased. R^2 -values dropped from 0.89 in February 2007 to 0.75 in April 2007 for WCPC1 vs. BCPC and from 0.95 in February 2007 to 0.40 in April 2007 for WCPC2 vs. BCPC.

On 14 June 2007, engineers from TSI examined the instruments at the University premises. New maintenance guidelines, which aimed to improve the life of the condensation wick were introduced. These included:

1. Not to operate the machine in its recycle-auto drain mode for the first 24-hours running period. Instead, it was to be operated in manual draining mode. When the instrument operates on the recycle auto-drain mode 80 % of the water needed to wet the condensation wick is taken from the instrument's reservoir. If the reservoir does not contain enough water, e.g. at the beginning of the running session (since at this point the reservoir is empty) insufficient water enters the condensation chamber, affecting particle growth and allegedly damaging the wick.
2. To wet the wick prior to installation in the particle counter. Other maintenance procedures referred to regular cleaning of the internal orifices of the machine (damper orifice, purge orifice and laser nozzle).

Despite implementing these guidelines, subsequent monitoring periods have confirmed that after approximately 6 weeks of continuous running, the end of the wick closest to the laser becomes damaged, and the WCPCs start to record low measurements. Unfortunately, the BCPC located at St. Enoch Sq. stopped operating in June 2007 and therefore, comparisons of PNC collected with both particle counter models after implementation of the new guidelines for the WCPCs were not possible. However, examination of time series plots revealed a significant decrease in the PNC approximately 2-3 months after a new wick was installed (Figure 5.16, period 5 to 27 September 2007). To prove that the damaged wick resulted in underestimation of PNC, the wick was turned around when the underestimation became apparent, so the end adjacent to the inlet, which was in good condition, was then installed closest to the laser. Figure 5.16 shows the sharp increase in concentration when the wick was turned around in both WCPCs (on 2 October in WCPC 1, Figure 5.16, top and on 18 October WCPC Figure 5.16, bottom).

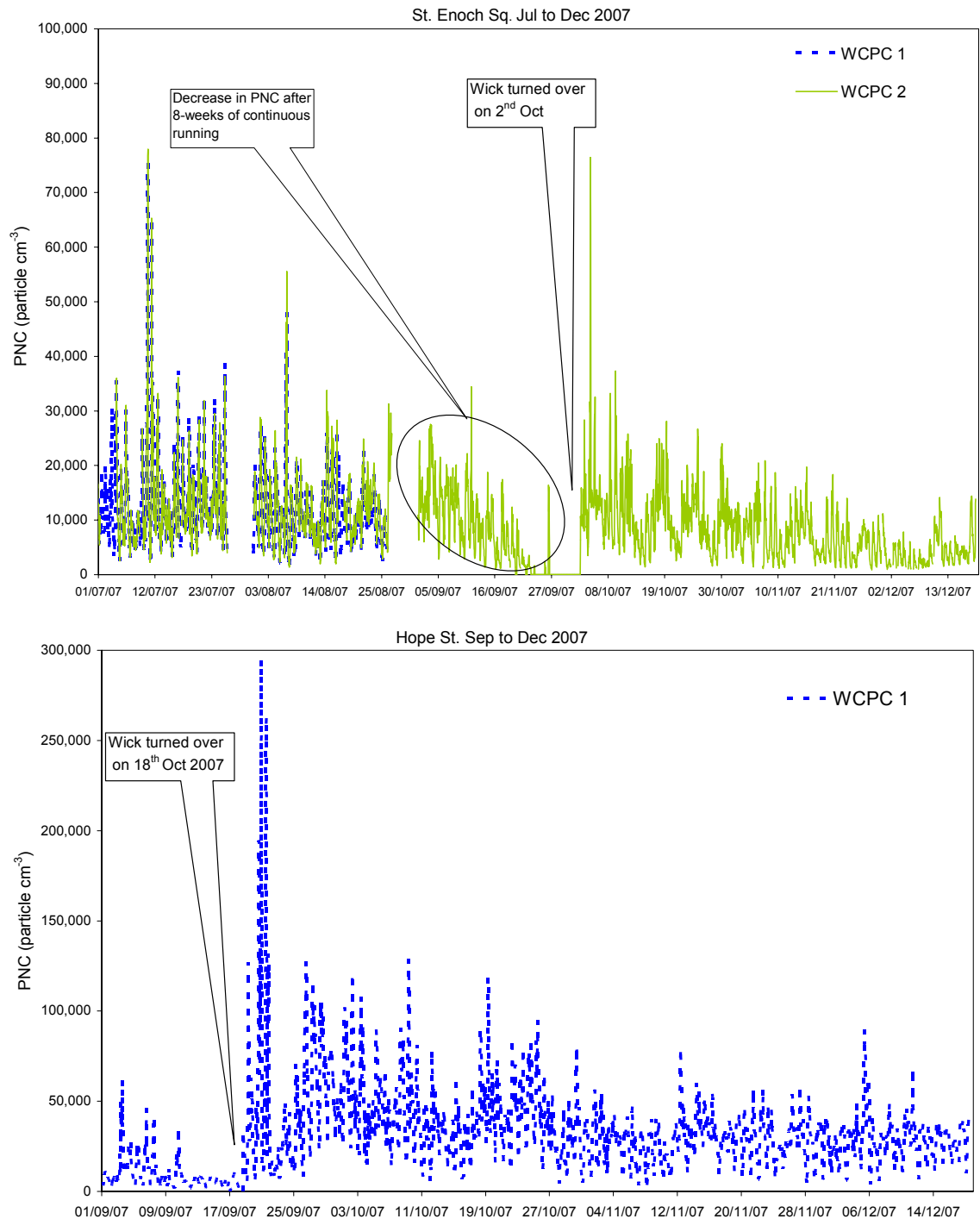


Figure 5.16 Time series plot of hourly particle number concentration (PNC) measured with the WCPC 1 (1 Jul- 25 Aug 2007) & WCPC 2 (1 Jul- 16 Dec 2007) at St. Enoch Sq. (top) and WCPC 1 (1 Sep-16 Dec 2007) at Hope St. (bottom).

PNC measured with the WCPC 2 increased from 0 to 10,800 particles cm⁻³ when the wick end in good condition was installed closest to the laser (Figure 5.16, top). PNC measured with the WCPC 1 raised from approximately 6,000-7,000 to

41,200 particles cm^{-3} , a concentration 6 times higher when the wick end in good condition was placed closer to the laser (Figure 5.16, bottom).

Since one of the aims of this project was to examine the different relationships between traffic-related air pollutants, it is important to understand how the underestimation of PNC influenced the relationship between PNC and nitrogen oxides.

The scatter plots of PNC for the three particle counters vs. NO_x and NO_2 for data collected in March 2006 (before the WCPCs were repaired) and data collected in February 2007 (after the WCPCs were repaired) are shown in Figure 5.17. The scatter plots of PNC vs. NO_x and NO_2 for March and April 2006 were not helpful in identifying the effects of the underestimation of PNC on the relationship between PNC and nitrogen oxides because during those months building works took place at St. Enoch Sq., resulting in emissions of particles, which confounded the relationship between traffic-emitted particles and nitrogen oxides.

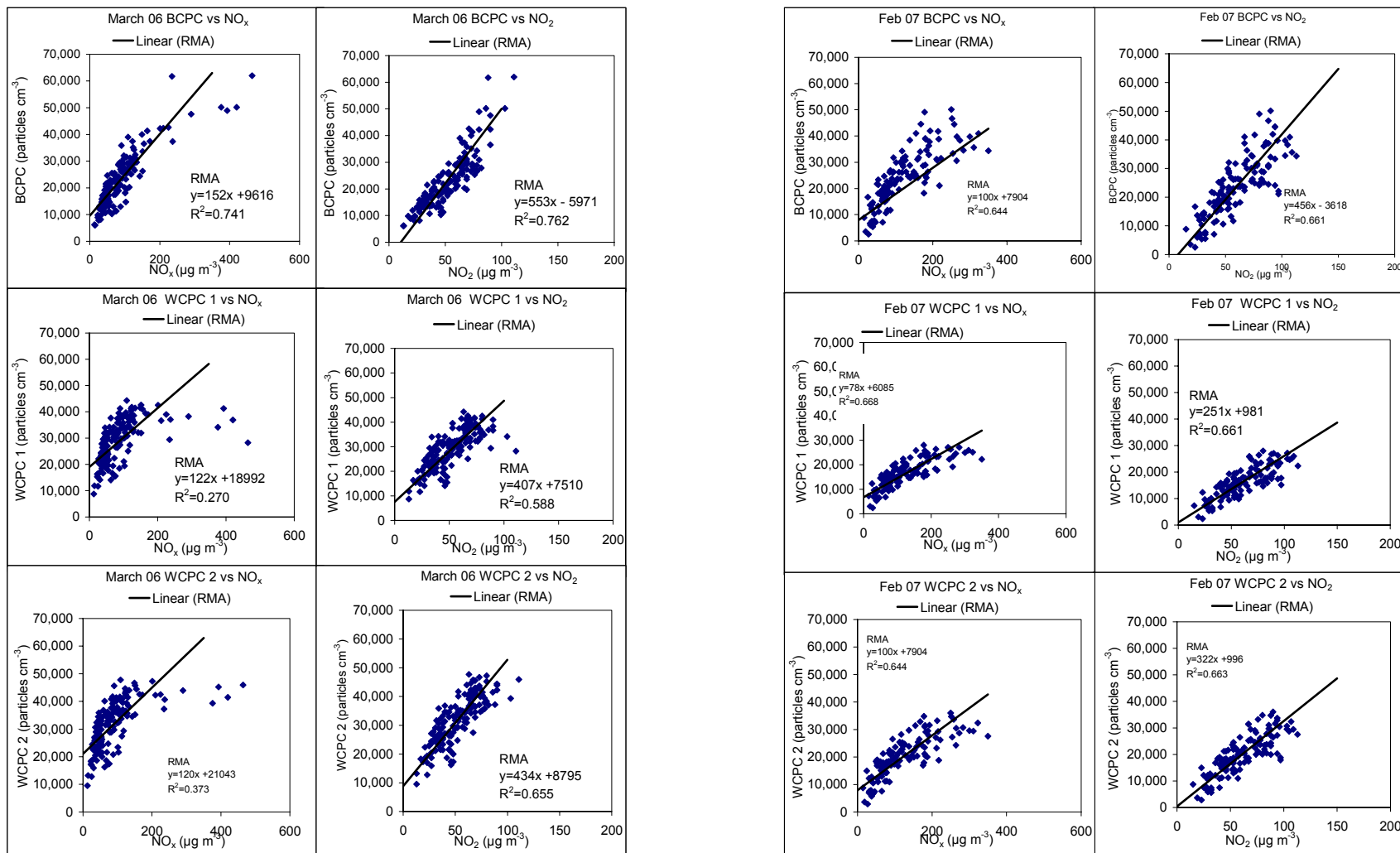


Figure 5.17 Scatter plots of hourly particle number concentration against NO_x and NO₂ for the butanol-based condensation particle counter (BCPC) and the water-based condensation particle counters (WCPC 1 & 2) from 2-8 Mar 2006, n=155 (left), and from 17-22 Feb 2007, n=128 (right), after the WCPCs underwent repairs. Data are 24-hours averages.

The scatter plots of WCPC1 & 2 vs. NO_x in March 2006, showed a fairly linear relationship below $40,000 \text{ particles cm}^{-3}$. However, above $40,000 \text{ particles cm}^{-3}$ the relationship flattens out. The WCPCs did not register concentrations higher than this value. Therefore, increases in NO_x and NO_2 were not followed by similar increases in PNC. In contrast, this trend was not observed in the relationship of PNC measured with the BCPC against NO_x and NO_2 , since this particle counter was able to measure concentrations over $40,000 \text{ particle cm}^{-3}$, albeit the dispersion of the data was greater at these high concentrations. NO_x concentrations explained up to 74 % of the variance (calculated as $R^2 \cdot 100$) in PNC as measured by the BCPC, though only a 27 % and 37 % of the variance in PNC measured by the WCPC1 & 2 respectively. The effect of the underestimation of PNC by the WCPC was less noticeable on the relationship of PNC vs. NO_2 . The relationships of WCPCs vs. NO_2 were more similar to BCPC vs. NO_2 than those of WCPCs and BCPC vs. NO_x .

The relationships of PNC vs. NO_x derived from data of February 2007 (after the WCPC were repaired) were similar for both particle counter models, unlike results for data of March 2006 (before the WCPC were repaired). NO_x explained 64-67 % of the variation in PNC for the two models. The intercepts of the relationship of WCPC vs. NO_x were similar to those of BCPC vs. NO_x , although the slopes of WCPC vs. NO_x were much smaller than those observed for BCPC vs. NO_x , because of the underestimation of PNC by the WCPCs.

Further evidence on the underestimation of PNC, as the wick aged and their influence on the relationship between PNC vs. nitrogen oxides is shown in Figure 5.18 for WCPC 2. Continuous PNC from February to July 2008 was plotted against NO_x and NO_2 data on a monthly basis. A new wick was installed in February and was left in the same position during the entire monitoring period, until the WCPC 2 stopped registering measurements. Scatters of PNC (WCPC 1) vs. nitrogen oxides have not been presented because the WCPC 1 experienced continuous drops on the flow rate which resulted in zero readings and therefore it does not add any information on the effect of wick aging on the PNC readings.

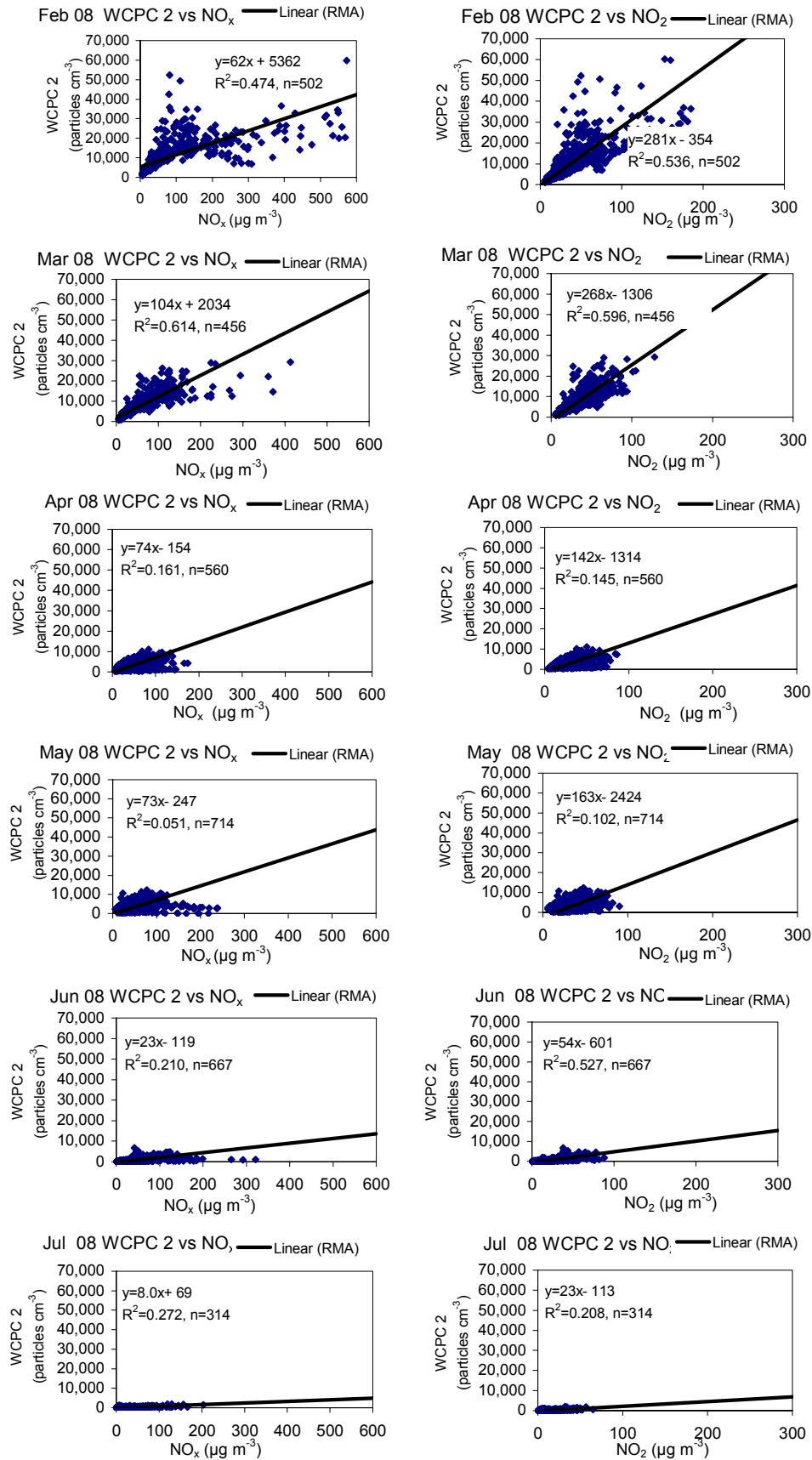


Figure 5.18 Scatter plots of hourly particle number concentration against NO_x and NO₂ for the water-based condensation particle counter 2 (WCPC 2) at St. Enoch Sq. (6 Feb-13 Jul 2008).

The relationship between PNC vs. NO_x and NO_2 changed partly because of different strengths of source emissions. However, the dramatic drop in the slope of both relationships (PNC vs. NO_x and NO_2) from May is apparent. In May, NO_x concentrations between $100\text{-}200\ \mu\text{g cm}^{-3}$ corresponded to PNC between $1000\text{-}5000\ \text{particles cm}^{-3}$, while the same NO_x concentrations in February and March matched PNC between $20,000$ and $30,000\ \text{particles cm}^{-3}$. The slope of the relationship dropped further in June and by 13 July the WCPC was not registering concentrations higher than $1,000\ \text{particles cm}^{-3}$.

5.1.3 Efficiency of the sequential extraction

5.1.3.1 PAHs concentrations

Concentrations for all of the PAHs were below LOD and therefore are not presented. This result was unexpected since anticipated PAHs concentrations were calculated from measurements at Montrose St., an urban background site in Glasgow. This presented a worst case scenario since St. Enoch Sq. and Hope St. are more polluted than this background site and therefore higher PAHs concentrations were expected.

The minimum concentrations expected for benz[a]pyrene was $2.4\ \text{ng per filter}$, which was higher than the instrumental LOD ($0.1\ \text{ng per filter}$) reported by Fisher et al. (2003) using preconcentration on an on-line solid phase extraction HPLC system with fluorescence detection. In Fisher's study, filters were extracted in $2.5\ \text{ml}$ of acetone and ultrasonicated at room T for $30\ \text{min}$. $1\ \text{ml}$ of the extract was diluted with $1.5\ \text{ml}$ of water and injected in the preconcentration system. In this study, filters were extracted in $2.5\ \text{ml}$ of a solution of hexane: acetone (1:1) and ultrasonicated at room T for $30\ \text{min}$. The extract was concentrated to $0.1\ \text{ml}$ by using a stream of N_2 .

After the analysis was performed, the NERC facility indicated that the instrumental LOD was $15\ \text{ng ml}^{-1}$, which lay below the expected concentration for benz[a]pyrene ($2.4\ \text{ng} / 2.5\ \text{ml} = 0.89\ \text{ng ml}^{-1}$) even with preconcentration to $0.1\ \text{ml}$ ($8.9\ \text{ng ml}^{-1}$).

5.1.3.2 Losses of metals during the PAH extraction

This section shows the results of the test carried out to examine losses of metals during the PAHs extraction (details of the extraction test were shown in section 4.7.3).

Table 5.12 shows the metal concentration (μg metal in g PM_{10}) in the three filter pairs, for the two extraction procedures: single metal extraction and sequential extraction of PAHs and metals. The % of metal lost during the PAHs extraction is also shown.

Table 5.12 Metal concentration (μg metal per g of PM_{10}) found in the single metal extraction and the sequential extraction (PAHs and metals).

Metal	Filter pair 1			Filter pair 2			Filter pair 3		
	($\mu\text{g g}^{-1}$) metals extraction	($\mu\text{g g}^{-1}$) PAHs & metals	Losses (%)	($\mu\text{g g}^{-1}$) metals extraction	($\mu\text{g g}^{-1}$) PAHs & metals	Losses (%)	($\mu\text{g g}^{-1}$) metals extraction	($\mu\text{g g}^{-1}$) PAHs & metals	Losses (%)
Ti	51.5	21.2	58.8	13.2	9.6	27.3	16.5	14.9	9.6
V	15.1	6.07	59.9	9.72	4.79	50.7	47.4	33.7	28.8
Cr	86.2	45.9	46.8	11.3	10.7	5.1	26.2	15.0	42.8
Mn	95.1	64.2	32.5	62.0	44.6	28.0	101	73.5	27.2
Fe	4607	1782	61.3	815	925	-13.6	1417	1622	-14.5
Ni	32.8	26.1	20.4	59.8	44.8	25.1	85.3	77.2	9.5
Cu	247	199	19.6	193	106	44.9	244	182	25.3
Zn	4595	969	78.9	1230	668	45.7	2107	1478	29.9
As	2.90	1.98	31.7	2.14	0.92	57.0	8.21	4.23	48.4
Cd	6.57	2.92	55.7	5.20	2.70	48.0	8.59	4.93	42.6
Pb	149	79.8	46.5	103	40.2	61.0	229	135	41.3

Considerable amounts of all metals were lost during the PAH extraction. The losses ranged from 5 % to nearly 80 %. The highest loss was observed for Ti, possibly due to the higher uncertainty in the calculation of those concentrations, since Ti concentrations were closer to the LOD compared with the other metals. Interestingly, metals with lower concentrations (V, As, Cd) had percentage losses similar to metals with concentrations two (Pb) or three (Zn) orders of magnitude higher.

Concentrations of Fe in the analysis of filter pairs 2 and 3 were higher in the filter halves extracted for PAHs and metals than those observed in the filter halves digested for metals only. This suggests contamination of Fe during the PAHs and metal extraction.

However, the aim of this project was to examine the functional relationships between metals and co-pollutants, rather than to gain knowledge of the absolute metal concentrations. Therefore, so long as the losses of metals are systematic, (i.e. metal concentration in the filter halves extracted for PAHs and metals correlate with metal concentration extracted in the single metal extraction) no error is introduced by using the metal concentrations to calculate the relationship between metals and co-pollutants.

Figure 5.19 shows the scatter plot, RMA relationship, and regression coefficient of the amount of metals extracted during the PAHs & metals extraction vs. the amount of metals extracted during the single metal extraction. All metals and filter pairs were included, apart from Zn and Fe which were removed from the dataset due to the contamination problems mentioned earlier.

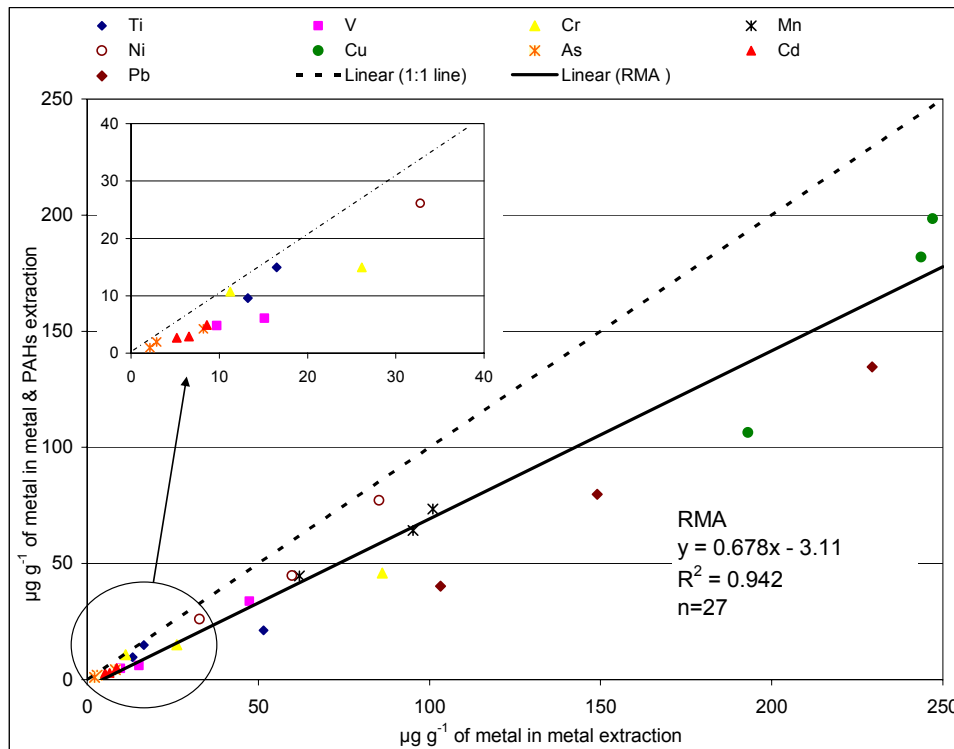


Figure 5.19 Scatter plot and RMA relationship between the amount of metals extracted during the sequential extraction (PAHs & metals) and the amount of metals extracted during the single metal extraction.

The high regression coefficient suggests that the amounts of metal lost during the PAHs extraction were systematic. The slope was significantly different from 1 ($p < 0.05$, 2-tailed) and the intercept was not significantly different from zero ($p < 0.05$).

5.2 DISCUSSION

5.2.1 Performance of PDTs

5.2.1.1 Precision of PDTs

The replicate precision of the PDTs measured as the RSD was below 8 % for 1 and 4-weeks exposure periods for NO₂ and the 1-week exposure period for NO_x (Table 5.2), which lies within the acceptable limit for these devices (AEA, 2008). The correlation coefficient between replicate measurements was very highly significant ($p < 0.001$, 2-tailed) and the RMA relationship was not significantly different from 1:1.

The higher RSD for the 1-week NO₂ exposure (7.4 %), compared to a 4-weeks exposure period (5.1 %) was possibly the result of the higher uncertainties when analysing relatively low masses of trapped nitrite. The minimum NO₂ concentration measured during the 1-week exposure periods was 7.13 µg m⁻³, which was close to the NO₂ PDTs LOD of 6.4 µg m⁻³ (Section 4.4.7), while the lowest NO₂ concentration measured during the 4-weeks periods was 17.1 µg m⁻³.

Replicate precision in this study compared well with observations reported by other authors: Heal et al. (1999) reported a mean RSD value of 2.4 % and 7.3 % for 1-week exposure and 4-weeks exposure periods, respectively using quartz, acrylic and foil tubes; the r-value for 1-week was 0.97. Kirby et al. (2000) reported a mean RSD of 3.8 % for a 2-week exposure period and $r=0.89$; and Hamilton and Heal (2004) a mean RSD of 8.5 % for a 1-week exposure.

5.2.1.2 Biases of PDTs

The results of the comparison of NO₂ measurements by PDTs and by chemiluminescence analyser showed a systematic overestimation of the NO₂ concentrations by the passive samplers, as shown by the RMA lines fitted to the observations from both measurement devices (Figure 5.6). The degree of overestimation was related to the length of the exposure period, with higher overestimation occurring for shorter exposure periods (1-week compared to 4-weeks,

Table 5.8). This suggested two opposing biases: imbalance of the outdoor photochemical equilibrium within the NO₂ in the tube, and a degradation of the trapped nitrite in the reagent over time.

The different degree of overestimation within and between monitoring sites (Table 5.4) suggests that application of a PDT adjustment factor would be difficult to implement. Any such factor should be exposure time and site specific.

The results of the comparison of two different exposure periods for the NO₂ PDTs, in a variety of monitoring sites, showed that concentrations derived from 4 consecutive weeks were lower than the concentrations relative to the average of 4 separate weeks exposures over the same period (Figure 5.2 and Table 5.3). This underestimation was statistically significant only at the monitoring sites with highest NO₂ concentrations (as measured by the chemiluminescence analyser: Montrose St. and St. Enoch Sq., Table 5.3). The magnitude of the underestimation (measured as the ratio of 4-weeks: 4*1 week) increased with increasing analyser NO₂ concentrations (data for St. Enoch Sq., Figure 5.5). Although the correlation coefficient was not statistically significant. This result might suggest a possible saturation of the TEA adsorbent at high NO₂ concentrations resulting in an ineffective trapping of NO₂. Passive diffusion analysis assumes an indefinite sink to the adsorbent and no desorption of the nitrite ions (Heal and Cape, 1997). However, the preparation method used in this study (dipping grids in a solution of 50% TEA: acetone) has been estimated to provide a molar concentration of TEA of approximately 66 μmol (Heal, 2007), which is well in excess of the amount of ambient NO₂ sampled. The highest mass of nitrite collected in the tube for 4-week exposure period at St. Enoch Sq. was 3000 ng (64 μg m⁻³), which corresponds to 65 nmol of nitrite, which is three orders of magnitude smaller than the estimated amount of TEA in the tubes. Therefore, saturation of TEA adsorbent does not seem to be the cause of underestimation.

A large study involving a variety of monitoring sites across the UK (including those in this study) with an NO₂ concentration range of 20 to 70 μg m⁻³, did not find significant correlation between increased underestimation by the PDTs (ratio PDTs: analyser) and increase NO₂ concentrations Heal (2007). However, acrylic PDTs

(those used in this study), which transmit 20 % of UV light, show a larger NO₂ underestimation by 4-weeks exposure periods compared with foil-covered PDTs (which do not transmit light). Heal (2007) concluded that the main reason for the observed underestimation in acrylic PDTs exposed for 4-week period, was light-dependant degradation of the trapped nitrite.

NO₂ overestimation by PDTs compared to chemiluminescence analyser measurements have been reported in previous studies. Heal et al. (1999, 2000, 2008) also reported overestimation by NO₂ PDTs at an urban background site (ratio PDTs: analyser=1.13, two urban centre sites (ratio PDTs: analyser= 1.36 and 1.5) and two roadside sites (ratios NO₂ PDTs: analyser =1.17 and 1.57) in Edinburgh and an urban centre site in Cambridge (ratio PDTs: analyser= 1.27).

Heal and Cape (1997) and Kirby et al. (2000) reported that a factor contributing to the overestimation by the PDTs was the formation of NO₂ in the tube by the reaction of co-diffusing NO and O₃ resulting in significant differences between NO₂ measurements by PDTs and by analyser.

The degree of overestimation will depend on the relative molar concentration of NO: NO₂ and O₃. When [O₃] > [NO] the formation of NO₂ is limited by NO concentration and when [O₃] < [NO] the formation of NO₂ is limited by O₃ concentration (Heal and Cape, 1997). In summer, O₃ is usually in excess over NO. Therefore, an increase in NO availability (i.e. ratio of NO: NO₂) should result in an increase of the overestimation. In this study, the ratio NO: NO₂ was just moderately correlated with the PDTs overestimation (NO₂ PDTs: analyser, Figure 5.7 b) at Hope St. and Montrose St. At St. Enoch Sq., NO concentration hardly fluctuated and therefore there was no statistical power for the regression, resulting in an $r \approx 0$ (Figure 5.7 b). However, O₃ concentration despite being present in excess (mean summer concentration 144 ppb) over NO (mean summer concentration 36 ppb) was moderately correlated with the overestimation by PDTs, instead of the of NO availability (i.e. ratio of NO: NO₂) which was anticipated to be the limiting factor in the NO₂ formation reaction.

The lower strength of the relationship between the ratio of PDTs: analyser vs. NO: NO₂ during the summer months (compared to that found by Kirby et al. (2000), $r=0.63$) was probably because O₃ was not actually in excess over NO at Hope St. and Montrose St. At these sites (both close to traffic sources and in street canyons) there are continuous NO emissions, which possibly deplete O₃ concentrations. Unfortunately, O₃ data for Hope St. and Montrose St. were not available to confirm this hypothesis.

On the other hand, depletion of O₃ by continuous NO emissions would have resulted in minimal overestimation of NO₂ at Hope St. and Montrose St. if this was the only cause of overestimation. However, the NO₂ overestimation at Hope St. was larger (mean PDTs: analyser=1.61) than at Montrose St. (mean PDTs: analyser=1.06). Therefore, other factors acting differently at both sites might have contributed to the observed overestimation.

The PDTs at Montrose St. were located in a deep window recess, thus, generally shielded from the wind compared to the PDTs at Hope St. and St. Enoch Sq., which were placed in more open locations. Increased wind-turbulence at the entrance of the tube has been associated with increased mass transfer of NO₂ along the tube (Gair and Penkett, 1995; Ferm and Svanger, 1998, Plaisance et al., 2004 and Busbin et al., 2006). Ferm and Svanger (1998) observed an overestimation of 85 % in the NO₂ concentrations sampled with unprotected PDTs (as those used in this study) compared with co-located PDTs with a net at the open end to protect them from the wind. The differences in NO₂ concentrations sampled with both tubes (with and without the net) indoors (with no wind) was negligible (Ferm and Svanger, 1998). Therefore, it is possible that the differences in wind turbulence at the three locations were responsible for the different degrees of overestimation.

The relationship between wind speed and NO₂ overestimation was not statistically significant (results not shown). However, this may be a reflection of the lack of representativeness of the wind speed data, as it was collected at a meteorological station located approximately 20 km from the monitoring sites. In addition, weekly

averaged wind speeds do not fully account for short-term fluctuations that could have caused turbulence at the entrance of the tube (Heal, 1999).

NO_x measurements derived from PDTs compared well with those derived from the analyser at Hope St. and Montrose St. (Table 5.6). However, at St. Enoch Sq. NO_x PDTs were an average of 60 % higher than those averaged from the analyser. NO concentrations derived from the PDTs were underestimated at the sites with highest NO concentrations (Montrose St. and Hope St.) but not at St. Enoch Sq. Mean NO concentrations during the studied period were 19.0 and 96.2 and 8.0 µg m⁻³ at Montrose St. and Hope St. and Enoch Sq., respectively. The fact that NO derived from PDTs was only underestimated at the sites with highest NO concentrations suggest inefficient capture of NO, possibly because of inefficient oxidation of NO to NO₂ at high NO concentrations.

The within-tube reaction of NO and O₃ to form NO₂ would result in NO underestimation. However, it should be noted that this should not affect the NO_x concentration, since the loss of NO results in a similar increase of NO₂ and therefore the effect would be offset. Thus, the slight underestimation of NO_x at Montrose St. (9 %, Table 5.6) was possibly the result of inefficient oxidation of NO to NO₂ at high NO concentrations. The agreement of NO_x PDTs with the analyser at Hope St. was a result of the offset effect of overestimation of NO₂ (caused by within tube reaction of NO and O₃) and underestimation of NO. Therefore, although measurements derived from PDTs may alter the distribution of NO₂ and NO, the NO_x concentrations compare well with those from the analyser.

The overestimation of NO_x at St. Enoch Sq. remains unclear in origin. A possible explanation might be that at this site the effect of shortening of the diffusion path due to wind-induced turbulence was greater than at Hope St. and Montrose St. This would affect the NO_x, NO₂ and NO concentrations.

A recent study by Vardoulakis et al. (2009) reported evidence of underestimation by NO_x PDTs compared to analyser measurements at two roadside and one background site in Birmingham for 4-5 week exposure period. The ratios PDTs: analyser were

lower than those observed in this study (0.21 and 0.51 for the roadside sites and 0.66 for the background site) because of the longer exposure periods resulted in an accumulated loss of NO concentration greater than that in this study, where the exposure periods were for 1-week. Vardoulakis et al. results and those observed in this study suggest an exposure-duration dependent underestimation of NO_x concentrations, possibly caused by inefficient oxidation of NO to NO₂.

Thus, from this and other studies the factors affecting the performance of PDTs appear to be:

1. Wind speed, which affects both NO₂ and NO_x PDTs, resulting in an overestimation of the concentrations compared to those derived from the analyser. This could be overcome by placing the PDTs in sheltered locations (as it has been shown at Montrose St.).
2. Ambient NO and O₃ concentration which results in overestimation of NO₂ by the PDTs when both NO and O₃ are available and affects the NO₂ and NO distribution estimated by the NO_x PDTs but not the overall NO_x concentration. This is complex to correct since NO and O₃ concentrations vary in time and space.
3. Light dependant degradation of the trapped nitrite, which could be overcome by using a material that does not transmit light, or limiting the exposure periods to 1-week.
4. Inefficient oxidation of NO to NO₂ (NO_x PDTs) at high NO concentrations.

However, if the PDTs are sheltered and exposure durations limited (1-week) (as was the case in Montrose St. in this study), PDTs appear to be an accurate method for measuring NO₂ and NO_x concentrations with deviations within the ±25 % specified by the EU Daughter Directive for NO₂ (EU, 1999). Currently, DEFRA guidelines for exposure of NO₂ PDTs do not recommend sheltering the PDTs and the recommended exposure time is 2-4 weeks (DEFRA, 2008). Local authorities, therefore should consider the use of shelter and 1-week exposure time.

5.2.2 Performance of the respirable dust samplers

At the outset of the project, it was anticipated that the respirable dust samplers may be useful devices for monitoring relatively long-term exposure (1-week sample resolution) of PM₄ and BC (measured as the absorbance of PM₄ filters) to be used as surrogates for PNC, water-soluble metals and PAHs. The initial evaluation tests showed good performance after new diaphragms were installed in the pumps. However, aging of the diaphragms had a considerable effect on the flow rate. During the monitoring campaign at Hope St., St. Enoch Sq. and Montrose St. flow rates were measured on days 1, 3 and 7 and the average was used to calculate the volume of air sampled during each sampling period. However, this measurement of the flow rate illustrated large variations that may have caused the observed poor precision between the mass and reflectance measurements from co-located respirable dust samplers (Figure 5.11).

The diaphragms appeared to become damaged more quickly at sites with higher PM₄ concentrations, perhaps as a result of the filters becoming loaded more quickly and therefore the diaphragm having to work harder to maintain the flow. This may explain why the precision of the sampling devices was acceptable during the inter-comparison test, which took place at Rottenrow, a background location with low PM₄ concentrations (5-10 µg m⁻³, Figure 5.10) but not at St. Enoch Sq., Hope St. and Montrose St. (8-30 µg m⁻³). It also may explain the larger variability in the replicate absorption coefficients found at Hope St, the site with the highest particle mass concentrations (Figure 5.11).

The precision was usually worse for the respirable dust absorption coefficients than for the mass concentration. This may have been the result of changes in the flow rate affecting the 'cut point' of the particles sampled. The set up flow rate was 2.2 L min⁻¹. However, it varied from 2.2 to 1.6 L min⁻¹. The 'cut point' of cyclones for a flow of 1.9 L min⁻¹ is 5 µm (British Medical Research Council, BMRC curve) and for 2 L min⁻¹ is 4 µm (ISO/CEN curve: ISO, 1995; CEN, 1992). Particle size has a considerable influence on the absorption properties (Horvath, 1986). The absorption coefficient of 4 µm diesel particles is 100 times lower than that for 5 µm

diesel particles, because of the variation in the concentration of BC in both particle sizes (Horvath, 1986).

Horvath (1995) found that the change of absorption coefficient with particle size for atmospheric aerosol was less pronounced than for pure diesel particles. This may explain the higher variability in the absorption coefficients observed at Hope St., the site most influenced by traffic and therefore expected to have higher concentration of diesel particles, compared to the other two sites.

The changes in the size of the particles did not affect the concentration as much as the reflectance because the changes in particle mass are not as sensitive to changes in sizes between 4 and 5 μm as the absorption properties (see Figure 1.2, Mass distribution of particles according to aerodynamic diameter).

This technical problem could have been partially addressed by recording the exact air volume sampled with a gas volume meter. Unfortunately, because of a lack of time, (by the time this could have been implemented the particle counters had failed) it would not have been possible to take simultaneous measurements of PM_{10} and PNC.

These results indicate that SKC pumps are not suitable for continuous running periods and highlight the importance of testing equipment in the field, under conditions (pollution level and atmospheric conditions) similar to those under which the monitoring campaign will take place.

5.2.3 Comparison of Partisol sampler and TEOM analyser

Underestimation of PM_{10} measured by the TEOM analyser compared with the European gravimetric method has been reported in previous studies (Allen et al., 1997; Smith et al., 1997; APEG, 1999; Green et al., 2001, Price et al., 2003; Charron et al., 2004, Green et al., 2006). This underestimation has been attributed to the loss of volatile and semi-volatile material, including ammonium nitrate and organic aerosols (Smith et al., 1997; Green et al., 2001; DEFRA, 2003, Charron et al., 2004). These studies have collected data from a single site from different cities. Examination of the discrepancies between TEOM and Partisol over small spatial

scales has been less documented. In this study, the UK correction factor applied to TEOM analyser (3, 1.03, 1.3), resulted in good agreement between both monitors at Hope St. and Marylebone Rd. (Tables 5.9 and 5.10, respectively) but not at St. Enoch Sq. and North Kensington (Tables 5.9 and 5.10, respectively). At St. Enoch Sq. application of the factor (3, 1.03, 1.3) resulted in statistically significant higher PM₁₀ measurements compared to those from the Partisol and at North Kensington, PM₁₀ TEOM data corrected with (3, 1.03, 1.3) resulted statistically significant lower PM₁₀ compared with PM₁₀ Partisol data. Given that the differences in PM₁₀ concentrations measured by both monitors are dependant on the concentrations of VOCs, the larger differences in PM₁₀ concentrations between the TEOM and Partisol at North Kensington suggest a higher concentration of VOCs at this site compared to the kerbside site (Marylebone Rd.). This result is surprising, as one would expect higher VOCs concentration at sites more influenced by traffic.

The results found at Glasgow cannot be taken as representing the annual pattern because of the limited data period analysed. Besides, simultaneous data was only collected on 8 days. Therefore, the observed differences in the agreement of Partisol and TEOM data between Hope St. and St. Enoch Sq. could also be because of temporal variation in the semi-volatile material rather than spatial variations between both sites.

The discrepancy calculated in this study between TEOM and Partisol at Marylebone Rd. differed from that calculated by Green et al. (2006) using data collected from 31 January 2000 to 31 December 2004. Green et al. found a better agreement between Partisol measurements and uncorrected TEOM data in contrast to the result observed in this study, where the UK correction factor (3, 1.03, 1.3) resulted in better agreement with Partisol measurements. This could be because of temporal variations in volatile organic compounds during the studied periods in both studies. Temporal variations in the underestimation of PM₁₀ TEOM data compared to Partisol sampler have been observed in several studies (Green, 2001; Muir, 2000, Price et al. 2003), with higher underestimation in winter than in summer possibly because of a greater amounts of volatile material present in airborne particles during this period.

The results from this and previous studies highlight the complexity of selecting a correction factor for TEOM measurements. The short time resolution of the TEOM analysers is one of their major advantages over the gravimetric method, alerting citizens to any high pollution episode. However, in order to do so, bias in the measurements must be minimised.

Price et al. (2003) and Speer (2003) indicated that the differences between the TEOM and Partisol could also arise from the moisture adsorbed by the aerosol particles in the Partisol filters. PM₁₀ hygroscopic components, including salts and organic aerosols adsorb water when RH exceeds their deliquescence value, which for an urban aerosol is around 70 % depending on the aerosol composition. Therefore, if moisture is not released during the pre-conditioning process prior to weighing the exposed filters, it will result in a higher gravimetric estimate of PM₁₀. Aerosols do not release their moisture content until RH decreases by up to 30-40 % (Price et al., 2003).

The PM₁₀ filters collected in Glasgow were expected to have released all moisture, since they were conditioned in a dessicator, where RH remained between 29-32 %. During the time the filter was weighed it remained subject to the room conditions, where RH did not exceed 60 %. Therefore, it is unlikely that particles adsorbed any substantial amount of moisture during this time. Therefore, at the Glasgow sites the observed differences between the Partisol and TEOM were more likely to be because of the loss of organic compounds by the TEOM. However, PM₁₀ filters from London were weighed according to EN 12341:1998, (BSI, 1998) where filters are conditioned prior to weighing at a RH of 50 % and therefore moisture might not have been totally released from the particulate mass.

At the time that the inter-comparison exercise was taking place in Glasgow, DEFRA published a report (DEFRA, 2006) indicating that the TEOM analyser did not meet the criteria of acceptance under the European Directive 1999/30/EC (EU, 1999) which uses the filter-based gravimetric sampler KFG as reference method. The corrected TEOM data failed to have an 'expanded uncertainty' below 25 %. The expanded uncertainty is calculated from the between instrument uncertainty (squared

differences between replicates divided by 2 times the number of replicates) and the relationship between the TEOM and reference method.

Some TEOM analysers from the UK monitoring network have been upgraded to Filter Dynamics Measurement System (FDMS) (AEA, 2006). The FDMS system operates at 30 °C rather than 50 °C to reduce particle losses and report fraction of volatile and non-volatile particles separately (AEA, 2006).

At the time of writing this thesis, in April 2009 DEFRA published the Volatile Correction Model (VCM) for correcting TEOM data. The VCM works by adding to the PM₁₀ TEOM data an estimated mass of volatile PM₁₀ calculated from measurements provided by nearby FDMS instruments (within 130 km) to assess the loss of PM₁₀ from the TEOM. The model has been demonstrated to work in most areas of the UK (www.volatile-correction-model.info/).

PM₁₀ TEOM measurements in Section 6 are presented with the UK correction factor (3, 1.03, 1.3) as it is provided in the NAQA.

5.2.4 Performance of the water-based condensation particle counter

Two factors contributed to the underestimation of particle concentration by the WCPCs compared to the BCPC. An underestimation of particle numbers occurred at high particle concentrations and a further underestimation occurred because of the ageing of the condensation wick, after approximately 6 weeks running. The former factor became systematic after the units were re-calibrated in February 2007 and therefore a correction factor could be applied. In contrast, it is not possible to correct the wick aging.

The relationships of WCPCs vs. BCPC in February 2007 were more linear (higher regression coefficients) than those observed in March 2006 (Figure 5.14). This translated into a more similar relationship between BCPC vs. NO_x and WCPCs vs. NO_x in February 2007 than that observed in March 2006 (Figure 5.17). In March 2006, the relationship of WCPCs vs. NO_x ‘flattened out’ at high concentrations as a result of the underestimation of particles by the WCPCs. However, this was not

observed in February 2007. In February 2007, the underestimation of particles was constant over the entire concentration range (Figure 5.14). However, the relationship of WCPCs vs. BCPC became scattered at high concentrations because of the higher uncertainty (20 %) when predicting concentrations over 50,000 particles cm^{-3} , compared with the estimated uncertainty when measuring lower concentrations (10 %) (TSI, 2002).

At concentrations over 10,000 particles cm^{-3} and over 20,000 particles cm^{-3} the BCPC and WCPC, respectively do not count single particles. Instead, the units measure the light scattered by the particles and transform this empirically into concentration using an internal photometric calibration table. This table was upgraded in the WCPCs when they were repaired. The range of photometric values in the calibration table in February 2007 was greater than that in March 2006, resulting in a higher linearity with BCPC measurements. Despite the improvement in the linearity between the two models, the relationship WCPC vs. BCPC was obscured by the ageing of the condensation wick. For instance, the regression coefficient between WCPC1 & 2 vs. BCPC dropped from 0.9 for WCPC1 & 2 vs. BCPC in February 2007, with new wicks installed, to 0.7 for WCPC1 vs. BCPC and 0.4 for WCPC2 vs. BCPC, in April after, 10 weeks of continuous running. After approximately 6 weeks running the end closest to the laser became discoloured and after approximately 8 weeks appeared burnt, resulting in an apparent underestimation of particles. In addition, white stains appeared on the middle of the wick. These white areas appeared dry. Water is constantly injected in the wick by means of a small pump. The liquid water is drawn by capillary action and gravity down the wick (Hering et al., 2005). The fact that some parts of the wick appeared dry could possibly result in particles not being grown efficiently resulting in underestimation. TSI have not provided a method for monitoring the condition of the wick, apart from subjective visual observation.

These changes in the slope appear to affect the relationship between PNC and NO_x making it hard to distinguish whether the changes in the slope were caused because of the atmospheric conditions or by an artefact of the particle counter operation.

Biswas et al. (2005) also reported an underestimation of the WCPC compared to the BCPC for particle concentrations above 40,000 particle cm⁻³, with ratios similar to those found in this study (0.6-0.8). The authors attributed the disagreement to the different photocalibration mode in both models.

Other possible sources of errors in the WCPCs include:

- Unstable flow. A lower flow rate results in larger growth of the aerosol, which would affect concentration accuracy. The leaking of water into the optics causes a drop in the flow rate. Tilting the instrument forwards more than 20 ° may cause the optical system to flood.
- The laser nozzle (where particles are counted) can become contaminated because of large particles. TSI recommended the use of a cyclone or sampler inlet to stop particles larger than 1 µm from entering the system. This cyclone must be cleaned every week. Other orifices controlling the flow-rate (the damper and flow control orifices) can also get clogged (Zerrath, 2007).
- Failure to start the draining period due to the pressure in the Sample Inlet being lower than in the drain bottle. TSI recommended connecting the Vent connector in cases when the inlet pressure is reduced. Despite this measure being implemented the instrument continued to show intermittent problems when draining.

Therefore, the WCPC is not yet a reliable particle counting technology as shown by the difference in concentrations measured compared with the BCPC. In addition, improvement of the lifetime of the growth tube and the problems related to the draining periods should be studied.

5.2.5 Efficiency of the sequential extraction

Substantial amounts of metals were lost during the combined PAHs & metal extraction (Table 5.12). These results differed from those found by Piñeiro et al. (2003), where no significant losses of metals were found, and the RSDs between the two procedures were reported below 15 %. The contrasting results are possibly

because of the higher metal concentration extracted in Piñeiro et. al's study, where the analysed filters were of TSP collected near a mine. The mass of metals in Piñeiro et. al's study (expressed as μg per filter) was two or three orders of magnitude greater than those extracted in this project. For example the mass of Ti, Cr, Mn in this work was $< 50 \mu\text{g}$ (as measured by the sum of μg extracted in the two filter halves extracted only for metals), while in Piñeiro's study Ti and Mn showed masses of approximately $300 \mu\text{g}$ and Cr around $150 \mu\text{g}$. As and Cd in this study showed masses $< 10 \mu\text{g}$. In Piñeiro et al. study results for As were reported on the analysis of a reference material (As content of $60 \mu\text{g g}^{-1}$) but not on the results obtained from analysis of TSP filters. Results for Cd were not reported by Piñeiro et al.

Thus, while the method developed by Piñeiro et al. may be appropriate for samples with high metal concentrations, its application to samples with a low concentration results in significant losses of metals.

However, these losses were systematic, i.e., the amount of metals found in the filter halves that underwent prior PAHs extraction were proportional to the amount of metal found in the filter halves that only underwent metal extraction. Therefore, the concentration of metals found in the filters previously extracted for PAHs can be used in the calculation of the correlation between metals vs. co-pollutants, since the absolute concentration does not affect the degree of correlation. However, for calculation of the absolute concentration, the amount of metal found in the PAHs & metal extract could be corrected by applying the regression equation presented in Figure 5.19.

The efficiency of the extraction procedure and the losses of metals during the PAHs extraction should have been tested prior to the analysis of the air samples to confirm the results reported by Piñeiro et al.

CHAPTER 6

SPATIAL & TEMPORAL VARIATIONS IN

PARTICLE CHARACTERISTICS (MASS,

NUMBER, ABSORBANCE, METAL

COMPOSITION) AND GASEOUS POLLUTANTS

IN GLASGOW AND LONDON

6.1 RESULTS

This chapter presents the results of the pollutant concentrations measured in Glasgow and London in the main study and the examination of the spatial and temporal variations of air pollutants.

6.1.1 Pollutant concentrations and diurnal variations

This section describes the concentrations and diurnal patterns of pollutants measured in Glasgow (at St. Enoch Sq., Hope St. and Montrose St.) and London (at North Kensington and Marylebone Rd.).

Due to technical problems with the monitoring equipment at the Glasgow sites, and missing data in the datasets provided by the NAQA, the sample sizes at each monitoring site are different.

A fault affected the WCPCs located in Hope St. and Montrose St. on the 13 July and 10 August respectively. Therefore, from that date onwards there was no PNC data from those sites.

Technical problems were also experienced with the Partisol samplers located at Hope St. and St. Enoch Sq. PM₁₀ data was only available on 8 June, 29 June-21 July at St. Enoch Sq. and 14- 22 June, 29 June, 2 July and 6-18 July at Hope St.

Table 6.1 summarises descriptive statistics of the pollutant observations at the Glasgow and London sites during the periods described above. Data were based on daily averaging periods.

Table 6.1 Descriptive statistics of traffic-related air pollutants at Glasgow (Hope St: kerbside/street canyon, St. Enoch Sq. urban centre; Montrose St: background/street canyon) (8 Jun to 31 Aug 2006) and London (Marylebone Rd: kerbside/street canyon; North Kensington: urban background).

	Hope St.			St. Enoch Sq.			Δ(Hope St-St. Enoch Sq.)			Montrose St.			Marylebone Rd.			North Kensington			Δ (Marylebone Rd. - North Kensington)			Edinburgh**	
	n	Median	IQR	N	Median	IQR	n	Median	IQR	n	Median	IQR	n	Median	IQR	n	Median	IQR	n	Median	IQR	PM ₁₀	PM _{2.5}
PNC (particles cm ⁻³)	35	23,564	10,475	79	12,851	3,128	30	12,458	7,889	63	11,095	2,940	26	109,953	35,393	26	23,407	9,784	26	82,276	36,781		
PM ₁₀ TEOM (μg m ⁻³)	58	27.0	16.0	76	19.0	11.0	56	11.4	10.7	-	-	-	26	52.1	10.3	26	22.5	7.58	26	29.5	13.0		
PM ₁₀ PARTISOL (μg m ⁻³)	31	32.9	12.0	24	21.6	12.5	17	13.6	10.7	-	-	-	26	45.0	9.00	26	25.5	10.8	25	17.0	15.0		
PM _{2.5} PARTISOL (μg m ⁻³)	-	-	-	-	-	-	-	-	-	-	-	-	26	30.0	7.00	26	15.5	7.00	26	13.0	11.8		
BS (μg m ⁻³)	-	-	-	-	-	-	-	-	-	-	-	-	26	57.0	28.2	-	-	-	-	-	-		
EC (μg m ⁻³)	-	-	-	-	-	-	-	-	-	-	-	-	26	3.55	1.36	23	1.75	0.776	23	1.95	1.90		
OC (μg m ⁻³)	-	-	-	-	-	-	-	-	-	-	-	-	26	6.81	1.42	23	5.62	1.58	23	0.483	3.10		
AbsPM [*] (10 ⁻⁵ m ⁻¹)	31	2.65	2.39	24	1.47	1.05	17	1.53	1.91	-	-	-	26	12.0	2.00	26	6.96	0.61	26	4.89	2.29		
NO _x (μg m ⁻³)	63	157	132	81	35.7	15.2	62	105	126	83	66.0	27.4	26	389	157	26	34.3	15.2	26	339	184		
NO ₂ (μg m ⁻³)	63	50.1	31.9	81	22.4	9.65	62	25.3	26.6	83	39.2	13.4	26	133	37.4	23	28.8	13.7	26	103	46.2		
NO (μg m ⁻³)	63	71.0	60.7	81	8.04	4.91	62	60.5	57.6	83	17.3	9.72	26	167	79.8	26	3.51	3.11	26	159	87.5		
CO (mg m ⁻³)	75	0.296	0.133	54	0.191	0.061	24	0.104	0.126	83	0.248	0.124	26	0.974	0.34	26	0.240	0.083	26	0.671	0.306		
SO ₂ (μg m ⁻³)	-	-	-	65	0.130	1.00	-	-	-	-	-	-	10	9.13	4.60	20	2.77	1.24	10	5.40	5.17		
O ₃ (μg m ⁻³)	-	-	-	82	35.6	18.3	-	-	-	-	-	-	26	9.09	7.00	26	43.3	15.0	26	-31.8	15.43		
1,3- Butadiene (μg m ⁻³)	31	0.077	0.082	-	-	-	-	-	-	-	-	-	19	0.463	0.157	-	-	-	-	-	-		
Benzene (μg m ⁻³)	33	0.563	0.313	-	-	-	-	-	-	-	-	-	21	2.35	1.32	-	-	-	-	-	-		
Toluene (μg m ⁻³)	30	2.36	1.36	-	-	-	-	-	-	-	-	-	22	9.74	2.95	-	-	-	-	-	-		
Ethylbenzene (μg m ⁻³)	20	0.530	0.287	-	-	-	-	-	-	-	-	-	21	5.02	0.418	-	-	-	-	-	-		
m/p-xylene (μg m ⁻³)	30	0.913	0.518	-	-	-	-	-	-	-	-	-	21	1.88	1.76	-	-	-	-	-	-		
o-xylene (μg m ⁻³)	33	1.54	1.01	-	-	-	-	-	-	-	-	-	22	1.33	0.678	-	-	-	-	-	-		
V (ng m ⁻³)	17	0.202	0.354	17	0.183	0.565	17	0.018	0.11	-	-	-	26	1.20	2.00	26	1.49	2.06	26	-0.191	0.238	0.680	0.580
Cr (ng m ⁻³)	17	0.190	0.187	17	0.141	0.328	17	0.122	0.15	-	-	-	-	-	-	-	-	-	-	-	-	0.200	0.110
Mn (ng m ⁻³)	17	0.428	1.23	17	1.57	1.46	17	0.550	0.84	-	-	-	26	0.723	0.802	26	0.352	0.488	26	0.310	0.241	1.10	0.300
Fe (ng m ⁻³)	17	24.4	15.9	17	26.0	16.5	17	0.833	15.5	-	-	-	26	6.91	11.1	26	5.04	5.91	26	2.15	5.40	11.7	2.81
Ni (ng m ⁻³)	17	0.392	0.675	17	0.473	0.593	17	0.074	0.78	-	-	-	26	0.429	0.473	26	0.803	0.97	26	-0.338	0.395	0.430	0.340
Cu (ng m ⁻³)	17	9.54	4.85	17	3.06	3.401	17	5.59	3.60	-	-	-	26	2.60	1.81	26	1.56	1.32	26	0.813	1.01	2.04	0.700
Zn (ng m ⁻³)	-	-	-	-	-	8.468	-	-	-	-	-	-	26	11.2	7.66	26	7.73	11.3	26	3.28	4.65	6.51	4.95
As (ng m ⁻³)	17	0.070	0.094	17	0.040	0.135	17	0.005	0.04	-	-	-	26	0.440	0.300	26	0.524	0.519	26	-0.073	0.161	0.210	0.190
Cd (ng m ⁻³)	17	0.057	0.033	17	0.054	0.036	17	-0.003	0.01	-	-	-	26	0.058	0.042	26	0.061	0.078	26	-0.007	0.039	0.200	0.200
Pb (ng m ⁻³)	17	1.32	0.894	17	0.714	1.51	17	0.012	1.17	-	-	-	26	1.96	2.22	26	2.44	3.45	26	-0.513	2.05	3.82	5.06
Wind speed*	84	5.54	3.43	84	5.54	3.43	-	-	-	84	5.54	3.43	25	11.7	4.69	25	11.7	4.69	-	-	-	-	-

PNC: particle number concentration; BS: black smoke; EC: elemental carbon; OC: organic carbon; * Abs PM_{2.5} at Marylebone Rd. & North Kensington; Abs PM₁₀ at Hope St. & St. Enoch Sq. IQR: Inter Quartile Range. *Wind speed data in Glasgow was measured at Bishopton (circa 18Km from the monitoring sites) and in London at Heathrow Airport (circa 16 km from North Kensington & 20 Km from Marylebone Rd.); ** Hibbs, (2002)

The highest concentrations for all pollutants were registered at the street canyon/kerbside sites Hope St. in Glasgow and Marylebone Rd. in London, highlighting the influence of traffic-related sources on air pollution.

Direct comparisons between the pollutant concentrations at London and Glasgow are somewhat compromised because the sampling periods and sample sizes were different for both cities. The data from London were deliberately selected to maximise the range of observed pollutant concentrations. The datasets were also of insufficient duration to represent intra-annual and inter-annual variations. The variability of pollutant concentrations, measured as the inter quartile range (IQR), was higher at the London sites than in Glasgow, possibly because the data for London corresponded to 26 days spread throughout the year, including winter and summer days. However, in Glasgow, the data period was limited to two months in summer, and therefore the variation in pollutant concentrations is expected to be smaller than for the London dataset.

In Glasgow, Montrose St. showed higher concentrations of gaseous pollutants than at St. Enoch Sq., whereas PNC were higher at St. Enoch Sq.

Averaged daily ratios of PNC, NO₂ and PM₁₀, for the paired kerbside/background sites (i.e. Hope St./ St. Enoch Sq. and Marylebone Rd./ North Kensington) were calculated to estimate the effect of local traffic on PNC, PM₁₀ and NO₂ (Table 6.2). PM₁₀ and NO₂ were selected, as these are the pollutants most widely used in epidemiological studies relating health effects to air pollution. PNC was selected because it has been suggested as being more harmful to human health than the mass of particles (Englert et al., 2004, Delfino et al., 2005). The mean daily ratios of EC and absorbance of PM_{2.5} (both surrogates of BC) for Marylebone Rd. and North Kensington have also been included in Table 6.2 with the purpose of examining which of them would be a better indicator of BC.

Table 6.2 Mean daily ratios of kerbside: background site concentrations in London and Glasgow.

	London			Glasgow		
	n	Mean	Range	n	Mean	Range
NO ₂	26	4.36	(1.36-8.43)	62	2.32	(1.20-5.43)
PNC	26	4.27	(1.78-6.53)	30	1.97	(0.70-3.08)
PM ₁₀ -TEOM	26	2.28	(0.94-3.59)	56	1.59	(0.65-2.50)
EC	26	1.96	(0.44-3.12)	-	-	-
AbsPM _{2.5}	26	1.68	(1.11-2.02)	-	-	-

PNC: particle number concentration; EC: elemental carbon;
Abs PM_{2.5}: absorbance of PM_{2.5}

NO₂ showed the highest spatial gradient (mean daily ratios were 4.36 and 2.32 in London and Glasgow, respectively) followed closely by PNC (4.27 and 1.97 in London and Glasgow, respectively). PM₁₀ showed the lowest ratio between the paired sites (2.28 and 1.59 in London and Glasgow, respectively). Ratios at the Glasgow sites were not calculated with simultaneous measurements for PNC, NO₂ and PM₁₀ because this resulted in a very small data set (n=10). Therefore, at Glasgow part of the difference in ratios between the pollutants could be due to temporal variability in pollutant concentrations. In addition, it should be borne in mind that the ratio for PNC was possibly underestimated due to the underestimation of PNC by the WCPC at Hope St.

EC showed a larger spatial contrast than absorbance of PM_{2.5} filters, suggesting that measurements of EC would be a better indicator for BC.

PM₁₀ and PM_{2.5} concentrations showed similar variability (measured as the IQR) at Marylebone Rd. and North Kensington, despite the differences in traffic flows at both sites. In addition, PM₁₀ and PM_{2.5} showed similar variability. In Glasgow, the variability of PM₁₀ at Hope St. and St. Enoch Sq. was also similar (IQR=16.0 and 11.0 µg m⁻³, in Hope St. and St. Enoch Sq., respectively). Median increments of PM₁₀ (concentrations of PM₁₀ at the kerbside with concentrations at the background site subtracted) were 29.5 µg m⁻³ at London and 11.5 at Glasgow (TEOM PM₁₀ measurements).

The differences in PM₁₀ concentration measured with the Partisol and TEOM analyser were described in section 5.1.2.2.

Median NO concentrations were higher than NO₂ at the kerbside sites (Hope St. and Marylebone Rd.) while at the least polluted sites (St. Enoch Sq., Montrose St. and North Kensington), the opposite trend was observed, with higher median NO₂ concentrations than median NO. The variability in NO concentrations was also higher than the variability in NO₂ at Hope St. (IQR were 60.7 µg m⁻³ and 31.9 µg m⁻³ for NO and NO₂, respectively) and Marylebone Rd. (IQR were 79.8 µg m⁻³ and 37.4 µg m⁻³ for NO and NO₂, respectively) highlighting the traffic contribution to NO. In contrast, the NO variability at the background sites was much smaller. The lowest NO concentrations of the five sites studied here were observed at North Kensington, the site located furthest away from direct traffic sources.

Median O₃ concentrations were much lower at Marylebone Rd. than at North Kensington, because of depletion of O₃ by NO at the kerbside site. (There were no O₃ data available at Hope St. so comparison between sites at Glasgow is not possible).

Toluene was the most abundant hydrocarbon at both sites (Hope St. and Marylebone Rd), followed by ethylbenzene and xylenes at Marylebone Rd. and xylenes and benzene at Hope St. 1,3-butadiene showed the lowest concentration at both sites.

The concentration ratio of toluene, ethylbenzene and xylenes to benzene provides information about additional non-traffic sources of toluene, ethylbenzene and xylenes, since traffic exhaust has specific known ratios (Simon et al., 2004). The median of the ratios toluene: benzene, ethylbenzene: benzene, m/p-xylene: benzene and o-xylene: benzene were 4.19, 0.94, 1.62, 2.73 at Hope St. and 4.14, 2.13, 0.8, 0.56 at Marylebone Rd.

Median metal concentrations were higher at Hope St. than at St. Enoch Sq. except for Mn, Fe and Ni. At the London sites, median concentrations of V, Ni, As, Cd and Pb

were higher at North Kensington, whereas median concentrations of Mn, Fe, Cu and Zn were higher at Marylebone Rd.

To put pollutant concentrations into a longer-term context the annual median 24-hours concentrations from 2006 are shown in Table 6.3.

Table 6.3 Summary of annual median concentrations in 2006 at Glasgow sites (Hope St. St. Enoch Sq. and Montrose St.) and London sites (Marylebone Rd. and North Kensington).

	Hope St.			St. Enoch Sq.			Δ (Hope St-St. Enoch Sq.)			Montrose St.			Marylebone Rd.			North Kensington			Δ (Marylebone Rd. - North Kensington)		
	n	Median	IQR	n	Median	IQR	n	Median	IQR	n	Median	IQR	n	Median	IQR	n	Median	IQR	n	Median	IQR
PNC (particles cm ⁻³)	-	-	-	288	13,682	6341	-	-	-	-	-	-	279	80,855	54,740	309	21,771	11,749	238	58,801	58,047
PM ₁₀ TEOM (µg m ⁻³)	304	33.6	21.8	336	19.5	10.3	285	13.2	17.6	-	-	-	356	47.3	21.4	365	23.3	10.5	356	20.4	21.1
PM ₁₀ PARTISOL (µg m ⁻³)	-	-	-	-	-	-	-	-	-	-	-	-	279	45.0	15.0	332	28.0	14.0	249	14.0	14.0
PM _{2.5} PARTISOL (µg m ⁻³)	-	-	-	-	-	-	-	-	-	-	-	-	316	30.0	12.0	343	17.0	12.0	299	9.00	12.5
BS (µg m ⁻³)	-	-	-	39	16.2	21.2	-	-	-	-	-	-	287	39.0	45.1	-	-	-	-	-	-
EC (µg m ⁻³)	-	-	-	-	-	-	-	-	-	-	-	-	271	2.77	2.72	206	2.03	1.36	178	0.733	2.73
OC (µg m ⁻³)	-	-	-	-	-	-	-	-	-	-	-	-	266	6.20	4.45	207	6.91	4.60	178	-0.152	4.08
NO _x (µg m ⁻³)	335	226	187	347	45.3	39.0	322	176	163	355	79.1	53.9	352	308	245	365	43.5	38.4	352	251	253
NO ₂ (µg m ⁻³)	336	68.0	33.5	347	30.2	17.4	324	34.4	28.5	355	46.0	22.3	352	114	64.5	365	35.0	22.3	352	73.4	70.5
NO (µg m ⁻³)	335	104	99.0	347	10.3	15.6	322	89.2	90.0	355	20.3	21.7	353	123	123	365	5.17	10.3	353	109	117
CO (mg m ⁻³)	347	0.387	0.204	323	0.261	0.130	310	0.113	0.152	360	0.330	0.201	246	0.97	0.45	355	0.24	0.14	236	0.674	0.463
SO ₂ (µg m ⁻³)	-	-	-	219	0.65	1.98	-	-	-	-	-	-	313	6.78	5.04	362	2.87	2.39	311	3.46	6.10
O ₃ (µg m ⁻³)	-	-	-	358	34.5	24.3	-	-	-	-	-	-	348	13.5	15.9	347	40.0	31.4	333	-21.8	25.7
1,3- Butadiene (µg m ⁻³)	336	0.134	0.162	-	-	-	-	-	-	-	-	-	240	0.387	0.17	-	-	-	-	-	-
Benzene (µg m ⁻³)	338	0.941	0.688	-	-	-	-	-	-	-	-	-	262	1.87	1.26	-	-	-	-	-	-
Toluene (µg m ⁻³)	338	3.29	2.25	-	-	-	-	-	-	-	-	-	284	7.54	6.13	-	-	-	-	-	-
Ethylbenzene (µg m ⁻³)	231	0.641	0.518	-	-	-	-	-	-	-	-	-	280	1.14	0.85	-	-	-	-	-	-
m/p-xylene (µg m ⁻³)	334	2.13	1.53	-	-	-	-	-	-	-	-	-	278	4.46	3.44	-	-	-	-	-	-
o-xylene (µg m ⁻³)	293	1.50	1.53	-	-	-	-	-	-	-	-	-	283	1.62	1.32	-	-	-	-	-	-

PNC: particle number concentration; BS: black smoke; EC: elemental carbon; OC: organic carbon

In Glasgow, annual median concentrations were higher than the median concentrations calculated during the monitoring campaign at the three sites, while in London annual median concentrations were similar to the median concentrations observed during the sampling periods. This is a result of the dates selected in London being spread throughout the year, while the monitoring campaign in Glasgow included only days during summer. In summer, meteorological conditions favour pollutant dispersion and concentrations are usually lower than during winter (DEFRA, 2007).

The annual median increments between Glasgow sites were slightly higher than those observed with data measured during this study, whereas the median increments in concentration at London sites were slightly lower than those observed for this study.

6.1.2 Temporal variability of pollutant concentrations at Glasgow

Figure 6.1 shows a time series plot of the hourly concentrations of NO₂, PM₁₀ and PNC at St. Enoch Sq., Hope St. and Montrose St.

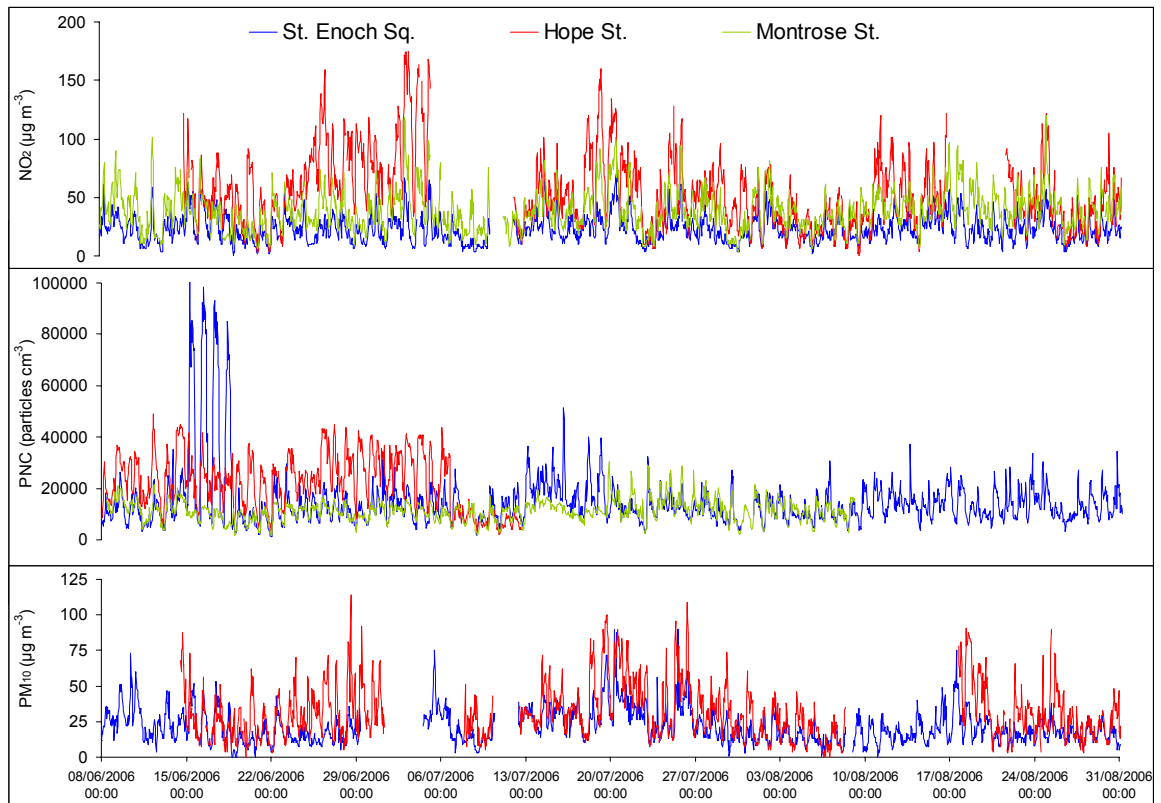


Figure 6.1 Time series of particle number concentration (PNC), PM_{10} and NO_2 at St. Enoch Sq. (urban centre), Hope St. (kerbside) and Montrose St. (urban background/street canyon) (8 Jun–31 Aug 2006). Data based on hourly averages.

NO_2 , PNC and PM_{10} concentrations followed similar temporal patterns at the three sites, except during an episode of high PNC at St. Enoch Sq., where concentrations reached $100,000$ particles cm^{-3} . These high concentrations did not coincide with a similar increase in NO_2 and PM_{10} . On these days (15–18 June), a street market took place in St. Enoch Sq. with open food cookers and fuel-power generators operating from 9 am to 5 pm, which may have caused the observed high particle concentrations. These days were removed from the subsequent correlation analysis since it was not a traffic-related episode.

The three pollutants follow a cyclical pattern corresponding to daily periods, though this diurnal pattern was more evident when data was averaged for each hour of the day than in the time series plot.

Figure 6.2 (left) shows the diurnal pattern of PNC, NO_x , PM_{10} , CO and SO_2 averaged for each hour of the day. Data was split between working days, Saturdays and

Sundays. To quantify the decrease in pollutant concentration during weekends, the concentration ratio weekday: weekend was calculated for each hour of the day (Figure 6.2, right). PNC daily averages are based on the period for which there were simultaneous PNC data available at the three sites (8 June to 13 July) so all pollutants at all sites have approximately the same number of data points.

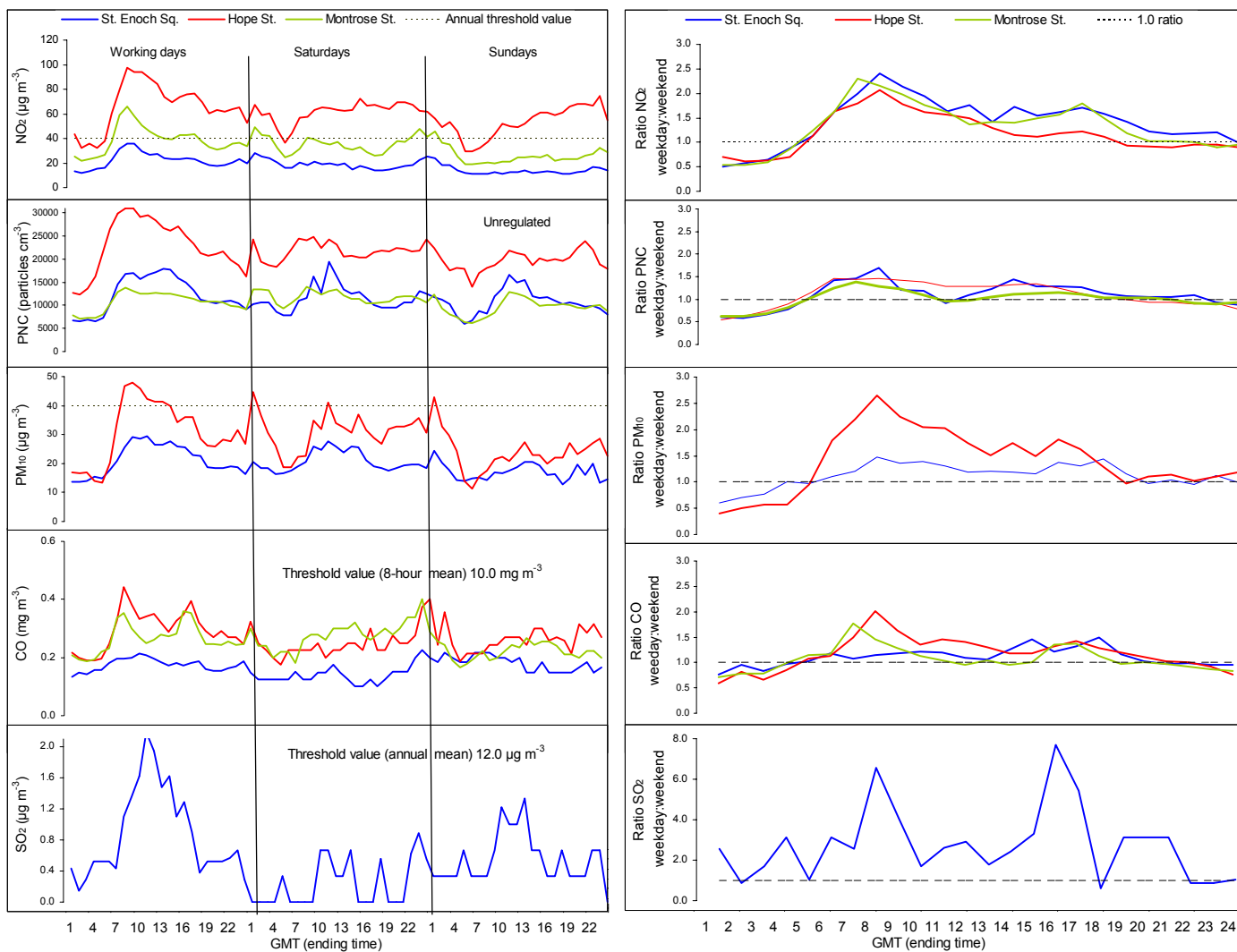


Figure 6.2 Time series plot of particle number concentration (PNC), PM₁₀ and NO₂ at Hope St., St. Enoch Sq. and Montrose St. on working days, Saturdays and Sundays (left) and time series plot of the ratios of weekday: weekend concentrations. Data averaged for each hour of the day (8 Jun-13 July 2006). PM₁₀ data at Montrose St. was not available.

The weekday profile shows typical urban traffic activity. The concentration of all pollutants rises rapidly between 6 and 9 am GMT (7 and 10 British Standard Time, BST) coinciding with the morning rush hour traffic. Then, concentrations decreased steadily until the late afternoon, when a peak, smaller than that in the morning was observed (between 3-5 pm GMT).

In general, all pollutant peaks were more prominent at Hope St. highlighting the major impact of traffic at this site. The diurnal increases in concentrations at Montrose St. were generally higher than at St. Enoch Sq. with the exception of PNC.

On weekends, the diurnal pattern was less defined which may be the result of traffic activities being less clearly defined on Saturdays and Sundays compared to weekdays. A first peak was observed in the early hours of Saturday and Sunday, probably because of nightlife activities, which include the circulation of a large number of taxis. Concentrations increased gradually reaching a peak around midday. From midday to midnight concentrations fluctuated with small peaks and dips, especially on Saturdays. The peak observed in PNC and PM₁₀ on Sundays originated mainly from the concentration measured on 31 July. On this day PNC and PM₁₀ rose up to 24,000 and 20,000 particles cm⁻³ at St. Enoch Sq. and Montrose St. respectively, while NO₂ remained very low (around 10 µg m⁻³ at both sites). Since data for weekends was based on a smaller dataset, this day had a considerable influence on the mean values.

The differences in concentrations between weekdays and the weekend allow the examination of the effect of a short-term traffic reduction in pollutant concentrations.

Not surprisingly, the hours of the day with the highest difference in concentration between weekdays and weekends were during the early morning (7-9 am) because of the weekday rush hour. Interestingly, the decrease in PM₁₀ concentrations during weekends was greater than that observed for PNC at Hope St. but not at St. Enoch Sq. When the hours when concentrations were higher over the weekends (1-4 am) were excluded from the dataset (so as not to confound the effect of traffic reduction on pollutant concentrations), the decrease in PM₁₀ concentrations on Sundays

compared to weekdays was 31 % at Hope St. and 25 % at St. Enoch Sq. The decrease in PNC at St. Enoch Sq and Hope St. was similar at both sites (18 %). At Montrose St. PNC was reduced by 15 % over the weekend. NO₂ concentrations decreased by 22 %, 44 % and 40 % at Hope St., St. Enoch Sq. and Montrose St. respectively.

The pollutant that showed the highest decrease during the weekend was SO₂. The concentrations during weekends were close to zero for most of the day. Therefore, although SO₂ concentrations were still low during weekdays the concentration ratio weekday: weekend was very high.

6.1.3 Correlations between a single pollutant measured at different sites

Table 6.4 shows the Spearman correlation coefficient and scatter plots of time series data of the same pollutant measured at different sites for hourly and daily averaged time. Because the instruments did not work simultaneously over the entire monitoring period at the Glasgow sites, the sample sizes for the correlation are different for each pollutant and paired site. This should be taken into account when comparing correlation coefficients.

Table 6.4 Spearman correlation coefficient (top) p-value (centre), sample size (bottom) and scatter plots of pollutant concentrations between monitoring sites for hourly and daily averaged data at Glasgow (Hope St., St. Enoch Sq. & Montrose St.: 8 Jun- 31 Aug) and London (Marylebone Rd. & North Kensington: selection of 26 days in 2006).

		Hope St. vs St. Enoch Sq.	Marylebone Rd. vs. North Kensington	Hope St. vs Montrose St.	Montrose St. vs St. Enoch Sq.
PNC	Hourly	0.473** 0.000 717	0.579** 0.000 609	0.552** 0.000 828	0.570** 0.000 1349
	Daily	0.433* 0.017 30	0.460* 0.018 26	0.548** 0.002 35	0.409** 0.002 57
PM ₁₀ TEOM	Hourly	0.673** 0.000 1386	0.504** 0.000 608	NA	
	Daily	0.727** 0.000 56	0.231 0.267 25	NA	
PM ₁₀ PARTISOL	Daily	0.358 0.158 17	0.342 0.094 25	NA	
	Daily	NA	0.350 0.080 26	NA	
EC	Hourly	NA	0.360** 0.000 546	NA	
	Daily	NA	0.134 0.541 23	NA	
OC	Hourly	NA	0.654** 0.000 546	NA	
	Daily	NA	0.037 0.868 23	NA	
AbsPM*	Daily	0.434 0.082 17	-0.026 0.900 26	NA	
NO _x	Hourly	0.524** 0.000 1552	0.426** 0.000 611	0.633** 0.000 1551	0.777** 0.000 1967
	Daily	0.332** 0.000 62	0.061 0.766 26	0.548** 0.001 63	0.719** 0.000 81
NO ₂	Hourly	0.497** 0.000 1552	0.371** 0.000 611	0.618** 0.000 1551	0.805** 0.000 1967
	Daily	0.491** 0.000 62	0.047 0.819 26	0.613** 0.000 63	0.796** 0.000 81
NO	Hourly	0.468** 0.000 1552	0.446** 0.000 611	0.614** 0.000 1551	0.740** 0.000 1967
	Daily	0.331** 0.009 62	0.036 0.860 26	0.466** 0.000 63	0.613** 0.000 81
CO	Hourly	0.261** 0.000 1168	0.329** 0.000 605	0.586** 0.000 1817	0.272** 0.000 1326
	Daily	0.169 0.257 47	0.061 0.766 26	0.636** 0.000 75	0.167 0.227 54

PNC: particle number concentration; EC: elemental carbon; OC: organic carbon* AbsPM₁₀ at Glasgow sites and AbsPM_{2.5} at London sites; NA: not available; **Correlation is significant at the 0.01 level.

Pollutant concentrations showed low to moderate correlation coefficients between monitoring sites. In general, the between site correlation coefficients were higher for nitrogen oxides than for PNC and PM₁₀ in Glasgow. In contrast, in London r-values were similar for PNC and PM₁₀ and these slightly higher than for nitrogen oxides.

Despite the higher contrast in absolute pollution concentration between the London sites compared to the Glasgow sites, correlation coefficients were not higher in London. The correlation coefficients for nitrogen oxides were actually lower between the London sites than between the Glasgow sites. This could be partly due to the smaller sample size and the larger distance between the monitoring sites in London (3 km) compared to Glasgow (300 m).

Hourly PM₁₀ was the pollutant that showed the highest correlation coefficient between monitoring sites in both cities. Only nitrogen oxides at the paired site Montrose St. & St. Enoch Sq. showed r-values higher than those observed for PM₁₀.

The correlation coefficient of daily PM₁₀ averaged from TEOM data, between Hope St. and St. Enoch Sq. was much higher than that observed for daily PM₁₀ collected with the Partisol. This might be because of the larger dataset available for the TEOM analyser and also because of the smaller experimental uncertainty associated with TEOM data compared with the gravimetric method (e.g. errors associated with the weighing and the conditioning of the filters).

PNC was moderately correlated between sites ($r=0.4-0.6$) in both cities. Correlation coefficients were lower than those observed for PM₁₀ (as measured by the TEOM analyser, $r=0.5-0.7$).

Measurements of EC were weakly correlated ($r=0.3$) and absorbance of PM (PM₁₀ at Glasgow sites and PM_{2.5} at London sites) was not correlated between paired sites.

Nitrogen oxides showed higher correlation coefficients at the Glasgow sites than at London, especially at the paired site Montrose St. vs. St Enoch Sq. where r-values were 0.8. NO concentrations at North Kensington were usually close to zero except on the 3 November where concentrations raised up to 200 $\mu\text{g m}^{-3}$ (data points deviating from the general trend in Table 6.4). On this day, concentrations of PM₁₀, and OC were also particularly high. This was probably the result of the bonfires that

took place to celebrate Guy Fawkes' Night, which fell on the following Sunday (5 November). When data for this day was removed from the dataset, correlation coefficients did not change significantly.

CO concentrations were scattered, with the exception of CO at the paired site Hope St. vs. Montrose St. The r-value at this site was higher than at the other two paired sites, especially for daily averaged time.

The averaging period did not significantly influence the correlation coefficient at the Glasgow sites. However, at the London sites hourly averaging time resulted in higher correlation coefficients than their daily counterparts especially for nitrogen oxides.

The correlation coefficients between metal concentrations at the paired sites Hope St. and St. Enoch and Marylebone and North Kensington are shown in Table 6.5.

Table 6.5 Spearman correlation coefficients of water-soluble metal concentration in PM₁₀ measured at Hope St. against St. Enoch Sq. in Glasgow (8 Jun-31 Aug 2006) and in PM_{2.5} at Marylebone Rd. against North Kensington in London (selection of 26 days in 2006).

		Hope St. vs St. Enoch Sq.	Marylebone Rd. vs. North Kensington
V	Correlation Coefficient	0.893**	0.935**
	Sig. (2-tailed)	0.000	0.000
	N	17	26
Cr	Correlation Coefficient	0.126	NA
	Sig. (2-tailed)	0.629	
	N	17	
Mn	Correlation Coefficient	0.529*	0.791**
	Sig. (2-tailed)	0.035	0.000
	N	17	26
Fe	Correlation Coefficient	0.250	0.493*
	Sig. (2-tailed)	0.350	0.010
	N	17	26
Ni	Correlation Coefficient	-0.015	0.768**
	Sig. (2-tailed)	0.955	0.000
	N	17	26
Zn	Correlation Coefficient		0.687**
	Sig. (2-tailed)	NA	0.000
	N		26
Cu	Correlation Coefficient	0.422	0.498**
	Sig. (2-tailed)	0.092	0.010
	N	17	26
As	Correlation Coefficient	0.850**	0.845**
	Sig. (2-tailed)	0.000	0.000
	N	17	26
Cd	Correlation Coefficient	0.174	0.575**
	Sig. (2-tailed)	0.552	0.002
	N	17	26
Pb	Correlation Coefficient	0.359	0.626**
	Sig. (2-tailed)	0.172	0.001
	N	17	26

** Correlation is significant at 0.01 level (2 tailed);* Correlation is significant at 0.05 level (2 tailed); NA: not available.

At the paired site Marylebone Rd. and North Kensington Fe, Cu, Cd and Pb showed moderate correlation coefficients and V, Mn, Ni and Zn showed high correlation coefficients. However, at the Glasgow sites correlation coefficients were high only for As and V ($r > 0.7$) and moderate for Mn ($r=0.5$).

6.1.4 Correlation between different pollutants measured at the same site

The scatter plots and Spearman correlation coefficient between traffic-related air pollutants at each monitoring site for hourly and daily averaging periods is shown in Table 6.6 (hourly averages Hope St.); Table 6.7 (daily averages Hope St.); Table 6.8 (hourly averages St. Enoch Sq.); Table 6.9 (daily averages St. Enoch Sq.); Table 6.10 (hourly averages Montrose St.); Table 6.11 (daily averages Montrose St.); Table 6.12 (hourly averages Marylebone) Table 6.13 (daily averages Marylebone Rd.) Table 6.14 (hourly averages North Kensington) and Table 6.15 (daily averages North Kensington).

Table 6.6 Spearman correlation coefficient and scatter plot of hourly averaged traffic-related air pollutants at Hope St. (8 Jun-31 Aug 2006), (horizontal variables: x axes and vertical variables: y axes).

		PNC	PM ₁₀ T	NO _x	NO ₂	NO	CO	1,3-Butadiene	Benzene	Toluene	Ethyl benzene	o-xylene	m/p-xylene	Wind speed	
PNC	Correlation Coefficient Sig. (2-tailed) N	1 837													
PM ₁₀ T	Correlation Coefficient Sig. (2-tailed) N	0.578** 0.000 463	1 1434												
NO _x	Correlation Coefficient Sig. (2-tailed) N	0.785** 0.000 488	0.786** 0.000 1244	1 1562											
NO ₂	Correlation Coefficient Sig. (2-tailed) N	0.741** 0.000 488	0.786** 0.000 1244	0.907** 0.000 1562	1 1562										
NO	Correlation Coefficient Sig. (2-tailed) N	0.776** 0.000 488	0.741** 0.000 1244	0.984** 0.000 1561	0.825** 0.000 1562	1 1562									
CO	Correlation Coefficient Sig. (2-tailed) N	0.568** 0.000 626	0.649** 0.000 1429	0.754** 0.000 1561	0.632** 0.000 1561	0.766** 0.000 1561	1 1825								
1,3-Butadiene	Correlation Coefficient Sig. (2-tailed) N	0.496** 0.000 259	0.575** 0.000 259	0.651** 0.000 259	0.690** 0.000 259	0.612** 0.000 259	0.596** 0.000 259	1 259							
Benzene	Correlation Coefficient Sig. (2-tailed) N	0.419** 0.000 259	0.509** 0.000 259	0.605** 0.000 259	0.612** 0.000 259	0.574** 0.000 259	0.611** 0.000 259	0.830** 0.000 259	1 259						
Toluene	Correlation Coefficient Sig. (2-tailed) N	0.375** 0.000 259	0.395** 0.000 259	0.518** 0.000 259	0.478** 0.000 259	0.505** 0.000 259	0.560** 0.000 259	0.707** 0.000 259	0.907** 0.000 259	1 259					
Ethyl benzene	Correlation Coefficient Sig. (2-tailed) N	0.374** 0.000 259	0.370** 0.000 259	0.428** 0.000 259	0.452** 0.000 259	0.400** 0.000 259	0.464** 0.000 259	0.638** 0.000 259	0.729** 0.000 259	0.797** 0.000 259	1 259				
o-xylene	Correlation Coefficient Sig. (2-tailed) N	0.359** 0.000 259	0.393** 0.000 259	0.470** 0.000 259	0.462** 0.000 259	0.452** 0.000 259	0.435** 0.000 259	0.605** 0.000 259	0.741** 0.000 259	0.789** 0.000 259	0.800** 0.000 259	1 259			
m/p-xylene	Correlation Coefficient Sig. (2-tailed) N	0.347** 0.000 259	0.376** 0.000 259	0.445** 0.000 259	0.417** 0.000 259	0.432** 0.000 259	0.505** 0.000 259	0.636** 0.000 259	0.798** 0.000 259	0.887** 0.000 259	0.954** 0.000 259	0.841** 0.000 259	1 259		
Wind speed	Correlation Coefficient Sig. (2-tailed) N	-0.282** 0.000 822	-0.136** 0.000 1432	-0.226** 0.000 1560	-0.208** 0.000 1560	-0.215** 0.000 1560	-0.166** 0.000 1809	0.022 0.725 2024	0.028 0.655 259	0.022 0.560 259	0.028 0.011 259	-0.036 0.017 259	-0.159* 0.017 259	0.017 -0.102 259	1 259

Significant correlations are in bold; **Correlation is significant at the 0.01 level (2-tailed), *Correlation is significant at the 0.05 level (2-tailed). PNC: particle number concentration; PM₁₀ T: PM₁₀ measured by TEOM analyser. Wind speed data were measured at Bishopton (circa 18.0 Km from the monitoring site). Data were provided by British Atmospheric Data Centre.

Table 6.7 Spearman correlation coefficient and scatter plot of daily averaged traffic-related air pollutants at Hope St. (8 Jun- 31 Aug 2006) (horizontal variables: x axes and vertical variables: y axes).

		V	Cr	Mn	Fe	Ni	Cu	As	Cd	Pb	PNC	PM ₁₀ P	Abs PM ₁₀	NO _x	NO ₂	NO	CO	1,3-Butadiene	Benzene	Toluene	m+p-xylene	o-xylene	Ethyl benzene	Wind speed
V	r Sig. (2-tailed) N	1 17																						
Cr	Correlation Coefficient Sig. (2-tailed) N	0.568* 0.017 17	1 17																					
Mn	Correlation Coefficient Sig. (2-tailed) N	0.794** 0.000 16	0.447 0.082 17	1 16																				
Fe	Correlation Coefficient Sig. (2-tailed) N	0.244 0.362 16	0.434 0.093 16	0.544* 0.029 16	1 17																			
Ni	Correlation Coefficient Correlation Coefficient N	0.699** 0.002 17	0.662** 0.004 17	0.565* 0.023 16	0.394 0.131 16	1 17																		
Cu	Correlation Coefficient Sig. (2-tailed) N	0.720** 0.001 17	0.497* 0.043 17	0.764** 0.001 16	0.321 0.226 16	0.755** 0.000 17	1 17																	
As	Correlation Coefficient Sig. (2-tailed) N	0.685** 0.003 16	0.440 0.088 16	0.857** 0.000 15	0.471 0.076 15	0.409 0.116 16	0.632** 0.009 16	1 17																
Cd	Correlation Coefficient Sig. (2-tailed) N	0.490 0.054 16	0.233 0.386 16	0.298 0.280 15	-0.025 0.929 15	0.243 0.365 16	0.225 0.402 16	0.690** 0.004 15	1 17															
Pb	Correlation Coefficient Sig. (2-tailed) N	0.444 0.074 17	0.495* 0.043 17	0.400 0.125 16	0.568* 0.022 16	0.228 0.379 17	0.262 0.309 17	0.726** 0.001 16	0.511* 0.043 16	1 17														
PNC	Correlation Coefficient Sig. (2-tailed) N	0.764** 0.006 11	0.711** 0.014 11	0.927** 0.000 10	0.661 0.038 10	0.918** 0.000 11	0.936** 0.000 11	0.539 0.108 10	0.224 0.533 10	0.355 0.285 11	1 35													
PM ₁₀ P	Correlation Coefficient Sig. (2-tailed) N	0.288 0.262 17	0.209 0.422 17	0.456 0.076 16	0.066 0.807 16	0.581* 0.014 17	0.703** 0.002 17	0.332 0.208 16	0.084 0.757 16	0.025 0.926 17	0.742** 0.000 25	1 25												
Abs PM ₁₀	Correlation Coefficient Sig. (2-tailed) N	0.056 0.830 17	0.129 0.622 17	0.226 0.399 16	-0.094 0.729 16	0.199 0.445 17	0.294 0.252 17	0.471 0.066 16	0.502* 0.048 16	0.130 0.619 17	0.346 0.090 25	0.278 0.179 25	1 25											

NO _x	Correlation Coefficient	-0.167	0.050	-0.267	-0.700*	0.317	0.550	-0.317	-0.287	-0.567	0.872**	0.850**	0.535*	1																															
	Sig. (2-tailed)	0.668	0.898	0.488	0.036	0.406	0.125	0.406	0.490	0.112	0.000	0.000	0.027	0.000																															
	N	9	9	9	9	9	9	9	8	9	19	17	17	63																															
NO ₂	Correlation Coefficient	0.117	0.293	-0.226	-0.594*	0.745*	0.477	-0.092	0.072	-0.293	0.845**	0.828**	0.499*	0.902**	1																														
	Sig. (2-tailed)	0.764	0.444	0.559	0.092	0.021	0.194	0.814	0.866	0.444	0.000	0.000	0.041	0.000	0.000																														
	N	9	9	9	9	9	9	9	8	9	19	17	17	63	63																														
NO	Correlation Coefficient	-0.250	0.083	-0.267	-0.583*	0.217	0.600	-0.233	-0.228	-0.450	0.854**	0.811**	0.582*	0.983**	0.828**	1																													
	Sig. (2-tailed)	0.516	0.831	0.488	0.099	0.576	0.088	0.546	0.588	0.224	0.000	0.000	0.014	0.000	0.000	0.000																													
	N	9	9	9	9	9	9	9	8	9	19	17	17	63	63	63																													
CO	Correlation Coefficient	0.205	0.222	0.250	-0.264	0.555*	0.659*	0.19604	0.215	0.042	0.637**	0.761**	0.434*	0.778**	0.602**	0.804**	1																												
	Sig. (2-tailed)	0.482	0.445	0.409	0.383	0.039	0.010	0.502	0.480	0.887	0.001	0.000	0.044	0.000	0.000	0.000	0.000																												
	N	14	14	13	13	14	14	14	13	14	25	22	22	63	63	63	75																												
1,3-Butadiene	Correlation Coefficient	0.202	0.004	0.289	-0.391	0.414	0.578*	0.305	0.377	-0.085	0.709**	0.714**	0.537**	0.951**	0.914**	0.933**	0.893**	1																											
	Sig. (2-tailed)	0.470	0.989	0.316	0.167	0.125	0.024	0.269	0.184	0.763	0.000	0.000	0.008	0.000	0.000	0.000	0.000	0.000	0.000																										
	N	15	15	14	14	15	15	15	14	15	33	23	23	19	19	19	25	33	33																										
Benzene	Correlation Coefficient	0.150	0.050	0.248	-0.226	0.414	0.518*	0.057	0.015	-0.043	0.550**	0.764**	0.321	0.933**	0.886**	0.921**	0.930**	0.801**	1																										
	Sig. (2-tailed)	0.594	0.860	0.392	0.436	0.125	0.048	0.840	0.958	0.879	0.001	0.000	0.135	0.000	0.000	0.000	0.000	0.000	0.000	0.000																									
	N	15	15	14	14	15	15	15	14	15	33	23	23	19	19	19	25	33	33	33																									
Toluene	Correlation Coefficient	0.450	0.339	0.609*	-0.156	0.539*	0.814**	0.471	0.312	0.179	0.646**	0.787**	0.463*	0.874**	0.814**	0.847**	0.866**	0.835**	0.856**	1																									
	Sig. (2-tailed)	0.092	0.216	0.021	0.594	0.038	0.000	0.076	0.277	0.524	0.000	0.000	0.026	0.000	0.000	0.000	0.000	0.000	0.000	0.000	0.000																								
	N	15	15	14	14	15	15	15	14	15	33	23	23	19	19	19	25	33	33	33	33																								
m + p-xylene	Correlation Coefficient	0.364	0.271	0.530	-0.121	0.532*	0.764**	0.411	0.213	0.107	0.335	0.804**	-0.238	0.538	0.465	0.533	0.679**	0.362	0.704**	0.662**	1																								
	Sig. (2-tailed)	0.182	0.328	0.051	0.681	0.041	0.001	0.128	0.464	0.704	0.148	0.002	0.457	0.058	0.109	0.061	0.005	0.116	0.001	0.001	0.000																								
	N	15	15	14	14	15	15	15	14	15	20	12	12	13	13	13	15	20	20	20	20																								
o-xylene	Correlation Coefficient	0.318	0.214	0.446	-0.165	0.632*	0.768**	0.371	0.374	0.125	0.426*	0.899**	0.038	0.759**	0.714**	0.765**	0.886**	0.524**	0.797**	0.797**	0.827**	1																							
	Sig. (2-tailed)	0.248	0.443	0.110	0.573	0.011	0.001	0.173	0.188	0.657	0.019	0.000	0.875	0.001	0.002	0.001	0.000	0.003	0.000	0.000	0.000	0.000																							
	N	15	15	14	14	15	15	15	14	15	30	20	20	16	16	16	22	30	30	30	30	30																							
Ethyl benzene	Correlation Coefficient	-0.250	0.143	-0.071	-0.071	-0.143	0.714**	-0.143	-0.290	0.000	0.673**	0.837**	0.516*	0.804**	0.764**	0.791**	0.810**	0.744**	0.792**	0.904**	0.901**	0.859**	1																						

Table 6.8 Spearman correlation coefficient and scatter plot of hourly averaged traffic-related air pollutants at St. Enoch Sq. (8 Jun- 31 Aug 2006), (horizontal variables: x axes and vertical variables: y axes).

		PNC	PM ₁₀ T	NO _x	NO ₂	NO	CO	SO ₂	O ₃	Wind speed
PNC	Correlation Coefficient	1.000								
	Sig. (2-tailed)	.								
	N	1896								
PM ₁₀ T	Correlation Coefficient	0.513**	1.000							
	Sig. (2-tailed)	0.000								
	N	1713	1857							
NO _x	Correlation Coefficient	0.765**	0.524**	1.000						
	Sig. (2-tailed)	0.000	0.000							
	N	1839	1852	1983						
NO ₂	Correlation Coefficient	0.662**	0.506**	0.924**	1.000					
	Sig. (2-tailed)	0.000	0.000	0.000						
	N	1839	1852	1983	1983					
NO	Correlation Coefficient	0.716**	0.427**	0.869**	0.634**	1.000				
	Sig. (2-tailed)	0.000	0.000	0.000	0.000					
	N	1839	1852	1983	1983	1983				
CO	Correlation Coefficient	0.357**	0.266**	0.475**	0.465**	0.395**	1.000			
	Sig. (2-tailed)	0.000	0.000	0.000	0.000	0.000				
	N	1214	1206	1330	1330	1330	1334			
SO ₂	Correlation Coefficient	0.185**	0.223**	0.265**	0.256**	0.236**	0.045	1.000		
	Sig. (2-tailed)	0.000	0.000	0.000	0.000	0.000	0.167			
	N	1456	1480	1597	1597	1597	951	1600		
O ₃	Correlation Coefficient	-0.240**	0.107**	-0.482**	-0.452**	-0.404**	-0.469**	0.050*	1.000	
	Sig. (2-tailed)	0.000	0.000	0.000	0.000	0.000	0.000	0.047		
	N	1841	1854	1979	1979	1979	1331	1596	1985	
Wind speed	Correlation Coefficient	-0.036	-0.043	-0.171**	-0.311**	0.049*	-0.204**	-0.058*	0.377**	1.000
	Sig. (2-tailed)	0.117	0.065	0.000	0.000	0.031	0.000	0.020	0.000	.
	N	1881	1841	1967	1967	1967	1319	1584	1969	2024

Significant correlations are in bold; **Correlation is significant at the 0.01 level (2-tailed), *Correlation is significant at the 0.05 level (2-tailed). PNC: Particle number concentration; PM10 T: PM10 measured by TEOM analyser; Wind speed data were measured at Bishopton (circa 18.0 Km from the monitoring site). Data were provided by British Atmospheric Data Centre.

Table 6.9 Spearman correlation coefficient and scatter plot of daily averaged traffic-related air pollutants at St. Enoch Sq. (8 Jun-31 Aug 2006) (horizontal variables: x axes and vertical variables: y axes).

		V	Cr	Mn	Fe	Ni	Cu	As	Cd	Pb	PNC	PM ₁₀ P	Abs PM ₁₀	NO _x	NO ₂	NO	CO	SO ₂	O ₃	Wind speed	
V	Correlation Coefficient Sig. (2-tailed) N	1.000 . 17																			
Cr	Correlation Coefficient Sig. (2-tailed) N	0.419 0.106 17	1.000 . 17																		
Mn	Correlation Coefficient Sig. (2-tailed) N	0.396 0.129 17	0.657** 0.004 17	1.000 . 17																	
Fe	Correlation Coefficient Sig. (2-tailed) N	0.480 0.060 17	0.620** 0.008 17	0.863** 0.000 17	1.000 . 17																
Ni	Correlation Coefficient Sig. (2-tailed) N	0.269 0.313 17	0.549* 0.022 17	0.635** 0.006 17	0.331 0.195 17	1.000 . 17															
Cu	Correlation Coefficient Sig. (2-tailed) N	0.514* 0.042 17	0.654** 0.004 17	0.855** 0.000 17	0.787** 0.006 17	0.637** 0.006 17	1.000 . 17														
As	Correlation Coefficient Sig. (2-tailed) N	0.745** 0.001 17	0.380 0.146 17	0.747** 0.001 17	0.773** 0.000 17	0.462 0.071 17	0.814** 0.000 17	1.000 . 17													
Cd	Correlation Coefficient Sig. (2-tailed) N	0.394 0.164 17	0.522* 0.046 17	0.732** 0.002 17	0.686** 0.005 17	0.729** 0.002 17	0.789** 0.004 17	0.701** 0.004 17	1.000 . 17												
Pb	Correlation Coefficient Sig. (2-tailed) N	0.386 0.155 15	0.603* 0.013 16	0.615* 0.011 16	0.606* 0.013 16	0.626** 0.009 16	0.824** 0.000 16	0.632** 0.009 15	0.793** 0.000 15	1.000 . 17											
PNC	Correlation Coefficient Sig. (2-tailed) N	0.521 0.056 17	0.620* 0.014 17	0.814** 0.000 17	0.732** 0.002 17	0.568* 0.027 17	0.832** 0.000 17	0.815** 0.007 17	0.703** 0.004 17	0.719** 0.004 17	1.000 . 17										
PM ₁₀ P	Correlation Coefficient Sig. (2-tailed) N	0.129 0.635 17	0.442 0.076 17	0.770** 0.000 17	0.560* 0.019 17	0.552* 0.022 17	0.601* 0.011 17	0.518* 0.040 17	0.527* 0.044 17	0.533* 0.034 17	0.292 0.176 23	1.000 . 24									
Abs PM ₁₀	Correlation Coefficient Sig. (2-tailed) N	0.695** 0.003 17	0.411 0.101 17	0.494* 0.044 17	0.611** 0.009 17	0.228 0.379 17	0.695** 0.002 17	0.761** 0.001 17	0.545* 0.036 17	0.518* 0.040 17	0.473* 0.023 23	0.234 1.000 24	0.415 0.069 20	1.000 . 20							
NO _x	Correlation Coefficient Sig. (2-tailed) N	0.524 0.080 15	0.709** 0.007 15	0.659* 0.014 15	0.747** 0.003 15	0.418 0.156 15	0.742** 0.004 15	0.758** 0.003 15	0.594* 0.042 15	0.725** 0.005 15	0.654** 0.023 75	0.644** 0.027 20	0.415 0.069 20	1.000 . 20							
NO ₂	Correlation Coefficient Sig. (2-tailed) N	0.510 0.090 15	0.670** 0.012 15	0.621* 0.024 15	0.709** 0.007 15	0.390 0.188 15	0.736** 0.004 15	0.531 0.075 15	0.654* 0.015 15	0.524** 0.000 75	0.686** 0.001 75	0.488* 0.029 20	0.915** 0.000 81	1.000 . 81							
NO	Correlation Coefficient Sig. (2-tailed) N	0.389 0.212 15	0.718** 0.006 15	0.657* 0.015 15	0.751** 0.003 15	0.371 0.212 15	0.699** 0.008 15	0.654* 0.015 15	0.581* 0.047 15	0.726** 0.005 15	0.612** 0.000 75	0.348 0.132 20	0.221 0.348 20	0.867** 0.000 81	0.623** 0.000 81	1.000 . 81					
CO	Correlation Coefficient Sig. (2-tailed) N	0.310 0.456 10	0.119 0.779 10	0.190 0.651 10	0.000 1.000 10	-0.095 0.823 10	0.048 0.911 10	0.120 0.778 10	-0.310 0.456 10	-0.238 0.570 10	0.357* 0.012 49	0.265 0.431 11	-0.279 0.407 11	0.486** 0.000 54	0.398** 0.003 54	0.456** 0.001 54	1.000 . 54				
SO ₂	Correlation Coefficient Sig. (2-tailed) N	-0.188 0.536 17	0.285 0.323 14	0.366 0.199 14	0.429 0.126 14	0.078 0.791 14	0.329 0.251 14	0.173 0.553 14	0.329 0.272 13	0.468 0.092 14	0.629** 0.570 50	-0.010 0.002 21	0.209 0.964 21	0.293* 0.098 21	0.116 0.019 64	-0.224 0.361 64	1.000 . 65				
O ₃	Correlation Coefficient Sig. (2-tailed) N	-0.319 0.289 17	-0.587* 0.027 17	-0.345 0.227 17	-0.473 0.088 17	-0.284 0.326 17	-0.371 0.191 17	-0.220 0.449 17	-0.456 0.117 17	-0.330 0.180 17	-0.234* 0.042 78	0.018 0.938 23	-0.207 0.367 23	-0.381** 0.000 80	-0.164 0.143 80	-0.574** 0.000 81	-0.559** 0.000 81	0.208 0.100 84	1.000 . 84		
Wind speed	Correlation Coefficient Sig. (2-tailed) N	-0.574* 0.025 17	-0.634** 0.008 17	-0.494 0.052 17	-0.509* 0.044 17	-0.382 0.144 17	-0.612* 0.012 17	-0.640* 0.010 17	-0.429 0.126 17	-0.589* 0.021 17	-0.303** 0.007 78	-0.510** 0.013 23	-0.348 0.104 23	-0.476** 0.000 80	-0.567** 0.006 80	-0.297** 0.006 80	-0.382** 0.005 80	-0.065 0.609 84	0.163 0.146 84	1.000 . 84	

Significant correlations are in bold; **Correlation is significant at the 0.01 level (2-tailed); *Correlation is significant at the 0.05 level (2-tailed); PNC: particle number concentration; PM₁₀P: PM₁₀ measured by PARTISOL sampler; Abs PM₁₀: absorption coefficient of PM₁₀. Wind speed data were measured at Bishopston (circa 18.0 Km from the monitoring site). Data were provided by British Atmospheric Data Centre.

Table 6.10 Spearman correlation coefficient and scatter plot of hourly averaged traffic-related air pollutants at Montrose St (8 Jun-31 Aug 2006), (horizontal variables: x axes and vertical variables: y axes).

		PNC	NO ₂	NO	NO _x	CO	Wind speed
PNC	Correlation Coefficient Sig. (2-tailed) N	1 . 1493					
NO _x	Correlation Coefficient Sig. (2-tailed) N	0.743** 0.000 1456	1 . 1998				
NO	Correlation Coefficient Sig. (2-tailed) N	0.721** 0.000 1456	0.944** 0.000 1998	1 . 1998			
NO ₂	Correlation Coefficient Sig. (2-tailed) N	0.683** 0.000 1456	0.951** 0.000 1998	0.804** 0.000 1998	1 . 1998		
CO	Correlation Coefficient Sig. (2-tailed) N	0.532** 0.000 1460	0.613** 0.000 1997	0.664** 0.000 1997	0.512** 0.000 1997	1 . 2005	
Wind speed	Correlation Coefficient Sig. (2-tailed) N	-0.134** 0.000 1477	-0.119** 0.000 1985	-0.212** 0.000 1985	-0.011 0.635 1985	-0.156** 0.000 1992	1 . 2024

Significant correlations are in bold;**Correlation is significant at the 0.01 level (2-tailed); PNC: particle number concentration. Wind speed data were measured at Bishopton (circa 18.6 Km from the monitoring site). Data were provided by British Atmospheric Data Centre.

Table 6.11 Spearman correlation coefficient and scatter plot of daily averaged traffic-related air pollutants at Montrose St. (8 Jun-31 Aug 2006), (horizontal variables: x axes and vertical variables: y axes).

		PNC	NO _x	NO	NO ₂	CO	Wind speed
PNC	Correlation Coefficient Sig. (2-tailed) N	1 . 63					
NO _x	Correlation Coefficient Sig. (2-tailed) N	0.624** 0.000 61	1 . 83				
NO ₂	Correlation Coefficient Sig. (2-tailed) N	0.659** 0.000 61	0.934** 0.000 83	1 . 83			
NO	Correlation Coefficient Sig. (2-tailed) N	0.509** 0.000 61	0.925** 0.000 83	0.746** 0.000 83	1 . 83		
CO	Correlation Coefficient Sig. (2-tailed) N	0.674** 0.000 61	0.646** 0.000 83	0.740** 0.000 83	0.460** 0.000 83	1 . 83	
Wind speed	Correlation Coefficient Sig. (2-tailed) N	-0.455** 0.000 62	-0.301** 0.006 82	-0.418** 0.000 82	-0.158 0.156 82	-0.440** 0.000 82	1 . 84

Significant correlations are in bold;**Correlation is significant at the 0.01 level (2-tailed); PNC: particle number concentration. Wind speed data were measured at Bishopton (circa 18.6 Km from the monitoring site). Data were provided by British Atmospheric Data Centre.

Table 6.12 Spearman correlation coefficient hourly averaged traffic-related air pollutants at Marylebone Rd. (selection of 26 days in 2006), (horizontal variables: x axes and vertical variables: y axes).

		PNC	PM ₁₀ T	EC	OC	NO _x	NO ₂	NO	CO	SO ₂	O ₃	1,3-butadiene	Benzene	Toluene	Ethyl benzene	o-xylene	m/p-xylene	wind speed
PNC	Correlation Coefficient Sig. (2-tailed) N	1 609																
PM ₁₀ T	Correlation Coefficient Sig. (2-tailed) N	0.773* 0.000 602	1 613															
EC	Correlation Coefficient Sig. (2-tailed) N	0.687** 0.000 607	0.787** 0.000 611	1 618														
OC	Correlation Coefficient Sig. (2-tailed) N	0.442** 0.000 607	0.787** 0.000 611	0.772** 0.000 618	1 618													
NO _x	Correlation Coefficient Sig. (2-tailed) N	0.863** 0.000 605	0.643** 0.000 611	0.781** 0.000 614	0.509** 0.000 614	1 616												
NO ₂	Correlation Coefficient Sig. (2-tailed) N	0.838** 0.000 605	0.856** 0.000 611	0.788** 0.000 614	0.546** 0.000 614	0.973** 0.000 616	1 616											
NO	Correlation Coefficient Sig. (2-tailed) N	0.861** 0.000 605	0.860** 0.000 611	0.769** 0.000 614	0.488** 0.000 614	0.997** 0.000 616	0.952** 0.000 616	1 616										
CO	Correlation Coefficient Sig. (2-tailed) N	0.525** 0.000 600	0.843** 0.000 611	0.546** 0.000 609	0.504** 0.000 609	0.611** 0.000 611	0.624** 0.000 611	0.597** 0.000 611	1 611									
SO ₂	Correlation Coefficient Sig. (2-tailed) N	-0.106* 0.035 394	0.053 0.287 399	0.091 0.067 403	0.405** 0.000 403	-0.077 0.125 401	-0.007 0.896 401	-0.100* 0.046 401	0.091 0.071 397	1 405								
O ₃	Correlation Coefficient Sig. (2-tailed) N	-0.702** 0.000 609	-0.523** 0.000 613	-0.459** 0.000 618	-0.259** 0.000 618	-0.732** 0.000 616	-0.639** 0.000 616	-0.755** 0.000 616	-0.443** 0.000 611	0.231** 0.000 405	1 620							
1,3-Butadiene	Correlation Coefficient Sig. (2-tailed) N	0.666** 0.000 501	-0.523** 0.000 613	0.591** 0.000 512	0.430** 0.000 512	0.809** 0.000 508	0.796** 0.000 508	0.804** 0.000 508	0.756** 0.000 506	-0.016 0.772 351	-0.639** 0.000 512	1 512						
Benzene	Correlation Coefficient Sig. (2-tailed) N	0.626** 0.000 448	0.669** 0.000 505	0.563** 0.000 459	0.350** 0.000 459	0.765** 0.000 459	0.753** 0.000 459	0.760** 0.000 459	0.658** 0.000 458	-0.029 0.615 297	-0.598** 0.000 459	0.888** 0.000 451	1 460					
Toluene	Correlation Coefficient Sig. (2-tailed) N	0.641** 0.000 506	0.634** 0.000 455	0.675** 0.000 517	0.553** 0.000 517	0.812** 0.000 513	0.806** 0.000 513	0.804** 0.000 513	0.742** 0.000 511	0.072 0.175 356	-0.608** 0.000 517	0.937** 0.000 513	0.860** 0.000 456	1 518				
Ethyl benzene	Correlation Coefficient Sig. (2-tailed) N	0.689** 0.000 511	0.691** 0.000 510	0.691** 0.000 518	0.571** 0.000 518	0.808** 0.000 514	0.802** 0.000 514	0.801** 0.000 514	0.741** 0.000 512	0.068 0.200 356	-0.615** 0.000 518	0.913** 0.000 513	0.839** 0.000 457	0.984** 0.000 518	1 519			
o-xylene	Correlation Coefficient Sig. (2-tailed) N	0.677** 0.000 511	0.555** 0.000 518	0.676** 0.000 518	0.556** 0.000 518	0.796** 0.000 514	0.786** 0.000 514	0.789** 0.000 514	0.724** 0.000 512	0.058 0.278 356	-0.615** 0.000 518	0.903** 0.000 513	0.834** 0.000 457	0.976** 0.000 518	0.982** 0.000 519	1 519		
m/p-xylene	Correlation Coefficient Sig. (2-tailed) N	0.656** 0.000 511	0.537** 0.000 518	0.661** 0.000 518	0.553** 0.000 518	0.781** 0.000 514	0.777** 0.000 514	0.773** 0.000 514	0.723** 0.000 512	0.062 0.244 356	-0.589** 0.000 518	0.908** 0.000 513	0.833** 0.000 457	0.970** 0.000 518	0.967** 0.000 519	0.967** 0.000 519	1 519	
wind speed	Correlation Coefficient Sig. (2-tailed) N	0.197** 0.000 590	0.165** 0.000 594	0.0057 0.889 599	-0.229** 0.000 599	0.191** 0.000 597	0.194** 0.000 597	0.192** 0.000 597	-0.022 0.593 395	-0.160** 0.001 601	-0.010 0.801 601	0.207** 0.000 500	0.233** 0.000 448	0.143** 0.001 505	0.128** 0.004 506	0.131** 0.003 506	0.105* 0.018 506	1 602

Significant correlations are in bold; **Correlation is significant at the 0.01 level (2-tailed), *Correlation is significant at the 0.05 level (2-tailed). PNC: Particle number concentration; PM₁₀T: PM₁₀ measured by TEOM analyser; EC: elemental carbon; OC: organic carbon. Wind speed data were measured at Heathrow Airport (circa 20.0 Km from the monitoring site). Data were provided by British Atmospheric Data Centre.

Table 6.13 Spearman correlation coefficient and scatter plots of daily traffic-related air pollutants at Marylebone Rd. (selection of 26 days in 2006), (horizontal variables: x axes and vertical variables: y axes).

		V	Mn	Fe	Ni	Cu	Zn	As	Cd	Pb	PNC	PM ₁₀ P	PM _{2.5} P	BS	EC	OC	Abs PM _{2.5}	NO _x	NO ₂	NO	CO	SO ₂	O ₃	1,3-butadiene	benzene	toluene	ethyl benzene	o-xylene	m/p-xylene	wind speed
V	Correlation Coefficient Sig. (2-tailed) N	1 26																												
Mn	Correlation Coefficient Sig. (2-tailed) N	0.583** 0.002 26	1 26																											
Fe	Correlation Coefficient Sig. (2-tailed) N	0.443* 0.024 26	0.877** 0.000 26	1 26																										
Ni	Correlation Coefficient Sig. (2-tailed) N	0.961** 0.000 26	0.647** 0.000 26	0.525** 0.006 26	1 26																									
Cu	Correlation Coefficient Sig. (2-tailed) N	0.221 0.278 26	0.706** 0.000 26	0.765** 0.000 26	0.328 0.102 26	1 26																								
Zn	Correlation Coefficient Sig. (2-tailed) N	0.337 0.093 26	0.865** 0.000 26	0.748** 0.000 26	0.408* 0.038 26	0.638** 0.000 26	1 26																							
As	Correlation Coefficient Sig. (2-tailed) N	0.237 0.244 26	0.556** 0.001 26	0.527** 0.006 26	0.252 0.214 26	0.562** 0.003 26	0.676** 0.000 26	1 26																						
Cd	Correlation Coefficient Sig. (2-tailed) N	0.215 0.293 26	0.561** 0.003 26	0.570** 0.002 26	0.281 0.164 26	0.674** 0.000 26	0.631** 0.001 26	0.601** 0.001 26	1 26																					
Pb	Correlation Coefficient Sig. (2-tailed) N	-0.038 0.855 26	0.495* 0.010 26	0.497** 0.010 26	-0.032 0.876 26	0.380 0.055 26	0.756** 0.000 26	0.521** 0.006 26	0.384 0.053 26	1 26																				
PNC	Correlation Coefficient Sig. (2-tailed) N	-0.116 0.572 26	-0.241 0.235 26	-0.211 0.302 26	-0.241 0.235 26	-0.605** 0.001 26	-0.255 0.209 26	-0.262 0.196 26	-0.362 0.069 26	-0.077 0.710 26	1 26																			
PM ₁₀ P	Correlation Coefficient Sig. (2-tailed) N	0.484* 0.014 25	0.311 0.130 25	0.120 0.569 25	0.436* 0.029 25	-0.185 0.377 25	0.245 0.238 25	0.024 0.907 25	-0.031 0.882 25	0.095 0.651 25	0.400* 0.048 25	1 25																		
PM _{2.5} P	Correlation Coefficient Sig. (2-tailed) N	0.381 0.055 26	0.536** 0.005 26	0.480* 0.013 26	0.340 0.089 26	0.034 0.868 26	0.360 0.071 26	0.243 0.232 26	0.192 0.348 26	0.187 0.361 26	0.476* 0.014 26	0.710** 0.000 25	1 26																	
BS	Correlation Coefficient Sig. (2-tailed) N	-0.035 0.866 26	-0.259 0.202 26	-0.281 0.164 26	-0.186 0.362 26	-0.494* 0.010 26	-0.247 0.224 26	-0.142 0.490 26	-0.334 0.095 26	-0.144 0.484 26	0.707** 0.000 26	0.352 0.084 25	0.279 0.167 26	1 26																
EC	Correlation Coefficient Sig. (2-tailed) N	0.451* 0.021 26	0.216 0.290 26	0.116 0.572 26	0.358 0.072 26	-0.069 0.737 26	0.034 0.871 26	-0.027 0.894 26	-0.089 0.666 26	-0.209 0.307 26	0.541** 0.004 26	0.506** 0.010 25	0.594** 0.001 26	0.477** 0.014 26	1 26															

Table 6.14 Spearman correlation coefficient hourly averaged traffic-related air pollutants at North Kensington (selection of 26 days in 2006), (horizontal variables: x axes and vertical variables: y axes).

	PNC	PM ₁₀ T	EC	OC	NO _x	NO ₂	NO	CO	SO ₂	O ₃	Wind speed
PNC	1 621										
PM ₁₀ T	0.264** 0.000 616	1 616									
EC	0.219** 0.000 620	0.329** 0.000 615	1 549								
OC	0.473** 0.000 620	0.328** 0.000 615	0.838** 0.000 549	1 549							
NO _x	0.787** 0.000 616	0.317** 0.000 611	0.643** 0.000 544	0.615** 0.000 544	1 616						
NO ₂	0.787** 0.000 616	0.312** 0.000 611	0.605** 0.000 544	0.597** 0.000 544	0.983** 0.000 616	1 616					
NO	0.681** 0.000 616	0.283** 0.000 611	0.645** 0.000 544	0.564** 0.000 544	0.869** 0.000 616	0.782** 0.000 616	1 616				
CO	0.690** 0.000 614	0.323** 0.000 610	0.495** 0.000 542	0.508** 0.000 542	0.695** 0.000 614	0.688** 0.000 614	0.639** 0.000 614	1 614			
SO ₂	0.328** 0.000 594	0.279** 0.000 589	0.343** 0.000 522	0.332** 0.000 522	0.421** 0.000 593	0.386** 0.000 593	0.426** 0.000 593	0.317** 0.000 591	1 594		
O ₃	-0.687** 0.000 615	-0.060 0.140 610	-0.472** 0.000 543	-0.404** 0.000 543	-0.840** 0.000 615	-0.829** 0.000 615	-0.711** 0.000 615	-0.619** 0.000 614	-0.260** 0.000 592	1 592	
Wind speed	-0.145** 0.000 602	-0.260** 0.000 597	-0.461** 0.000 536	-0.602** 0.000 536	-0.469** 0.000 597	-0.487** 0.000 597	-0.333** 0.000 597	-0.218** 0.000 595	-0.187** 0.000 575	0.348** 0.000 596	1 602

Significant correlations are in bold; * Correlation is significant at the 0.05 level (2-tailed); ** Correlation is significant at the 0.01 level (2-tailed); PNC: particle number concentration; PM₁₀ T: PM₁₀ measured by the TEOM analyser; EC: elemental carbon; OC: organic carbon. Wind data was measured at Heathrow Airport (circa 16 Km from the monitoring site). Data were provided by British Atmospheric Data Centre.

Table 6.15 Spearman correlation coefficient and scatter plots of daily traffic-related air pollutants at North Kensington (horizontal variables: x axes and vertical variables: y axes).

		V	Mn	Fe	Ni	Cu	Zn	As	Cd	Pb	PNC	PM ₁₀ P	PM _{2.5} P	EC	OC	Abs PM _{2.5}	NO _x	NO ₂	NO	CO	SO ₂	O ₃	wind speed
V	Correlation Coefficient Sig. (2-tailed) N	1.000 . 26																					
Mn	Correlation Coefficient Sig. (2-tailed) N	0.505** 0.009 26	1.000 . 26																				
Fe	Correlation Coefficient Sig. (2-tailed) N	0.416* 0.035 26	0.848** 0.000 26	1.000 . 26																			
Ni	Correlation Coefficient Sig. (2-tailed) N	0.689** 0.000 26	0.573** 0.002 26	0.589** 0.002 26	1.000 . 26																		
Cu	Correlation Coefficient Sig. (2-tailed) N	-0.114 0.580 26	0.584** 0.002 26	0.617** 0.001 26	0.023 0.913 26	1.000 . 26																	
Zn	Correlation Coefficient Sig. (2-tailed) N	0.164 0.424 26	0.634** 0.001 26	0.683** 0.000 26	0.224 0.271 26	0.649** 0.000 26	1.000 . 26																
As	Correlation Coefficient Sig. (2-tailed) N	0.019 0.926 26	0.414* 0.035 26	0.539** 0.004 26	0.173 0.398 26	0.501** 0.009 26	0.722** 0.000 26	1.000 . 26															
Cd	Correlation Coefficient Sig. (2-tailed) N	0.209 0.305 26	0.672** 0.000 26	0.717** 0.000 26	0.336 0.094 26	0.624** 0.001 26	0.769** 0.000 26	0.722** 0.000 26	1.000 . 26														
Pb	Correlation Coefficient Sig. (2-tailed) N	0.205 0.316 26	0.508** 0.008 26	0.584** 0.002 26	0.186 0.363 26	0.658** 0.000 26	0.837** 0.000 26	0.814** 0.000 26	0.743** 0.000 26	1.000 . 26													
PNC	Correlation Coefficient Sig. (2-tailed) N	-0.318 0.114 26	-0.252 0.214 26	-0.119 0.564 26	-0.533** 0.005 26	0.240 0.237 26	0.189 0.355 26	0.247 0.223 26	0.202 0.324 26	0.319 0.112 26	1.000 . 26												
PM ₁₀ P	Correlation Coefficient Sig. (2-tailed) N	0.436* 0.026 26	0.587** 0.002 26	0.593** 0.001 26	0.544** 0.004 26	0.212 0.298 26	0.466* 0.016 26	0.551** 0.004 26	0.627** 0.001 26	0.487* 0.012 26	0.026 0.900 26	1.000 . 26											

In general, the correlation coefficients between traffic-related air pollutants were higher at the two kerbside sites, Hope St. and Marylebone Rd., than at the other less polluted sites. The following sections describe the correlations between co-pollutants.

6.1.4.1 Correlations between particle characteristics and gaseous pollutants

At all the studied sites, PNC and NO_x were the pollutant pair with the highest correlation coefficients. Generally, there were no significant differences between the r-values derived from daily and hourly averaged data, with the exception of Hope St. At this site daily averaged data showed higher r-values than their hourly counterparts. At Hope St., the relationship for hourly PNC vs. NO_x, NO₂ and NO showed a curved relationship at high PNC, possibly due to the underestimation of particles by the WCPC, explained in section 5.1.2.3. In contrast, at Marylebone Rd. (where PNC were measured with a BCPC) PNC vs. nitrogen oxides showed a fairly linear relationship for the whole concentration range. At North Kensington, slightly higher r-values were observed for daily averaged data.

PNC vs. gaseous pollutants

PNC were highly correlated to nitrogen oxides at all the studied sites ($r=0.6-0.9$, Table 6.6 to 6.15). Correlation coefficients were slightly higher between PNC vs. NO_x ($r=0.6-0.9$) than between PNC vs. NO₂ and NO.

Correlations of PNC with CO were moderate to high ($r=0.5-0.7$) at Hope St. (Tables 6.6 and 6.7), Montrose St. (Tables 6.10 and 6.11), Marylebone Rd. (only hourly data) (Tables 6.12) and North Kensington (Tables 6.14 and 6.15) but low ($r=0.3$) at St. Enoch Sq. (Tables 6.8 and 6.9) and daily data at Marylebone Rd. (Table 6.13). r-values were slightly higher for daily averaged data at the less polluted sites (North Kensington, and Montrose St.), whereas at Marylebone Rd. hourly averaged data showed significantly higher correlation coefficients than daily averaged data. At Hope St. r-values for hourly averaged data were slightly lower than their daily

counterparts, probably because of the underestimation of particles by the WCPC as indicated earlier.

PNC were not correlated to SO₂ concentrations at any of the sites for which data was available: St. Enoch Sq. (Tables 6.8 and 6.9), Marylebone Rd. (Tables 6.12 and 6.13) and North Kensington (Tables 6.14 and 6.15).

PNC showed a high negative correlation with O₃ concentrations ($r \approx -0.7$) at Marylebone Rd. (Tables 6.12 and 6.13) and North Kensington (Tables 6.14 and 6.15) but not at St. Enoch Sq. (Tables 6.8 and 6.9) ($r = -0.2$). There were no data available for O₃ at Hope St.

Correlations of PNC with 1,3-butadiene and BTEX were moderate at Hope St. ($r \approx 0.4-0.7$, Tables 6.6 and 6.7) and high at Marylebone Rd. ($r \approx 0.6-0.8$, Tables 6.12 and 6.13). At both sites the r -values were higher for PNC vs. 1,3-butadiene and benzene than for PNC vs. toluene, ethylbenzene and xylenes. Daily averaged data showed higher correlation coefficients (generally $r > 0.6$) than their hourly counterparts: $r < 0.5$ at Hope St. (Tables 6.6 and 6.7) and $r < 0.5$ at Marylebone Rd. (Tables 6.12 and 6.13). 1,3-butadiene and BTEX data at Montrose St., St. Enoch Sq. and North Kensington were not available.

PM₁₀ and PM_{2.5} vs. gaseous pollutants

PM₁₀ was highly correlated with NO_x, NO₂, NO and CO at the kerbside sites: $r \approx 0.6-0.9$ at Hope St. (Tables 6.6 and 6.7) and Marylebone Rd. (Tables 6.12 and 6.13) and moderate to low correlated at the background sites: St. Enoch Sq. ($r \approx 0.5-0.6$, Tables 6.8 and 6.9) and North Kensington ($r \approx -0.3-0.4$, Tables 6.14 and 6.15). The r -values did not change significantly with the averaging period. Daily averaged periods showed slightly higher correlation coefficients than their hourly counterparts at the background sites. At Hope St., both r -values were similar and at Marylebone Rd., hourly averaged periods showed higher correlation coefficients than daily averaged periods. There were no data available at Montrose St. for PM₁₀.

Hourly PM₁₀ showed a negative and moderate correlation coefficient with O₃ at Marylebone Rd. ($r=-0.5$, Table 6.12) but not at St. Enoch Sq. ($r=0.1$, Table 6.8). Daily PM₁₀ was not correlated with O₃ at any of the sites. There were no O₃ data available at Hope St. and Montrose St.

PM₁₀ was not correlated to SO₂ at Marylebone Rd. (Tables 6.12 and 6.13). Correlations were moderate for daily PM₁₀ vs. SO₂ but not hourly at St. Enoch Sq. (Table 6.9) and North Kensington (Table 6.15).

Correlations of PM₁₀ with 1,3-butadiene and BTEX were moderate ($r\approx 0.4-0.6$) at Hope St. (Tables 6.6 and 6.7) and high ($r\approx 0.6-0.7$) at Marylebone Rd. (Tables 6.14 and 6.15), with higher correlation coefficients for daily averaged periods than hourly averaged periods.

PM_{2.5} (data only available at North Kensington and Marylebone Rd. for daily averaging periods) showed moderate to low correlation coefficients with nitrogen oxides ($r\approx 0.4$, Tables 6.12 to 6.15).

Correlations of PM_{2.5} vs. CO, 1,3-butadiene, BTEX and SO₂ showed a different pattern at both sites. At Marylebone Rd. (Tables 6.12 and 6.13) PM_{2.5} was moderately correlated with CO, 1,3-butadiene and BTEX ($r\approx 0.5$) and not correlated with SO₂. In contrast, at North Kensington (Tables 6.14 and 6.15) PM_{2.5} did not show correlation with CO, 1,3-butadiene and BTEX, but correlations with SO₂ were moderate ($r\approx 0.5$).

PM_{2.5} (only daily averaged data available) was not correlated with O₃ at Marylebone Rd. and North Kensington (Tables 6.12 to 6.15).

Surrogates of BC vs. gaseous pollutants

The surrogates of BC (EC, absorbance of PM, and BS) showed the highest correlation coefficients with nitrogen oxides ($r\approx 0.5-0.9$). Absorbance of PM also showed a high correlation with 1,3-butadiene and BTEX at Marylebone Rd. (Table 6.13) but not at Hope St. Hourly EC and BS (data only available at Marylebone Rd.)

also showed a high correlation coefficient with 1,3-butadiene and BTEX (Tables 6.12 and 6.13). In general, correlation coefficients were higher for absorbance of PM vs. gaseous pollutants than for EC and BS vs. gaseous pollutants.

Correlations of EC, absorbance of PM and BS with CO were generally low. Hourly EC vs. CO showed moderate correlation coefficients ($r \approx 0.5$) at Marylebone Rd. and North Kensington (Tables 6.12 and 6.15). Absorbance of PM vs. CO showed a moderate correlation coefficient ($r \approx 0.5$) at St. Enoch Sq. (Table 6.9), Hope St. (Table 6.7), and North Kensington (Table 6.15), but not at Marylebone Rd. ($r = 0.2$, Table 6.13).

EC and absorbance of $PM_{2.5}$ were moderately correlated with SO_2 at North Kensington but not at Marylebone Rd.

OC was moderately correlated with nitrogen oxides and CO at North Kensington (Tables 6.14 and 6.15) and Marylebone Rd. (Tables 6.12 and 6.13). Correlations of OC with O_3 were high at North Kensington ($r = -0.7$) but not at Marylebone Rd. ($r = -0.2$). Hourly OC but not daily averages were moderately correlated with 1,3-butadiene and BTEX at Marylebone Rd. ($r \approx 0.5$, Table 6.12, the only site with data available for both BTEX and OC).

6.1.4.2 Correlations between surrogates of BC, PM and PNC

Correlations between PNC and PM_{10} were very high ($r = 0.6-0.8$) at the most polluted sites: Hope St. (Tables 6.8, 6.9) and Marylebone Rd. (Tables 6.12 and 6.13), moderate at St. Enoch Sq. ($r \approx 0.5$, Tables 6.6 and 6.7) and low at North Kensington ($r < 0.3$, Tables 6.14 and 6.15). There were no PM_{10} data available for Montrose St.

Correlations of PNC with $PM_{2.5}$ (daily data available at Marylebone Rd. and North Kensington) showed similar correlation coefficients to those observed between PNC and PM_{10} (Tables 6.12 to 6.15).

In general, absorbance of $PM_{2.5}$ was the BC surrogate that showed the highest correlation coefficients with PNC, PM_{10} and $PM_{2.5}$. Correlations of BC surrogates vs.

PNC, PM_{10} and $PM_{2.5}$ were high at Marylebone Rd. ($r= 0.5-0.9$, Tables 6.12 and 6.13) and moderate to low at North Kensington ($r < 0.6$, Table 6.13). At St. Enoch Sq. and Hope St. absorbance of PM_{10} (the only BC surrogate for which there were data available) was not correlated with PNC.

At Marylebone, absorbance of $PM_{2.5}$ showed the highest correlation coefficients with PNC, PM_{10} and $PM_{2.5}$ ($r=0.5-0.9$) followed by EC ($r=0.5-0.6$) and BS ($r=0.3-0.7$). PNC showed higher correlation coefficients with BC surrogates ($r>0.7$, Table 6.13) than PM_{10} and $PM_{2.5}$ ($r<0.6$ for PM_{10} and $PM_{2.5}$ vs. EC and absorbance of $PM_{2.5}$; $r < 0.4$ for PM_{10} and $PM_{2.5}$ vs. BS, Table 6.13). Correlations at different averaging periods were only available for PNC and PM_{10} vs. EC. Both correlation coefficients were higher for hourly averaging periods than their daily counterparts.

At North Kensington, in contrast to results observed at Marylebone Rd. PNC was not correlated to EC and absorbance of $PM_{2.5}$ (Table 6.15). The correlation coefficient for absorbance of $PM_{2.5}$ vs. PM_{10} and $PM_{2.5}$ were similar than those for EC vs. PM_{10} and $PM_{2.5}$. $PM_{2.5}$ showed higher r-values with surrogates of BC ($r\approx 0.7$, Table 6.15) than PM_{10} ($r\approx 0.5$, Table 6.15). Correlations at different averaging periods were only available for PNC and PM_{10} vs. EC. Hourly averaged data showed slightly higher correlation coefficients than their daily counterparts.

At St. Enoch Sq., there was a small dataset available of simultaneous measurements of PNC and BS. NPL only installed a BS monitor in 2007. PNC data was plotted against BS for the period January to May 2007 (until the BCPC stopped functioning). The scatter plot is shown in Figure 6.3.

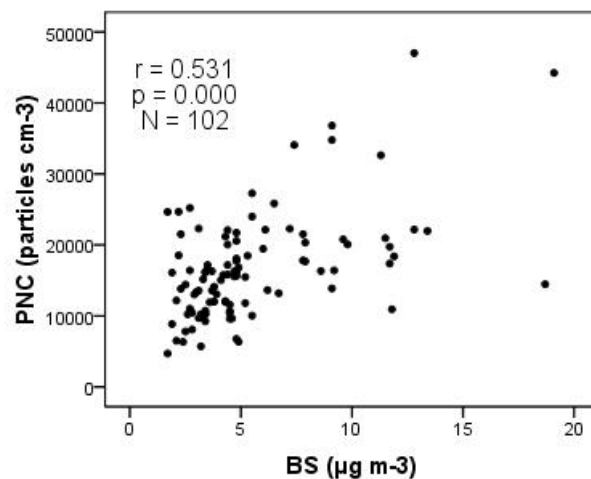


Figure 6.3 Scatter plot and Spearman correlation coefficient of daily averaged particle number concentration (PNC) against black smoke (BS) at St. Enoch Sq. (Data period: Jan-May 07).

The scatter plot of PNC vs. BS showed highly dispersed BS values above $10 \mu\text{g m}^{-3}$. The correlation coefficient was only moderate, although statistically significant (0.01 level, 2-tailed) due to the large dataset.

Regarding the correlations between BC surrogates, absorbance of $\text{PM}_{2.5}$, EC and BS all of them were highly correlated with each other. However, at North Kensington it was observed that the high correlation between EC and absorbance of $\text{PM}_{2.5}$ was driven by two high values (see scatters in Table 6.15). When these values were excluded from the dataset, the correlation coefficient dropped to 0.2.

6.1.4.3 Correlations between gaseous air pollutants

Nitrogen oxides were moderately to highly correlated with CO, 1,3-butadiene and BTEX at all sites and for both averaging periods ($r=0.6-0.9$, Tables 6.6 to 6.15), except for daily averaged nitrogen oxides vs. CO at Marylebone Rd. ($r < 0.3$, Table 6.13).

Correlations of SO_2 with nitrogen oxides, CO and BTEX were generally low and not statistically significant.

BTEX were highly correlated between each other. At Marylebone Rd. the correlation coefficients were very similar (Tables 6.12 and 6.13) whereas at Hope St. benzene

vs. toluene showed a higher r-value ($r=0.9$) than that observed for benzene vs. ethylbenzene and xylenes ($r=0.7$) (Table 6.6 and 6.7), suggesting a possible non-traffic related source for ethylbenzene and xylenes. r-values were similar for hourly and daily averaging periods.

6.1.4.4 Correlations between water-soluble metals and traffic-related air pollutants

At the Glasgow sites, metals vs. NO_x and metals vs. PNC exhibited generally higher correlation coefficients compared to metals vs. PM_{10} and metals vs. absorbance of PM_{10} filters. At St. Enoch Sq., Mn, Fe, Cu, As, Cd and Pb were highly correlated with NO_2 and NO_x ($r=0.6-0.7$), PNC ($r=0.7-0.8$), and absorbance of PM_{10} ($r=0.5-0.8$). Mn, Fe, Cu, As, Cd and Pb were also correlated with PM_{10} ($r = 0.5-0.75$) and Ni showed moderate correlation with PNC ($r=0.56$). Measurements of SO_2 and CO did not show correlation with any of the metal concentrations.

At Hope St. a rather different pattern of inter-pollutant correlations was observed. For example (unlike at St. Enoch Sq.) Fe, As, Cd, and Pb were not statistically significantly correlated with PNC. However, V, Cr, Mn, Cu, and Ni were statistically significantly correlated with PNC ($r=0.7-0.9$). Mn, Cu, As, Cd and Pb were not significantly correlated with NO_2 , in contrast to results observed at St. Enoch Sq. However, Ni was highly correlated with NO_2 and Fe showed a negative correlation with nitrogen oxides. Ni and Cu were highly correlated with PM_{10} ($r=0.6$ and $r=0.7$ respectively). None of the metals were correlated with absorbance of PM_{10} . Measurements of 1,3-butadiene and BTEX (available only at Hope St.) were highly correlated with Cu, PNC and NO_x .

At Marylebone Rd. (Table 6.13) most of the metals showed negative correlations with nitrogen oxides, PNC, absorbance of $\text{PM}_{2.5}$ and EC, though r-values were only statistically significant for Cu. Ni and V showed significant but low correlation with PM_{10} ($r\approx 0.4$), Mn and Fe with $\text{PM}_{2.5}$ ($r\approx 0.5$). Mn, Fe, Cu, Zn and Cd showed moderate correlations with OC ($r\approx 0.5-0.6$).

At North Kensington PNC did not show positive correlations with metal concentrations (Table 6.15). Mn, Fe, Cu, Zn, As, Cd and Pb were moderately to highly correlated with NO₂, ($r \approx 0.5-0.8$, except Mn); EC ($r \approx 0.5-0.7$); absorbance of PM_{2.5} ($r \approx 0.5-0.7$) and OC ($r \approx 0.5-0.6$, except Mn). All those metals apart from Cu were also moderately to highly correlated with PM_{2.5} ($r \approx 0.5-0.8$) and PM₁₀ ($r \approx 0.5$). SO₂ was moderately correlated with Mn, Fe, Cu, Zn ($r \approx 0.5$), and highly correlated with Cd ($r = 0.7$), though the correlation coefficient was driven by an outlier registered on the 3 November (probably due to the bonfires on Guy Fawkes night) which can be clearly observed in the scatters in Table 6.15. When this data point was removed from the data set the only metal that remained correlated with SO₂ was Cd. Measurements of CO showed correlation coefficients below 0.5 with metal concentrations.

6.1.5 Correlations between the increments in pollutant concentrations

This section shows the scatter plots, RMA relationship and regression coefficient of the daily increments in PNC and metals vs. increments in pollutant concentrations between Hope St. and St. Enoch Sq. in Glasgow and Marylebone Rd. and North Kensington in London (Tables 6.16, 6.17, 6.18 and 6.19). The increments refer to the concentration at the kerbside sites with the concentration at the background sites subtracted (i.e. Marylebone Rd. – North Kensington and Hope St. – St. Enoch Sq.).

RMA regression equations were calculated for the pollutants that had been considered in the aims of the project as possible surrogates for PNC and those that, although not considered, showed a high regression coefficient with PNC.

Table 6.16 Scatter plot, RMA relationship, and regression coefficient (R^2) of the increments in PNC vs. increments in co-pollutants. The increments refer to the daily concentrations at Hope St. with the daily concentrations at St. Enoch Sq. subtracted (8 Jun-31 Aug 2006).

Relationship	N	intercept	Lower	Upper	slope	Lower	Upper	R^2	
		(particles cm^{-3})	CI (95%)	CI (95%)	(particles $\text{cm}^{-3}/\mu\text{gm}^{-3}$)	CI (95%)	CI (95%)		
$\Delta\text{PNC vs. } \Delta\text{PM}_{10}$	10	-15,408	-24,916	-5,899	1273	767	1,780	0.702	
$\Delta\text{PNC vs. } \Delta\text{AbsPM}_{10}$	10	-10,980	-25,416	3,456	8657	2,426	14,889	0.026	
$\Delta\text{PNC vs. } \Delta\text{NO}_x$	14	7,408	5,262	9,554	42.3	30.9	53.7	0.787	
$\Delta\text{PNC vs. } \Delta\text{NO}_2$	14	6,880	3,733	10,027	155	97.1	213	0.590	
$\Delta\text{PNC vs. } \Delta\text{NO}$	14	7,751	5,975	9,527	87.0	66.9	107	0.843	
$\Delta\text{PNC vs. } \Delta\text{CO}$	19	1,881	-3,031	6,792	75842	45,232	106,452	0.305	

PNC: particle number concentration; AbsPM₁₀: absorbance of PM₁₀. $R^2 > 0.5$ in bold

Table 6.17 Scatter plot, RMA relationship, and regression coefficient (R^2) of the increments in PNC vs. increments in co-pollutants. The increments refer to the daily concentrations at Marylebone Rd. with the daily concentrations at North Kensington subtracted (selection of 26 days in 2006).

Relationship	N	intercept	Lower	Upper	slope	Lower	Upper	R^2	
		(particles cm^{-3})	CI (95%)	CI (95%)	(particles $\text{cm}^{-3}/\mu\text{gm}^{-3}$)	CI (95%)	CI (95%)		
$\Delta\text{PNC vs. } \Delta\text{PM}_{10}$	25	26,073	9,211	42,935	3,078	2,225	3,930	0.552	
$\Delta\text{PNC vs. } \Delta\text{PM}_{2.5}$	26	37,570	21,150	53,989	3,520	2,444	4,596	0.429	
$\Delta\text{PNC vs. } \Delta\text{AbsPM}_{2.5}$	26	-22,769	-46,142	604	21,533	16,877	26,188	0.715	
$\Delta\text{PNC vs. } \Delta\text{EC}$	26	37,570	21,150	53,989	3,520	2,444	4,596	0.429	
$\Delta\text{PNC vs. } \Delta\text{OC}$	26	74,419	59,879	88,959	8,153	4,720	11,587	0.715	
$\Delta\text{PNC vs. } \Delta\text{NO}_x$	26	732	-15,715	17,179	233	189	278	0.777	
$\Delta\text{PNC vs. } \Delta\text{NO}_2$	26	-12,534	-32,686	7,619	933	742	1,125	0.744	
$\Delta\text{PNC vs. } \Delta\text{NO}$	26	6,161	-9,726	22,047	469	377	561	0.765	
$\Delta\text{PNC vs. } \Delta\text{CO}$	26	652	-32,831	34,135	119,440	72,968	165,913	0.076	

PNC: particle number concentration; AbsPM_{2.5}: absorbance of PM_{2.5}; EC: elemental carbon; OC: organic carbon. $R^2 > 0.5$ in bold

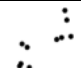
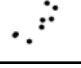

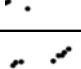
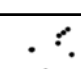


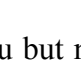
The increments in NO_x explained approximately 80 % of the variance ($R^2 \times 100$) in PNC at both paired sites. Absorbance of PM ($\text{PM}_{2.5}$ at the London sites and PM_{10} at the Glasgow sites) explained 70 % of the variance in PNC at London but was not associated with PNC in Glasgow. OC also explained 70 % of the variance in PNC at London, whereas EC explained only 43 % of the variation in PNC.

The greater slopes at London compared to Glasgow were partly caused by the underestimation of PNC at Hope St. in Glasgow. The RMA slope is calculated as the SD of PNC divided by the SD of the co-pollutant. Therefore, an underestimation of the SD of PNC results in a smaller slope.

Assuming NO_x originates exclusively in traffic, the intercepts of ΔPNC vs. ΔNO_x represent the concentration of non-traffic related PNC. The intercepts were much greater at Glasgow than at London. This difference was possibly caused by the underestimation of the slope at Hope St. explained above, since a smaller slope results in a greater intercept.

Table 6.18 shows the RMA relationships, regression coefficients, and scatter plots of the increments in Cu and Ni vs. increments in PNC and nitrogen oxides at Glasgow sites.

Table 6.18 Scatter plot, RMA relationship, and regression coefficient (R^2) of the increments in Cu and Ni vs. increments in PNC and nitrogen oxides. The increments refer to the daily concentrations at Hope St. with the daily concentrations at St. Enoch Sq. subtracted (8 Jun-31 Aug 2006).

Relationship	N	intercept (particles cm^{-3})	Lower CI (95%)	Upper CI (95%)	slope (particles $\text{cm}^{-3}/$ $\mu\text{g m}^{-3}$)	Lower CI (95%)	Upper CI (95%)	R^2	
$\Delta\text{Cu vs. } \Delta\text{PNC}$	11	3.63	1.54	5.72	4.0E-04	2.3E-04	2.3E-04	0.657	
$\Delta\text{Cu vs. } \Delta\text{NO}_x$	8	0.499	-2.95	3.95	0.037	0.018	0.056	0.650	
$\Delta\text{Cu vs. } \Delta\text{NO}_2$	8	0.739	-2.51	3.98	0.151	0.076	0.226	0.670	
$\Delta\text{Cu vs. } \Delta\text{NO}$	8	0.696	-2.95	4.34	0.072	0.032	0.112	0.587	
$\Delta\text{Ni vs. } \Delta\text{PNC}$	9	0.018	-0.25	0.29	5.3E-05	3.3E-05	7.4E-05	0.760	
$\Delta\text{Ni vs. } \Delta\text{NO}_x$	8	-2.33	-4.26	-0.40	0.014	0.003	0.024	0.187	
$\Delta\text{Ni vs. } \Delta\text{NO}_2$	8	-2.24	-3.74	-0.74	0.055	0.021	0.090	0.475	
$\Delta\text{Ni vs. } \Delta\text{NO}$	8	-2.26	-4.22	-0.29	0.026	0.005	0.048	0.110	

PNC: particle number concentration, $R^2 > 0.5$ in bold.

The increments in NO_x explained approximately 70 % of the variance in Cu but not in Ni. PNC explained approximately 70 % of the variance in Ni and 80 % of the variance in Cu. The R^2 values for the remaining metals and co-pollutants were below 0.4 and are not shown.

The slope of $\Delta\text{metal vs. } \Delta\text{NO}_x$ was larger for Cu than for Ni, suggesting that vehicle exhaust contributes more to Cu than Ni concentrations.

Table 6.19 shows the RMA relationships, regression coefficients and scatter plots of the increments in Mn, Fe and Cu vs. increments in PNC and nitrogen oxides at the London sites.

Table 6.19 Scatter plot, RMA relationship, and regression coefficient (R^2) of the increments in Mn, Fe and Cu vs. increments in OC. The increments refer to the daily concentrations at Marylebone Rd. with the daily concentrations at North Kensington subtracted (selection of 26 days in 2006).

Relationship	N	intercept	Lower	Upper	slope	Lower	Upper	R^2	
		(particles cm ⁻³)	CI (95%)	CI (95%)	(particles cm ⁻³ / μg m ⁻³)	CI (95%)	CI (95%)		
ΔMn vs. ΔOC	22	0.77	-5.75	-1.85	0.08	17.2	8.93	0.508	
ΔFe vs. ΔOC	18	-5.68	-2.85	0.09	1.55	0.44	0.83	0.511	
ΔCu vs. ΔOC	23	0.27	-2.30	0.17	0.53	1.37	2.39	0.609	

OC: organic carbon. $R^2 > 0.5$ in bold.

At the paired sites in London OC was the only pollutant that showed a regression coefficient with the increments in metals above 0.5. However, the correlations were driven by three data points (see scatters in Table 6.18). When this data was removed from the dataset, the regression coefficients were < 0.3 .

6.1.6 Variation of traffic-related air pollutants with wind speed and direction

The correlation coefficient between wind speed and traffic-related air pollutants at each monitoring site for hourly and daily averaged data is shown in the correlation matrix in Tables 6.5 to 6.14. The correlations were higher for daily averaged data than for their hourly counterparts.

The wind flows created between buildings and streets dominate pollutant dispersion and can create significant spatial differences in pollutant concentrations, which depend on the wind direction (Scaperdas and Colvile, 1999). This is especially important within street canyons where localised wind flows are created, blowing pollutants against or away from the monitoring station.

Figures 6.4 and 6.5 show the wind rose diagrams for daily averaged wind speed at Bishopton (Glasgow) and Heathrow Airport (London). The length of the bars indicates the frequency intervals and the colour indicates the wind speed.

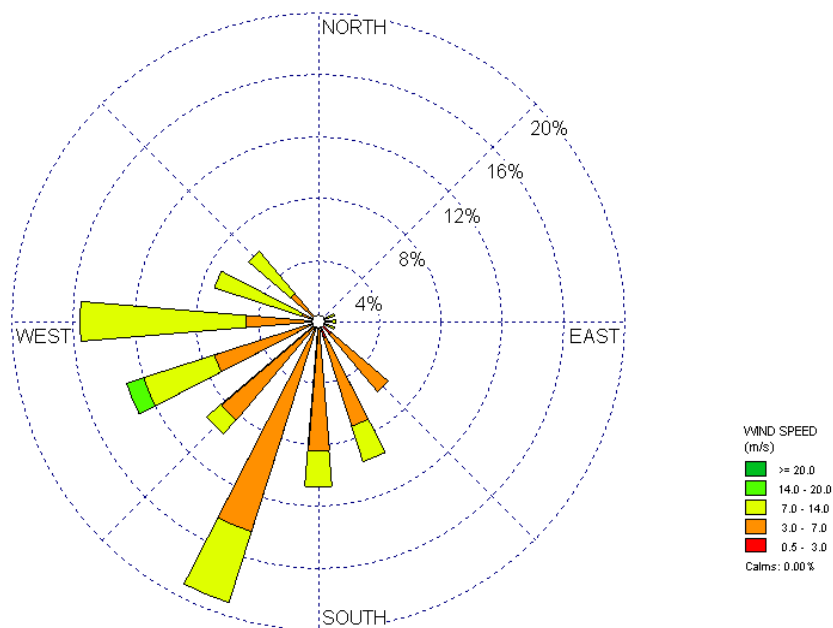


Figure 6.4 Daily wind rose at Bishopton (Glasgow) (8 Jun- 31 Aug 2006).

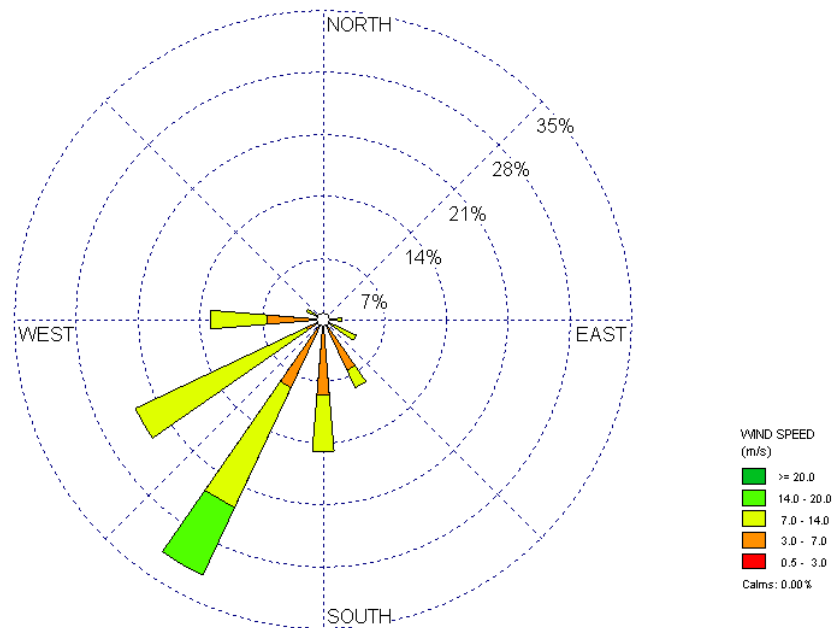


Figure 6.5 Daily wind rose at Heathrow Airport (London) (selection of 26 days in 2006).

In both cities, the prevailing wind direction was SW. In London, a higher frequency was observed from the direction 225-270°, whereas in Glasgow westerly winds were more frequent. Wind speeds were mostly between 3-7 m s⁻¹ in Glasgow (Figure 6.5) and between 7-14 m s⁻¹ in London (Figure 6.6).

The relative position of the monitoring stations located within street canyons is important to assess the airflow patterns within the canyon. At Hope St. the prevailing wind direction was partly perpendicular (W) and partly parallel (S) to the street; at Montrose St. westerly winds were oblique to the street and southerly winds perpendicular to the street and at Marylebone Rd. westerly winds were parallel to the street and SW winds were oblique to the street (Figure 6.6).

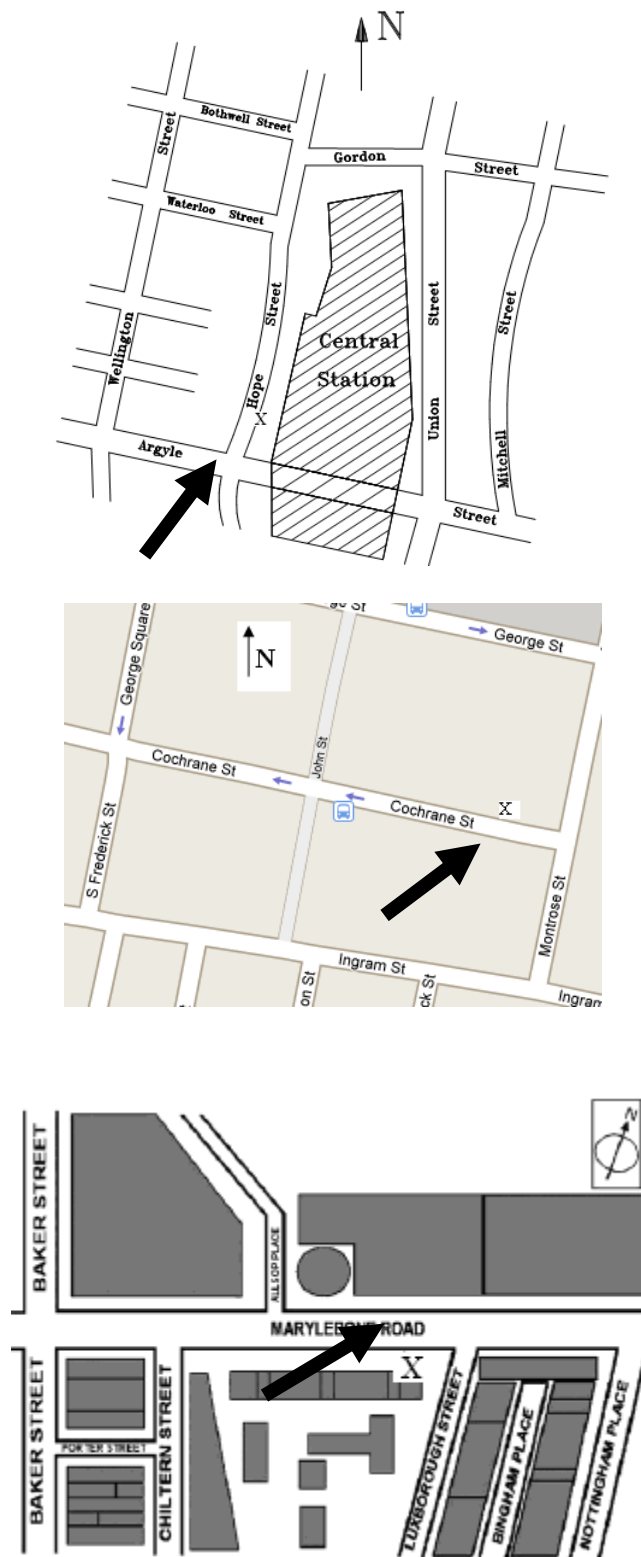


Figure 6.6 Schematic representation of the street canyon at Hope St (top, modified from Crowther, 2002) Montrose St. (centre, Google earth); and Marylebone Rd (bottom, modified from Vardoulakis et al. (2007)). X location of sampling site. The arrow indicates the prevailing wind direction.

At the background sites, St. Enoch Sq. and North Kensington, an increase in wind speed resulted in a decrease in all pollutant concentrations, with the exception of PNC at North Kensington, which were not affected by wind speed.

At the street canyon sites, daily pollutant concentrations behave differently with increasing wind speed. High wind speed resulted in an increase in PNC and nitrogen oxides (PNC and nitrogen oxides vs. wind speed $r \approx 0.4$) at Marylebone Rd. (Table 6.13), but decrease at Hope St. (PNC and nitrogen oxides vs. wind speed, $r \approx -0.5$, Table 6.9) and Montrose St. (PNC vs. wind speed, $r = -0.4$ and nitrogen oxides vs. wind speed $r = -0.2$ to -0.4 , Table 6.11). PM_{10} and $PM_{2.5}$ were unaffected by wind speed at Marylebone Rd. (PM_{10} and $PM_{2.5}$ vs. wind speed, $r = 0.0$ and -0.2 respectively, Table 6.13), but PM_{10} showed a negative association (although not significant) with wind speed at Hope St. (PM_{10} vs. wind speed, $r = -0.4$, Table 6.9). The concentrations of water-soluble metals decreased with increasing wind speed at both sites (r-values were generally between -0.4 and -0.8).

To further understand the effect of wind speed on the pollutant concentrations the correlations between the increments in concentrations (which correspond to the on-road emissions at the street canyons, since the background concentration has been subtracted), against wind speed were examined. At Marylebone Rd. concentrations of all measured pollutants except CO , O_3 , V and As showed positive correlations with increasing wind speed. In contrast, at Hope St. all pollutants showed a decrease in concentration with increasing wind speed.

6.2 DISCUSSION

6.2.1 Spatial Variability of Air Pollutants

Direct comparisons between the concentrations at London and Glasgow have to be made with caution because sampling periods and sample sizes were different in the two cities. In addition, the monitoring periods were relatively short and cannot be considered to be representative of the annual trend.

Concentrations of particles and gaseous pollutants were much higher at the kerbside sites (Hope St. and Marylebone Rd.) than at the background sites (North Kensington, St. Enoch Sq. and Montrose St.) because of the major impact of nearby traffic at the former sites. The large influence of traffic emissions at the kerbside sites was also revealed in the higher diurnal variability in pollutant concentrations observed at Hope St. and Marylebone Rd. compared to St. Enoch Sq., Montrose St. and North Kensington (Figure 6.1).

The following paragraphs discuss in detail the concentrations for each pollutant found at the different sites.

Median NO₂ concentrations exceeded the 24-hours annual UK threshold value (40 µg m⁻³) at Marylebone Rd. and Hope St. The corresponding background sites (North Kensington for Marylebone Rd. and St. Enoch Sq. for Hope St.) showed much lower concentrations with a daily median difference in concentration between paired sites of 24 µg m⁻³ in Glasgow and 103 µg m⁻³ in London.

Median NO₂ concentrations at Montrose St. were higher than those observed at St. Enoch Sq., despite the fact that the monitoring inlet at Montrose St. was located 20 m above the ground. However, since the buildings at Montrose St. form a street canyon, pollutants are likely to have been re-circulated leading to an increase in concentrations. This result highlights the importance of local street topography to air pollutant concentrations. Interestingly, PNC were similar at both the Montrose St. and St. Enoch Sq. sites. It could be thought that the higher concentrations of nitrogen oxides but not PNC at Montrose St. compared to St. Enoch Sq. could be the result of

the underestimation of particles by the WCPC located at Montrose St. However, from the inter-comparison study between the WCPC and BCPC at St. Enoch Sq. it was found that underestimation of particles happened above 30,000 particle cm^{-3} and at Montrose St. concentrations did not reach 20,000 particle cm^{-3} . This result seems to indicate that the increase in pollutant concentrations due to the re-circulation of air within the canyon was more important than the vertical dilution, for nitrogen oxides but not for PNC. PNC during transport upwards from the street level may have undergone coagulation and condensation processes resulting in a shift of the diameters to larger values leading to a decrease in the numbers (Hussein et al., 2005).

NO_2 concentrations at the kerbside sites in this study were higher than those reported at other urban traffic sites. For example higher than those reported by Lewné et al. (2004) in Germany (annual mean 33 $\mu\text{g m}^{-3}$), Netherlands (annual mean 34 $\mu\text{g m}^{-3}$) and Sweden (annual mean 30 $\mu\text{g m}^{-3}$). However, NO_2 concentrations at North Kensington and St. and Enoch Sq. were similar to those reported by Lewné et al. (2004) in Germany, Netherlands, and Sweden at sites with similar characteristics. It should be noted that these comparisons are a rough estimate as the year of monitoring in Lewné and this study were different.

The kerbside Marylebone Rd. showed higher PNC than those observed at other UK and EU sites. PNC concentrations at the kerbside in Glasgow (Hope St.) tended to be lower than in other cities. For example, mean PNC at Marylebone Rd. were higher than those reported by Longley et al. (2005) in a street canyon in Manchester (27,000 particles cm^{-3}) and Harrison et al. (1999) at a kerbside site in Birmingham (96,000 particles cm^{-3}). The lower PNC observed at Hope St. compared to Manchester and Birmingham could be partly because of the underestimation of PNC by the WCPC. In addition, the above comparison should be interpreted with care as the monitoring periods were different for each study.

Mean PNC at the urban background site at North Kensington were similar to those reported in other urban background sites in Alkmaar (25,800 particles cm^{-3}), Erfurt (25,900 particles cm^{-3}), Helsinki (20,300 particles cm^{-3}) (Ruuskanen et al., 2001) and Birmingham (23,000 particles cm^{-3}) (Shi et al., 1999) and lower than in Helsinki,

Athens and Amsterdam (PNC ranged from 13,000 to 20,000 particles cm^{-3}) (Puustinen et al., 2007).

Mean PNC at the urban centre St. Enoch Sq. were lower than those reported at other UK sites. For example, median concentrations (for the same period as the study in Glasgow) at an urban centre at Manchester Piccadilly were 23,068 particles cm^{-3} and at another urban centre in Birmingham Centre were 17,629 particles cm^{-3} . The urban centre sites in Belfast and Port Talbot showed similar concentrations to those found in St. Enoch Sq. (13,829 and 13,214 particles cm^{-3} , respectively) (data obtained from the NAQA).

The large difference in PNC between the background sites (St. Enoch Sq. and North Kensington) compared to the kerbside sites (Hope St. and Marylebone Rd.) was in line with results reported by other studies. Puustinen et al. (2007) found twice the PNC at sites heavily influenced by traffic than at urban centres, in Amsterdam and Birmingham. Aalto et al. (2006) found PNC between 2 to 6 times higher at traffic sites than at urban background sites, in Stockholm, Rome and Barcelona.

PM_{10} and $\text{PM}_{2.5}$ averaged over 2006 exceeded the annual UK threshold value (50 $\mu\text{g m}^{-3}$ and 25 $\mu\text{g m}^{-3}$ for PM_{10} and $\text{PM}_{2.5}$, respectively) at Marylebone Rd. PM_{10} concentrations at St. Enoch Sq. and PM_{10} and $\text{PM}_{2.5}$ concentrations at North Kensington were higher than those reported at sites with similar characteristics in Helsinki (12.0 and 8.0 $\mu\text{g m}^{-3}$), Amsterdam (29.9 and 17.6 $\mu\text{g m}^{-3}$), Athens (46.0 and 20.6 $\mu\text{g m}^{-3}$), and Birmingham (17.2 and 10.2 $\mu\text{g m}^{-3}$) for PM_{10} and $\text{PM}_{2.5}$ respectively (Puustinen et al., 2007).

The similar variability of PM_{10} and $\text{PM}_{2.5}$ (Partisol measurements, see IQR data in Table 6.2) suggest that both pollutants are affected by similar sources and dispersion is also similar. Interestingly, this variability was similar at both London sites, Marylebone Rd. and North Kensington, despite Marylebone Rd. being much more influenced by traffic emissions, suggesting that over the entire day both sites undergo similar variations in PM_{10} and $\text{PM}_{2.5}$ concentrations.

The higher PM₁₀ concentrations collected with the TEOM analyser compared to the Partisol sampler at Marylebone Rd. may have been due to the inaccuracy of using the UK correction factor for PM₁₀ (1.3) and have been discussed in detail in Chapter 5.

The higher spatial contrast for PNC and NO₂ compared to PM₁₀ between the kerbside sites and background sites (Table 6.2) indicates that vehicle emissions mostly contribute to PNC and NO₂ and to a lesser extent to PM₁₀. Similar differences in concentrations between kerbside and background sites have been observed at other paired sites in Copenhagen by Kezel et al. (2003) (ratios were between 3.1 and 5.7 for PNC, 5.7 and 8.7 for NO_x and 2.9 for PM₁₀) and Stockholm by Johansson et al. (2007) (ratios of 5.6 for PNC, 4.6 and 8.2 for NO_x and 2.0 and 2.5 for PM₁₀). Therefore, results from this and other studies suggest that particle mass does not reflect sufficiently the spatial variability in traffic-related air pollution. PNC and /or NO₂ appear more appropriate to assess the spatial variability of traffic-related air pollutants. Bearing in mind the more serious health impact of particle numbers compared to PM₁₀ these results have serious implications for air pollution policies, since air quality management addresses PM₁₀ but there is no threshold value for particle numbers.

The higher EC concentrations at Marylebone Rd. compared to North Kensington highlight the high contribution of traffic to EC. However, concentrations of OC were similar at both sites, suggesting a regional background concentration of secondary organic aerosol. These results are in line with previous data from 2002-2004 at the same sites (Jones and Harrison, 2005).

The absorption coefficient of PM₁₀ and PM_{2.5} (Table 6.1), which has been shown to be a good surrogate for BC/soot (Cyrus et al., 2003b; Brunekreef et al., 2005) was higher than those reported by Götschi et al. (2005) in a study of 21 EU cities (annual means of absorption coefficient of PM_{2.5} ranged from 1.4 to 4.3 × 10⁻⁵ m⁻¹) and those reported by Puustinen et al. (2007) at urban sites in Helsinki (1.3 × 10⁻⁵ m⁻¹), Athens (3.5 × 10⁻⁵ m⁻¹), Amsterdam (3.5 × 10⁻⁵ m⁻¹) and Birmingham (1.3 × 10⁻⁵ m⁻¹).

The higher SO₂ concentration and variability at Marylebone Rd. compared to that found at North Kensington (Table 6.1) reflects the contribution of traffic to this pollutant. Nevertheless, concentrations were lower than the UK 24-hours threshold value (125 µg m⁻³). Similarly, CO concentrations were well below the UK 8-hours threshold value (10 mg m⁻³).

The lower concentrations of O₃ at Marylebone Rd. compared to North Kensington reflect the depletion of O₃ by reaction with the continually emitted NO to form NO₂.

Benzene and 1,3-butadiene concentrations at Hope St. and Marylebone Rd. (Table 6.1) were lower than the UK annual threshold values (5.00 µg m⁻³ and 2.25 µg m⁻³ respectively). The ratio toluene: benzene was very similar at both sites (4.19 at Hope St. and 4.14 at Marylebone Rd.), suggesting that no other sources apart from traffic contribute to toluene concentrations at both sites. The toluene: benzene ratio was higher than those observed at background sites in Toulouse (2.9-3.7) (Simon et al., 2004), which confirms observations by Gelencser et al. (1997) that the toluene: benzene ratio decreases as the distance from the pollution source increases.

Compared to other locations worldwide, benzene concentrations in Glasgow (0.563 µg m⁻³ at Hope St.) were lower than those reported in other similar locations. However, in London concentrations were higher (2.35 µg m⁻³ at Marylebone Rd.) than those found in other locations. Beckerman et al. (2008) reported benzene concentration of 0.7 and 0.9 µg m⁻³, near an expressway in Canada as measured with passive samplers.

A metal enrichment at the kerbside compared to background site St. Enoch Sq. was observed in Glasgow, reflecting the contribution of traffic to metal concentrations. The fact that this trend was not observed at the London sites, where concentrations of V, Pb, As and Ni at North Kensington were higher than at Marylebone Rd. could be the result of a local contribution of metals in water-soluble form at North Kensington. These emissions could originate from a Ni refinery located 3.2 km NW from North Kensington (data retrieved from the UK Environment Agency). It could

be that on the timescale in which the air parcel reaches Marylebone Rd., these metals are oxidised and therefore insoluble in water.

Although direct comparison between concentrations at Glasgow and London cannot be made because metals at Glasgow were in the PM₁₀ fraction whereas at London metals were in the PM_{2.5} fraction, it was interesting to note that the concentrations at the Glasgow sites were greater than those at the London sites, especially for Fe and Cu. This is probably because these two metals dominate in the PM₁₀ fraction. A study in Edinburgh also found much higher concentrations of soluble Fe and Cu in PM₁₀ than in PM_{2.5} (Table 6.1) compared to other metals (Hibbs, 2002). Comparisons with other urban sites were limited because of the limited literature on the analysis of water-soluble metals in PM from urban environments. Instead, most of the reviewed studies focused on total metal content.

6.2.2 Diurnal pattern of traffic-related air pollutants in Glasgow

The diurnal pattern of PM₁₀, PNC, NO₂, CO and SO₂ on weekdays was typical of anthropogenic sources, with peaks matching the morning and late afternoon rush hours. Similar patterns have been observed in other cities (Cyrus et al., 2003a; Harrison and Jones, 2005).

Over the weekend, the profiles were less defined, probably as a result of traffic flows being lower and more evenly distributed through the day compared to weekdays, in turn making pollutant concentrations more dominated by meteorological factors than by traffic flows (Ketzler et. al., 2003). Besides this, the weekend profiles were based on a smaller dataset. The reduction of traffic on Sundays allows the investigation of how much pollutant concentrations are reduced, assuming the effects of meteorology and long-range transport of pollutants do not vary between weekdays and weekends.

NO₂ is considered a good tracer for traffic activity (Harrison et al., 2003b). Therefore, the larger reduction in NO₂ over the weekend compared to weekdays, at St. Enoch Sq. (44 %), suggests a larger reduction of traffic at this site, compared to Hope St. (22 %). Then, one could also expect a higher reduction in PNC and PM₁₀ at

St. Enoch Sq. compared to Hope St. However, the reduction in PM_{10} over the weekend was larger at Hope St. (31%) than at St. Enoch Sq. (25 %) and PNC showed similar reductions at both sites (18%). Regarding the magnitude of the decrease of each pollutant at each site over the weekend, at Hope St. PM_{10} showed a larger decrease than NO_2 , while at St. Enoch Sq. the opposite trend was observed. PNC showed a smaller decrease than PM_{10} and NO_2 at both sites.

The greater reduction of PM_{10} at Hope St. can be explained by the fact that a higher proportion of PM_{10} at this site originates from traffic, compared to St. Enoch Sq. St. Enoch Sq. is located further away from the roadside, thus with a smaller traffic influence compared to Hope St. Therefore, a larger proportion of PM_{10} comes from regional background aerosols, whose concentrations change less from weekdays to weekends, assuming steady weather conditions.

The similar decrease of PNC at both sites is attributed to the fact that PNC do not depend only on primary emissions but also on particle formation processes: nucleation of particles by condensation of pre-existing vapours and condensation of vapours into existing particles (Kulmala et al., 2004). These particle formation processes have been observed in periods of low primary emissions and high temperature (Stainer et al., 2004), in both rural and urban areas (Wichmann et al., 2000; Laakso et al., 2003; Kulmala et al., 2004; Rodríguez et al., 2007). Therefore, although traffic emissions were reduced at both sites during the weekend, particles can still be formed in the atmosphere.

In summary, although traffic contributed more to NO_2 than to PNC and PM_{10} , a short-term reduction in traffic resulted in a larger decrease of PM_{10} than NO_2 at the kerbside Hope St. In contrast, at the urban centre St. Enoch Sq. the reduction in NO_2 was larger than that for PM_{10} . This is due to the larger contribution of background PM_{10} at St. Enoch Sq. compared to Hope St., where a higher fraction of PM_{10} are traffic-related.

6.2.3 Correlations of the same pollutant measured at different sites.

Low to moderate correlation coefficients of a single pollutant between sites suggest their emission sources are localised and pollutants are not homogeneously dispersed. The between site correlation coefficients for PM₁₀ were higher than for PNC in Glasgow but not in London (Table 6.4). This could be the result of a relatively higher contribution to PM₁₀ from regionally transported aerosols in Glasgow. In contrast, in London because of the higher traffic flows compared to Glasgow a larger fraction of PM₁₀ may originate from local traffic resulting in a higher contribution of ultrafine particles to PM₁₀. This results in a more similar distribution for PM₁₀ and PNC in London than that observed in Glasgow. Thus, the spatial variability of particles may be different for each city and conclusions may not be applicable between different locations. Therefore, it seems reasonable that each city should conduct a study on the spatial variability of the pollutants addressed to avoid exposure misclassification (Wilson et al., 2005).

The higher correlation coefficients between nitrogen oxides at the paired site Montrose St. and St. Enoch Sq. compared to the other paired sites in Glasgow (Table 6.4) was attributed to the more similar traffic characteristics at these two sites compared to Hope St. Hope St. is subject to congestion and the traffic is characterised as having a stop-start traffic flow. Therefore, it is continuously affected by fresh emissions. It could be argued that the larger dataset at the paired site St. Enoch Sq. and Montrose St. (n=1967) compared to the other paired sites (n=1552) resulted in higher r-values. However, correlations with data collected on the same days as at the paired sites Hope St. vs. Montrose and Hope St. vs. St. Enoch Sq. showed similar r-values. Interestingly, CO showed a higher correlation coefficient between Montrose St. and Hope St. than between Montrose St. and St. Enoch Sq. This could be the result of the “trapping effect” of pollutant concentrations at street canyons and the long life time of CO (90 days, Crowther, 2002), which may result in a more similar dispersion pattern for this pollutant at Montrose St. and Hope St. than at St. Enoch Sq.

In London, the low correlations for nitrogen oxides between paired sites (Table 6.4) reflect the different traffic flows at both sites, and suggest that meteorological conditions do not disperse nitrogen oxides homogeneously over the city.

The lack of correlation of the absorbance of PM₁₀ between paired sites is thought to be the result of the different factors affecting the absorption properties of particles. A higher correlation coefficient was expected, since the material with the highest absorption properties, BC, forms the core of accumulation mode particles from combustion sources (Kittelson et al., 1998), which can travel long distances (Puustinen et al., 2007) and therefore are expected to be correlated between sites. However, the magnitude of the reflectance depends not only on the BC content. It is strongly influenced by the size of the particles (decreasing for larger sizes) and the degree of dilution of absorbing and non-absorbing transparent particles (Horvath, 1986). The light absorption of BC increases considerably when it is included in a large transparent particle, due to the lower density (Horvath, 1986). Particle size distribution changes in time and space: size distributions during rush hours are expected to differ from those observed at periods with lower emissions, since as particles travel away from their emission source they shift to larger sizes (Ketzler et al., 2003; Gidhagen et al., 2005), changing their optical properties. Therefore, it is not surprising that the mix of particles with absorption properties is not homogeneous at the three sites, resulting in the low observed correlations. This assumption is partly confirmed by the fact that EC (the measurement of which is not influenced by particle size and non-absorbing particles) did show a positive correlation between Marylebone Rd. and North Kensington ($r=0.36$). A further discussion on the properties affecting the absorption properties is included in section 6.2.2.

In general, hourly averaging time resulted in higher correlation coefficients than their daily counterparts for all pollutants that were measured at both timescales, suggesting correlations are driven by the peaks and troughs in pollutant concentrations during rush hours, rather than by the dispersing effect of meteorology over a 24 hour period. If the force driving the correlations was the effect of

meteorology, then correlations with daily averages would be higher than their hourly counterparts, since the homogenising effects of meteorology is more notable over a entire day rather than on an hourly basis.

The moderate correlation found for nitrogen oxides, PM₁₀ (in London) and PNC and surrogates of BC (EC and absorbance of PM) across sites indicates that a single monitoring site would not represent the temporal variation of these pollutants.

Ketzel et al. (2003) reported similar correlation coefficients to those found in this work for NO_x and PM₁₀ between urban background (20 m above the ground in an urban centre) and city-background (30 km away from urban centre) sites in Copenhagen. r-values were 0.61, 0.76 for half-hour measurements of NO_x, and PM₁₀. Moraska et al. (2002) found PM₁₀ and NO_x moderate to highly correlated between background sites in Brisbane (r=0.4-0.68 for PM₁₀ and 0.31-0.77 for NO_x). The correlation coefficients were lower between sites with higher concentrations as a result of local sources not varying similarly across sites. High correlation coefficients between PM₁₀ at urban and suburban sites have also been reported by Grivas et al. (2007) in Athens. r-values ranged from 0.55 to 0.85, with higher r-values for sites with similar traffic characteristics.

Several studies in Europe have reported higher between-site correlation coefficients for PNC than those observed in this study. Buzorious et al. (1999) reported correlation coefficients between 0.58-0.94 for 24-hours PNC between sites of similar traffic characteristics in Helsinki. Ketzel et al. (2003) reported 24-hours r-values of 0.58 between street and roof-level sites in Copenhagen. Aalto et al. (2005) found 24-hours correlation coefficient of 0.67, 0.69 and 0.84 between background and traffic sites in Rome, Stockholm and Barcelona respectively. Puustinen et al. (2007) reported r-values for 24-hours averages of PNC of 0.67-0.76 between urban background sites and high and low traffic sites in a study in Amsterdam, Athens, Birmingham and Helsinki from 2002 to 2004. r-values for hourly averages were lower (0.56-0.66). In a study in Augsburg, Cyrus et al. (2008) found correlation coefficients between 24-hours averages of up to 0.8 between urban background sites in winter and summer.

However, in California, Sardar et al. (2004) found high correlations ($r= 0.7$) between 24-hours PNC measured at receptor sites, only in summer. The dataset for the entire year (2002) resulted in an r -value of 0.3.

The difference in the strength of the between-site correlation coefficient for PNC could be the result of different meteorological factors affecting the formation and dispersion of PNC. Interestingly, most of the studies mentioned above showed higher correlation coefficients with daily averaged data than with hourly averaging periods, in contrast to the results observed in this study. High correlation between daily averaged data reflects the homogenising effect of meteorology (Sardar et al., 2004). Whereas high correlation between hourly averaged data reflects the diurnal variation of air pollutants, which is driven by the traffic flows. In addition, the occurrence of particle formation events may contribute to a higher correlation coefficient between daily averaged data than between hourly averaged data (Sardar et al., 2004).

Regarding the correlation of metals at paired sites, the high degree of correlation of V and As in London and Glasgow suggests a possible regional component from industrial combustion sources. V is a surrogate for oil combustion (Divita et al., 1996) and As is associated with coal combustion and smelters (Pinto et al., 1998). The lack of correlation of Cr, Ni and Pb between paired sites in Glasgow could be the result of the higher uncertainty on the calculation of the concentrations of these metals, as their values were close to their respective LODs. The lower correlation coefficients for the rest of the metals in London and Glasgow suggest that concentrations of these metals were influenced by local sources at each site, rather than traffic, whose emissions did not vary in a similar way. Studies on spatial correlation between metal concentrations in urban areas were not identified in the literature reviewed and therefore comparisons are not presented.

6.2.4 Correlation between different pollutants measured at the same site

The high correlation between PNC, PM₁₀, nitrogen oxides, CO and BTEX reflects their common source in traffic. Nitrogen oxides showed the highest correlation

coefficients with PNC at all sites and both averaging periods (Tables 6.6 to 6.15) and therefore they would be the best surrogate to represent PNC.

In general, most of the pollutant pair combinations showed higher correlation coefficients at the kerbside sites: Marylebone Rd. (Tables 6.13 and 6.14) and Hope St. (Tables 6.6 and 6.7) compared to the less polluted sites: St. Enoch Sq. (Tables 6.8 and 6.9), Montrose St. (Tables 6.10 and 6.11) and North Kensington (Tables 6.14 and 6.15). This suggests that as the distance from the emission source increases and pollutants undergo physical and chemical transformations and dilution with background air, between-pollutant correlations become weaker.

The following sections discuss in detail the different correlation patterns observed between traffic-related air pollutants among the different monitoring sites.

6.2.4.1 Correlations between particle characteristics and gaseous pollutants

PNC, PM₁₀ and PM_{2.5} vs. nitrogen oxides

NO_x can be considered as a tracer of traffic activity and therefore pollutants highly correlated with NO_x can be considered to originate mostly from traffic exhaust (Harrison et al., 2003b). In this study, PNC vs. NO_x showed a higher degree of correlation across the different studied sites than PM₁₀ and PM_{2.5} vs. NO_x. This suggests PNC come mostly from traffic exhaust at all sites, whereas additional sources contribute to PM₁₀ and PM_{2.5} and lower the strength of the correlation with NO_x. The high correlation between PNC and nitrogen oxides also implies that both pollutants undergo similar dispersion processes.

The higher correlation coefficients between PM₁₀ vs. NO_x at the kerbside sites: Marylebone Rd. (Tables 6.12 and 6.13) and Hope St. (Tables 6.6 and 6.7) compared to their corresponding background sites: North Kensington and St. Enoch Sq., suggests a higher contribution of combustion particles to PM₁₀ at the kerbside site and possibly a regional contribution to PM₁₀ at the background sites, resulting in a lower degree of correlation with NO_x. This result is in line with the previous finding

of a higher reduction in PM_{10} at kerbside sites compared to background sites with a reduction in traffic flows (section 6.1.1).

These results imply that the composition of PM_{10} is not homogenous across the city, with a higher proportion of traffic-related particles at kerbside sites compared to background sites. Thus, PM_{10} do not fully represent exposure to traffic-related air pollutants and both particle mass and particle number should be considered in epidemiological studies.

The high temporal correlation between PNC and NO_x at sites representative of population exposure: St. Enoch Sq. (Tables 6.8 and 6.9) and North Kensington, (Tables 6.14 and 6.15) implies that short-term health studies based on time series analysis may not be able to distinguish between the health effects of these pollutants.

The lower correlation coefficient at Hope St. for hourly PNC vs. nitrogen oxides and CO compared to their daily counterparts was attributed to the underestimation of PNC by the WCPC located at Hope St. The peaks in nitrogen oxides were not followed by a proportional increase in the number of particles, resulting in a lower correlation coefficient than expected. This trend was clearly observed in the scatter plots of hourly PNC vs. NO_x and NO (Table 6.6) where a change in the shape of the scatter plots is observed at high PNC. The slope dropped, indicating a smaller increase in PNC relative to the increases in NO_x . This effect was less noticeable for daily averaged data because when hours are averaged over a day the peaks in concentration are smoothed (it should be noted that the underestimation was larger at rush hours where PNC were higher) and thus the overall underestimation was smaller than that observed for the hourly data for high concentrations. Therefore, at Hope St. correlation coefficients of PNC vs. co-pollutants were underestimated.

The correlations found in this study are in line with results reported in previous studies where higher correlations have been found between PNC and NO_x than between PNC and PM_{10} Cyrys et al. (2003a), Ketznel et al. (2004) and Harrison and Jones (2005).

The correlation coefficients observed for PNC and nitrogen oxides found in this study were higher than those reported by Moraska et al. (1998), PNC vs. NO_x , $r=0.45$, for 4 hours averaging period, in a background site in Brisbane and Cyrus et al. (2003a), hourly PNC vs. NO_2 $r=0.55$ (pooled data from two urban centres in Erfurt). Correlation coefficients were comparable to those observed by Penttinen et al. (2001), daily PNC vs. NO_x $r=0.81$, at a traffic site in Helsinki; Noble et al., (2003), hourly PNC vs. NO_x , $r=0.81$, at two traffic sites in Texas, and Paatero et al. (2005) where daily PNC vs. NO_2 showed r -values ranging from 0.33 to 0.67 in 5 European cities (Augsburg, Barcelona, Helsinki, Rome and Stockholm). Correlation coefficients found in this work and most of the reviewed literature were lower than those reported by Ketzler et al. (2004), where $r=0.93$ for hourly PNC ($0.01\text{-}0.7\ \mu\text{m}$) vs. NO_x in a street canyon. The higher r -value reported in Ketzler et al.'s study was possibly influenced by the fact that the size fraction of particle number considered corresponded only to ultrafine particles, which are primary emitted particles from the combustion of fuel as NO_x . Total PNC ($\text{AED} < 3\ \mu\text{m}$) also include particles from secondary formation processes.

Harrison and Jones (2005) examined correlations between hourly PNC vs. NO_x and PM_{10} at 5 UK sites including St. Enoch Sq., North Kensington and Marylebone Rd. Data were averaged from 2000 to 2003 for the analysis at North Kensington and Marylebone Rd. and from 2001 to 2003 at St. Enoch. The r -values of PNC vs. NO_x (calculated from the regression coefficients reported in Harrison and Jones's paper), were lower than those observed in this study at North Kensington ($r=0.16$) and comparable to those obtained at St. Enoch Sq. ($r=0.55$) and Marylebone Rd. ($r=0.79$). It should be noted that in this study, Spearman correlation coefficients (non-parametric methods) were used for the correlation analysis whereas in Harrison and Jones's study Pearson coefficients (parametric methods) were used. In general, air pollution data is not normally distributed and therefore non-parametric methods are used.

Harrison and Jones (2005) examined the influence of wind direction on the correlations and report lower correlations with south-westerly winds at North

Kensington, since this direction was associated with higher wind speeds favouring pollutant dispersion. In this study, south-westerly winds were also the prevailing wind direction, as is usually the case in the UK. Unfortunately, the limited dataset in this study did not allow for the stratification of correlation coefficients according to wind direction. The higher correlations observed in this study at North Kensington, could be a result of lower wind speeds during the monitoring period compared to Harrison and Jones' study (averaged data from 2000-2003). Another possible reason could be the presence of a higher amount of long range transported accumulation particles in Harrison and Jones' study, leading to a lower correlation of PNC with NO_x . The study presented here confirms Harrison and Jones' findings and highlights that the correlation between PNC vs. NO_x changes over time due the temporal variation in pollutant concentrations and the influence of meteorological variables.

The correlation coefficients between PM_{10} and nitrogen oxides found in the present study were similar to those reported by Harrison et al. (1997) at an urban centre in Birmingham ($r=0.46$ and 0.70 for summer and winter, respectively) for hourly PM_{10} vs. NO_2 and Cyrus et al. (2003a) at a site located 30 m away from a busy road in Erfurt (daily PM_{10} vs. NO_2 , $r=0.71$). Correlation coefficients in the present study were higher than those reported by Noble et al. (2003) using data pooled from two traffic sites in Texas (hourly PM_{10} vs. NO_2 , $r=0.13$); Pentinem et al. (2001) at an urban centre in Helsinki (daily PM_{10} vs. NO_2 , $r=0.16$) and Johansson et al. (2007) at a kerbside in Stockholm (daily PM_{10} vs. NO_x , $r=0.37$). Johansson et al. attributed the low correlation of PM_{10} vs. NO_x to the high contribution of road wear to PM_{10} , with 90 % of cars using studded tyres. In Texas, the arid climate probably makes resuspension of soil an important component of PM_{10} . The situation in Glasgow seems to be different, with PM_{10} at sites heavily influenced by traffic closely associated with PNC.

Regarding the effect of the averaging time on the degree of correlation between PNC and nitrogen oxides, Cyrus et al. (2003a) found higher correlation coefficients between daily PNC vs. NO_2 at a background site than their hourly counterparts, while Sardar et al. (2003) observed higher r-values for daily averaging time only in

summer (June to August) at receptor sites (downwind from the traffic source). As mentioned above, PNC are influenced by particle formation processes, which depend on specific conditions (including pre-existing organic compounds, solar radiation, and oxidant species such as O_3) that are specific at each site. If these processes are important, daily averaged data may better represent the correlation with nitrogen oxides. However, if concentrations are driven by primary traffic emissions, which similarly influence nitrogen oxides and PNC, then hourly averages are expected to show higher correlations.

PNC, PM_{10} and $PM_{2.5}$ vs. CO, SO_2 and O_3

Correlations of PNC, PM_{10} and $PM_{2.5}$ vs. CO showed a similar pattern than those observed for PNC, PM_{10} , $PM_{2.5}$ vs. nitrogen oxides. Higher correlation coefficients were observed at the kerbside sites: Hope St. (Tables 6.6 and 6.7) and Marylebone Rd. (Tables 6.12 and 6.13) than at the background sites: St. Enoch Sq. (Tables 6.8 and 6.9) and North Kensington (Tables 6.14 and 6.15), with higher r-values for hourly averaged data than daily averages. These results highlight the similar traffic sources and dispersion sources affecting particle number, mass, nitrogen oxides and CO. High correlation between PNC and PM_{10} vs. CO at street canyons has been reported by Ketzal et al. (2003), in Copenhagen ($r=0.84$ and 0.67 for PNC vs. CO and PM_{10} vs. CO, respectively for 30 minutes averaging period). Whereas lower correlation coefficients have been found at background sites. For example at a background site in Brisbane, Morawska reported an r -value= 0.33 for PM_{10} vs. CO (4 hours averaging period).

The lack of correlation of PNC and PM_{10} vs. SO_2 at Marylebone Rd. (Tables 6.12 and 6.13) suggests that other sources apart from traffic may contribute to SO_2 concentrations, and also different dispersion processes may affect particle, number, mass and SO_2 .

The latter hypothesis is supported by the fact that at St. Enoch Sq., SO_2 showed a similar diurnal pattern to PNC and PM_{10} (Figure 6.2) but correlations for hourly PNC and PM_{10} vs. SO_2 were low (Table 6.8). Cyrus et al. (2003a) also showed a low

correlation between 30 minutes PNC vs. SO₂ ($r=0.33$) in a street canyon in Copenhagen. However, in contrast to results observed in this study, their daily averaged data showed higher r -values $r=0.57$.

The insignificant correlation between PNC and SO₂ also suggest SO₂ did not contribute to a large extent to particle formation processes (Jeong et al., 2006). This is also supported by the negative correlation of PNC vs. O₃ at Marylebone Rd. (Tables 6.12 and 6.13) and North Kensington (Tables 6.14 and 6.15). In addition to traffic emissions, particles are also formed via oxidation of SO₂ and organic compounds by O₃ or hydroxyl radical (Kulmala et al. 2004). Positive associations between PNC and O₃, have been reported and attributed to particle formation processes involving photochemical reactions of O₃ and pre-existing vapours. In Los Angeles, Sardar et al. (2004) reported a correlation coefficient of $r=0.59$ for hourly PNC vs. O₃.

PNC, PM₁₀ and PM_{2.5} vs. hydrocarbons

Correlations of PNC, PM₁₀ and PM_{2.5} with hydrocarbons were generally higher with benzene and 1,3-butadiene than with toluene, ethylbenzene and xylenes. This is explained by the fact that benzene and 1,3-butadiene arise mostly from traffic exhaust (Dollar et al., 2000; Ho et al., 2004) and have less reactivity with the OH radical (Atkinson et al., 2000; Mono, 2001) than ethylbenzene and xylenes. In addition, toluene, besides being added to unleaded fuel in order to increase the octane index (Ho et al., 2004), is also commonly used as a solvent in industrial applications alongside ethylbenzene and xylenes (Zhu et al., 2008). The effects of these non-traffic related sources and the higher reactivity with the OH radical, possibly contributed to a weakening of the correlation coefficient of PNC, PM₁₀ and PM_{2.5} with toluene, ethylbenzene and xylenes compared to that observed for benzene and 1,3-butadiene.

Higher correlation coefficients between PNC and benzene but not with toluene, ethylbenzene and xylenes were also reported by Beckerman et al. (2008), in a study of pollutant gradients with distance from a highway in Toronto. Fisher et al. (2000)

reported a similar correlation coefficient between PM_{10} vs. benzene than that found in this study (r -value = 0.66 between ΔPM_{10} vs. Δ benzene). The correlation coefficient for Δ absorbance of PM_{10} vs. Δ benzene was higher than that found in this study ($r=0.85$). The increments in concentration (Δ) were the difference in concentration at homes with a high traffic influence and the concentration at homes with a low traffic influence.

Surrogate of BC vs. gaseous pollutants.

The surrogate of BC that best correlated with nitrogen oxides and hydrocarbons was absorbance of PM (PM_{10} at London, Tables 6.13 and 6.15) and $PM_{2.5}$ at Glasgow, Tables 6.7 and 6.9). However, the degree of correlation was much higher at London than at Glasgow, suggesting that the aerosol composition (i.e. substances responsible for the absorbing properties of the material deposited on the filter) significantly influences the degree of correlation of absorbance vs. co-pollutants and therefore results observed in an area may not be extrapolated to other locations.

6.2.4.2 Correlations between particle characteristics: number, mass and darkness

The higher correlation coefficients between PNC vs. PM_{10} at the kerbside sites compared to the background sites suggests that a larger proportion of ultrafine particles contributes to PM_{10} at kerbside sites compared to background sites. This result is in line with the higher correlations of PM_{10} vs. NO_x observed at the kerbside sites compared to the background sites. Since a high proportion of PM_{10} at kerbside sites originates in exhaust emissions, correlations of PM_{10} vs. NO_x are higher at kerbside sites compared to background sites.

The high correlation between PM_{10} and $PM_{2.5}$ highlights the previous finding (section 6.2.4.1) that most PM_{10} are formed by fine particulate matter, rather than coarse aerosols ($>2.5 \mu m$).

The correlation coefficients between PNC vs. PM_{10} observed in this study were higher than those reported by Morawska et al. (1998) ($r=0.25$) in an urban

background in Brisbane; Cyrus et al. (2003a), in a study in an urban centre and city background in Erfurt (r values for the bulked data were $r=0.57$, for hourly data and $r=0.37$, for daily data), and Sardar et al. (2004) at source and receptor sites in Los Angeles ($r= -0.16-0.27$, for hourly averaged data and $r=-0.32-0.10$, for averaged daily data). Harrison and Jones (2005) examined the correlations between PNC and PM_{10} at Marylebone Rd. North Kensington and St. Enoch Sq. with data from 2000 to 2003. Results at St. Enoch Sq. and North Kensington were higher than those observed in this study. Correlation coefficients (derived from the reported R^2) were $r=0.6$ for hourly and daily averaged data at St. Enoch Sq. and $r=0.2$ and $r=0.4$ for hourly and daily data at North Kensington. At Marylebone Rd. r -values for daily data were considerably lower ($r=0.5$) than their hourly counterparts ($r=0.8$), in contrast to results observed in this study ($r=0.8$ and $r=0.4$ for hourly and daily averaged data, Tables, 6.12 and 6.13). The higher correlation coefficient for hourly averaged data observed in this work suggests that over the years, from 2000-2003 to 2006 a larger proportion of PM_{10} might arise from traffic, since hourly correlations are driven by the diurnal traffic flows.

The higher correlation coefficient between PNC vs. surrogate of BC at Marylebone Rd. ($r=0.5-0.9$, Tables 6.12 and 6.13) compared to the other sites ($r=0.0-0.5$, Tables 6.6 to 6.9 and 6.14, 6.15) highlights the higher contribution of BC particles at sites heavily influenced by traffic.

The correlation of PM_{10} and $PM_{2.5}$ but not PNC with BC surrogates at North Kensington, suggest a regionally transported source of combustion particles dispersed along PM_{10} and $PM_{2.5}$.

EC, BS and absorbance of PM, all make reference to the fraction of graphitic carbon, the main absorbing material present in PM (Horvath, 1993). Therefore, similar correlation coefficients with co-pollutants were expected. However, the r -values varied substantially. For example, at Marylebone Rd. (the only site with data available for all BC surrogates) r -values for PNC vs. BS were 0.54, while PNC vs. EC and absorbance of $PM_{2.5}$ were 0.71 and 0.87 respectively.

Two factors can explain these discrepancies. First, BS measurements were possibly influenced by the inaccuracy of the formulae used to transform the reflectance into BS concentrations. The transformation uses the ISO: 9835 formula which was estimated taking into account the optical properties of the composition of particles in the 1950/1960s and corroborated in 1970. In those times the majority of black particles originated from coal combustion, while nowadays they are mostly emitted by diesel and gasoline from vehicle engines (Horvath, 1996). Taking into account that the optical properties of particles depend on particle size and composition, it is quite likely that the ISO curve no longer accurately represents the mass of soot.

Secondly, BS and absorbance of PM are both indirect measurements of BC. However, BC and EC are not strictly equivalent, although most studies refer to both of them as elemental graphite, “soot”. BC and EC make reference to two different properties: BC is a measure of the optical properties of the carbonaceous material while EC makes reference to the thermal properties (Cyrus et al., 2003b).

The factors that most affect BC measurements relate to the particle size and the mixture of black particles with non-absorbing particles (SiO_2 , Al_2O_3 , PbO , MnO , NaCl , sulphides, ammonium sulphate, etc.). Large amounts of non-absorbing particles result in a higher value of the absorption coefficient (Horvath, 1995). In addition, some fine mineral species such as MgO and hematite ($\alpha\text{-Fe}_2\text{O}_3$) also have high refractive index values (Hamilton et al., 1995) and therefore will be accounted as BC (Marr et al., 2007). However, these discrepancies are expected to be small since these species are uncommon in urban atmospheres (Horvath, 1995).

The amount of EC measured is strongly dependant on the method used to determine it. Schmid et al. (2001) reported a difference of up to one order of magnitude and RSDs between 37 % and 46 % for EC measured using different thermo-optical methods and the German reference method VDI (VDI, 1996).

Some of these factors might explain why the correlation of absorbance of $\text{PM}_{2.5}$ with EC was significant at Marylebone Rd. (Table 6.13) but scattered at North Kensington (Table 6.15, note that the r-value was driven by two high values shown in the scatter

plot; when these values were removed from the dataset the r-value dropped to 0.2). PM_{2.5} at North Kensington was probably influenced by a variety of sources, since it is located in an urban background site. Therefore, it might be expected to have more variability of black to non-black particles compared with the composition of PM_{2.5} at Marylebone Rd., which is expected to be mostly black particles from vehicle exhaust. Cyrus et al. (2003b) also reported variability in the correlation coefficient of absorbance of PM_{2.5} and EC between traffic sites ($r=0.97$) and background sites ($r=0.65$), although overall, the r-values in Cyrus' study were higher than those observed in this work. Ruuskanen et al. (2001) also reported a correlation coefficient of 0.9 between absorbance of PM_{2.5} and EC. Both studies used the VDI method mentioned above, while EC data used in this work were measured using the thermal-optical method.

The lower correlation coefficient between PNC vs. BS and absorbance of PM₁₀ at St. Enoch Sq. compared to Marylebone Rd., might be also related to the higher variability of absorbing and non-absorbing particles at St. Enoch Sq. At St. Enoch Sq., background particles possibly make a larger contribution to the total PNC than at Marylebone Rd. where most particles possibly arise from traffic emissions. In addition, BS concentrations were much lower at St. Enoch Sq. ($5 \mu\text{g m}^{-3}$) than at Marylebone Rd. ($43 \mu\text{g m}^{-3}$), resulting in lower statistical power. The reason why absorbance of PM₁₀ was not correlated with PNC at Hope St., in contrast to observations at Marylebone Rd. remained unclear. It could be argued that the non-black aerosol fraction in the size range 2.5-10 μm might affect the reflectance measurements, resulting in lower correlations with PNC (it should be noted that at Marylebone Rd. absorbance measurements were from PM_{2.5} filters, while at Hope St. absorbance measurements were from PM₁₀ filters). However, this hypothesis contrasts with observations reported by Fisher et al. (2000), Janssen et al. (2001) and Cyrus et al. (2003b). In these studies, absorbance of PM_{2.5} was highly correlated with absorbance of PM₁₀. The only plausible explanation is that the composition of PM_{2.5-10} in Glasgow was different to that in those studies. In addition, it should be noted that the correlation of PNC vs. absorbance of PM₁₀ at Hope St. was affected by

underestimation of high PNC events, by the WCPC and that this possibly affected the correlations.

6.2.4.3 Correlations between water-soluble metals and traffic-related air pollutants

The different pattern of correlations between metals and co-pollutants at the background and kerbside/street canyon sites, and between the two kerbside/street canyon sites (Tables 6.7, 6.9, 6.13 and 6.15) was thought to be the result of the different wind-induced dispersion regimes in open spaces compared to street canyons.

When air enters a canyon it is channelled and mixed with the on-road emissions creating a recirculation flow that depends on the relative orientation of the canyon with respect to the wind direction. The canyon at Hope St. was on a north-south axis while the canyon at Marylebone Rd. was on a west-east axis. At both sites, the prevailing wind direction was SW, which is oblique to the direction of the canyons. This creates both a flow along the street canyon and a re-circulation vortex as a consequence of the parallel and perpendicular components of the wind respectively, resulting in a spiralling flow along the length of the canyon (Scaperdas and Colvile, 1999). When the source of pollution is located at the ground level this recirculation vortex blows the on-road emissions against the leeward side of the street.

At Marylebone Rd. the monitoring station was located at the upwind side of the street (Figure 6.6). Therefore, southerly winds (which blow perpendicular to the street) will induce a recirculation vortex blowing pollutants against the monitoring station. Figure 6.7 shows a schematic representation of the recirculation regime created when wind blows perpendicular to the street.

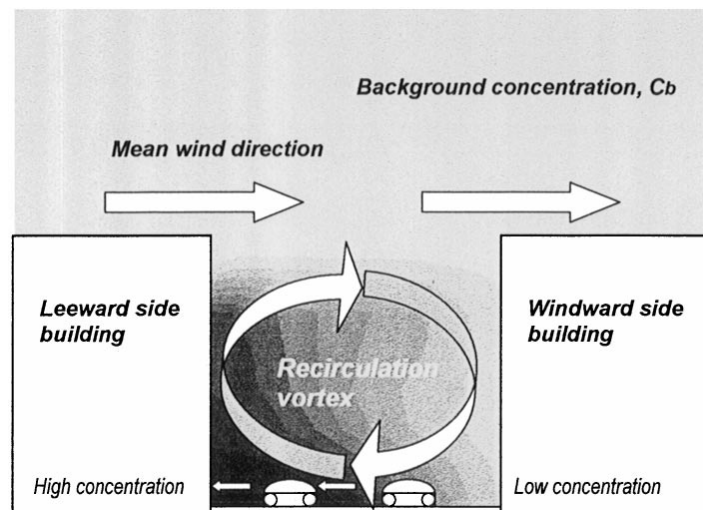


Figure 6.7 Schematic representation of wind flow and spatial variation of pollutant concentrations created when wind blows parallel to a regular street canyon (Scaperdas and Colville, 1999).

This might explain the observed increase in the increments in pollutant concentrations (i.e. the on road emissions at Marylebone Rd.) with increasing wind speed. The absolute concentrations of metals at Marylebone Rd. decreased with increasing wind speed possibly because they were diluted with the incoming background air (Table 6.13).

In contrast, Hope St. was located on the downwind side of the street (Figure 6.6) relative to westerly winds. Therefore, wind blowing in this direction dilutes pollutant concentrations resulting in a decrease of the increments and absolute concentrations (Table 6.7). Southerly winds enter parallel to the canyon, diluting traffic pollutants with background air.

In addition to the effect of the air-flows within the canyon on the pollutant concentrations, the physical characteristics of air pollutants also influence their response to wind speed. The fact that the increments in PNC were unaffected by wind speed at Marylebone Rd. is in line with findings by Charron and Harrison (2003) that 71 % of PNC at Marylebone Rd. are nucleation particles (11-30 nm), which are not affected by wind speed (Charron and Harrison, 2003; Agus et al., 2007).

6.2.5 Correlations between the increments in pollutant concentrations

The high regression coefficient between the 24-hours averaged measurements of traffic-related air pollutants at the individual sites (Tables 6.7, 6.9, 6.11, 6.13 and 6.15) allows the examination of the relationship between the differences in the concentration of these pollutants between paired sites with the aim of estimating one pollutant by measuring the other.

By subtracting a background concentration from the concentrations at the kerbside sites the slope is more directly related to the emission sources at the kerbside and the intercept relates to local non-traffic related emissions.

The increments in NO_x concentrations explained the highest percentage of the variation in PNC at both paired sites in London and Glasgow (Table 6.16). Therefore spatial variations in NO_x could be used to estimate spatial variations in PNC.

The smaller slope and larger intercept in the relationship ΔPNC vs. ΔNO_x at Glasgow compared to London may have been the result of the underestimation of particles by the WCPC at Hope St. The SD of PNC was possibly smaller than it should be, due to the underestimation of PNC at high particle events, resulting in a smaller slope and consequently a larger intercept.

The examination of the relationship between the increments in pollutant concentrations is a very straightforward and novel method to estimate spatial variations in the concentrations of one pollutant from measurements of another pollutant.

6.2.6 Summary of correlations between traffic-related air pollutants

The moderate correlations between PNC, PM_{10} and nitrogen oxides between paired sites in London and Glasgow suggest that the use of a single monitoring site to assess average exposure of population in time series epidemiological studies may lead to exposure misclassification, as variations observed at one single site do not adequately represent variations over large areas.

Nitrogen oxides showed the most consistent associations with PNC across all the studied sites in Glasgow ($r=0.7-0.8$) and London ($r=0.6-0.9$) for hourly and daily averaging periods and therefore they would be the best surrogate for PNC.

PM_{10} can represent PNC at sites heavily influenced by traffic (r -values for PNC vs. PM_{10} were 0.6 and 0.7 at Hope St. and Marylebone Rd. respectively). However, as the distance from the traffic emission source increases, the strength of correlation decreases (r -values < 0.5 at St. Enoch Sq. and North Kensington). Therefore, at background sites PM_{10} do not represent well exposure to PNC. Therefore, the use of PM_{10} as a surrogate for air pollution in epidemiological studies is likely to underestimate the association between actual exposure to a range of pollutants and health effects since correlations of PM_{10} with co-pollutants were lower than correlations of PNC with co-pollutants, especially at sites representative of population exposure, such as St. Enoch Sq. (urban centre) and North Kensington (urban background).

Absorbance of PM showed a different degree of correlation with PNC and nitrogen oxides in Glasgow and London, possibly due to the different composition of the light absorbing material in both cities. Therefore, its use as a surrogate for PNC must be examined at individual locations since results from one site cannot be extrapolated to other sites.

The averaging period, hourly and daily did not significantly influence the strength of the correlation coefficients, suggesting that correlations are mostly driven by the diurnal pattern of traffic flows, and over the day the effects of meteorology do not significantly affect this pattern. If the correlations between pollutants were the effect of meteorology and long-transported air masses, then correlations between daily averages would be higher than their hourly counterparts, since the homogenising effects of meteorology and long-transported air masses are more noticeable over an entire day rather than on an hourly basis.

The high correlation of nitrogen oxides and PNC ($r=0.6-0.9$) implies that it is not possible to distinguish between their health effects. The high correlation of PNC vs.

PM₁₀ at kerbside sites ($r=0.8$) but low correlation at background sites ($r=0.3-0.6$) implies that the separate health effects of PNC and PM₁₀ can be distinguished at background sites but not at sites influenced by traffic sources.

Water-soluble metals (Fe, Cu, As, Pb and Zn) were highly correlated to nitrogen oxides at background sites but not at kerbside sites, possibly as a consequence of small-scale variations in pollutant dispersion induced by wind regimes created within street canyons.

The spatial variations in NO_x can be used to represent spatial variations in PNC. Examination of the relationship between the increments in concentrations of both pollutants has shown to be a very simple and novel method for measuring the spatial variation of one pollutant by using measurements of another pollutant.

CHAPTER 7

USE OF NO₂ AND NO_x PDTs AS SURROGATES FOR AIR POLLUTION METRICS

7.1 RESULTS

This section describes the results of the study into the use of PDTs to measure the spatial variability of NO₂ and the use of NO₂ and NO_x measurements as surrogates for other pollutants.

Section 7.1.1. shows the results of NO₂ concentrations measured simultaneously using PDTs at seven urban/suburban sites across Glasgow and 7.1.2 the NO₂ concentration profile with increasing distance from a major road in Glasgow. All exposure periods were 7 days.

7.1.1 Use of PDTs to estimate the spatial variability of NO₂ in Glasgow

Table 7.1 shows the summary statistics of NO₂ concentrations measured at 7 sites in Glasgow. The measuring period was from 15 February to 10 May 2005.

Table 7.1 Descriptive statistics of NO₂ ($\mu\text{g m}^{-3}$) measured by PDTs at different sites in Glasgow (sites arranged from west to east).

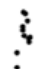


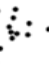



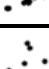
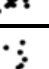
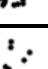
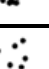

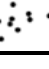
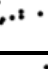
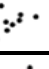
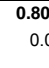

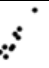
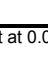
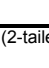
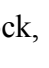
Site Name	Site classification	n	Mean	Median	SD	Q1	Q3
Cardonald	Suburban	12	34	34	10	31	40
Montrose St.	Urban background	12	59	56	11	54	60
St. Enoch Sq.	Urban centre	8	54	54	8.3	51	61
Springburn	Suburban	11	34	35	13	28	39
Dalmarnock	Urban industrial	12	22	20	11	16	25
Carmyle	Urban industrial	12	28	26	10	22	35
Baillieston	Urban background	12	27	27	12	18	34

SD: standard deviation; Q1: first quartile; Q3: third quartile

There was a substantial difference in NO₂ concentrations (around 30 $\mu\text{g m}^{-3}$) between urban sites (Montrose St. and St. Enoch Sq.) and those located in suburban and background areas. The decreases in NO₂ concentration appeared to be clearly related to the proximity of the sites to traffic sources. Suburban sites (Cardonald and Springburn) showed higher concentrations than those observed at urban background and industrial sites (Dalmarnock, Carmyle and Baillieston).

Table 7.2 shows the scatter plot and correlation coefficients of NO₂ PDTs across the different sites.

Table 7.2 Scatter plots and Spearman correlation coefficient between NO₂ PDTs measured at different sites in Glasgow.

		Cardonald	Montrose St.	St Enoch Sq.	Springburn	Dalmarnock	Carmyle	Baillieston
Cardonald	Correlation Coefficient	1						
	Sig. (2-tailed)							
	N	12	12	8	11	12	12	12
Montrose St.	Correlation Coefficient	0.187	1					
	Sig. (2-tailed)	0.560						
	N	12	12	8	11	12	12	12
St Enoch Sq.	Correlation Coefficient	0.847**	0.757*	1				
	Sig. (2-tailed)	0.008	0.030					
	N	8	8	8	11	12	12	12
Springburn	Correlation Coefficient	0.676*	0.261	0.566	1			
	Sig. (2-tailed)	0.022	0.438	0.185				
	N	11	11	7	11	12	12	12
Dalmarnock	Correlation Coefficient	0.259	0.802**	0.513	0.406	1		
	Sig. (2-tailed)	0.416	0.002	0.194	0.215			
	N	12	12	8	11	12	12	12
Carmyle	Correlation Coefficient	0.426	0.713*	0.630	0.560	0.801**	1	
	Sig. (2-tailed)	0.167	0.009	0.094	0.073	0.002		
	N	12	12	8	11	12	12	12
Baillieston	Correlation Coefficient	0.493	0.705*	0.444	0.430	0.837**	0.660	1
	Sig. (2-tailed)	0.103	0.010	0.271	0.187	0.001	0.020	
	N	12	12	8	11	12	12	12

Significant correlations are in bold.**Correlation is significant at the 0.01 level (2-tailed); *Correlation is significant at 0.05 level (2-tailed)

NO₂ concentrations were statistically significantly correlated among the following sites: St. Enoch Sq., Cardonald and Springburn; Montrose, Dalmarnock, and Carmyle; St. Enoch Sq. and Montrose St.

The high correlation coefficients between Montrose St. vs. Dalmarnock, Carmyle and Baillieston were driven by an outlier in the period from 8 March to 15 March (see scatters in Table 7.2). When this value was excluded from the dataset the correlation coefficients were no longer significant.

7.1.2 Use of PDTs to assess the spatial variability of NO₂ with increasing distance from a major road

Figure 7.1 shows the results of the NO₂ decay profile with increasing distance from Cathedral St. in Glasgow, a road with a traffic flow of approximately 8,000-15,000 vehicles day⁻¹ (Henderson, 2005). An exponential, power and logarithmic decay were tested as best fit for the observations. The regression curves are presented in Figure 7.1 for five separate exposure periods and for the NO₂ averaged concentration over the five periods. The UK 24-hours Air Quality limit value for NO₂ is also shown.

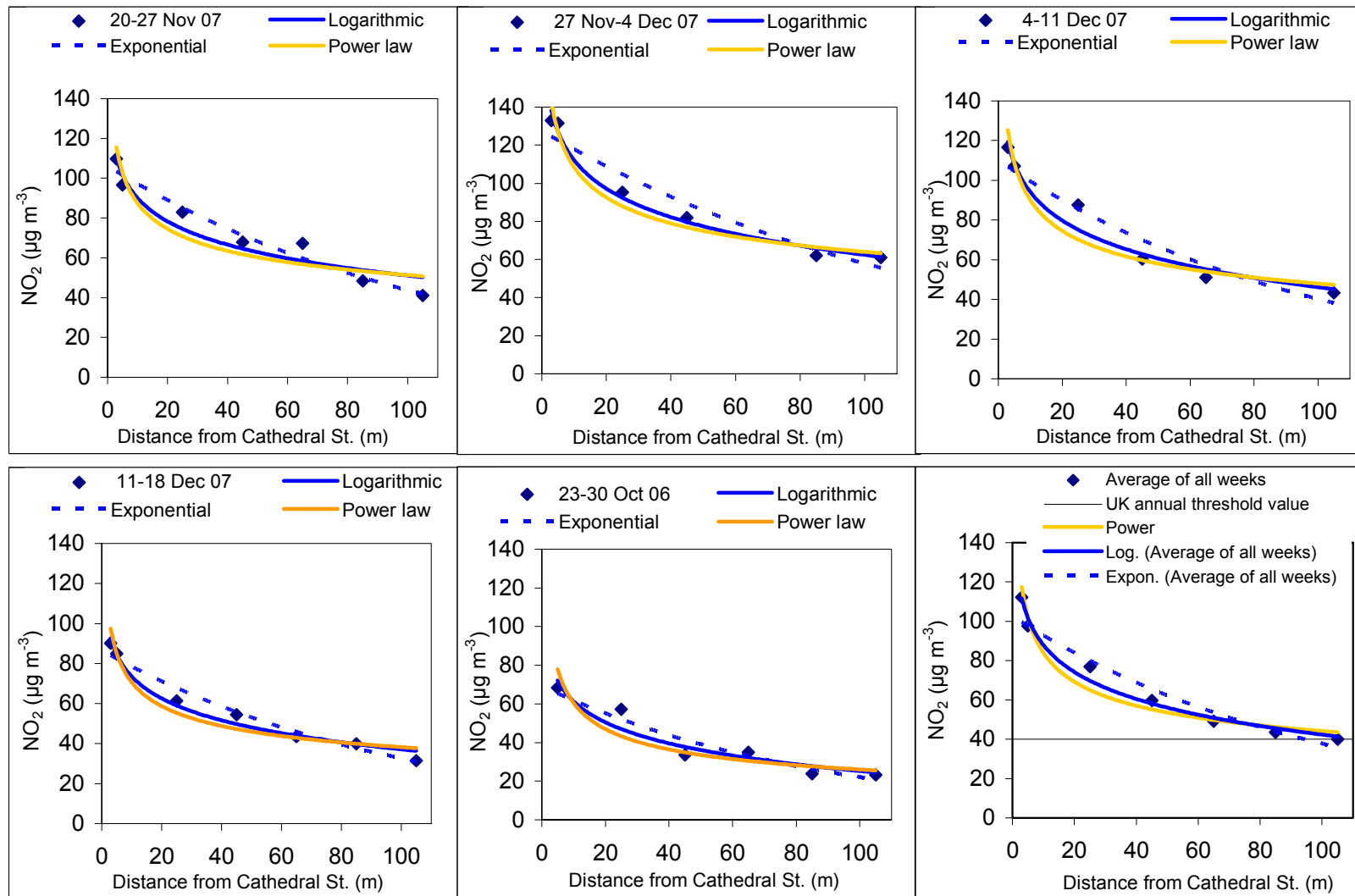


Figure 7.1 Scatter plots, logarithmic, exponential, and power law curves of 5 week averaged NO₂ concentrations and the averaged of the concentrations over the five weeks measured by PDTs against distance from Cathedral St. (8,000-15,000 vehicles day⁻¹).

Two PDTs, one located at 65 m and the other at 85 m were vandalised on weeks 27 November to 4 December and 4 to 11 December, respectively.

NO₂ concentrations decreased monotonically, but not linearly with the distance to the road. Close to the road (3-40 m) the decrease was much sharper, with a lower rate at long distances.

The logarithmic and exponential curves represented the NO₂ decline better than the power law. The curvature of the power decay was very strong, exhibiting lower concentrations over the sharp decline from 5 to 40 m.

The 24-hours NO₂ Air Quality limit value in the UK (40 µg m⁻³) was achieved in most of the measurement periods at a distance of approximately 100 m from the road.

The values of the equation parameters, regression coefficients and p-values for the logarithm, exponential and power law are shown in Table 7.3.

Table 7.3 Estimated parameters, regression coefficients (R²) and p-value of the exponential, logarithmic and power relationship between NO₂ concentrations measured using PDTs at different distances from Cathedral St (x). (8,000-15,000 vehicles day⁻¹).

Period	NO ₂ (x) = a ₁ - b Log(x)				NO ₂ (x) = a ₀ e ^{-kx}				NO ₂ (x) = a ₂ x ^{-b}			
	a ₁	b	R ²	p	a ₀	k	R ²	p	a ₂	b	R ²	p
23-30 Oct 06	97.3	36.0	0.904	0.004	69.1	-0.011	0.921	0.002	162	-0.252	0.772	0.009
20-27 Nov 07	129	38.9	0.918	0.001	106	-0.009	0.967	0.000	207	-0.259	0.973	0.004
27 Nov-4 Dec 07	162	49.7	0.985	0.000	128	-0.008	0.939	0.001	191	-0.304	0.903	0.001
4-11 Dec 07	142	48.0	0.959	0.001	110	-0.010	0.931	0.002	148	0.298	0.907	0.002
11-18 Dec 07	110	36.4	0.981	0.000	86.5	-0.010	0.975	0.000	140	-0.366	0.851	0.001
Average over all the weeks	134	19.8	0.984	0.000	103	-0.01	0.955	0.000	159	-0.279	0.950	0.001

a₁ and a₂ in the logarithmic and power relationships respectively are the concentration at x=1 m, since the logarithm and power function converge to an asymptote as x → 0. a₀ is the concentration at x=0.

a₀ (concentration at x=0) was smaller than a₁ and a₂ (concentration at x=1) reflecting the underestimation of NO₂ at short distances when using an exponential model, as shown in Figure 7.1. a₂ was larger than a₁, reflecting the NO₂ overestimation of the power relationship at distances close to the road.

The regression coefficients for the logarithmic relationship were generally statistically significant at a higher level than the exponential and power functions, and therefore it would represent better the concentration profile.

7.1.3 Use of NO₂ PDTs as surrogates for PNC

Figure 7.2 shows the RMA relationship between PNC and NO₂ measured by PDTs and weekly NO₂ averaged data measured with the chemiluminescence analyser.

NO₂ PDTs showed high regression coefficients ($R^2 > 0.6$) with weekly averaged PNC at the three sites. The regression coefficients were similar to those obtained with weekly averaged data from the analyser at Montrose St. and Hope St. However, at St. Enoch Sq. the R^2 was higher for PNC vs. NO₂ PDTs ($R^2=0.621$), than for PNC vs. NO₂ analyser ($R^2=0.412$).

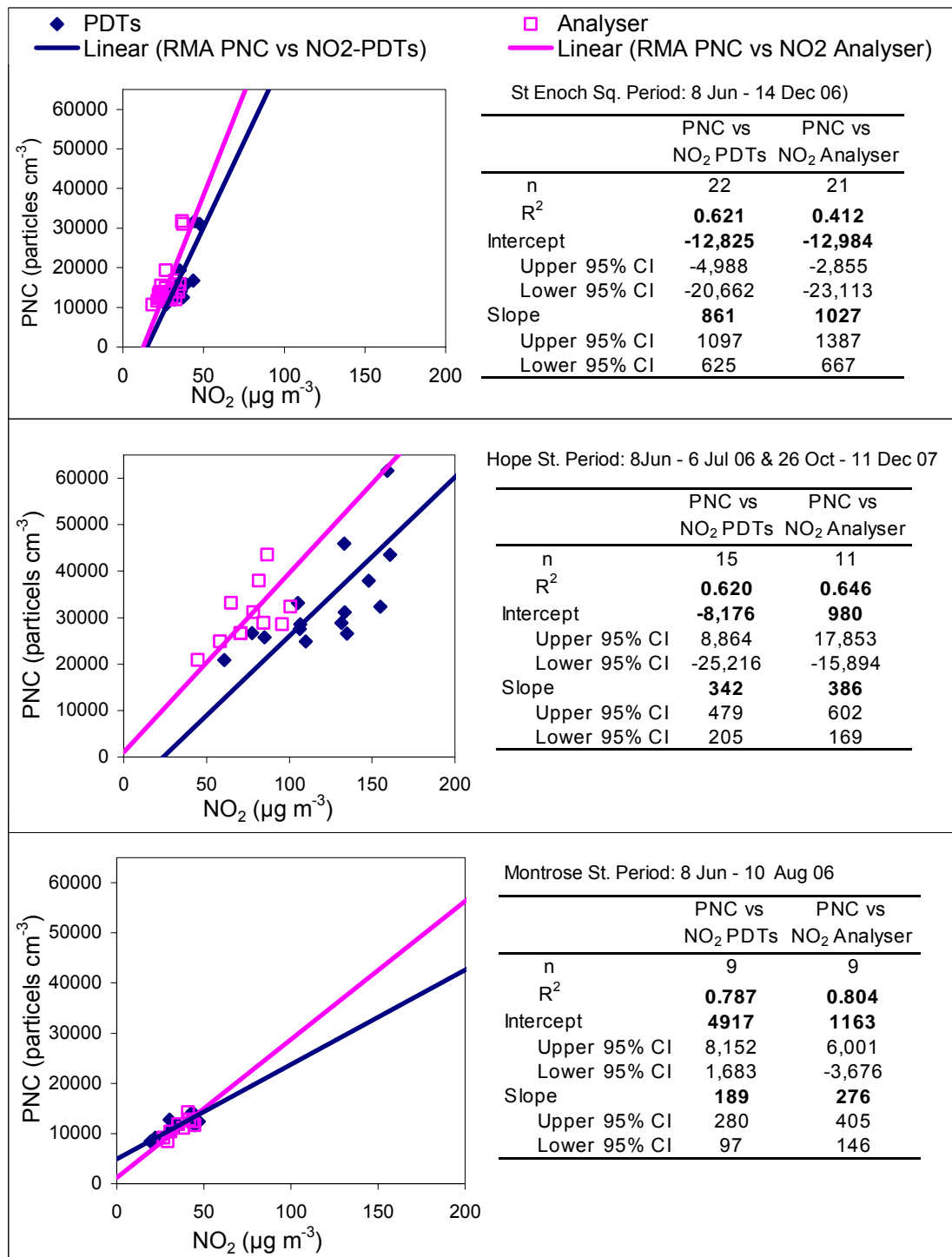


Figure 7.2 Scatter plots, RMA relationship, and regression coefficient (R^2) of weekly averaged particle number concentration (PNC) vs. NO_2 at St. Enoch Sq. (top), Hope St. (center) and Montrose St. (bottom).

At St. Enoch Sq. and Montrose St. the regression lines for PNC vs. NO_2 PDTs and NO_2 analyser were relatively similar, particularly for NO_2 concentrations below

$50 \mu\text{g m}^{-3}$. The slope and intercept of PNC vs. NO_2 PDTs lay within the CI range of the slope and intercept of PNC vs. NO_2 analyser. Thus, NO_2 PDTs measurements could be used instead of NO_2 analyser measurements to represent PNC. However, at Hope St. PNC predicted from NO_2 analyser data would be much higher than those obtained if calculated using NO_2 PDTs measurements. The CI for the slope and intercept were relatively broad for both regression equations PNC vs. NO_2 (PDTs and analyser).

The relationship between PNC and NO_x PDTs has not been presented because during the period for which NO_x PDTs data were available (May to August 2007) the BCPC and the two WCPCs were malfunctioning. Maintenance of the BCPC by NPL ended in June 2007 and the two WCPCs experienced some technical problems. Therefore, data for PNC during this period were not reliable.

7.1.4 Use of NO_2 & NO_x PDTs as surrogates for hydrocarbons

This section shows the functional relationships between weekly measurements of NO_2 and NO_x measured by PDTs and the corresponding averaged concentrations of hydrocarbons measured by the NO_x analyser at Hope St. (the only site for which hydrocarbons data were available in Glasgow).

The scatter plot and RMA relationships of hydrocarbons vs. NO_2 and NO_x are shown in Figure 7.3 and Figure 7.4, respectively.

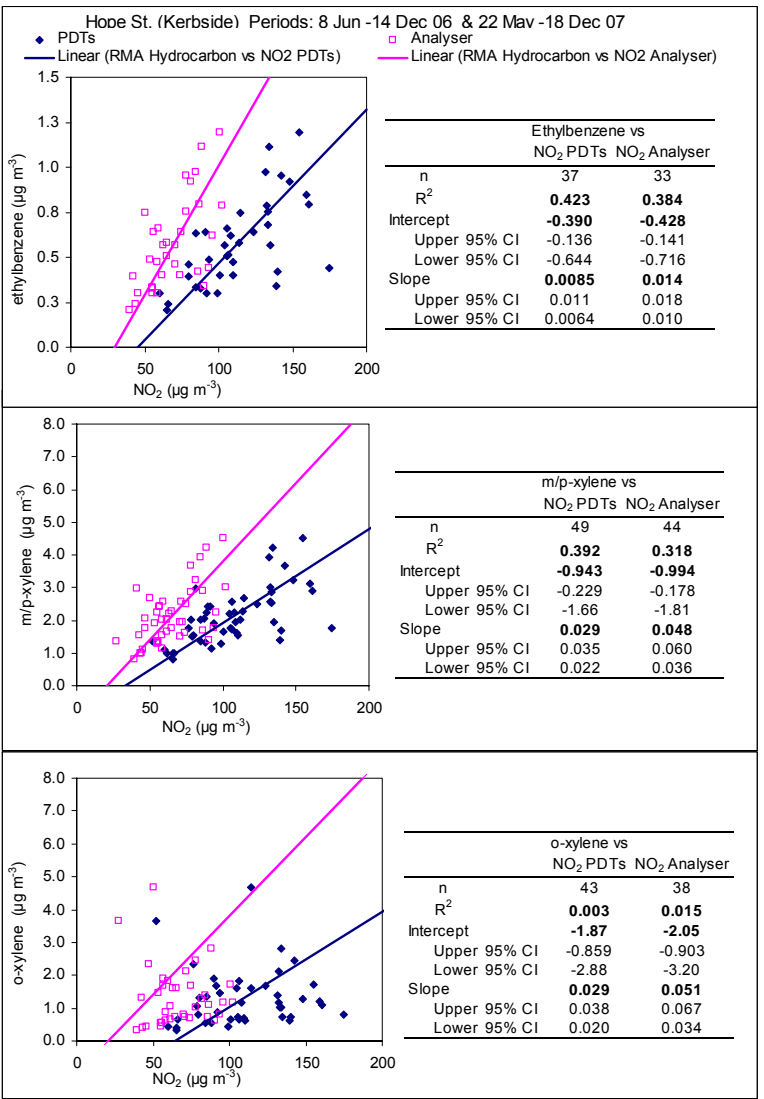
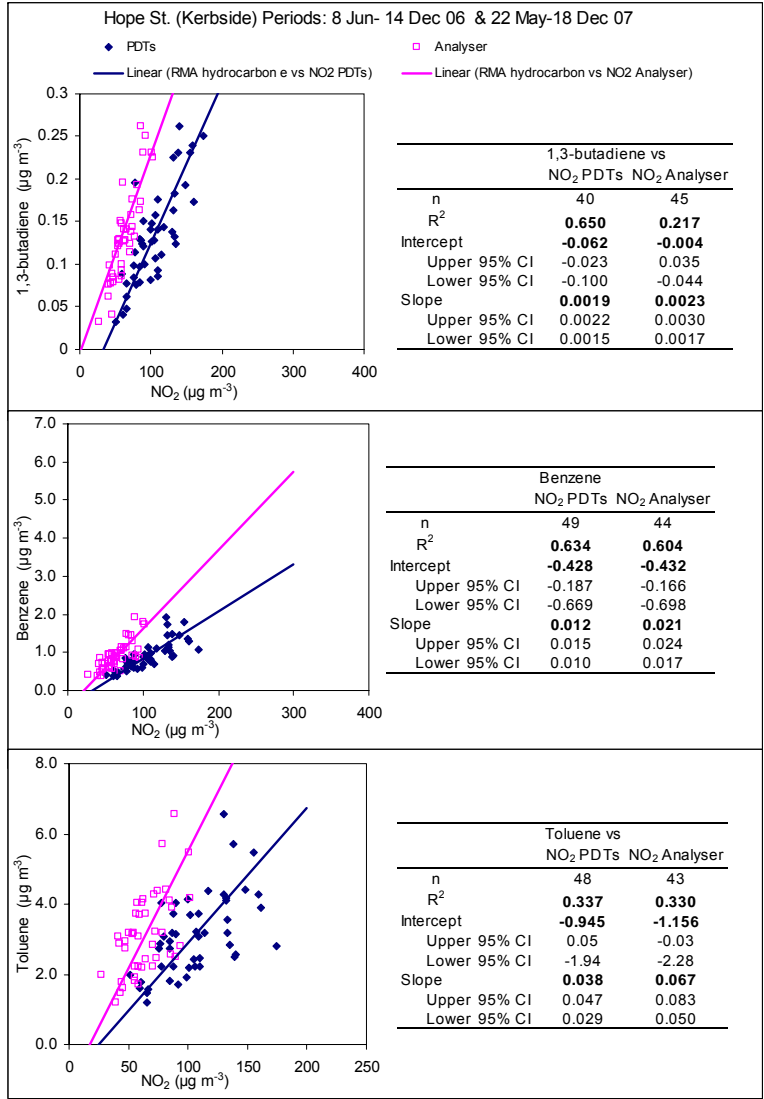


Figure 7.3 Scatter plots, RMA relationship and regression coefficient (R^2) of weekly averaged hydrocarbons vs. NO₂ derived from passive diffusion tubes (PDTs) and analyser.

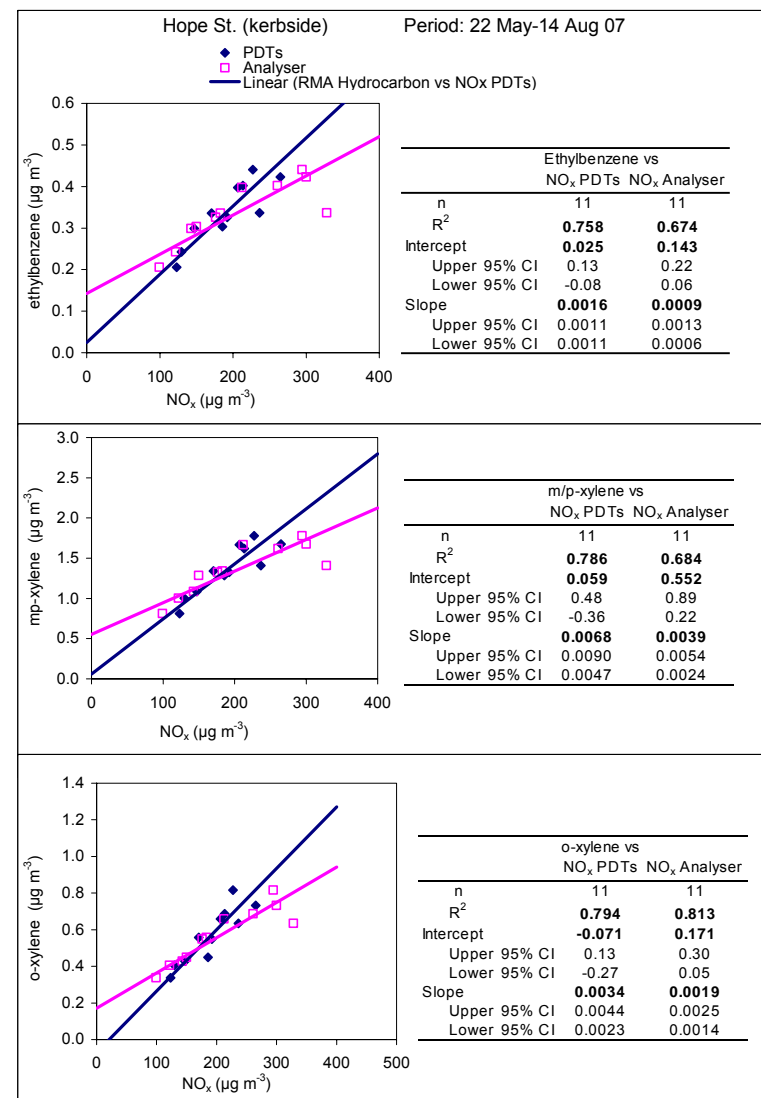
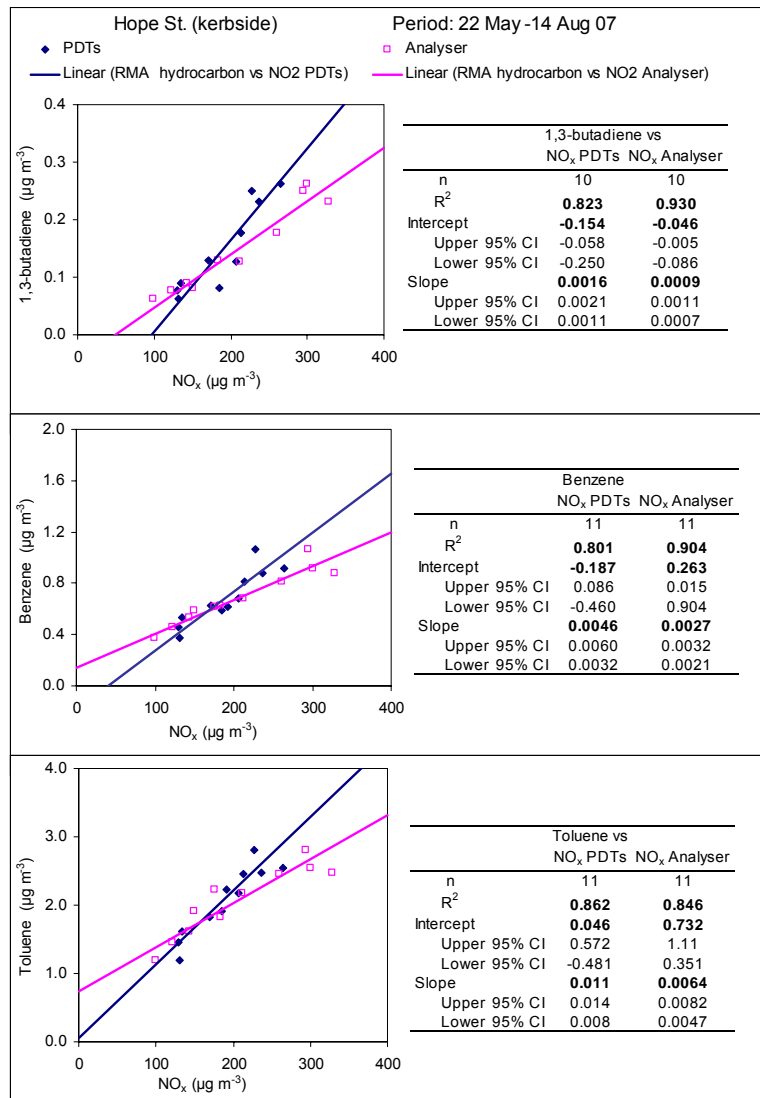


Figure 7.4 Scatter plots, RMA relationship and regression coefficient (R^2) of weekly averaged hydrocarbons vs. NO_x derived from passive diffusion tubes (PDTs) and analyser.

Regression coefficients were higher for hydrocarbons vs. NO_x ($R^2 > 0.8$) than for hydrocarbons vs. NO_2 ($R^2 \approx 0.6$) for 1,3-butadiene and benzene vs. NO_2 and $R^2 < 0.4$ for toluene, ethylbenzene, m/p-xylene and o-xylene vs. NO_2 . This could be partly the result of the different measurement periods for NO_2 and NO_x . It should be noted that NO_x measurements were a sub-set of NO_2 measurements. Regression coefficients of hydrocarbons vs. NO_2 for the same period as for hydrocarbons vs. NO_x resulted in R^2 values of 0.9 for NO_2 vs. benzene, 1,3-butadiene and toluene and R^2 values of 0.8 for NO_2 vs. m/p-xylene and o-xylene (data not shown).

The regression lines for hydrocarbons vs. NO_x PDTs and hydrocarbons NO_x vs. analyser crossed at approximately $200 \mu\text{g m}^{-3}$. Hydrocarbon concentrations derived from NO_x PDTs measurements would be overestimated at NO_x concentrations below $200 \mu\text{g m}^{-3}$ and underestimated at NO_x concentrations above $200 \mu\text{g m}^{-3}$ compared to those derived from the analyser.

The slope of hydrocarbon vs. NO_2 analyser was higher than that for hydrocarbons vs. NO_2 PDTs. The slope of hydrocarbons vs. NO_2 PDTs was outside the CI range of hydrocarbon vs. NO_2 analyser. Therefore, hydrocarbon concentrations derived from NO_2 PDTs will be significantly different to those derived from NO_2 analyser.

7.1.5 Use of NO_2 & NO_x as surrogates for BS

Figure 7.5 shows the scatter plots, RMA relationship and regression coefficients of BS vs. NO_2 and NO_x derived from PDTs at St. Enoch Sq.

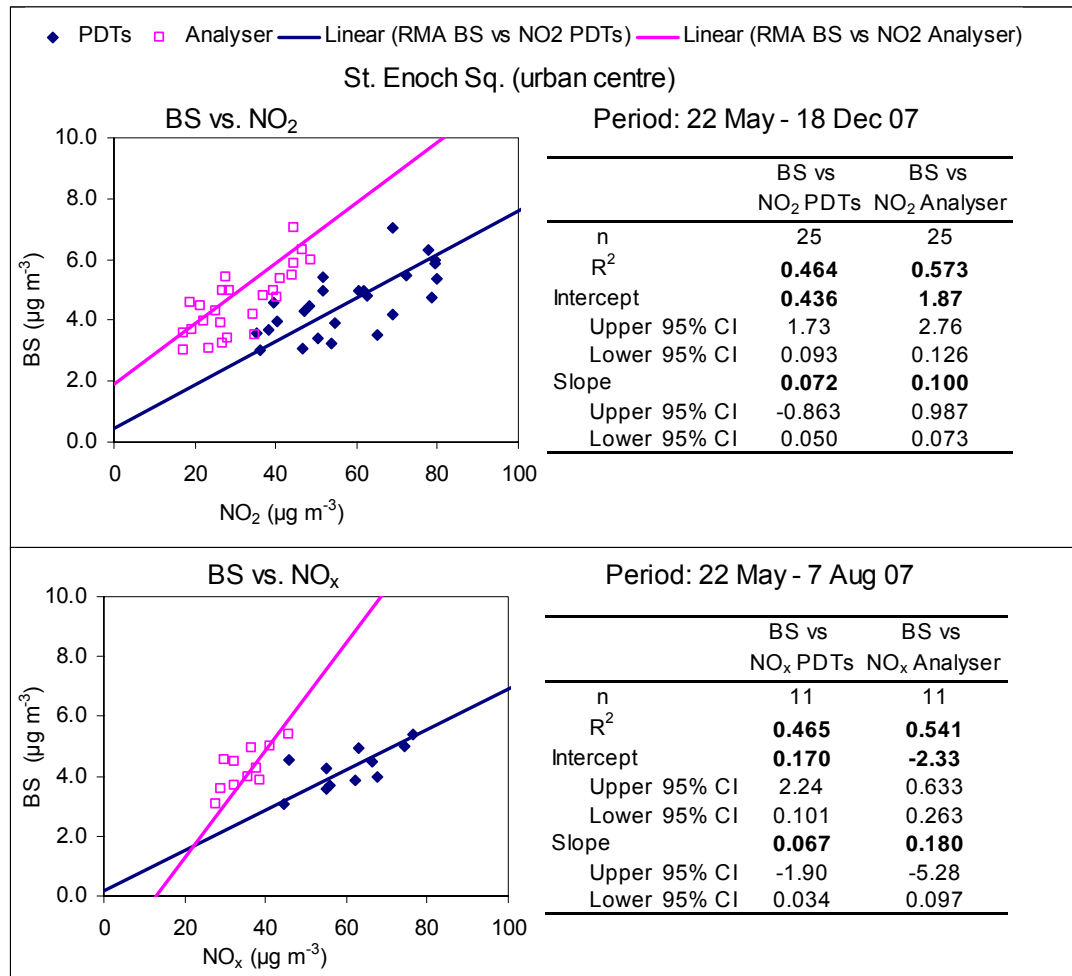


Figure 7.5 Scatter plots, RMA relationship and regression coefficient (R^2) of weekly averaged black smoke (BS) vs. NO₂ and NO_x derived from PDTs and analyser.

The regression coefficients of BS against NO₂ and NO_x were moderate ($R^2 \approx 0.5$). Data averaged from the analyser showed slightly higher regression coefficients with BS than measurements from the PDTs.

The RMA relationships for BS vs. NO₂ and NO_x PDTs showed smaller slopes than those for BS vs. NO₂ and NO_x analyser. Therefore, BS concentrations derived from PDTs would underestimate those derived from the analyser.

7.2 DISCUSSION

7.2.1 Use of PDTs to examine the spatial variability of NO₂

PDTs were shown to be a simple and cost-effective method to measure weekly NO₂ concentrations across the city. Correlation coefficients of weekly NO₂ were only statistically significant between sites of similar characteristics. This result suggests that correlations were mostly influenced by similar variations in traffic emission between sites rather than by the homogenising effect of meteorology. Therefore, weekly NO₂ concentrations measured at a single site would not be expected to represent the NO₂ variations across the city.

The correlation of weekly NO₂ PDTs between Montrose St. and St. Enoch Sq. was less statistically significant ($p < 0.05$, 2-tailed, Table 7.2) than that observed for hourly and daily averaged NO₂ from the analyser ($p < 0.01$, 2-tailed) (Table 6.4). This might be partly due to the higher accuracy of the hourly and daily measurements (derived from the analyser) compared to those derived from the PDTs. The biases affecting the performance of the PDTs were not the same at St. Enoch Sq. and Montrose St, as discussed in section 5.2.1.2, and this could have affected the strength of correlation between sites. Alternatively, since NO₂ concentrations at Montrose St. and St. Enoch Sq. were strongly influenced by the diurnal traffic flows (Figure 6.3) a higher correlation between hourly data than between weekly exposure periods would be expected.

Examination of the exponential, power and logarithmic relationship to explain the decay of NO₂ with distance from Cathedral St. showed that the logarithmic model better described the NO₂ decay. These results are in line with those observed by Roorda-Knape (1998), Gilbert et al. (2003) and Pleijel et al. (2004). In contrast, Arya (1999) based on gradient transport theory predicted a NO₂ decay in the form $C(x) x^{-\beta}$ where β depends on atmospheric stability and surface roughness and is assumed to vary between 0.5 and 1. Singer et al. (2004) observed this relationship in a study of NO₂ concentrations and distance from a highway in California. Although, the observed value for β was lower than that predicted by Arya ($\beta = 0.356$, $R^2 = 0.80$). In this study the β was also lower than 0.5 (average over the 5 exposure periods,

$\beta=0.279$, $R^2=0.95$, Table 7.3). The decline predicted by the power law was much steeper than the observed measurements, resulting in underestimation of the concentrations between 20 and 40 m from the emission source.

Cape et al. (2004) observed an exponential decay, which can be derived from Gaussian dispersion under certain idealized conditions (quasi-steady emission strength, isotropic dispersion, atmospheric stability, and chemical stability of the compound) (Seinfeld and Pandis, 1998). In the present study, the curvature of the exponential decay fell above the observed measurements (Figure 7.2), overestimating NO_2 concentrations over the distance interval 5 to 40 m.

The logarithmic regression best represented the observed measurements. A limitation of the logarithmic model is that when the distance approaches to zero the concentration approaches to ∞ , therefore extrapolation to zero is not possible and the distance at which the concentration is maximum has to be held at 1 m. Similarly, at large distances, as the model does not converge to a horizontal asymptote, values become negative (Faus-Kessler et al., 2008). In contrast, with the exponential model is possible to estimate concentrations at $x=0$.

In order to compare the decay rates estimated from the logarithmic regression with those described by Pleijel et al. (2004) in a study in Sweden and Gilbert et al. (2003) in a study in Canada, the five logarithmic regression equations (Table 7.3) were transformed to a relative scale as described in Pleijel et al. (2004). A background concentration (extrapolated from the regression equations) was subtracted from the intercept and the resulting intercept and the slope divided by the concentration at a reference point (Equation 7.1).

$$C_{rel} = \frac{(\text{intercept} - C_{BG}) - \log x}{C_{ref}} \quad \text{Equation 7.1}$$

C_{rel} : concentration respect a reference point (in this case 3 m from the emission source)

C_{BG} : background concentration

C_{ref}: reference concentration (in this case the concentration at x=3 m)

Pleijel et al. selected as a reference point the concentration at 10 m from the road since that was the concentration closest to road available in the study and a background concentration of $6 \mu\text{g m}^{-3}$. In this work, the concentration closest to the road was that observed at 3 m, and the background concentration was calculated by extrapolation at 300 m for each equation, since background levels have been reported at this distance (Gilbert et al., 2003, Pleijel et al. 2004, Beckerman et al. 2006). Table 7.4 shows the equation parameters of the scaled relationship of concentration with the logarithm of the distance, together with results obtained by Gilbert et al. (2003) and Pleijel et al. (2004).

Table 7.4 Estimated parameters of the logarithmic relationship of the relative NO₂ concentration (*C_{rel}*, reference distance of 3 m away from road in present study and 10 m in Gilbert et al. and Pleijel et al. studies) contributed by a major road and the distance to the road.

$C_{rel}(x) = a_1 - b \text{Log}(x)$			
Reference	a_1	b	R^2
Present study	0.98	0.39	0.980
Gilbert et al. 2003*	1.45	0.45	NA
Pleijel et al. 2004	1.53	0.51	0.950

*as calculated by Pleijel et al. (2004). NA: not available

The rate of decay predicted by Pleijel et al. (2004) and that calculated by Pleijel et al. with Gilbert et al.'s results showed a steeper decrease than that estimated in this study. The intercept of the relationship estimated in this study was also smaller than that predicted by Pleijel et al. (2004). These differences may be the result of the following factors:

1. Different spatial scales covered in the different studies (1,310 m in Gilbert et al. and 1,000 m in Pleijel et al. compared to 105 m in the present study).
2. Different vehicle flows (100,000 vehicles day⁻¹ in Gilbert et al., averaged of 32,000 vehicles day⁻¹ and 18,900 vehicles day⁻¹, compared to 8,000-15,000 vehicles day⁻¹ in the present study).
3. Differences in landscape roughness and wind speed. An increase in any of these would result in higher decay rates (Pleijel et al., 2004).

4. Differences in O₃ availability in the three studies. NO₂ formation due to reaction of NO and O₃ as air is advected from the source would result in a lower decay rate.

The turbulence regime is likely to vary at different distances from the road, and therefore decay rates from different studies with different traffic flows and covering different distances are not comparable (Cape et al., 2004).

On the other hand, the effect of the NO₂ overestimation in PDTs observed in this study (discussed in Section 6.1) might have contributed to a lower decay rate than expected. Overestimation is likely to be greater at larger distances from the road (where NO and O₃ are available to react within the tube) compared to the locations closer to the source (where all NO is depleted by O₃ and therefore there is not enough NO to react within the tube) (Kirby et al., 2003). Higher overestimation at increasing distance would result in a lower observed decay rate. The overestimation of concentrations at large distances but not at close distances results in a smoother decay with smaller decay constant. These biases in the PDTs were not reported in either Gilbert et al. or Pleijel et al.'s studies. Gilbert et al. used Ogawa NO₂ passive samplers and Pleijel et al. a variant of Palme's tubes with a shorter tube length (5 cm compared to 7 cm) and a steel screen at the open end to prevent NO₂ overestimation caused by turbulence diffusion.

Pedestrians along Cathedral St. were exposed to concentrations of NO₂ in excess of the UK 24-hours Air Quality limit value (40 µg m⁻³). NO₂ concentrations of 40 µg m⁻³ were only achieved beyond 60 m from the kerbside (average of the distance calculated from the logarithmic relationship for the five exposure periods). This should be taken into account in urban planning to contribute to the better health of citizens.

7.2.2 Use of PDTs as surrogate for traffic-related air pollutants

The relatively high regression coefficients between PNC vs. NO₂ PDTs (Figure 7.2); hydrocarbons vs. NO₂ and NO_x PDTs (Figures 7.3 and 7.4) and BS vs. NO₂ and NO_x

PDTs (Figure 7.5) suggest that PDTs may be a useful tool to represent spatial variations in PNC, hydrocarbon and BS concentrations. NO_x appeared to be a slightly better surrogate than NO_2 , explaining 80-90 % of the variation in hydrocarbon concentrations and 50 % of the variation in BS concentrations.

However, possibly because of the bias affecting PDTs, the RMA relationships of PNC, hydrocarbons and BS vs. NO_2 and NO_x PDTs vs. were different to those derived using NO_2 averaged data from the chemiluminescence analyser. Since the biases affecting PDTs are difficult to correct, as discussed in Chapter 5, PDTs may not provide reliable estimates of absolute concentrations of PNC, hydrocarbons and BS.

Weekly NO_2 (as measured by the PDTs) and weekly averaged data from the analyser resulted in higher r-values with hydrocarbons than their hourly and daily counterparts at Hope St. This is possibly the result of the different dispersion patterns of hydrocarbons and NO_2 . As discussed in Section 6.2.3.1, hydrocarbon concentrations are influenced by chemical reactions with hydroxyl radical. Therefore, for pollutants that do not follow similar dispersion patterns, correlations seem to be higher for longer averaging periods.

These results are in line with those reported by Wheeler et al. (2008), in a study in Canada using passive samplers with a 2-week exposure period. Correlation coefficients for data of 54 sites between NO_2 and benzene and toluene were approximately 0.8 in summer, winter, and spring. In a study of pollutant gradients with distance from a highway in Toronto, Beckerman et al. (2008) found that weekly measurements of benzene, toluene, ethylbenzene and xylenes were highly correlated to NO_2 and NO_x , with the highest r-values for benzene ($r=0.85$) and lowest for xylenes ($r=0.46$). Correlations with data collected within a street canyon were much more scattered, highlighting the influence of site specific topography on the pollutant correlations.

To sum up, NO₂ PDTs were shown by this study and related publications to have potential to be a useful and inexpensive method to explain spatial differences in other traffic-related air pollutants including PNC, BS, benzene and 1,3-butadiene.

CHAPTER 8

CONCLUSIONS, FURTHER WORK & LIMITATIONS OF THE PROJECT

8.1 LIMITATIONS OF THE STUDY & FURTHER WORK

The measurement period and monitoring sites examined in this study were limited, due to logistical problems preventing setting up equipment in certain locations and limited technical support for the challenging fieldwork attempted. In addition, the continuous problems mentioned with the WCPCs in Glasgow restrained the time available to measure at other locations.

The small dataset and different monitoring periods in Glasgow and London limited the comparability of the pollutant concentrations at both sites.

The degree of correlation between PNC and other traffic-related air pollutants was possibly influenced by the biases associated with the underestimation of particles by the WCPCs.

Examination of the correlations between pollutants was limited due to the small data set, which did not allow examination of the correlations by wind sector.

The different pattern of correlation between kerbside-street canyon and background sites illustrates that further investigation is necessary to better understand how different complex, built environments affect the correlation between pollutants, so as to inform health studies of the different exposure patterns.

Regression analysis between the increments in pollutant concentrations was shown to be a promising tool to estimate toxic and complex of measuring pollutants from NO_x concentrations. However, the study was limited to one paired location in each city. Examination of the regression between pollutants at the background sites paired with other sites should be carried out to confirm that the relationships found in this study can be extrapolated to larger areas.

Regarding the sequential extraction of PAHs and metals from PM filters, the sonication time used in this study to extract PAHs and estimated to be equivalent to the microwave digestion time used by Piñeiro et al. (2003) should be re-evaluated, in addition to possible metal losses during sonication compared to microwave digestion

(e.g. by performing a single and sequential extraction of an appropriate reference material).

This research has found significant associations between nitrogen oxides and PNC at locations relevant to human exposure. Future investigation could focus on validating the derived relationships by deriving PNC from observed nitrogen oxides concentrations and comparing them with observed PNC.

The uncertainty in the pollutant measurements may have affected the correlation between pollutants. This should be addressed in future research.

8.2 CONCLUSIONS

Large differences in mean concentrations of PNC, PM₁₀ and NO₂ were found between kerbside and background sites in Glasgow and London as a result of the higher traffic contribution to these pollutants at kerbside sites. The spatial gradients were similar for PNC and NO₂ and these were much larger than for PM₁₀, indicating that traffic contributes more to PNC and NO₂ than to PM₁₀. Consequently, NO₂ but not PM₁₀ represent well the spatial variation in PNC.

Temporal correlations between paired sites were moderate for PM₁₀ and PNC in London and Glasgow and moderate for NO₂ in London but high in Glasgow. This implies that PNC and PM₁₀ are not homogeneously distributed and therefore the use of a single monitoring site in epidemiological studies to represent average exposure of the population may lead to exposure misclassification. The different degree of correlation for NO₂ found in both cities suggests that results of exposure assessment studies cannot be extrapolated from city to city. However, it should be noted that the differences in the correlation coefficients found in London and Glasgow could be influenced by the proximity of the monitoring sites: being closer in Glasgow (300 m) than in London (4 km).

NO₂ and NO_x showed a high degree of correlation with other more toxic traffic-related air pollutants (PNC, water-soluble metals: Fe, Cu, As, Cd, Pb, 1,3-butadiene and BTEX) at background sites (St. Enoch Sq. and North Kensington) which are representative of population exposure and at different averaging periods representative of short-term exposure (hourly, daily). Thus, it can be concluded that NO₂ and NO_x represent well the mix of traffic-related air pollutants and could be used as a surrogate for PNC, 1-3-butadiene, BTEX and water-soluble Fe, Cu, As, Cd, Pb at background sites. However, the strength of the correlation did not persist in complex street canyon environments. The correlations between pollutants seem to be affected by small-scale variations in pollutant dispersion induced by the wind regimes created within street canyons.

The daily spatial variations (kerbside-background increments) in NO₂ and NO_x concentrations can be used to estimate up to 70 % of the spatial variation in PNC in Glasgow and London and 70 % of the spatial variation in Cu and Ni at Glasgow but not at London.

Absorbance of PM did not show a consistent correlation with PNC at all sites and therefore its use as surrogate for PNC cannot be generalised to all locations. Absorbance of PM_{2.5} showed a high degree of correlation with PNC at the kerbside site, but not at the background site in London. The increments in absorbance of PM_{2.5} explained up to 71 % of the spatial variation of PNC in London, and therefore it could be used a surrogate for PNC in this city. In contrast, absorbance of PM₁₀ (available for Glasgow) showed a low correlation coefficient with PNC at the background and kerbside site.

The similar between-pollutant and between-site correlation coefficients observed for hourly and daily averaged concentrations suggest that pollutant variations are driven by the diurnal pattern of traffic flows over the day and that meteorological effects do not affect this pattern. If the correlations were the effect of meteorology and long-transported air masses, then correlations between daily averages would be higher than their hourly counterparts, since the homogenising effects of meteorology and long-transported air masses are more evident over an entire day rather than on an hourly basis.

Systematic biases affected the performance of the PDTs. Overestimation by the NO₂ PDTs compared to chemiluminescence analyser readings may have been the result of reaction between co-diffusing NO and O₃ and by reduction of the diffusion path caused by wind turbulence at the entrance of the tube at locations where the tubes were exposed to high wind speed (St. Enoch Sq. and Hope St.). This overestimation may have been partly offset by underestimation caused by degradation of the absorbed nitrite over long periods of exposure. Nevertheless, at locations where PDTs were sheltered from high wind speeds (as at Montrose St.) and where exposure was limited to 1 week the accuracy of PDTs was within the ± 25 % specified by the EU Daughter Directive for NO₂. (EU, 1999).

NO_x concentrations measured with PDTs compared well with measurements from the analyser. This was thought to be the result of the cancelling out of two opposing biases: overestimation of NO₂ (discussed above) and an exposure-duration dependent underestimation of NO concentrations. Thus, although NO_x PDTs may disagree compared to the analyser on the distribution of NO₂ and NO they provide an accurate estimation of NO_x concentrations.

Weekly NO₂ and NO_x concentrations derived from PDTs explained up to 70 % of the variance in PNC and hydrocarbons. Therefore, they could be used to represent the temporal and spatial variations of these pollutants, although they could not be used to estimate the absolute concentrations, due to the biases mentioned. The advantage of this technique lies in its low cost and simple operation which allows measurement over wide areas to allow the creation of detailed maps of air pollution to assess population exposure in health studies.

A logarithmic relationship was found to best describe the relationship between NO₂ concentrations and increasing distance from a major road in Glasgow. Pedestrians were exposed to high NO₂ concentrations, with concentrations being over the UK's 24-hours Air Quality limit value for distances up to 60 m from the road.

An important conclusion, not stated in the research aims but which emerged during the study, was that the WCPCs consistently underestimated PNC measured by a BCPC. The underestimation could be corrected with the use of a regression equation between both particle counter models. However, results from this study showed a reduction in PNC after 6 weeks of continuous running possibly because of a reduced condensation efficiency caused by the aging of the growth tube where condensation of particles takes place. Results from this evaluation show that the WCPC is not yet a reliable particle counting technology and improvement of the lifetime of the growth tube should be studied.

8.3 IMPLICATIONS FOR EPIDEMIOLOGICAL STUDIES

So far, there are very few epidemiological studies that have looked at the effects of PNC on health. Most of the studies have used PM_{10} and NO_2 as surrogates for air pollution. The EU and the UK regulate only PM_{10} and NO_2 , however there is not a threshold value for PNC.

This study has shown that PNC is a better indicator of traffic-related air pollution than PM_{10} . Therefore, taking into account the growing importance of PNC in health effects, PNC should be regularly monitored to generate data so that epidemiological studies can also include PNC besides PM_{10} in their health assessments. The information derived from these studies could inform air quality policies to establish a limit value for PNC.

This study has shown that PNC are only moderately correlated between sites across the two studied cities and therefore monitoring at multiple locations is recommended to assess exposure within urban populations. Since PNC are difficult and expensive to measure, their concentration could be derived from NO_2 measurements. This study has shown similar spatial gradients between kerbside and background sites for NO_2 and PNC. The increments in NO_2 concentration between kerbside and background sites could be used to represent the increments in PNC. However, a specific relationship should be derived for each paired site, and each urban area.

The high correlation of nitrogen oxides and PNC implies that epidemiological studies based on time series analyses may not distinguish between their separate health effects. The separate health effects of PNC and PM_{10} might be more clearly distinguished in studies covering background areas (where both pollutants appear to be less well correlated). However, at sites influenced by traffic the correlation between PNC and PM_{10} appears to increase and different health effects of PNC and PM_{10} may not be distinguishable.

8.4 IMPLICATIONS FOR AIR QUALITY MONITORING

Local authorities should consider sheltering their NO₂ PDTs and reducing the sampling period to 1-week as these conditions have shown deviations compared to the reference method (chemiluminescence analyser) within the $\pm 25\%$ specified by the EU Daughter Directive for NO₂ (EU, 1999).

The respirable sampler, which consisted of a personal SKC pump and a cyclone, was shown to be unsuitable for long term measurement of the reflectance of respirable PM as the SKC pumps are not stable for continuous running periods.

The WCPC is not yet a reliable particle counting technology, as shown by the difference in concentrations measured compared with the BCPC. In addition, ways to improve the lifetime of the particle growth tube must be studied.

REFERENCES

- Aalto, P., Hameri, K., Paatero, P., Kulmala, M., Bellander, T., Berglind, N., Bouso, L., Castano-Vinyals, G., Sunyer, J., Cattani, G., Marconi, A., Cyrys, J., Von Klot, S., Peters, A., Zetzsche, K., Lanki, T., Pekkanen, J., Nyberg, F., Sjoval, B. & Forastiere, F. (2005) Aerosol particle number concentration measurements in five European cities using TSI-3022 condensation particle counter over a three-year period during health effects pollution on susceptible subpopulations. *Journal of the Air & Waste Management Association*, 55, 1064-1076.
- Ackermann-Lieblich, U., Leuenberger, P., Schwartz, J., Schindler, C., Monn, C., Bolognini, G., Bongard, J. P., Brandli, O., Domenighetti, G., Elsasser, S., Grize, L., Karrer, W., Keller, R., Keller-Wossidlo, H., Kunzli, N., Martin, B. W., Medici, T. C., Perruchoud, A. P., Schoni, M. H., Tschopp, J. M., Villiger, B., Wuthrich, B., Zellweger, J. P. & Zemp, E. (1997) Lung function and long term exposure to air pollutants in Switzerland. Study on Air Pollution and Lung Diseases in Adults (SAPALDIA) Team.
- Abelsohn, A., Sanborn, M. D., Jessiman, B. J. & Weir, E. (2002) Identifying and managing adverse environmental health effects: 6. Carbon monoxide poisoning. *Canadian Medical Association Journal*, 166, 1685-1690.
- ACGHI (1999) American Conference of Governmental Industrial Hygienists (ACGIH): Threshold Limit Values for Chemical Substances and Physical Agents and Biological Exposure Indices, 1-77.
- Adamson, I. Y. R., Prieditis, H., Hedgecock, C. & Vincent, R. (2000) Zinc Is the Toxic Factor in the Lung Response to an Atmospheric Particulate Sample. *Toxicology and Applied Pharmacology*, 166, 111-119.
- AEA (2006) FAQ www.airquality.co.uk
- AEA (2008). EAE Energy & Environment. Diffusion Tubes for ambient NO₂ monitoring. Practical Guidance. Report AEA/ENV/R/2504, to DEFRA and the devolved administrations.
- Agus, E. L., Young, D. T., Lingard, J. J. N., Smalley, R. J., Tate, J. E., Goodman, P. S. & Tomlin, A. S. (2007) Factors influencing particle number concentrations, size distributions and modal parameters at a roof-level and roadside site in Leicester, UK. *Science of The Total Environment*, 386, 65-82.
- AIRNET (2004) Air Pollution and the risks to human health – a toxicological perspective.
- Aksoy, M. D. (1985) Benzene as a leukemogenic and carcinogenic agent *American Journal of Industrial Medicine*, 8, 9-20.
- Allen, G., Sioutas, C., Koutrakis, P., Reiss, R., Lurmann, F.W., Roberts, P.T (1997) Evaluation of the TEOM method for measurement of ambient particulate mass in urban areas. *Journal of the Air and Waste Management Association*, 47, 682-689.

- Analitis, A., Katsouyanni, K., Dimakopoulou, K., Samoli, E., Nikoloulopoulos, A. K., Petasakis, Y., Touloumi, G., Schwartz, J., Anderson, H. R., Cambra, K., Forastiere, F., Zmirou, D., Vonk, J. M., Clancy, L., Kriz, B., Bobvos, J. & Pekkanen, J. (2006) Short-Term Effects of Ambient Particles on Cardiovascular and Respiratory Mortality. *Epidemiology*, 17, 230-233.
- APEG (1999) Airborne particles expert group. Source apportionment of airborne particulate matter in the UK. Report prepared by APEG for the Department for The Environment, Food and Rural Affairs. London.
- AQEG (2004) Air Quality Expert Group. Nitrogen Dioxide in the UK. Report prepared by AQEG for the Department for The Environment, Food and Rural Affairs. London. Available online at: http://www.defra.gov.uk/environment/airquality/aqeg_Last accessed: 15 Apr 2005.
- AQEG (2005) Air Quality Expert Group Particulate matter in the United Kingdom. Report prepared by AQEG for the Department for The Environment, Food and Rural Affairs. London. Available online at: <http://www.defra.gov.uk/environment/airquality/publications/particulate-matter/index.htm>. Last accessed 20 Jan 2008.
- AQEG (2007) Air Quality Expert Group Trends in primary nitrogen oxide in the UK. Report prepared by AQEG for the Department for The Environment, Food and Rural Affairs. London. Available online at: <http://www.defra.gov.uk/environment/airquality/publications/primaryno2-trends/index.htm>. Last accessed 7 Jan 2009.
- Arya, S.P. (1999) Air pollution meteorology and dispersion. , New York and Oxford: Oxford University Press.
- Atkins, C. H. F., Sandalls, J., Law, D. V., Hough, A. M., Stevenson, K., (1986). The measurement of nitrogen dioxide in the outdoor environment using passive diffusion tube samplers. AERE-R12133, Harwell Laboratory.
- Atkinson, R. (2000) Atmospheric chemistry of VOCs and NO_x. *Atmospheric Environment*, 34, 2063-2101.
- Atkinson, R. W., Anderson, H.R., Sunyer, J., Ayres, Baccini, J.M., Vonk, J.M., Boumgh, A., Forastiere, F., Forsberg, B., Touloumi, Bg., Schwartz, J., Katsouyanni, K. (2003) Acute Effects of Particulate Air Pollution on Respiratory Admissions. *In Revised Analyses of Time-series of Air Pollution and Health. Special Report: Health Effects Institute: Boston, MA* .
- ATSDR, 2005. Agency for Toxic Substances and Disease Registry. Toxicology profile for polyaromatic hydrocarbons. ATSDR's Toxicological Profiles on CD-ROM, CRC Press, Boca Raton, FL.
- Aunan, K. & Pan, X.-C. (2004) Exposure-response functions for health effects of ambient air pollution applicable for China - a meta-analysis. *Science of The Total Environment*, 329, 3-16.

- Ayers, G. P. (2001) Comment on regression analysis of air quality data. *Atmospheric Environment*, 35, 2423-2425.
- BADC (2008). British Atmospheric Data Centre. Available on line (registration needed) at <http://cdat.badc.nerc.ac.uk/cgi-bin/dxui.pyn> Last accessed 17 Feb 2008
- BSI (1969) Methods for the measurement of air pollution. Part 2: Determination of concentrations of suspended matter, British Standard 1747:Part 2:1969, British Standards Institute, London
- BSI (1998). BS EN 12341:1998. Air quality—determination of the PM₁₀ fraction of suspended particulate matter— reference method and field test procedure to demonstrate reference equivalence of measurement methods. British Standards Institute, London.
- Baltensperger, U., Weingartner, E., Burtscher, H., Keskinen, J. (2001) *Dynamic mass and surface area measurements*. In Willeke, K., Baron, B.A (Eds) *Aerosol measurement: principles, techniques and applications*, (pp. 87-418) New York: Willey.
- Bayram, H., Sapsford, R. J., Abdelaziz, M. M. & Khair, O. A. (2001) Effect of ozone and nitrogen dioxide on the release of proinflammatory mediators from bronchial epithelial cells of nonatopic nonasthmatic subjects and atopic asthmatic patients in vitro. *Journal of Allergy and Clinical Immunology*, 107, 287-294.
- Baulig, A., Poirault, J. J., Ausset, P., Schins, R., Shi, T., Baralle, D., Dorlhene, P., Meyer, M., Lefevre, R., Marano, F. (2004) Physicochemical Characteristics and Biological Activities of Seasonal Atmospheric Particulate Matter Sampling in Two Locations of Paris *Environmental Science and Technology*, 38, 5985-92.
- Beelen, R., Hoek, G., Fischer, P., Brandt, P. A. van den. & Brunekreef, B. (2007) Estimated long-term outdoor air pollution concentrations in a cohort study. *Atmospheric Environment*, 41, 1343-1358.
- Bell, M. L., Dominici, F., Samet, J. M. (2005) A Meta-Analysis of Time-Series Studies of Ozone and Mortality With Comparison to the National Morbidity, Mortality, and Air Pollution Study. *Epidemiology*, 16, 436-445.
- Beckerman, B., Jerrett, M., Brook, J. R., Verma, D. K., Arain, M. A. & Finkelstein, M. M. (2008) Correlation of nitrogen dioxide with other traffic pollutants near a major expressway. *Atmospheric Environment*, 42, 275-290.
- Bethel, R. A., Epstein, J., Sheppard, D. (1983) Sulfur dioxide-induced bronchoconstriction in freely breathing, exercising, asthmatic subjects. *American Review of Respiratory Disease* 128, 987-990.
- Berverland, I. J., Heal, M. R., Agius, R. M., Hibbs, L. R., Elton, R. & Fowler, D. (2002) The metal content of airborne particles in Edinburgh: application to epidemiological research. Final Project Report to Department of Health.

- Biswas, S., Fine, P. M.; Geller, M. D.; Hering, S. V.; Sioutas, C. (2005) Performance evaluation of a recently developed water-based condensation particle counter. *Aerosol Science and Technology*, 39, 419-427.
- Bjorseth, A., Ramdahl, T., (Ed.) (1985) *Sources and emissions of PAH. In: Emission Sources and Recent Progress in Analytical Chemistry. Handbook of Polycyclic Aromatic Hydrocarbons, vol. 2*, New York and Barcel, Marcel Dekker.
- Brauer, M. & Brook, J. R. (1997) Ozone personal exposures and health effects for selected groups residing in the Fraser Valley. *Atmospheric Environment*, 31, 2113-2121.
- Brauer, M., Hrubá, F., Mihalíková, E., Fabiánová, E., Miskovic, P., Plzиковá, A., Lendacká, M., Vandenberg, J. & Cullen, A. (2000) Personal exposure to particles in Banska Bystrica, Slovakia. *Journal of Exposure Analysis and Environmental Epidemiology* 10, 478-487.
- Brauer, M., Ebel, S. T., Fisher, T. V., Brumm, J., Petkau, A. J. & Vedal, S. (2001) Exposure of chronic obstructive pulmonary disease patients to particles: Respiratory and cardiovascular health effects. *Journal Exposure Analytical Environmental Epidemiology*, 11, 490-500.
- Brauer, M., Brumm, J., Vedal, S., Petkau, A. J. (2002) Exposure Misclassification and Threshold Concentrations in Time Series Analyses of Air Pollution Health Effects. *Risk Analysis*, 22, 1183 - 1193.
- Brauer, M., Hoek, G., Vliet, P. van, Meliefste, K., Fischer, P., Gehring, U., Heinrich, J., Cyrys, J., Bellander, T., Lewne, M., Brunekreef, B. (2003) Estimating Long-Term average particulate air pollution concentrations: application of traffic indicators and geographic information systems. *Epidemiology*, 14, 228-239.
- Braun-Fahrlander, C., Vuille, J. C., Sennhauser, F. H., Neu, U., Kunzle, T., Grize, L., Gassner, M., Minder, C., Schindler, C., Varonier, H. S. & Wuthrich, B. (1997) Respiratory health and long-term exposure to air pollutants in Swiss schoolchildren. SCARPOL Team. Swiss Study on Childhood Allergy and Respiratory Symptoms with Respect to Air Pollution, Climate and Pollen. *American Journal of Respiratory Critical Care Medicine*. 155, 1042-1049.
- Briggs, D. J., Collins, S., Elliott, P., Fischer, P., Kingham, S., Lebret, E., Pryn, K., Reeuwijk, H. V., Smallbone, K. & Veen, A. V. D. (1997) Mapping urban air pollution using GIS: a regression-based approach. *International Journal of Geographical Information Science*, 11, 699-718.
- Briggs, D. J., De Hoogh, C., Gulliver, J., Wills, J., Elliott, P., Kingham, S. & Smallbone, K. (2000) A regression-based method for mapping traffic-related air pollution: application and testing in four contrasting urban environments. *The Science of The Total Environment*, 253, 151-167.
- Brown, R. K., Wyatt, H., Price, J. F., Kelly, F. J. (1996) Pulmonary dysfunction in cystic fibrosis is associated with oxidative stress *European Respiratory Journal* 9, 334-339

- Brown, D. M., Wilson, M. R., Macnee, W., Stone, V. & Donaldson, K. (2001) Size-Dependent Proinflammatory Effects of Ultrafine Polystyrene Particles: A Role for Surface Area and Oxidative Stress in the Enhanced Activity of Ultrafines. *Toxicology and Applied Pharmacology*, 175, 191-199.
- Brown, D. M., Donaldson, K., Stone, V. (2004) Effects of PM₁₀ in human peripheral blood monocytes and J774 macrophages. *Respiratory Research*, 5.
- Brown, D. M., Hutchison, L., Donaldson, K. & Stone, V. (2007) The effects of PM₁₀ particles and oxidative stress on macrophages and lung epithelial cells: modulating effects of calcium-signalling antagonists. *American Journal of Physiology and Lung Cell Molecular Physiology* 292, L1444-1445.
- Brown, R. J. C. (2008) The use and abuse of limits of detection in environmental analytical chemistry. *The Scientific World Journal*, 8, 796-801.
- Browning, E. (1965) *Toxicity and Metabolism of Industrial Solvents*, (pp.412–462). New York: Elsevier
- Brunekreef, B., Holgate, S. T. (2002) Air pollution and health. *The Lancet*, 369, 1233-1242.
- Brunekreef, B., Janssen, N. A., De Hartog, J. J., Oldenwening, M., Meliefste, K., Hoek, G., Lanki, T., Timonen, K. L., Vallius, M., Pekkanen, J., Van Grieken, R. & (2005) Personal, indoor, and outdoor exposures to PM_{2.5} and its components for groups of cardiovascular patients in Amsterdam and Helsinki. *Research Reports Health Effects Institute*, No. 127, 1-70.
- Buczynska, A. J., Krata, A., Stranger, M., Locateli Godoi, A. F., Kontozova-Deutsch, V., Bencs, L., Naveau, I., Roekens, E. & Van Grieken, R. (2009) Atmospheric BTEX-concentrations in an area with intensive street traffic. *Atmospheric Environment*, 43, 311-318.
- Buddingh, F., Bailey, M.J., Wells, B., Haesemeyer, J. (1981) Physiological significance of benzo(a)pyrene adsorbed to carbon blacks: Elution studies, AHH determinations. *American Industrial Hygiene Association Journal* 42, 503-509
- Burnett, R. T., Brook, J., Dann, T., Delocla, C., Philips, O., Cakmak, S., Vincent, R., Goldberg, M.S, Krewski, D. (2000) Association between particulate- and gas-phase components of urban air pollution and daily mortality in eight Canadian cities. *Inhalation Toxicology*, 12, 15-39
- Busbin, D. D., Feigley, C. E., Salzberg, D., Underhill, D. W. (2006) A second look at the Palmes' Diffusive Sampler. *Journal of the Air & Waste Management Association* 56, 1431-1439.
- Buschini, A., Cassoni, F., Anceschi, E., Pasini, L., Poli, P. & Rossi, C. (2001) Urban airborne particulate: genotoxicity evaluation of different size fractions by mutagenesis tests on microorganisms and comet assay. *Chemosphere*, 44, 1723-1736.

- Campen, M. J., Nolan, J. P., Schladweiler, M. C. J., Kodavanti, U. P., Evansky, P. A., Costa, D. L., Watkinson, W. P. (2001) Cardiovascular and thermoregulatory effects of inhaled PM-associated transition metals: A potential interaction between nickel and vanadium sulfate. *Toxicological Sciences*, 64, 243-252.
- Carslaw, D. C. & Beevers, S. D. S. D. (2004) Investigating the potential importance of primary NO₂ emissions in a street canyon. *Atmospheric Environment*, 38, 3585-3594.
- Carslaw, D. C. & Beevers, S. D. (2005) Estimations of road vehicle primary NO₂ exhaust emission fractions using monitoring data in London. *Atmospheric Environment*, 39, 167-177.
- Castaño-Vinyals, G., D'errico, A., Malats, N. & Kogevinas, M. (2004) Biomarkers of exposure to polycyclic aromatic hydrocarbons from environmental air pollution. *Occupational and Environmental Medicine*, 61, e12.
- Cape, J. N., Tang, Y. S., Van Dijk, N., Love, L., Sutton, M. A. & Palmer, S. C. F. (2004) Concentrations of ammonia and nitrogen dioxide at roadside verges, and their contribution to nitrogen deposition. *Environmental Pollution*, 132, 469-478.
- Carter, J. D., Ghio, A. J., Samet, J. M. & Devlin, R. B. (1997) Cytokine Production by Human Airway Epithelial Cells after Exposure to an Air Pollution Particle Is Metal-Dependent. *Toxicology and Applied Pharmacology*, 146, 180-188.
- Castillejos, M., Gold, D. R., Dockery, T. Tosteson, T. Baum, & Speizer, F. (1992) Effects of ambient ozone on respiratory functions and symptoms in school children in Mexico City. *The American Review of Respiratory Diseases*, 145, 276-282
- CEN 1992 prEN481 European Standardization Committee (CEN): Size Fraction Definitions for Measurement for Measurement of Airborne Particles in Workplaces, CEN, Brussels.
- Chang, C. T. & Chen, B. Y. (2008) Toxicity assessment of volatile organic compounds and polycyclic aromatic hydrocarbons in motorcycle exhaust. *Journal of Hazardous Materials*, 153, 1262-1269.
- Charron, A. & Harrison, R. M. (2003) Primary particle formation from vehicle emissions during exhaust dilution in the roadside atmosphere. *Atmospheric Environment*, 37, 4109-4119.
- Charron, A., Harrison, R. M., Moorcroft, S. & Booker, J. (2004) Quantitative interpretation of divergence between PM₁₀ and PM_{2.5} mass measurement by TEOM and gravimetric (Partisol) instruments. *Atmospheric Environment*, 38, 415-423.
- Champion, J. A. & Mitragotri, S. (2006) From the Cover: Role of target geometry in phagocytosis. *Proceedings of the National Academy of Sciences of the United States of America*, 103, 4930-4934.

- Chauhan, A. J., Inskip, H. M., Linaker, C. H., Smith, S., Schreiber, J., Johnston, S. L. & Holgate, S. T. (2003) Personal exposure to nitrogen dioxide (NO₂) and the severity of virus-induced asthma in children. *The Lancet*, 361, 1939-1944.
- Chen, F., Ding, M., Castranova, V. & Shi, X. (2001) Carcinogenic metals and NF-kappaB activation. *Molecular and Cellular Biochemistry*, 222, 159-171.
- Chin, B. Y., Choi, M. E., Burdick, M. D., Strieter, R. M., Risby, T. H. & Choi, A. M. K. (1998) Induction of apoptosis by particulate matter: role of TNF-alpha and MAPK. *American Journal of Physiology*, 275, L942-949.
- Chávez, E., Jay, D. & Bravo, C. (1987) The mechanism of lead-induced mitochondrial Ca²⁺ efflux *Journal of Bioenergetics and Biomembranes*, 19, 285-295.
- Chow, J. C. (1995) Measurement methods to determine compliance with ambient air quality standards for suspended particulates. *Journal of the Air and Waste Management Association*, 45, 320-382.
- Costa, D. L., Dreher, K. L. (1997) Bioavailable transition metals in particulate matter mediate cardiopulmonary injury in healthy and compromised animal models. *Environmental Health Perspectives*, 105, 1053-1060.
- Crowther, J. M., Galeil, A. & Hassan, A.A (2002) Three-Dimensional Numerical Simulation of Air Pollutant Dispersion in Street Canyons *Water, Air, and Soil Pollution*, 2, 279-295.
- Cyrus, J., Heinrich, J., Brauer, M. & Wichmann, H. E. (1998) Spatial variability of acidic aerosols, sulfate and PM₁₀ in Erfurt, Eastern Germany. *Journal of Exposure Analysis and Environmental Epidemiology* 8, 447-464.
- Cyrus, J., Stölzel, M., Heinrich, J., Kreyling, W. G., Menzel, N., Wittmaack, K., Tuch, T. & Erich Wichmann, H. E. (2003a) Elemental composition and sources of fine and ultrafine ambient particles in Erfurt; Germany. *Science of the Total Environment*, 143-156.
- Cyrus, J., Heinrich, J., Hoek, G., Meliefste, K., Lewne, M., Gehring, U., Bellander, T., Fischer, P., Vliet, P. V., Brauer, M., Wichmann, H. E. & Brunekreef, B. (2003b) Comparison between different traffic-related particle indicators: Elemental carbon (EC), PM_{2.5} mass, and absorbance. *Journal of exposure analysis and environmental epidemiology* 13, 134-143.
- Cyrus, J., Pitz, M., Heinrich, J., Wichmann, H. E. & Peters, A. (2008) Spatial and temporal variation of particle number concentration in Augsburg, Germany. *Science of The Total Environment*, 401, 168-175.
- Cyrus, J., Pitz, M., Heinrich, J., Wichmann, H. E. & Peters, A. (2008) Spatial and temporal variation of particle number concentration in Augsburg, Germany. *Science of The Total Environment*, 401, 168-175.
- Damji, K. S. & Richters, A. (1989) Reduction in T lymphocyte subpopulations following acute exposure to 4 ppm nitrogen dioxide. *Environmental Research*, 49, 217-224.

- DEFRA (2003) Department for the Environment, Food and Rural Affairs (DEFRA), 2003. Technical Guidance LAQM. TG(03), Local Air Quality Management, London.
- DEFRA (2006). UK Equivalence Programme for Monitoring of Particulate Matter. Final Report for: Department for the Environment, Food and Rural Affairs; Welsh Assembly Government; Scottish Executive; Department of Environment for Northern Ireland. Ref: BV/AQ/AD202209/DH/2396
- DEFRA (2007). The Air Quality Strategy for England, Scotland, Wales and Northern Ireland. Department for Environment, Food and Rural Affairs in partnership with the Scottish Executive, Welsh Assembly Government and Department of the Environment Northern Ireland.
- DEFRA (2008) Diffusion Tubes for Ambient NO₂ Monitoring: Practical Guidance. AEAT/ENV/R/2504
- Delfino, R. J., Sioutas, C. & Malik, S. (2005) Potential Role of Ultrafine Particles in Associations between Airborne Particle Mass and Cardiovascular Health *Environmental Health Perspectives* 113, 934–946.
- DETR (1997) UK Smoke and Sulphur Dioxide Network Instruction Manual, AEAT-1806, AEA Technology, Harwell.
- DETR (2000a) Department for the Environment, Transport and the Regions (DETR), 2000a. The Air Quality Strategy for England, Scotland, Wales and Northern Ireland, London.
- DETR (2000b) Department for the Environment, Transport and the Regions (DETR), 2000b. First Phase Air Quality Review and Assessment: A Summary, London.
- Devlin, R. B., Horstman, D. P., Gerrity, T. R., Becker, S., Madden, M. C., Biscardi, F., Hatch, G.E. & Koren, H. S. (1999) Inflammatory response in humans exposed to 2.0 ppm nitrogen dioxide. *Inhalation Toxicology*, 11, 89-109.
- Dick, C. A. J., Brown, D. M., Donaldson, K. & Stone, V. (2003) The role of free radicals in the toxic and inflammatory effects of four different ultrafine particle types. *Inhalation Toxicology*, 15, 39-52.
- Divita, F., Ondov, J. M., Suarez, A. E. (1996) Size spectra and atmospheric growth of V-containing aerosols in Washington DEC. *Aerosol Science and Technology* 25, 256-273.
- Dockery, D. W., Pope III C. A., Xu, X., Spengler, J. D., Ware, J. H., Fay, M. E., Ferris Jr, B. G. & Speizer, F. E. (1993) An association between air pollution and mortality in six U.S. cities. *New England Journal of Medicine*, 329, 1753-9.
- Dockery, D. W. & Stone, P. H. (2007) Cardiovascular risks from fine particulate air pollution. *New England Journal of Medicine*, 356, 511-3.

- Dollard, G. J., Dumitrean, P., Telling, S., Dixon, J. & Derwent, R. G. (2007) Observed trends in ambient concentrations of C2-C8 hydrocarbons in the United Kingdom over the period from 1993 to 2004. *Atmospheric Environment*, 41, 2559-2569.
- Dominici, F. & Burnett, R. (2003) Risk Models for Particulate Air Pollution. *Journal of Toxicology and Environmental Health Part A*, 66, 1883-1890.
- Donaldson, K., Brown, D. M., Mitchell, C., Dineva, M., Beswick, P. H., Gilmour, P. & Macnee, W. (1997) Free radical activity of PM₁₀: iron-mediated generation of hydroxyl radicals. *Environmental Health Perspectives*, 105, 1285-1289.
- Donaldson, K., Brown, D., Clouter, A., Duffin, R., Macnee, W., Renwick, L., Tran, L. & Stone, V. (2002) The Pulmonary Toxicology of Ultrafine Particles. *Journal of Aerosol Medicine*, 15, 213-220.
- Donaldson, K., Borm P. (2007) *Particle Toxicology*, New York, Taylor and Francis.
- Donbrow, M. (1996) Instrumental methods in analytical chemistry: their principles and practice. Vol 1. Pitman.
- EC (1996). European Commission. Council Directive 96/62/EC of 27 September 1996 on ambient air quality assessment and management. ([Air Quality Framework Directive](#)).
- Englert, N. (2004) Fine particles and human health--a review of epidemiological studies. *Toxicology Letters*, 149, 235-242.
- EN 14907 Ambient air quality - Standard gravimetric measurement method for the determination of the PM_{2,5} mass fraction of suspended particulate matter. CEN, Brussels, 2005.
- EU (1999). 'Council Directive 1999/30/EC Relating to Limit Values for sulphur Dioxide, Nitrogen Dioxide and Oxides of Nitrogen, Particulate Matter and Lead in Ambient Air', Official Journal of the European Communities L163/41.
- Faus-Kessler, T., Kirchner, M. & Jakobi, G. (2008) Modelling the decay of concentrations of nitrogenous compounds with distance from roads. *Atmospheric Environment*, 42, 4589-4600.
- Fernandez Espinosa, A. J., Ternero Rodriguez, M., Barragan De La Rosa, F. J. & Jimenez Sanchez, J. C. (2002) A chemical speciation of trace metals for fine urban particles. *Atmospheric Environment*, 36, 773-780.
- Fernández-Martínez, G., López-Mahía, P., Muniategui-Lorenzo, S., Prada-Rodríguez, D., Fernández-Fernández, E. (2001) Measurement of Volatile Organic Compounds in Urban Air of La Coruña, Spain *Water, Air, & Soil Pollution*, 129, 267-288.
- Ferm, M. & Svanberg, P.-A. (1998) Cost-efficient techniques for urban- and background measurements of SO₂ and NO₂. *Atmospheric Environment*, 32, 1377-1381.

- Field, R. A., Goldstone, M. E., Lester, J. N. & Perry, R. (1992) The sources and behaviour of tropospheric anthropogenic volatile hydrocarbons. *Atmospheric Environment. Part A. General Topics*, 26, 2983-2996.
- Filleul, L., Rondeau, V., Vandentorren, S., Le Moual, N., Cantagrel, A., Annesi-Maesano, I., Charpin, D., Declercq, C., Neukirch, F., Paris, C., Vervloet, D., Brochard, P., Tessier, J. F., Kauffmann, F. & Baldi, I. (2005) Twenty five year mortality and air pollution: results from the French PAARC survey. *Occupational and Environmental Medicine*, 62, 453-460.
- Fischer, P. H., Hoek, G., Van Reeuwijk, H., Briggs, D. J., Lebret, E., Van Wijnen, J. H., Kingham, S. & Elliott, P. E. (2000) Traffic-related differences in outdoor and indoor concentrations of particles and volatile organic compounds in Amsterdam. *Atmospheric Environment*, 34, 3713-3722.
- Forastiere, F., Stafoggia, M., Picciotto, S., Bellander, T., D'ippoliti, D., Lanki, T., Von Klot, S., Nyberg, F., Paatero, P., Peters, A., Pekkanen, J., Sunyer, J. & Perucci, C. A. (2005) A Case-Crossover Analysis of Out-of-Hospital Coronary Deaths and Air Pollution in Rome, Italy. *American Thoracic Society*, 172, 1549-1555.
- Frampton, M. W., Smeglin, A. M., Roberts, J. N. J., Finkelstein, J. N., Morrow, P. E. & Utell, M. J. (1989) Nitrogen dioxide exposure in vivo and human alveolar macrophage inactivation of influenza virus in vitro. *Environmental Research*, 48, 179-192.
- Frampton, M. W., Ghio, A. J., Samet, J. M., Carson, J. L., Carter, J. D., Devlin, R. B. (1999) Effects of aqueous extracts of PM₁₀ filters from the Utah Valley on human airway epithelial cells. *American Journal of Physiology - Lung Cellular and Molecular Physiology*, 277, L960-L967.
- Frampton, M. W., Boscia, J., Roberts, N. J. Jr., Azadniv, M., Torres, A., Cox, C., Morrow, P. E., Nichols, J., Chalupa, D., Frasier, L.M., Gibb, F. R., Speers, D. M., Tsai, Y., Utell, M. J. (2002) Nitrogen dioxide exposure: effects on airway and blood cells. *American Journal of Physiology - Lung Cellular and Molecular Physiology*, 282, L155-165.
- Fusco, D., Forastiere, F., Michelozzi, P., Spadea, T., Ostro, B., Arca, M. & Perucci, C. A. (2001) Air pollution and hospital admissions for respiratory conditions in Rome, Italy. *European Respiratory Journal* 17, 1143-1150.
- Garza, A., Vega, R., Soto, E. (2006) Cellular mechanisms of lead neurotoxicity. *Medical science monitor: international medical journal of experimental and clinical research*, 12, RA57-65.
- Gauderman, W. J., Avol, E., Lurmann, F., Kuenzli, N., Gilliland, F., Peters, J. & McConnell, R. (2005) Childhood asthma and exposure to traffic and nitrogen dioxide. *Epidemiology* 16, 737-743.
- Gair, A. J. & Penkett, S. A. (1995) The effects of wind speed and turbulence on the performance of diffusion tube samplers. *Atmospheric Environment*, 29, 2529-2533.

- GCC (2008) Glasgow City Council. Retrieved from <http://www.glasgow.gov.uk> Last accessed 26 Sep 2008.
- Gelencser, A., Siszler, K. & Hlavay, J. (1997) Toluene:Benzen Concentration Ratio as a Tool for Characterizing the Distance from Vehicular Emission Sources. *Environmental Science & Technology*, 31, 2869-2872.
- Gerboles, M., Amantini, L., (1993). Validation of measurement by NO₂ passive sampler. A comparison with chemiluminescent monitor. Technical Note TNI/93/107, Environment Institute, Joint Research Centre, Ispra Italy.
- Gerde, P., Muggenburg, B. A., Lundborg, M. & Dahl, A. R. (2001) The rapid alveolar absorption of diesel soot-adsorbed benzo[a]pyrene: bioavailability, metabolism and dosimetry of an inhaled particle-borne carcinogen. *Carcinogenesis*, 22, 741-749
- Gerlofs-Nijland, M. E, Dormans J. A, Bloemen, H. J, Leseman, D. L, John, A., Boere, F., Kelly, F. J., Mudway, I.S., Jimenez, A.A., Donaldson, K., Guastadisegni, C., Janssen N.A., Brunekreef, B., Sandstrom, T., van Bree L., Cassee, F. R. (2007) Toxicity of coarse and fine particulate matter from sites with contrasting traffic profiles. *Inhaationl Toxicology*,;19, 1055-69.
- Germani, M. S. & Zoller, W. H. (1994) Solubilities of elements on in-stack suspended particles from a municipal incinerator. *Atmospheric Environment*, 28, 1393-1400.
- Ghio, A. J. (1999) Metals associated with both the water-soluble and insoluble fractions of an ambient air pollution particle catalyze an oxidative stress. *Inhalation toxicology* 11, 37-49.
- Ghio, A. J., Kim, C. & Devlin, R. B. (2000) Concentrated Ambient Air Particles Induce Mild Pulmonary Inflammation in Healthy Human Volunteers. *American Journal of Respiratory and Critical Care Medicine*, 162, 981-988
- Ghio, A. J., Piantadosi, C. A., Wang, X., Dailey, L. A., Stonehuerner, J. D., Madden, M. C., Yang, F., Dolan, K. G., Garrick, M. D. & Garrick, L. M. (2005) Divalent metal transporter-1 decreases metal-related injury in the lung. *American Journal of Physiology- Lung Cellular and Molecular Physiology* 289, L460-467.
- Gidhagen, L., Johansson, C., Langner, J. & Foltescu, V. L. (2005) Urban scale modelling of particle number concentration in Stockholm. *Atmospheric Environment*, 39, 1711-1725.
- Gilbert, N. L., Woodhouse, S., Stieb, D. M. & Brook, J. R. (2003) Ambient nitrogen dioxide and distance from a major highway. *The Science of The Total Environment*, 312, 43-46.
- Goldberg, M. S., Burnett, R. T., Yale, J. F., Valois, M. F. & Brook, J. R. (2006) Associations between ambient air pollution and daily mortality among persons with diabetes and cardiovascular disease. *Environmental Research*, 100, 255-267.
- Götschi, T., Hazenkamp-Von Arx, M. E., Heinrich, J., Bono, R., Burney, P., Forsberg, B., Jarvis, D., Maldonado, J., Norbäck, D., Stern, W. B., Sunyer, J., Torén, D., Verlato,

- G., Villani, S. & Künzli, N. (2005) Elemental composition and reflectance of ambient fine particles at 21 European cities. *Atmospheric Environment*, 39, 5947-5958.
- Gregg, A. S., Sing, K. S. (1995) *Adsorption, surface area and porosity*, London, Academic Press.
- Green, D., Fuller, G., Barrat, B. (2001) Evaluation of TEOM correction factors for assessing the EU Stage 1 limit values of PM₁₀. *Atmospheric Environment*, 35, 2589-2593.
- Grivas, G., Chaloulakou, A. & Kassomenos, P. (2008) An overview of the PM₁₀ pollution problem, in the Metropolitan Area of Athens, Greece. Assessment of controlling factors and potential impact of long range transport. *Science of The Total Environment*, 389, 165-177.
- Hamilton, R., Gorbunov, B. & Semenov, M. (1995) A new version of black smoke method. *Journal of Aerosol Science*, 26, S189-S190.
- Hamilton, R. P. & Heal, M. R. (2004) Evaluation of method of preparation of passive diffusion tubes for measurement of ambient nitrogen dioxide. *Journal of Environmental Monitoring*, 6, 1217.
- Han, X. & Naeher, L. P. (2006) A review of traffic-related air pollution exposure assessment studies in the developing world. *Environment International*, 32, 106-120.
- Harrison, R. M., Deacon, A.R., Jones, M. R., Appleby, R.S. (1997) Sources and processes affecting concentrations of PM₁₀ and PM_{2.5} particulate matter in Birmingham (U.K.). *Atmospheric Environment*, 31, 4103-4117.
- Harrison, R. M., Jones, M. & Collins, G. (1999) Measurements of the physical properties of particles in the urban atmosphere. *Atmospheric Environment*, 33, 309-321.
- Harrison, R. M., Charron, A., Lawrence, R. & Jones, A. M. (2000) Mass Closure and Source Apportionment Studies of Urban Atmospheric Aerosol. Division of Environmental Health and Risk Management, School of Geography, Earth and Environmental Sciences, The University of Birmingham, United Kingdom.
- Harrison, R.M. 2003a PM₁₀ sources and composition and their relevance for human health. University of Birmingham. Available online at:
http://atmos.chem.le.ac.uk/group/ppt/harrison_031705.ppt. Last accessed 27 Oct 2008.
- Harrison, R. M., Tilling, R., Callen, N., Romero, M. S., Harrad, S. & Jarvis, K. (2003b) A study of trace metals and polycyclic aromatic hydrocarbons in the roadside environment. *Atmospheric Environment*, 37, 2391-2402.
- Harrison, R. M. & Jones, A. M. (2005) Multisite Study of Particle Number Concentrations in Urban Air. *Environmental Science and Technology*, 39, 6063-6070.

- Heal, M. R., Cape, J.N (1997) A numerical evaluation of chemical interferences in the measurement of ambient nitrogen dioxide by passive diffusion samplers. *Atmospheric Environment*, 31, 1911-1923.
- Heal, M. R., O'donoghue, M. A. & Cape, J. N. (1999) Overestimation of urban nitrogen dioxide by passive diffusion tubes: a comparative exposure and model study. *Atmospheric Environment*, 33, 513-524.
- Heal, M., Kirby, C., Cape, J. N. (2000) Systematic Biases in Measurement of Urban Nitrogen Dioxide using Passive Diffusion Samplers *Environmental Monitoring and Assessment*, 62, 39-54.
- Heal, M.R. (2005) University of Edinburgh, Edinburgh. Personal communication.
- Heal, M. R., Hibbs, L. R., Agius, R. M. & Beverland, I. J. (2005) Total and water-soluble trace metal content of urban background PM₁₀, PM_{2.5} and black smoke in Edinburgh, UK. *Atmospheric Environment*, 39, 1417-1430.
- Heal, M.R. (2007) University of Edinburgh, Edinburgh. Personal communication.
- Heflich, R. H., Fifer, E. K., Djuric, A., Beland, F. A. (1985) DNA adduct formation and mutation induction by nitropyrenes in Salmonella and Chinese hamster ovary cells: relationships with nitroreduction and acetylation. *Environmental Health Perspectives*, 135-143.
- HEI (1995). Health Effects Institute. Diesel exhaust: a critical analysis of emissions, exposure and health effects. Cambridge, MA.
- HEI (2003) Health Effects Institute. Revised analyses of time-series studies of air pollution and health. Special report. Boston, MA.
- Henderson, D. (2005) PhD Thesis Exposure assessment and characterization in air pollution epidemiology, University of Strathclyde, Glasgow.
- Hering, S., Stolzenburg, M., Quant, F., Oberreit, D. & Keady, P. (2005) A Laminar-Flow, Water-Based Condensation Particle Counter (WCPC). *Aerosol Science and Technology*, 39, 659-672.
- Hetland, R. B., Cassee, F.R., Låg, M., Refsnes, M., Dybing, E., Schwarze, P.E (2005) Cytokine release from alveolar macrophages exposed to ambient particulate matter: Heterogeneity in relation to size, city and season. *Particle and Fibre Toxicology*, 2:4
- Heunks, L. M. A. & Dekhuijzen, P. N. R. (2000) Respiratory muscle function and free radicals: from cell to COPD.
- Hibbs, L.R. (2002) PhD Thesis: Metal Content of Airborne Particulate Matter in Edinburgh. University of Edinburgh, Edinburgh.
- Hinds, W. C. (1982) *Aerosol Technology: properties, behaviour, and measurement of airborne particles* New York, Wiley.

- Ho, K. F., Lee, S. C., Guo, H. & Tsai, W. Y. (2004) Seasonal and diurnal variations of volatile organic compounds (VOCs) in the atmosphere of Hong Kong. *Science of The Total Environment*, 322, 155-166.
- Hoek, G., Brunekreef, B., Goldbohm, S., Fisher, P. & Brandt, A. V. D. (2002a) Association between mortality and indicators of traffic-related air pollution in the Netherlands: a cohort study. *The Lancet*, 360, 1203-1209.
- Hoek, G., Meliefste, K., Cyrus, J., Lewne, M., Bellander, T., Brauer, M., Fischer, P., Gehring, U., Heinrich, J., Van Vliet, P. & Brunekreef, B. (2002b) Spatial variability of fine particle concentrations in three European areas. *Atmospheric Environment*, 36, 4077-4088.
- Holz, O., Mücke, M., Paasch K., Böhme, S., Timm P., Richter, K., Magnussen, H., Jörres, R.A. (2002) Repeated ozone exposures enhance bronchial allergen responses in subjects with rhinitis or asthma. *Clinical and experimental Allergy*, 32, 681-689.
- Hong, Y. C., Hwang, S. S., J.H., K., Lee, K. H., Lee, H. J., Yu, S. D. & Kim, D. S. (2007) Metals in particulate pollutants affect peak expiratory flow of schoolchildren. *Environmental Health Perspectives*, 115, 430-434.
- Horstman, D. H. & Folinsbee, L. J. (1989) Sulfur dioxide-induced bronchoconstriction in asthmatics exposed for short durations under controlled conditions: a selected review In: M.J. Utell and R. Frank, Editors, Susceptibility to inhaled pollutants, American Society for Testing and Materials, Philadelphia (1989).
- Horvath, H., Jager, J., Kreiner, I. & Norek, C. (1986) Determination of the size-dependent light absorption coefficient of aerosols. *Journal of Aerosol Science*, 17, 258-260.
- Horvath, H. (1993) Atmospheric light absorption--A review. *Atmospheric Environment. Part A. General Topics*, 27, 293-317.
- Horvath, H. (1995) Size segregated light absorption coefficient of the atmospheric aerosol. *Atmospheric Environment*, 29, 875-883.
- Horvath, H. (1996) Black smoke as a surrogate for PM10 in health studies. *Atmospheric Environment*, 30, 2649-2650.
- IARC (1973). International Agency for Research on Cancer. Volume 3 Certain Polycyclic Aromatic Hydrocarbons and Heterocyclic Compounds. Lyon, France.
- IARC (1982). International Agency for Research on Cancer. Monograph vol. 29 Summaries & Evaluations. Benzene. Lyon, France.
- IARC (1989). International Agency for Research on Cancer. Vol. 46 Diesel and Gasoline Engine Exhausts and Some Nitroarenes. Lyon, France.
- IARC (2008). International Agency for Research on Cancer. Monograph vol. 97 1,3-Butadiene, Ethylene Oxide and Vinyl Halides (Vinyl Fluoride, Vinyl Chloride and Vinyl Bromide). Lyon, France.

- ICPS (1996) International Program in Chemical Safety. Environmental Health criteria 171. Diesel and fuel exhaust emissions. Geneva, Switzerland.
- ICPS (1999) International Programme on Chemical Safety. Environmental Health Criteria 213. Carbon (2nd edition). Geneva, Switzerland.
- ISO (1993), International Organization for Standardization ISO 9835 . Ambient air-Determination of a black smoke index, 1-9. Geneva, Switzerland.
- ISO (1995) International Organization for Standardization. Air quality-particle size fraction definition for health related sampling, ISO Standard 7708. International Organization for Standardization, Geneva, Switzerland.
- Ito, K., Inoue, S., Hiraku, Y. & Kawanishi, S. (2005) Mechanism of site-specific DNA damage induced by ozone. *Mutation Research/Genetic Toxicology and Environmental Mutagenesis*, 585, 60-70.
- Janes, H., Sheppard, L. & Lumley, T. (2005) Case-crossover analyses of air pollution exposure data: referent selection strategies and their implications for bias. *Epidemiology*, 16, 717-26.
- Janssen, N. A. H., Van Vliet, P. H. N., Aarts, F., Harssema, H. & Brunekreef, B. (2001) Assessment of exposure to traffic related airpollution of children attending schools near motorways. *Atmospheric Environment*, 35, 3875-3884.
- Janssen, N. A. H., Brunekreef, B., Vliet, P. van, Aarts, F., Meliefste, K., Harssema, H. & Fischer, P. (2003) The relationship between air pollution from heavy traffic and allergic sensitization, bronchial hyperresponsiveness, and respiratory symptoms in Dutch schoolchildren. *Environmental Health Perspectives*, 111, 1512-1518.
- Jarvis, K. E., Gray, A.L., Houk, R.S. (1992) *Handbook of Inductively Coupled Plasma Mass Spectrometry*, Blackie, London.
- Jeong, C. H., Evans, G. J., Hopke, P., Chalupa, D. & Utell, M. J. (2006) Influence of atmospheric dispersion and new particle formation events on ambient particle number concentration in Rochester, United States, and Toronto, Canada. *Journal of the Air and Waste Management Association*, 56, 431-443.
- Jerrett, M., Burnett, R. T., Kanaroglou, P., Eyles, J., Finkelstein, N., Giovis, C., Brook, J. R. (2001) A GIS - environmental justice analysis of particulate air pollution in Hamilton, Canada. *Environment and Planning A*, 33, 955 – 973.
- Jerrett, M., Arain, A., Kanaroglou, P., Beckerman, B., Potoglou, D., Sahuvaroglu, T., Morrison, J., Giovis, C., (2005) A review and evaluation of intraurban air pollution exposure models. *Journal of Exposure Analysis and Environmental Epidemiology*, 15, 185-204.
- Jimenez, L. A., Thompson, J., Brown, D. A., Rahman, I., Antonicelli, F., Duffin, R., Drost, E. M., Hay, R. T., Donaldson, K. & Macnee, W. (2000) Activation of NF- κ B by PM₁₀ Occurs via an Iron-Mediated Mechanism in the Absence of I κ B Degradation. *Toxicology and Applied Pharmacology*, 166, 101-110.

- Jimenez, L. A., Drost, E. M., Gilmour, P. S., Rahman, I., Antonicelli, F., Ritchie, H., Macnee, W. & Donaldson, K. (2002) PM₁₀-exposed macrophages stimulate a proinflammatory response in lung epithelial cells via TNF-alpha. *American Journal of Physiology Lung Cellular and Molecular Physiology*, 282, L237-248.
- Johansson, C. & Noman, M. (2007) Spatial & temporal variations of PM₁₀ and particle number concentrations in urban air. *Environmental Monitoring and Assessment*, 127, 477-87.
- Jones, A. M. & Harrison, R. M. (2005) Interpretation of particulate elemental and organic carbon concentrations at rural, urban and kerbside sites. *Atmospheric Environment*, 39, 7114-7126.
- Jorres, R., Nowak, D., Grimminger, F., Seeger, W., Oldigs, M. & Magnussen, H. (1995) The effect of 1 ppm nitrogen dioxide on bronchoalveolar lavage cells and inflammatory mediators in normal and asthmatic subjects. *European Respiratory Journal*, 8, 416-424.
- Junker, M., Kasper, M., Rössly, M., Camenzind, N., Künzli, N., Monn, C., Theis, G. & Braun-Fahrländer, C. (1999) Airborne particle number profiles, particle mass distributions and particle-bound PAH concentrations within the city environment of Basel: an assessment as part of the BRISKA Project. *Atmospheric Environment*, 34, 3171-3181.
- Katsouyanni, K., Touloumi, G., Samoli, E., Gryparis, A., Le Tertre, A., Monopoli, Y., Rossi, G., Zmirou, D., Ballester, F., Boumghar, A., Anderson, H. R., Wojtyniak, B., Paldy, A., Braunstein, R., Pekkanen, J., Schindler, C. & Schwartz, J. (2001) Confounding and Effect Modification in the Short-Term Effects of Ambient Particles on Total Mortality: Results from 29 European Cities within the APHEA2 Project. *Epidemiology*, 12, 521-531.
- Kawasaki, S., Takizawa, H., Takami, K., Desaki, M., Okazaki, H., Kasama, T., Kobayashi, K., Yamamoto, K., Nakahara, K., Tanaka, M., Sagai, M. & Ohtoshi, T. (2001) Benzene-Extracted Components Are Important for the Major Activity of Diesel Exhaust Particles . Effect on Interleukin-8 Gene Expression in Human Bronchial Epithelial Cells. *American Journal of Respiratory cell and molecular biology*, 24, 419-426.
- Ketzel, M., Wählin, P., Berkowicz, R. & Palmgren, F. (2003) Particle and trace gas emission factors under urban driving conditions in Copenhagen based on street and roof-level observations. *Atmospheric Environment*, 37, 2735-2749.
- Kingham, S., Briggs, D., Elliott, P., Fischer, P. & Erik, L. (2000) Spatial variations in the concentrations of traffic-related pollutants in indoor and outdoor air in Huddersfield, England. *Atmospheric Environment*, 34, 905-916.
- Kingham, S., Pearce, J. & Zawar-Reza, P. (2007) Driven to injustice? Environmental justice and vehicle pollution in Christchurch, New Zealand. *Transportation Research Part D: Transport and Environment*, 12, 254-263.

- Kirby, C., Fox, M., Waterhouse, J. & Drye, T. (2000) Influence of environmental parameters on the accuracy of nitrogen dioxide passive diffusion tubes for ambient measurement. *Journal of Environmental Monitoring*, 3, 150-158.
- Kittelson, D. B. (1998) Engines and nanoparticles: a review. *Journal of Aerosol Science*, 29, 575-588.
- Knaapen, A. M., Shi, T., Borm, P.J.A., Schins, R.P.F. (2002) Soluble metals as well as the insoluble particle fraction are involved in cellular DNA damage induced by particulate matter *Molecular and Cellular Biochemistry*, 234-235, 317-326.
- Koch, K. A., Pena, M. M. O. & Thiele, D. J. (1997) Copper-binding motifs in catalysis, transport, detoxification and signaling. *Chemistry & Biology*, 4, 549-560.
- Kok De, T. M., Hogervorst, J. G., Briedé, J. J., Herwijnen Van, M. H., Maas, L. M., Moonen, E. J., Driee, H. A., Kleinjans, J. C. (2005) Genotoxicity and physicochemical characteristics of traffic-related ambient particulate matter. *Environmental and molecular mutagenesis*, 46, 71-80.
- Kodavanti, U. P., Jaskot, R. H., Costa, D. L. & Dreher, K. L. (1997) Pulmonary proinflammatory gene induction following acute exposure to residual oil fly ash: roles of particle associated metals. *Inhalation Toxicology*, 9, 679-701.
- Krewski, D., Burnett, R. T., Goldberg, M. S., Hoover, K., Siemiatycki, J., Jarret, M., Abrahamowicz, M., White, W. H. (2000) Reanalysis of the Harvard Six Cities Study and the American Cancer Society Study of Particulate Air Pollution and Mortality. Special Report; Health Effects Institute: Cambridge MA.
- Krewski, D., Burnett, R.T., Goldberg, M.S., Hoover, K.; Siemiatycki, J., Abrahamowicz, M., White, W.H. (2004) Validation of the Harvard Six Cities Study of Particulate Air Pollution and Mortality. *New England Journal of Medicine*, 350, 198-199.
- Kulmala, M., Vehkamäki, H., Petaja, T., Dal Maso, M., Lauri, A., Kerminen, V. M., Birmili, W. & McMurry, P. H. (2004) Formation and growth rates of ultrafine atmospheric particles, a review of observations. *Journal of Aerosol Science*, 35, 143-176.
- Künzli, N., Kaiser, R., Medina, S., Studnicka, M., Chanel, O., Filliger, P., Herry, M., Horak, J. F., Puybonnieux-Textier, V., Quenel, P., Schneider, J., Seethaler, R., Vergnaud, J. C. & Sommer, H. (2000) Public-health impact of outdoor and traffic-related air pollution: a European assessment. *The Lancet*, 356, 795-801.
- Künzli, N., Medina, S., Kaiser, R., Quénel, P., Horak Jr, F. & Studnicka, M. (2001) Assessment of Deaths Attributable to Air Pollution: Should We Use Risk Estimates based on Time Series or on Cohort Studies? *American Journal of Epidemiology*, 153, 1050-1055.
- Kyotani, T. & Iwatsuki, M. (2002) Characterization of soluble and insoluble components in PM_{2.5} and PM₁₀ fractions of airborne particulate matter in Kofu city, Japan. *Atmospheric Environment*, 36, 639-649.

- Laakso, L., Hussein, T., Aarnio, P., Komppula, M., Hiltunen, V., Viisanen, Y. & Kulmala, M. (2003) Diurnal and annual characteristics of particle mass and number concentrations in urban, rural and Arctic environments in Finland. *Atmospheric Environment*, 37, 2629-2641.
- Laden, F., Schwartz, J., Speizer, F. E. & Dockery, D. W. (2006) Reduction in Fine Particulate Air Pollution and Mortality: Extended Follow-up of the Harvard Six Cities Study. *American Journal of Respiratory and Critical Care Medicine*, 173, 667-672.
- Lagorio, S., Forastiere, F., Pistelli, R., Iavarone, I., Michelozzi, P., Fano, V., Marconi, A., Ziemacki, G. & Ostro, B. (2006) Air pollution and lung function among susceptible adult subjects: a panel study. *Environmental Health*, 5, 11.
- LAQM (2003). Local Air Quality Management. Update and Screening Assessment 2003. Environmental Protection Services, Glasgow City Council.
- LAQN (2008) London Air Quality Network, Report 13. Environmental Research Group, Kings College.
- Lanki, T., Pekkanen, J., Aalto, P., Elosua, R., Berglind, N., D'ippoliti, D., Kulmala, M., Nyberg, F., Peters, A., Picciotto, S., Salomaa, V., Sunyer, J., Tiittanen, P., Von Klot, S., Forastiere, F. & For the, H. S. G. (2006) Associations of traffic related air pollutants with hospitalisation for first acute myocardial infarction: the HEAPSS study *Occupational and Environmental Medicine*. 63, 844-851.
- Levy, J. I., Hammitt, J. K. & Spengler, J. D. (2000) Estimating the Mortality Impacts of Particulate Matter: What Can Be Learned from Between-Study Variability? *Environmental Health Perspectives*, 108, 109-117.
- Levy, D., Sheppard, L., Checkoway, H., Kaufman, J., Lumley, T., Koenig, J. & Siscovick, D. (2001) A case-crossover analysis of particulate matter air pollution and out-of-hospital primary cardiac arrest. *Epidemiology*, 12, 193-199.
- Li, N., Sioutas, S., Cho, A., Schmitz, D., Misra, C., Sempf, J., Wang, M., Oberley, T., Froines, J. & Nel, A. (2003a) Ultrafine Particulate Pollutants Induce Oxidative Stress and Mitochondrial Damage *Environmental Health Perspectives* 111, 455-460.
- Li, N., Hao, M., Phalen, R. F., Hinds, W. C. & Nel, A. E. (2003b) Particulate air pollutants and asthma: A paradigm for the role of oxidative stress in PM-induced adverse health effects. *Clinical Immunology*, 109, 250-265.
- Lim, L. H., Harrison, R. M. & Harrad, S. (1999) The Contribution to Traffic to Atmospheric Concentrations of Polycyclic Aromatic Hydrocarbons. *Environmental Science and Technology*, 33, 3538-3542.
- Lingard, J. J. N., Agus, E. L., Young, D. T., Andrews, G. E., Tomlin, A. S. (2006) Observations of urban airborne particle number concentrations during rush-hour conditions: analysis of the number based size distributions and modal parameters. *Journal of Environmental Monitoring*, 8, 1203 - 1218.

- Loader, A. (1997) Instruction Manual: UK Smoke and Sulphur Dioxide Networks. AEA Technology, Oxfordshire, UK.
- Lloyd, D. R., Phillips, D. H. & Carmichael, P. L. (1997) Generation of Putative Intrastrand Cross-Links and Strand Breaks in DNA by Transition Metal Ion-Mediated Oxygen Radical Attack. *Chemical Research Toxicology*, 10, 393-400.
- Longley, I. D., Inglis, D. W., Gallagher, M. W., Williams, P. I., Allan, J. D. & Coe, H. (2005) Using NO_x and CO monitoring data to indicate fine aerosol number concentrations and emission factors in three UK conurbations. *Atmospheric Environment*, 39, 5157-516.
- Luhana, L., Sokhi, R., Warner, L., Mao, H., Boulter, P., McCrae, I., Wright, J. & Osborn, D. (2004) PARTICULATES: Characterization of Exhaust Particulate Emissions from Road Vehicles. Fifth Framework Programme Competitive and Sustainable Growth Sustainable Mobility and Intermodality, European Commission. Geneva, Switzerland.
- Lundborg, M., Bouhafs, R., Gerde, P., Ewing, P., Camner, P., Dahlen, S.-E. & Jarstrand, C. (2007) Aggregates of ultrafine particles modulate lipid peroxidation and bacterial killing by alveolar macrophages. *Environmental Research*, 104, 250-257.
- Madden, M. C., Richard, J. H. Dailey, L. A., Hatch, G. E, Ghio, A. J. (2000) Effect of ozone on diesel exhaust particle toxicity in rat lung, *Toxicology and Applied Pharmacology*, 168, 140-148.
- Mantis, J., Chaloulakou, A. & Samara (2005) PM₁₀-bound polycyclic aromatic hydrocarbons (PAHs) in the Greater Area of Athens Greece. *Chemosphere*, 59, 593-604.
- Marston, G. (1999) Atmospheric Chemistry. Annual Reports on the Progress of Chemistry, Section C, 95:235-276.
- Marr, I. L., Rosser, D. P. & Meneses, C. A. (2007) An air quality survey and emissions inventory at Aberdeen Harbour. *Atmospheric Environment*, 41, 6379-6395.
- Mathieu-Nolf, M. (2002) Poisons in the Air: A Cause of Chronic Disease in Children. *Clinical Toxicology*, 40, 483 - 491.
- Matti Maricq, M. (2007) Chemical characterization of particulate emissions from diesel engines: A review. *Journal of Aerosol Science*, 38, 1079-1118.
- McMaster & MacMaster (1998) Gas Chromatography-Mass Spectrometry a practical user's guide. New York: Wiley.
- Mcclellan, R. O. (2000) *Particle interactions with the respiratory tract. In Particle-lung interactions* New York, Marcel Dekker Inc.
- Mehlman, M. A. (1983) Current Toxicological Information as the Basis for Sulfur Oxide Standards. *Environmental Health Perspectives*, 52, 261-66.

- Miguel, A. H., Kirchstetter, T. W., Harley, R.H., Hering, S. V (1998) On-Road Emissions of Particulate Polycyclic Aromatic Hydrocarbons and Black Carbon from Gasoline and Diesel Vehicles. *Environmental Science and Technology*, 32, 450–455.
- Miller, J. C., Miller, J. N., Statistics for Analytical Chemistry, Third Edition ed., Ellis Horwood PTR Prentice Hall, 1993, p. 115
- Miller, B. (2008) Institute of Occupational Medicine, Edinburgh. Personal communication.
- Monod, A., Sive, B. C., Avino, P., Chen, T., Blake, D. R. & Sherwood Rowland, F. (2001) Monoaromatic compounds in ambient air of various cities: a focus on correlations between the xylenes and ethylbenzene. *Atmospheric Environment*, 35, 135-149.
- Monteiller, C., Tran, L., Macnee, W., Faux, S., Jones, A., Miller, B. & Donaldson, K. (2007) The pro-inflammatory effects of low-toxicity low-solubility particles, nanoparticles and fine particles, on epithelial cells in vitro: the role of surface area.
- Moolgavkar, S. H. (2003) Air Pollution and Daily Mortality in Two U.S. Counties: Season-Specific Analyses and Exposure-Response Relationships. *Inhalation Toxicology*, 15, 877 - 907.
- Moschandreas, D. J., Relwani, S. M., Taylor, K. C. & Mulik, J. D. (1990) A laboratory evaluation of a nitrogen dioxide personal sampling device. *Atmospheric Environment. Part A. General Topics*, 24, 2807-2811.
- Morawska, L., Thomas, S., Bofinger, N., Wainwright, D. & Neale, D. (1998) Comprehensive characterization of aerosols in a subtropical urban atmosphere: particle size distribution and correlation with gaseous pollutants. *Atmospheric Environment*, 32, 2467-2478.
- Morawska, L., Vishvakarman, D., Mengersen, K. & Thomas, S. (2002) Spatial variation of airborne pollutant concentrations in Brisbane, Australia and its potential impact on population exposure assessment. *Atmospheric Environment*, 36, 3545-3555.
- Morgenstern, V., Zutavern, A., Cyrys, J., Brockow, I., Gehring, U., Koletzko, S., Bauer, C. P., Reinhardt, D., Wichmann, H. E. & Heinrich, J. (2007) Respiratory health and individual estimated exposure to traffic-related air pollutants in a cohort of young children.
- Muir, D. (2000) New Directions: The suitability of tapered element oscillating microbalances (TEOMs) for PM₁₀ monitoring in Europe. The use of PM₁₀ data as measured by TEOM for compliance with the European Air Quality Standard. *Atmospheric Environment*, 34, 3209-3211.
- Mumtaz, M. M., George, J.D., Gold, K.W., Cibulas, W., Derosa, C.T. (1996) ATSDR evaluation of health effects of chemicals. IV. Polycyclic aromatic hydrocarbons (PAHs): understanding a complex problem. *Toxicology and Industrial Health* 12, 742-971.
- NAEI (2007) National Atmospheric Emission Inventory. UK Emissions of Air Pollutants 1970 to 2005. Available on line at:

- http://www.airquality.co.uk/archive/reports/cat07/0801140937_2005_Report_FINA_L.pdf Last accessed 10 Feb 2008
- Nafstad, P., Haheim, L. L., Oftedal, B., Gram, F., Holme, I., Hjermann, I. & Leren, P. (2003) Lung cancer and air pollution: a 27 year follow up of 16 209 Norwegian men. *Thorax*, 58, 1071-1076.
- NAQA National Air Quality Archive Data retrieved from:
http://www.airquality.co.uk/archive/data_and_statistics.php Last accessed: 12 Jun 2008.
- NAQAa National Air Quality Archive: Classification of BS sites.
http://www.airquality.co.uk/archive/reports/cat13/0602211414_site2004.csv Last accessed 1 Oct 2008.
- NAQAb National Air Quality Archive: Classification of AUN sites in Glasgow:
http://www.airquality.co.uk/archive/detailed_zone.php?zone_id=6 Last accessed 1 Oct 2008.
- NAQAc National Air Quality Archive: Classification of AUN sites in London.
http://www.airquality.co.uk/archive/detailed_zone.php?zone_id=15 Last accessed 1 Oct 2008.
- NAQAd National Air Quality Archive: Monitoring of PNC:
http://www.airquality.co.uk/archive/particle_data.php Last accessed 1 Oct 2008.
- Namdeo, A. & Bell, M. C. (2005) Characteristics and health implications of fine and coarse particulates at roadside, urban background and rural sites in UK. *Environment International*, 31, 565-573.
- Nemmar, A., Vanbilloen, H., Hoylaerts, M. F., Hoet, P. H. M., Verbruggen, A. & Nemery, B. (2001) Passage of Intratracheally Instilled Ultrafine Particles from the Lung into the Systemic Circulation in Hamster.
- Nisbet, I. C. T. & Lagoy, P. K. (1992) Toxic equivalency factors (TEFs) for polycyclic aromatic hydrocarbons (PAHs). *Regulatory Toxicology and Pharmacology*, 16, 290-300.
- Noble, C., Mukerjee, S., Gonzales, M., Rodes, C. E., Lawless, P. A., Natarajan, S., Myers, E. A., Norris, G. A., Smith, L., Å-Zkaynak, H., Neas, L. M. (2003) Continuous measurement of fine and ultrafine particulate matter, criteria pollutants and meteorological conditions in urban El Paso, Texas. *Atmospheric Environment*, 37, 827-840.
- Nordenhäll, C., Pourazar, J., Ledin, M.C., Levin, J.O., Sandström, T., Adelroth, E. (2001) Diesel exhaust enhances airway responsiveness in asthmatic subjects. *European Respiratory Journal* 17, 900-915.
- Office for National Statistics. Retrieved from www.statistics.gov.uk on 21 Aug 2008.

- O'Neill, M. S., Jerrett, M., Kawachi, I., Levy, J. I., Cohen, A. J., Gouveia, N., Wilkinson, P., Fletcher, T., Cifuentes, L. & Schwartz, J. (2003) Health, wealth, and air pollution: advancing theory and methods. *Environmental Health Perspectives*, 111, 1861–1870
- Oberdörster, G., Sharp, Z., Atudorei, V., Elder, A. A., Gelein, R., Lunts, A. A., Kreyling, W., Cox, C. (2002) Extrapulmonary translocation of ultrafine carbon particles following whole-body inhalation exposure of rats. *Journal of Toxicology and Environmental Health - Part A*, 65, 1531 - 1543.
- Oberdörster, G., Sharp, Z., Atudorei, V., Elder, A., Gelein, R., Kreyling, W., Cox, C. (2004) Translocation of inhaled ultrafine particles to the brain. *Inhalation Toxicology* 16, 437-445.
- Omori, T., Fujimoto, G., Yoshimura, I., Nitta, H. & Ono, M. (2003) Effects of particulate matter on daily mortality in 13 Japanese cities. *Journal of Epidemiology*, 13, 314-322.
- Ono-Ogasawara, M., Smith, T. (2004) Diesel Exhaust Particles in the Work Environment and their Analysis. *Industrial Health* 42, 389–399.
- Ostro, B., Sánchez, J. M. & Eskeland, G. S. (1996) Air pollution and mortality results from a study of Santiago, Chile. *Journal of Exposure Analysis and Environmental Epidemiology*, 6, 97-114.
- Ostro, B., Feng, W.Y., Broadwin, R., Green, S., Lipsett, M. (2007) The effects of components of fine particulate air pollution on mortality in California: Results from CALFINE. *Environmental Health Perspectives*, 115, 13-19.
- Osunsanya, T., Prescott, G. & Seaton, A. (2001) Acute respiratory effects of particles: mass or number?
- Paatero, P., Aalto, P., Picciotto, S., Bellander, T., Castaño, G., Cattani, G., Cyrus, J., Kulmala, M., Lanki, T., Nyberg, F., Pekkanen, J., Peters, A., Sunyer, J. & Forastiere, F. (2005) Estimating time series of aerosol particle number concentrations in the five HEAPSS cities on the basis of measured air pollution and meteorological variables. *Atmospheric Environment*, 39, 2261-2273.
- Pan, C. J. G., Schmitz, D. A., Cho, A. K., Froines, J. & Fukuto, J. M. (2004) Inherent Redox Properties of Diesel Exhaust Particles: Catalysis of the Generation of Reactive Oxygen Species by Biological Reductants. *Toxicological Sciences*, 81, 225-232.
- Palmes, E. D., Gunnison, A. F., Dimattio, J. & Tomczyk, C. (1976) Personal sampler for nitrogen dioxide. *American Industrial Hygiene Association Journal*, 37, 570-577.
- Papageorgopoulou, A., Manoli, E., Touloumi, E., Samara, C. (1999) Polycyclic aromatic hydrocarbons in the ambient air of Greek towns in relation to other atmospheric pollutants. *Chemosphere*, 39, 2183-2199.
- Peacock, J. L., Symonds, P., Jackson, P., Bremner, S. A., Scarlett, J. F., Strachan, D. P. & Anderson, H. R. (2003) Acute effects of winter air pollution on respiratory function

- in schoolchildren in southern England. *Occupational and Environmental Medicine*, 60, 82-89.
- Peng, R. D., Dominici, F., Pastor-Barriuso, R., Zeger, S. L. & Samet, J. M. (2005) Seasonal Analyses of Air Pollution and Mortality in 100 U.S Cities. *American Journal of Epidemiology*, 161, 585-594.
- Pekkanen, J., Peters, A., Hoek, G., Tiittanen, P., Brunekreef, B., De Hartog, J., Heinrich, J., Ibaldo-Mulli, A., Kreyling, W. G., Lanki, T., Timonen, K. L. & Vanninen, E. (2002) Particulate Air Pollution and Risk of ST-Segment Depression During Repeated Submaximal Exercise Tests Among Subjects With Coronary Heart Disease: The Exposure and Risk Assessment for Fine and Ultrafine Particles in Ambient Air (ULTRA) Study. *Circulation*, 106, 933-938.
- Penard-Morand, C., Charpin, D., Raheison, C., Kopferschmitt, C., Caillaud, D., Lavaud, F. & Annesi-Maesano, I. (2005) Long-term exposure to background air pollution related to respiratory and allergic health in schoolchildren. *Clinical and experimental allergy*. 35, 1279-1287.
- Penttinen, P., Alm, S., Ruuskanen, J. & Pekkanen, J. (2000) Measuring reflectance of TSP-filters for retrospective health studies. *Atmospheric Environment*, 34, 2581-2586.
- Penttinen, P., Timonen, K. L., Tiittanen, P., Mirme, A., Ruuskanen, J. & Pekkanen, J. (2001) Ultrafine particles in urban air and respiratory health among adult asthmatics. *European Respiratory Journal*, 17, 48-435.
- Peters, A., Wichmann, H. E., Tuch, T., Heinrich, J. & Heyder, J. (1997) Respiratory effects are associated with the number of ultrafine particles. *American Journal of respiratory and critical care medicine*, 155:1376-1386.
- Peters, A., Dockery, D. W., Muller, J. E. & Mittleman, M. A. (2001) Increased Particulate Air Pollution and the Triggering of Myocardial Infarction. *Circulation*, 103, 2810-2815.
- Pinto, J.P., Stevens, R.K., Willis, R.D., Kelllogg, R., mamane, Y., Novak, J., Santroch, J., Benes, I., Lenicek, J., Bures, V. (1998). Czech air quality monitoring and receptor modelling study. *Environmental Science and Technology*, 32:843-854.
- Pinto, J. P., Lefohn, A. S. & Shadwick, D. S. (2004) Spatial variability of PM_{2.5} in urban areas in the United States. *Journal of the Waste and Air Management Association*, 54, 440-9.
- Piñeiro-Iglesias, M., Lopex-Mahia, P., Muniategui-Lorenzo, S., Prada-Rodriguez, D., Querol, X. & Alastuey, A. (2003) A new method for the simultaneous determination of PAH and metals in samples fo atmospheric particulate matter. *Atmospheric Environment*, 37, 4171-7175.
- Pleijel, H., Karlsson, G. P. & Gerdin, E. B. (2004) On the logarithmic relationship between NO₂ concentration and the distance from a highroad. *Science of the Total Environment*, 332, 261-264.

- Plaisance, H., Piechocki-Minguy, A., Garcia-Fouque, S., Galloo, J. C. (2004) Influence of meteorological factors on the NO₂ measurements by passive diffusion tube. *Atmospheric Environment*, 38, 573–580.
- Pope, C. A., III, Thun, M. J., Namboodiri, M. M., Dockery, D. W., Evans, J. S., Speizer, F. E. & Heath, C. W., Jr. (1995) Particulate air pollution as a predictor of mortality in a prospective study of U.S. adults. *Respiratory and critical care medicine*. 151, 669-674.
- Pope, C. A. III Burnett, R. T., Thun, M. J., Calle, M. J., Krewski, D., Ito, K., Thurston, G.D. (2002) Lung cancer, cardiopulmonary mortality and long-term exposure to fine particulate air pollution. *Journal of American Medical Association*, 287, 1132-1141.
- Pope, C. A., III, Burnett, R. T., Thurston, G. D., Thun, M. J., Calle, E. E., Krewski, D. & Godleski, J. J. (2004) Cardiovascular Mortality and Long-Term Exposure to Particulate Air Pollution: Epidemiological Evidence of General Pathophysiological Pathways of Disease. *Circulation*, 109, 5-7.
- Pope, C. A. III, Ezzati, M. I & Dockery, D. W. (2009) Fine-Particulate Air Pollution and Life Expectancy in the United States. *New England Journal of Medicine*, 360: 376-386.
- Pourazar, J., Mudway, I. S., Samet, J. M., Helleday, R., Blomberg, A., Wilson, S.J., Frew, A. J., Kelly, F.J. & Sandstrom, T. (2005) Diesel exhaust activates redox-sensitive transcription factors and kinases in human airways. *American Journal of Physiology and Lung Cell Molecular Physiology*; 289, 724-30.
- Price, M., Bulpitt, S. & Meyer, M. B. (2003) A comparison of PM₁₀ monitors at a Kerbside site in the northeast of England. *Atmospheric Environment*, 37, 4425-4434.
- Pritchard, R. J., Ghio, A. J., Lehmann, J. R., Winsett, D. W., Tepper, J. S., Park, P., Gilmour, M. I., Dreher, K. L. & Costa, D. L. (1996) Oxidant Generation and Lung Injury after Particulate Air Pollutant Exposure Increase with the Concentrations of Associated Metals. *Inhalation Toxicology*, 8, 457 - 477.
- Prockop, L. D. & Chichkova, R. I. (2007) Carbon monoxide intoxication: An updated review. *Journal of the Neurological Sciences*, 262, 122-130.
- Puustinen, A., Hämeri, K., Pekkanen, J., Kulmala, M., De Hartog, J., Meliefste, K., Ten Brink, H., Kos, G., Katsouyanni, K., Karakatsani, A., Kotronarou, A., Kavouras, I., Meddings, C., Thomas, S., Harrison, R., Ayres, J. G., Van Der Zee, S. & Hoek, G. (2007) Spatial variation of particle number and mass over four European cities. *Atmospheric Environment*, 41, 6622-6636.
- QUARG (1996) Quality Urban Air Review Group Airborne Particulate Matter in the United Kingdom: Third Report of the Quality of Urban Air Review Group. London.
- Rahman, I. & Macnee, W. (2000) Oxidative stress and regulation of glutathione in lung inflammation. *European Respiratory Journal*, 16, 534-554.

- Raub, J. A. & Benignus, V. A. (2002) Carbon monoxide and the nervous system. *Neuroscience & Biobehavioral Reviews*, 26, 925-940.
- Reissell, A., Macdonald, C., Roberts, P. & Arey, J. (2003) Characterization of biogenic volatile organic compounds and meteorology at Azusa during the SCOS97-NARSTO. *Atmospheric Environment*, 37, 181-196.
- Risom, L., Moller, P. & Loft, S. (2005) Oxidative stress-induced DNA damage by particulate air pollution. *Mutation Research*, 592, 119-137.
- Roberts, S. & Martin, M. A. (2006) Investigating the mixture of air pollutants associated with adverse health outcomes. *Atmospheric Environment*, 40, 984-991.
- Rodríguez, S., Van Dingenen, R., Putaud, J.-P., Dell'acqua, A., Pey, J., Querol, X., Alastuey, A., S. Chenery, K.-F. Ho, Harrison, R. M. Tardivo, B. Scarnato, R., Gianelle, V. (2007) A study on the relationship between mass concentrations, chemistry and number size distribution of urban fine aerosols in Milan, Barcelona and London. *Atmospheric Chemistry and Physics Discussions*, 7, 605-639.
- Roemer, W., Hoek, G., Brunekreef, B., Haluszka, J., Kalandidi, A. & Pekkanen, J. (1998) Daily variations in air pollution and respiratory health in a multicentre study: the PEACE project. Pollution Effects on Asthmatic Children in Europe. *European Respiratory Journal*, 12, 1354-1361.
- Roemer, W., Hoek, G., Brunekreef, B. (2000a) Pollution effects on asthmatic children in Europe, the PEACE study. *Clinical and Experimental Allergy*, 30, 1067-1075.
- Roemer, W., Hoek, G., Brunekreef, B., Clench-Aas, J., Forsberg, B., Pekkanen, J., Schutz, A. (2000b) PM₁₀ elemental composition and acute respiratory health effects in European children (PEACE project). *European Respiratory Journal*, 15, 553-559.
- Roorda-Knape, M. C., Janssen, N. A. H., De Hartog, J. J., Van Vliet, P. H. N., Harssema, H. & Brunekreef, B. (1998) Air pollution from traffic in city districts near major motorways - design and calibration. *Atmospheric Environment*, 32, 1921-1930.
- Rossner Jr, P., Binkova, B., Milcova, A., Solansky, I., Zidzik, J., Lyubomirova, K. D., Farmer, P. B. & Sram, R. J. (2007) Air pollution by carcinogenic PAHs and plasma levels of p53 and p21WAF1 proteins. *Mutation Research/Fundamental and Molecular Mechanisms of Mutagenesis*, 620, 34-40.
- Röösly, M., Theis, G., Kunzli, N., Staehelin, J., Mathys, P., Oglesby, L., Camenzind, M. & Braun-Farlander, C. (2001) Temporal and spatial variation of the chemical composition of PM₁₀ at urban and rural sites in the Basel area, Switzerland. *Atmospheric Environment*, 35, 3701-3713.
- Ruijin, L., Ziqiang, M. & Jingfang, X. (2007) Effects of sulfur dioxide derivatives on four asthma-related gene expressions in human bronchial epithelial cells. *Toxicology Letters*, 175, 71-81.

- Rupprecht, E. G. & Patashnick, H. (1991) Continuous PM-10 measurement using the tapered element oscillating microbalance. *Journal of the Air and Waste Management Association* 41, 1079–1083, (since 2006 Thermo Fisher Scientific)
- Rupprecht, E. G. and Patashnick, H. (1999) Operation/Service Manual, Partisol-Plus Model 2025 Sequential Air Sampler. Revision B.001. New York, USA. (since 2006 Thermo Fisher Scientific)
- Rupprecht & Patashnick, (2006) Personal communication.
- Ruuskanen, J., Tuch, T., Ten Brink, H., Peters, A., Khlystov, A., Mirme, A., Kos, G., Brunekreef, B., Wichmann, H., Buzorius, G., Vallius, M., Kreyling, W. G. & Pekkanen, J. (2001) Concentrations of ultrafine, fine and PM_{2.5} particles in three European cities. *Atmospheric Environment*, 35, 3729-3738.
- Rusznak, C., Devalia, J.L., Sapsford, R.,J., Davies, R.,J. (1996) Ozone-induced mediator release from human bronchial epithelial cells in vitro and the influence of nedocromil sodium. *European Respiratory Journal* 9, 2298-2305.
- Saldiva, P. H. N., Pope, C. A. III, Schwartz, J., Dockery, D. W., Lichtenfels, A. J., Salge, J. M., Barone, I. & Bohm, G. M. (1995) Air pollution and mortality in elderly people—a time series study in Sao-Paulo, Brazil. *Archives of Environmental Health*, 50, 159-163.
- Salvi, S., Blomberg, A., Rudell, B., Kelly, F., Sandstrom, T., Holgate, Stephen t. & Frew, A. (1999) Acute Inflammatory Responses in the Airways and Peripheral Blood After Short-Term Exposure to Diesel Exhaust in Healthy Human Volunteers. *American Journal of Respiratory and Critical Care Medicine*. 159, 702-709.
- Salvi, S. S., Nordenhall, C., Blomberg, A., Rudell, B., Pourazar, J., Kelly, F. J., Wilson, S., Sandstrom, T., Holgate, S. T. & Frew, A. J. (2000) Acute Exposure to Diesel Exhaust Increases IL-8 and GRO-alpha Production in Healthy Human Airways. *American Journal of Respiratory and Critical Care Medicine*. 161, 550-557.
- Samet, J. M., Dominic, I. F., Curriero, F. C., Coursac, I. & Zeger, S. L. (2000) Fine particulate air pollution and mortality in 20 US Cities: 1987-1994. *New England Journal of Medicine*, 343, 1742-1749.
- Samoli, E., Aga, E., Touloumi, G., Nisiotis, K., Forsberg, B., Lefranc, A., Pekkanen, J., Wojtyniak, B., Schindler, C., Niciu, E., Brunstein, R., Dodic Fikfak, M., Schwartz, J. & Katsouyanni, K. (2006) Short-term effects of nitrogen dioxide on mortality: an analysis within the APHEA project. *European Respiratory Journal*, 27, 1129-1138.
- Sandip, D. S., Johnson, C. M. W., Cocker Iii, D. R. & Norbeck, J. M. (2004) Emission rates of PM and elemental carbon from in use diesel engines. *Environmental Science and Technology*, 38, 2544 -2550.
- Sardar, S. B., Fine, P. M., Yoon, H., Sioutas, C. (2004) Associations between Particle Number and Gaseous Co-Pollutant Concentrations in the Los Angeles Basin. *Journal of the Air and Waste Management Association*, 54, 992-1005.

- Scaperdas, A. & Colvile, R. N. (1999) Assessing the representativeness of monitoring data from an urban intersection site in central London, UK. *Atmospheric Environment* 33, 661-674.
- Schierhorn, K., Zhang, M., Matthias, C. & Kunkel, G. (1999) Influence of Ozone and Nitrogen Dioxide on Histamine and Interleukin Formation in a Human Nasal Mucosa Culture System. *American Journal of Respiratory Cell and Molecular Biology*, 20, 1013-1019.
- Schins, R. P. F., Mcalinden, A., Macnee, W., Jimenez, L. A., Ross, J. A., Guy, K., Faux, S. P. & Donaldson, K. (2000) Persistent Depletion of I Kappa B Alpha and Interleukin-8 Expression in Human Pulmonary Epithelial Cells Exposed to Quartz Particles. *Toxicology and Applied Pharmacology*, 167, 107-117.
- Schmid, H., Laskus, L., Jürgen Abraham, H., Baltensperger, U., Lavanchy, V., Bizjak, M., Burba, P., Cachier, H., Crow, D., Chow, J., Gnauk, T., Even, A., Ten Brink, H. M., Giesen, K.-P., Hitzenberger, R., Hueglin, C., Maenhaut, W., Pio, C., Carvalho, A., Putaud, J.-P., Toom-Sauntry, D. & Puxbaum, H. (2001) Results of the "carbon conference" international aerosol carbon round robin test stage I. *Atmospheric Environment*, 35, 2111-2121.
- Schober, W., Lubitz, S., Belloni, B., Gebauer, G., Lintelmann, J., Matuschek, G., Weichenmeier, I., Eberlein, K., Ouml, Nig, B., Buters, J. & Behrendt, H. (2007) Environmental Polycyclic Aromatic Hydrocarbons (PAHs) Enhance Allergic Inflammation by Acting on Human Basophils. *Inhalation Toxicology*, 19, 151-156.
- Schroeder, W. H., Dobson, M., Kane, D. M. & Johnson, N. D. (1987) Toxic trace elements associated with airborne particulate matter: A review. *Journal of the Air Pollution Control Association*, 37, 1267-1285.
- Schwartz, J. (1991) Particulate air pollution and daily mortality in Detroit *Environmental Research*, 56, 202-211.
- Schwartz, J. (2004) The effects of particulate air pollution on daily deaths: a multi-city case crossover analysis. *Occupational and Environmental Medicine*, 61, 956-961.
- Schwartz, J., Litonjua, A., Suh, H., Verrier, M., Zanobetti, A., Syring, M., Nearing, B., Verrier, R., Stone, P., Maccallum, G., Speizer, F. E. & Gold, D. R. (2005) Traffic related pollution and heart rate variability in a panel of elderly subjects. *Thorax*, 60, 455-461.
- Seagrave, J., Knall, C., McDonald, J. D., Mauderly, J. L. (2004) Diesel particulate material binds and concentrates a proinflammatory cytokine that causes neutrophil migration. *Inhalation Toxicology*, 16, 93-98.
- Seaton, A., Godden, D., Macnee, W. & Donaldson, K. (1995) Particulate air pollution and acute health effects. *The Lancet*, 345, 176-178.
- Sem, G. J. (2002). Design and performance characteristics of three continuous flow condensation particle counters: A Summary. *Atmospheric Research*, 62, 267-294.

- Seigneur, C., Pun, B., Lohman, K. & Wu, S. Y. (2003) Regional Modeling of the Atmospheric Fate and Transport of Benzene and Diesel Particles. *Environment Science and Technology*, 37, 5236-5246.
- Seinfeld, J. H. & Pandis, S. N. (1998) *Atmospheric Chemistry and Physics*, New York, John Wiley & Sons, Inc.
- Shi, J. P., Khan, A. A. & Harrison, R. M. (1999) Measurements of ultrafine particle concentration and size distribution in the urban atmosphere. *The Science of The Total Environment*, 235, 51-64.
- Shi, J. P., Mark, D. & Harrison, R. M. (2000) Characterization of Particles from a Current Technology Heavy-Duty Diesel Engine. *Environmental Science and Technology*, 34, 748-755.
- Shi, J. P., Evans, D. E., Khan, A. A. & Harrison, R. M. (2001) Sources and concentration of nanoparticles (<10 nm diameter) in the urban atmosphere. *Atmospheric Environment*, 35, 1193-1202.
- Shi, T., Schins, R. P., Knaapen, A. M., Kuhlbusch, T., Pitz, M., Heinrich, J., Borm, P. J. (2003) Hydroxyl radical generation by electron paramagnetic resonance as a new method to monitor ambient particulate matter composition. *Journal of Environmental Monitoring*, 5, 550-6.
- Simon, V., Baer, M., Torres, L., Olivier, S., Meybeck, M. & Della Massa, J. P. (2004) The impact of reduction in the benzene limit value in gasoline on airborne benzene, toluene and xylenes levels. *Science of The Total Environment*, 334-335, 177-183.
- Singer, B. C., Hodgson, A. T., Hotchi, T. & Kim, J. J. (2004) Passive measurement of nitrogen oxides to assess traffic-related pollutant exposure for the East Bay Children's Respiratory Health Study. *Atmospheric Environment*, 38, 393-403.
- Sioutas, C., Delfino, R.J., Singh, M. (2005) Exposure Assessment for Atmospheric Ultrafine Particles (UFPs) and Implications in Epidemiologic Research. *Environmental Health Perspectives*, 113, 947-955.
- SKC Inc. USA, Operating Instructions Universal sampling pump Catalog. No. 224-4XR <http://www.skcinc.com/pumps/224-44XR.asp> Last accessed 01 Oct 2008.
- Smith, S., Stribley, T., Barratt, B., Perryman, C. (1997). Determination of PM₁₀ by Partisol, TEOM, ACCU and Cascade Impactor Instruments in the London Borough of Greenwich. *Clean Air* 27, 70-73.
- Speer, R. E., Edney, E.O., Kleindienst, T.E. (2003) Impact of organic compounds on the concentrations of liquid water in ambient PM_{2.5}. *Journal of Aerosol Science* 34, 63-77
- Steenenbergh, P. A., Van Amelsvoort, L., Lovik, M., Hetland, R. B., Alberg, T., Halatek, T., Bloemen, H. J. T., Rydzynski, K., Swaen, G., Schwarze, P., Dybing, E. & Cassee, F. R. (2006) Relation between sources of particulate air pollution and biological effect

- parameters in samples from four European cities: An exploratory study. *Inhalation Toxicology*, 18, 333-346.
- Stohs, S. J. & Bagchi, D. (1995) Oxidative mechanisms in the toxicity of metal ions. *Free Radical Biology and Medicine*, 18, 321-336.
- Stenfors, N., Pourazar, J., Blomberg, A., Krishna, M.T., Mudway, I., Helleday, R., Kelly, F.J., Frew, A.J., Sandström, T. (2002) Effect of ozone on bronchial mucosal inflammation in asthmatic and healthy subjects. *Respiratory Medicine*, 96, 352-358.
- Stenfors, N., Nordenhall, C., Salvi, S. S., Mudway, I., Soderberg, M., Blomberg, A., Helleday, R., Levin, J. O., Holgate, S. T., Kelly, F. J., Frew, A. J. & Sandstrom, T. (2004) Different airway inflammatory responses in asthmatic and healthy humans exposed to diesel. *European Respiratory Journal*, 23, 82-86
- Stuchbury, G. (2006). Personal communication.
- Sullivan, J., Ishikawa, N., Sheppard, L., Siscovick, D., Checkoway, H. & Kaufman, J. (2003) Exposure to Ambient Fine Particulate Matter and Primary Cardiac Arrest among Persons With and Without Clinically Recognized Heart Disease. *American Journal of Epidemiology*. 157, 501-509.
- Sunyer, J., Atkinson, R., Ballester, F., Le Tertre, A., Ayres, J. G., Forastiere, F., Forsberg, B., Vonk, J. M., Bisanti, L., Anderson, R. H., Schwartz, J. & Katsouyanni, K. (2003) Respiratory effects of sulphur dioxide: a hierarchical multicity analysis in the APHEA 2 study. *Occupational and Environmental Medicine*. 60, e2.
- Thomson, E. M., Kumarathasan, P., Calderon-Garciduenas, L. & Vincent, R. (2007) Air pollution alters brain and pituitary endothelin-1 and inducible nitric oxide synthase gene expression. *Environmental Research*, 105, 224-233.
- TSI, 2002 Model 3022A Condensation Particle Counter Instruction Manual, P/N 1933763, 2002.
- TSI, 2005 Model 3785 Water-based Condensation Particle Counter Operation and Service Manual, P/N 1933001P/N 1933763, 2005.
<http://www.tsi.com/Product.aspx?Pid=250> Last accessed 1 Oct 2008.
- Tsien, A., Diaz-Sanchez, D., Ma, J. & Saxon, A. (1997) The Organic Component of Diesel Exhaust Particles and Phenanthrene, a Major Polyaromatic Hydrocarbon Constituent, Enhances IgE Production by IgE-Secreting EBV-Transformed Human B Cells in Vitro. *Toxicology and Applied Pharmacology*, 142, 256-263.
- Tornqvist, H., Mills, N. L., Gonzalez, M., Miller, M. R., Robinson, S. D., Megson, I. L., Macnee, W., Donaldson, K., Soderberg, S., Newby, D. E., Sandstrom, T. & Blomberg, A. (2007) Persistent Endothelial Dysfunction in Humans after Diesel Exhaust Inhalation. *American Journal of Respiratory and Critical Care Medicine* 176, 395-400.
- Tunnicliffe, W. S., Harrison, R.M., Kelly, F.J., Dunster, C., Ayres, J.G. (2003) The effect of sulphurous air pollutant exposures on symptoms, lung function, exhaled nitric oxide,

and nasal epithelial lining fluid antioxidant concentrations in normal and asthmatic adults. *Occupational and environmental medicine* 60, e15.

Upadhyay, D., Panduri, V., Ghio, A. & Kamp, D. W. (2003) Particulate Matter Induces Alveolar Epithelial Cell DNA Damage and Apoptosis: Role of Free Radicals and the Mitochondria. *American Journal of Respiratory Cell and Molecular Biology*. 29, 180-187.

USEPA (1997) Report AP-42 Compilation of Air Pollutant Emission Factors. Volume I, 5th edition. Environmental Protection Agency, Washington DC. Available on line at: <http://www.epa.gov/oms/ap42.htm> Last accessed 13 Dec 2007.

USEPA (1998a) Quality Assurance Guidance Document 2.12 Monitoring PM_{2.5} in Ambient Air Using Designated Reference or Class I Equivalent Methods.

USEPA (1998b) PM_{2.5} Mass Weighing Laboratory Standard Operating Procedures for the Performance Evaluation Program.

USEPA. (1998c) 625/R-96/010b. Compendium of methods for the determination of toxic organic compounds in ambient air. Second Ed. Environmental Protection Agency, Washington DC. Available on line at: <http://www.epa.gov/ttnamti1/files/ambient/airtox/tocomp99.pdf>

USEPA (2002). Health Assessment Document For Diesel Engine Exhaust. USEPA EPA/600/8-90/057F. 1 May 2002. U.S. Environmental Protection Agency, Office of Research and Development, National Center for Environmental Assessment, Washington, DC

ULTRA (1998a) SOP/UoW-F-2.0 Measurements of PM_{2.5} with the Harvard Impactor.

ULTRA (1998b) SOP/KTL-L-1.0 Determination of absorption coefficient using reflectometric method.

Valavanidis, A., Fiotakis, K., Bakeas, E. & Vlahogianni, T. (2005) Electron paramagnetic resonance study of the generation of reactive oxygen species catalysed by transition metals and quinoid redox cycling by inhalable ambient particulate matter *Redox Report*, 10, 37-51.

Valko, M., Rhodes, C. J., Moncol, J., Izakovic, M. & Mazur, M. (2006) Free radicals, metals and antioxidants in oxidative stress-induced cancer. *Chemico-Biological Interactions*, 160, 1-40.

Van Eeden, S. F., Yeung, A., Quinlan, K. & Hogg, J. C. (2005) Systemic Response to Ambient Particulate Matter: Relevance to Chronic Obstructive Pulmonary Disease. *The Proceedings of the American Thoracic Society* 2, 61-67.

Vardoulakis, S., Lumberras, J. & Solazzo, E. (2009) Comparative evaluation of nitrogen oxides and ozone passive diffusion tubes for exposure studies. *Atmospheric Environment*, 43, 2509-2517.

- Vaughan, N. P., Milligan, B. D. & Ogden, T. L. (1989) Filter weighing reproducibility and the gravimetric detection limit. *Annals of Occupational Hygiene*, 33, 331-337.
- Vautard, R., Honoré, C., Beekmann, M. & Rouil, L. (2005) Simulation of ozone during the August 2003 heat wave and emission control scenarios. *Atmospheric Environment*, 39, 2957-2967.
- VDI. Verein Deutscher Ingenieure, 2465, Part 1: Measurements of Soot (Immission) Chemical Analysis of Elemental Carbon by Extraction and Thermal Desorption of Organic Carbon. Berlin, 1996.
- Venkataraman, C., Friedlander, S. K., (1994) Size distribution of polycyclic aromatic hydrocarbons and elemental carbon. 1. Sampling, measurement methods and source characterization. *Environmental Science & Technology*, 28, 555-562.
- Veranth, J., Kaser, E., Veranth, M., Koch, M. & Yost, G. (2007) Cytokine responses of human lung cells (BEAS-2B) treated with micron-sized and nanoparticles of metal oxides compared to soil dusts. *Particle and Fibre Toxicology*, 4, 2.
- Vincent, J. H. (1985). On the practical significance of electrostatic lung deposition of isomeric and fibrous aerosols. *Journal of Aerosol Science*, 16, 511-519.
- Vogel, C. F., Sciullo, E., Wong, P., Kuzmicky, P., Kado, N., Matsumura, F. (2005) Induction of Proinflammatory Cytokines and C-Reactive Protein in Human Macrophage Cell Line U937 Exposed to Air Pollution Particulates *Environmental Health Perspectives*, 113, 1536-1541.
- Voutsas, D. & Samara, C. (2002) Labile and bioaccessible fractions of heavy metals in the airborne particulate matter from urban and industrial areas. *Atmospheric Environment*, 36, 3583-3590.
- Walters, S., Phupinyokul, M. & Ayres, J. (1995) Hospital admission rates for asthma and respiratory disease in the West Midlands: their relationship to air pollution levels. *Thorax*. 50, 948-954.
- Wellenius, G. A., Schwartz, J. & Mittleman, M. A. (2005) Air Pollution and Hospital Admissions for Ischemic and Hemorrhagic Stroke Among Medicare Beneficiaries. *Stroke*, 36, 2549-2553.
- Wheeler, B. W. & Ben-Shlomo, Y. (2005) Environmental equity, air quality, socioeconomic status, and respiratory health: a linkage analysis of routine data from the Health Survey for England. *Journal of Epidemiology and Community Health*, 59, 948-954
- Wheeler, A. J., Smith-Doiron, M., Xu, X., Gilbert, N. L. & Brook, J. R. (2008) Intra-urban variability of air pollution in Windsor, Ontario--Measurement and modelling for human exposure assessment. *Environmental Research*, 106, 7-16.
- Whitby, K. T. & Sverdrup, G. M., (1980) California aerosols: their physical and chemical characteristics, in *The Character and Origins of Atmospheric Aerosols: A Digest of Results from the California Aerosol Characterization Experiment (ACHEX)*, Hidy, G. M., Mueller, P. K., Grosjean, D., Appel, B. R., and Wesolowski, J. J. (Eds.), 477-

517. *Advances in Environmental Science and Technology*. Vol. 9. Wiley, New York, NY.
- Wichmann, H. E., Spix, C., Tuch, T., Wölke, G., Peters, A., Heinrich, J., Kreyling, W. & Heyder, J. (2000) Daily mortality and fine and ultrafine particles in Erfurt, Germany part I: role of particle number and particle mass. *Research Report (Health Effects Institute)*, 98, 87-94.
- Winterton, D. L., Kaufman, J., Keener, C.V., Quigley, S., Farin, F.M., Williams, P.V., Koenig, J.Q. (2001) Genetic polymorphisms as biomarkers of sensitivity to inhaled sulphur dioxide in subjects with asthma. *Annals of Allergy Asthma Immunology*, 86, 232-238
- WHO (1996) World Health Organization. Diesel fuel and exhaust emissions. Geneva, Switzerland.
- WHO (2003) World Health Organization. Health aspects of air pollution with particulate matter, ozone and nitrogen dioxide. Geneva, Switzerland.
- WHO (2004) World Health Organization. Health aspects of air pollution. Results from the WHO projects "Systematic effects of air pollution in Europe". Geneva, Switzerland
- WHO (2005) World Health Organization. Health effects of transport-related air pollution; Geneva, Switzerland.
- Wiebert, P., Sánchez-Crespo, A., Seitz, J., Falk, R., Philipson, K., Kreyling, W. G., Moller, W., Sommerer, K., Larsson, S. & Svartengren, M. (2006) Negligible clearance of ultrafine particles retained in healthy and affected human lungs. *European Respiratory Journal*. 28, 286-290.
- Wilson, M. R., Lightbody, J. H., Donaldson, K., Sales, J. & Stone, V. (2002) Interactions between Ultrafine Particles and Transition Metals in Vivo and in Vitro. *Toxicology and Applied Pharmacology*, 184, 172-179.
- Wilson, J. G., Kingham, S., Pearce, J. & Sturman, A. P. (2005) A review of intraurban variations in particulate air pollution: Implications for epidemiological research. *Atmospheric Environment*, 39, 6444-6462.
- Wong, T. W., Tam, W. S., Yu, T. S. & Wong, A. H. S. (2002) Associations between daily mortalities from respiratory and cardiovascular diseases and air pollution in Hong Kong, China. *Occupational and Environmental Medicine*, 59, 30-35.
- Wrobel, A., Rokita, E. & Maenhaut, W. (2000) Transport of traffic-related aerosols in urban areas. *The Science of the Total Environment*, 257, 199-211.
- Xia, T., Korge, P., James, N. W., Ning, N. L., Venkatesen, M. I., Sioutas, C. & Nel, A. (2004) Quinones and Aromatic Chemical Compounds in Particulate Matter Induce Mitochondrial Dysfunction: Implications for Ultrafine Particle Toxicity. *Environmental Health Perspectives*, 112, 1347-1358.

- Yanagisawa, R., Takano, H., Inoue, K., Ichinose, T., Sadakane, K., Yoshino, S., Yamaki, K., Kumagai, Y., Uchiyama, K., Yoshikawa, T. & Morita, M. (2003) Enhancement of acute lung injury related to bacterial endotoxin by components of diesel exhaust particles.
- Yang, Q., Chen, Y., Krewski, D., Burnett, R. T., Shi, Y. & Mcgrail, K. M. (2005) Effect of short-term exposure to low levels of gaseous pollutants on chronic obstructive pulmonary disease hospitalizations. *Environmental Research*, 99, 99-105.
- Zanobetti, A. P. & Schwartz, J. P. (2000) Race, Gender, and Social Status as Modifiers of the Effects of PM₁₀ on Mortality. *Journal of Occupational & Environmental Medicine*, 42, 469-474.
- Zemp, E., Elsasser, S., Schindler, C., Kunzli, N., Perruchoud, Andre p., Domenighetti, G., Medici, T., Ackermann-Liebrich, U., Leuenberger, P., Monn, C., Bolognini, G., Bongard, J.-P., Brandli, O., Karrer, W., Keller, R., Schoni, Martin h., Tschopp, J.-M., Villiger, B. E. A., Zellweger, J.-P. & The sapaldia team (1999) Long-Term Ambient Air Pollution and Respiratory Symptoms in Adults (SAPALDIA Study). *American Journal of Respiratory and Critical Care Medicine* 159, 1257-1266.
- Zerrath, A. (2007). TSI Incorporated. Personal Communication.
- Zhu, Y., Hinks, W.C., Kim, S., Shen, S. & Sioutas, C., (2002a) Study of ultrafine particles near a major highway with heavy-duty diesel traffic. *Atmospheric Environment*, 36, 4323-4335.
- Zhu, Y., Hinds, W.C., Kim, S. & Sioutas, C. (2002b) Concentration and size distribution of ultrafine particles near a major highway. *Journal of the Air and Waste Management Association*, 52, 1032-1042.
- Zhu, X., Fan, Z., Wu, X., Meng, Q., Wang, S. W., Tang, X., Ohman-Strickland, P., Georgopoulos, P., Zhang, J., Bonanno, L., Held, J. & Liou, P. (2008) Spatial Variation of Volatile Organic Compounds in a "Hot Spot" for Air Pollution. *Atmospheric Environment*, 42, 7329-7338.
- Zielinski, H., Mudway, I.S., Kelly, F.J. (1998) PM₁₀ and the Respiratory Tract: What Do We Know? *Polish Journal of Environmental Studies* 7, 273-277.